eman ta zabal zazu

Universidad del País Vasco
Euskal Herriko Unibertsitatea

Sustainable C–H Functionalization within Peptide & Heterocyclic Chemistry

Itziar Guerrero Azurmendi

Doctoral Thesis

Supervised by Dr. Arkaitz Correa

Química Sintética e Industrial

Departamento de Química Orgánica I

Donostia-San Sebastián, October 2020

List of Publications

1. *Site-Selective Trifluoromethylation Reactions of Oligopeptides.*
   Guerrero, I.; Correa, A.
   Asian J. Org. Chem. **2020**, *9*, 898.

2. *Cu-Catalyzed Site-Selective C(sp^2)–H Radical Trifluoromethylation of Trp-Containing Peptides.*
   Guerrero, I.; Correa, A.
   Org. Lett. **2020**, *22*, 1754. (Highlighted in Synfacts 2020, 16, 609)

3. *Metal-Catalyzed C–H Functionalization Processes with "Click"- Triazole Assistance*.
   Guerrero, I.; Correa, A.
   Eur. J. Org. Chem. **2018**, 6034. (Front-journal cover)

4. *Iron-Catalyzed C(sp^3)–H Functionalization of N,N-dimethylanilines with Isocyanides*.
   Guerrero, I.; San Segundo, M.; Correa, A.
   Chem. Commun. **2018**, 54, 1627.

5. *Co-Catalyzed C(sp^3)–H Oxidative Coupling of Glycine and Peptide Derivatives*.
   San Segundo, M.; Guerrero, I.; Correa, A.
   Org. Lett. **2017**, *19*, 5288.

Table of contents

Abbreviations and Acronyms

bpy = 2,2′-Bipyridyl

CDC = Cross-Dehydrogenative Coupling

Cod = 1,5-Cyclooctadiene

Cys = Cysteine

DCC = N,N′-Dicyclohexylcarbodiimide

DCE = 1,2-Dichloroethane

DCIB = 1,2-Dichloroisobutane

DCM = Dichloromethane

DDQ = 2,3-Dichloro-5,6-dicyano-p-benzoquinone

DFT = Density Functional Theory

DG = Directing Group

DMA = *N*,*N*-Dimethylacetamide

DMF = *N*,*N*-Dimethylformamide

DMAP = N,N-Dimethylpyridin-4-amine

DMPU = N,N′-Dimethylpropylene urea

DMSO = Dimethyl sulfoxide

dppe = 1,2-Bis(diphenylphosphino)ethane

dppf = 1,1′-Ferrocenediyl-bis(diphenylphosphine)

d.r. = Diastereomeric ratio

DTPB = Di-*tert*-Butyl peroxybenzoate

ee = Enantiomeric excess

EWG = Electron With-Drawing Group

Gly = Glycine

HBpin = 4,4,5,5-Tetramethyl-1,3,2-dioxaborolane

HMPA = Hexamethylphosphoramide

His = Histidine

Mp = Melting point

n.d. = Not Determined

NHC = N-Heterocyclic Carbene

n.r. = No Reaction

OA = Oxidative Addition

PDFA = Difluoromethylene phosphobetaine

PET = Positron Emission Tomography

Phe = Phenylalanine

PMP = *p*-Methoxyphenyl

ppy = 2-Phenylpyridine

RCC = Radiochemical conversion

RE = Reductive Elimination

RSD = Relative Standard Deviation

r.t. = Room temperature

SEAr = Electrophilic Aromatic Substitution

SET = Single Electron Transfer

TBAB = Tetrabutylammonium bromide

TBHP = *Tert*-Butyl hydroperoxide

TEEDA = N,N,N′,N′-Tetraethylethylenediamine

TEMPO = 2,2,6,6-tetramethyl-1-piperidinyloxy

THF = Tetrahydrofuran

Trp = Tryptophan

TS = Transition State

Tyr = Tyrosine

Abstract

Chemistry is known to play a crucial role in the universal commitment to achieve sustainable methodologies in which the reduction of energy consumption and the production of waste constitute great challenges for the advancement of Science. In this context, Organic and Organometallic Chemistry have experienced exceptional development in recent years, providing access to new environmentally friendly synthetic protocols based on the use of metal catalysts. In particular, cross-coupling reactions for C–H functionalization have emerged as a powerful alternative within modern Chemistry to overcome previous synthetic problems. In this regard, CDC (*Cross-Dehydrogenative Coupling*) processes are of great interest since they not only minimize the generation of chemical waste but also can be carried out under very mild reaction conditions. Given the experience of our group in the development of robust and general catalytic C–H functionalization events, we envisioned that the use of earth-abundant and often less-toxic first-row transition metals (Cu, Fe, and Co) could be a viable tool for sustainable development. In particular, we became interested in the modification and assembly of amino acid and peptide derivatives, in a sustainable manner, due to their high importance in research areas such as proteomics and drug discovery. Likewise, the use of 1,2,3-triazoles as versatile DGs in the realm of C–H functionalization has not reached yet its full synthetic potential. Thus, we decided to focus our doctoral studies on the development of sustainable methodologies for the diversification of heterocycles and peptides, which are structures of utmost importance in medicinal chemistry.

Concerning CDC-type reactions, the α-C(*sp*3)−H bond adjacent to a heteroatom like nitrogen is known to be activated under oxidative reaction conditions to form the corresponding imine/iminium-type electrophilic intermediate. In this respect, two new methodologies have been developed based on this strategy. On the one hand, we have carried out the α-heteroarylation and aminocarbonylation of glycine derivatives with indoles or formamides, respectively, by cobalt or iron catalysis. Furthermore, these processes have been extended to peptide compounds without racemization of the chiral centers present in the molecule (*Chapter 2*). On the other hand, an Ugi-type oxidative reaction between *N*,*N*-dimethylanilines and isocyanides with a Fe(II)/ oxidant system has been disclosed enabling the synthesis of α-amino amides (*Chapter 3*).

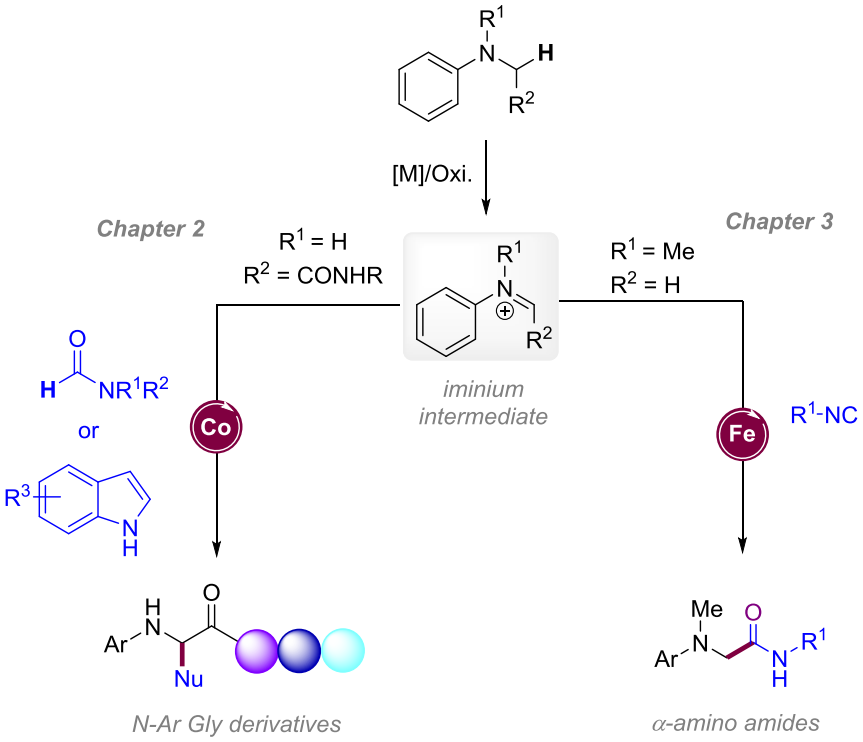

Scheme 1 CDC Processes.

Subsequently, we expanded our studies towards the modification of other amino acid residues developing a copper-catalyzed selective C(sp^2)–H trifluoromethylation of tryptophan derivatives with the commercially available Langlois reagent ($NaSO_2CF_3$). Moreover, the procedure enabled the access to a wide variety of peptide compounds of great structural complexity (*Chapter 4*).

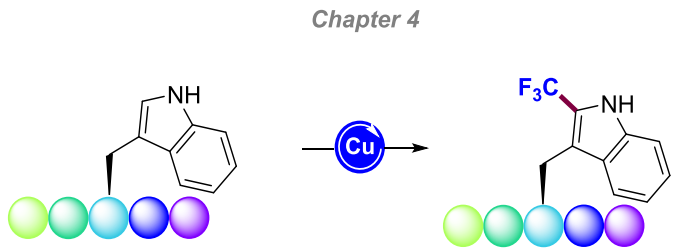

Scheme 2 Copper-Catalyzed Selective C(sp^2)–H Trifluoromethylation of Tryptophan Derivatives.

We have also explored the use of 1,2,3-triazoles prepared through "click" processes as versatile and efficient directing groups to carry out comparatively less studied *meta*-C(sp^2)–H functionalization reactions. In particular, we have studied the ruthenium-catalyzed *meta*-sulfonylation of arenes through σ-activation (*Chapter 5*).

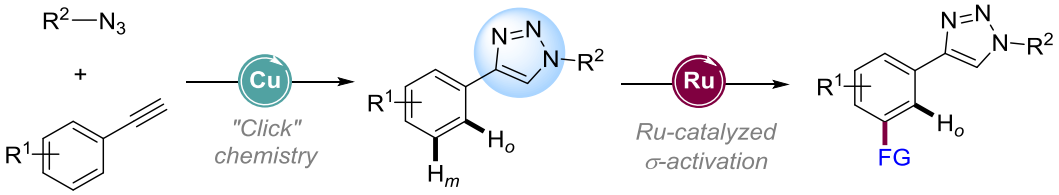

Scheme 3 Ruthenium-Catalyzed Meta-C(sp^2)–H Functionalization Directed by 1,2,3-Triazole Derivatives.

Resumen de Tesis Doctoral

La Química desempeña un indudable papel de liderazgo en el compromiso universal para alcanzar un desarrollo sostenible en el que la reducción del gasto energético y producción de residuos constituyen grandes retos para el avance de la Ciencia. En este contexto, la Química Orgánica y Organometálica han experimentado un excepcional desarrollo en los últimos años proporcionando acceso a nuevas metodologías sintéticas respetuosas con el medio ambiente basadas en el uso de catalizadores metálicos. En particular, las reacciones de acoplamiento que transcurren *via* funcionalización de enlaces C–H han experimentado un espectacular desarrollo y este campo se ha establecido como una importante disciplina dentro de la Química Moderna. Los procesos CDC (*Cross-Dehydrogenative Coupling*) están de máxima actualidad ya que no sólo minimizan la generación de residuos químicos cumpliendo el principio de economía atómica sino que además pueden llevarse a cabo de forma muy sencilla e incluso en presencia de aire y agua, evitando así el uso de complicadas técnicas experimentales. Nuestro grupo de investigación ha centrado su atención en el desarrollo de nuevos procesos catalíticos de funcionalización de enlaces C–H abogando de manera firme y directa por la innovación y desarrollo hacia una química sostenible proporcionando ventajosas soluciones a problemas sintéticos de indudable interés como el uso de materias primas de bajo coste y metales de baja toxicidad como hierro y cobalto. El principal objetivo de esta Tesis Doctoral consiste en el diseño de nuevos métodos sintéticos medioambientalmente atractivos que permitan obtener diversidad química en estructuras heterocíclicas y peptídicas, ambas de amplia presencia en química médica.

Por un lado y en relación a los procesos de CDC, se han desarrollado dos nuevas metodologías. La primera consiste en la α-heteroarilación y aminocarbonilación de derivados de glicina con indoles o formamidas, respectivamente, por activación de enlaces C(sp^3)–H adyacentes al grupo amino en presencia de catalizadores de cobalto o hierro. Este proceso se ha extendido a compuestos peptídicos demostrando además que la reacción transcurre sin la racemización de los centros quirales presentes en dichas moléculas (*Chapter 2).*

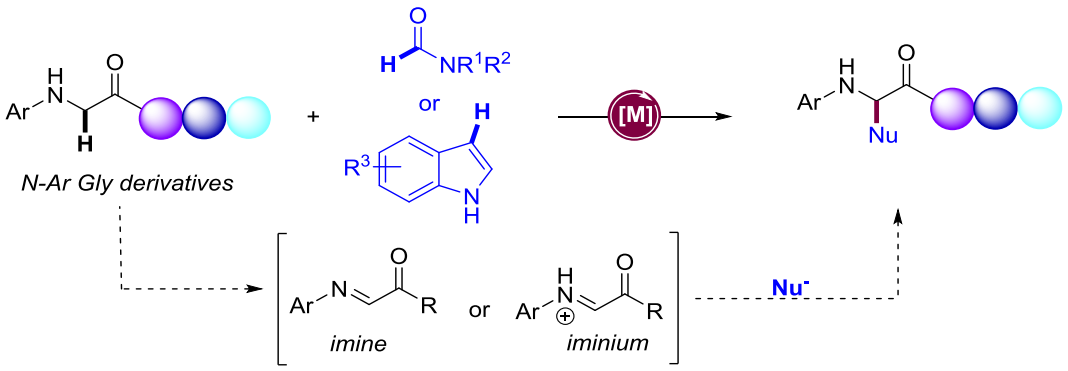

Scheme 4 Procesos CDC entre Indoles/Formamidas y Aminoácidos o Derivados.

El segundo acoplamiento oxidativo estudiado en esta Tesis Doctoral consiste en la reacción oxidativa de Tipo Ugi entre *N,N*-dimetilanilinas e isocianuros con la combinación de catalizadores de Fe(II) y un oxidante. Al igual que los anteriores, estod procesos cursan a través de especies electrófilas intermedias de tipo imina o iminio (*Chapter 3*).

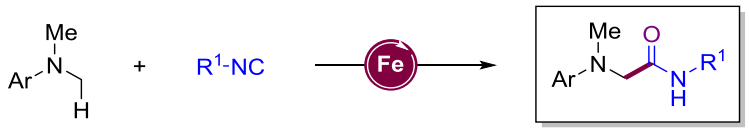

Scheme 5 Reacción Oxidativa de tipo Ugi entre N,N-Dimetilanilinas e Isocianuros Catalizada por Hierro.

Por otro lado, se ha puesto a punto con gran éxito un proceso de trifluorometilación C(sp^2)–H selectiva de derivados de triptófano catalizado por sales de Cu(I). Entre las ventajas del método se encuentra el uso del reactivo comercial de Langlois ($NaSO_2CF_3$), así como la simplicidad operacional del método que transcurre en presencia de aire. Esta técnica nos ha permitido acceder a variedad de compuestos peptídicos de gran complejidad estructural (Chapter 4).

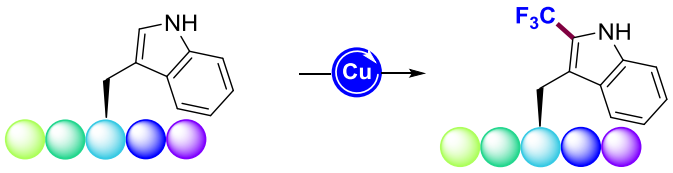

Scheme 6 Trifluorometilación C(sp²)–H Selectiva de Derivados de Triptófano Catalizada por Cobre.

Nuestro último objetivo ha consistido en explorar el uso de triazoles preparados a través de procesos "Click" en reacciones de funcionalización C(sp^2)–H en posición *meta*, comparativamente menos exploradas. Para ello nos hemos centrado en el uso de catalizadores de Ru, los cuales permiten a través de la formación de los correspondientes rutenaciclos activar el C(sp^2)–H en posición *para* al metal y por tanto promover de manera formal una *meta*-funcionalización (*Chapter 5*).

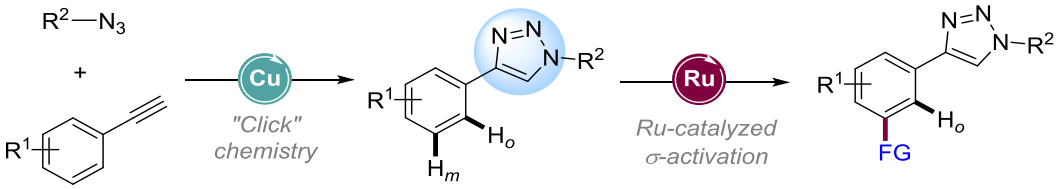

Scheme 7 Sulfonilacion C(sp^2)–H en Posición Meta Dirigida por 1,2,3-Triazoles.

Chapter 1.

General Introduction

1.1. Metal-Catalyzed Cross-Coupling Reactions

In the last decades, chemists have been struggled to seek for new methodologies that enable the selective transformation of organic molecules with further applications in biochemistry and material sciences as well as agrochemical and pharmaceutical industries, among others. Since the seminal work based on Pd-catalysts in the 70's by Heck, Negishi and Suzuki,[1] transition metal-catalyzed cross-coupling reactions have been one of the most important breakthroughs in the realm of organic chemistry. The landscape of this field has totally changed until the point that it became hard to perform a total synthesis of complex molecules without the use of transition metal catalysts. There are uncountable the innovative tactics for new C–C/C–X bond formation that are based on this strategy.[2]

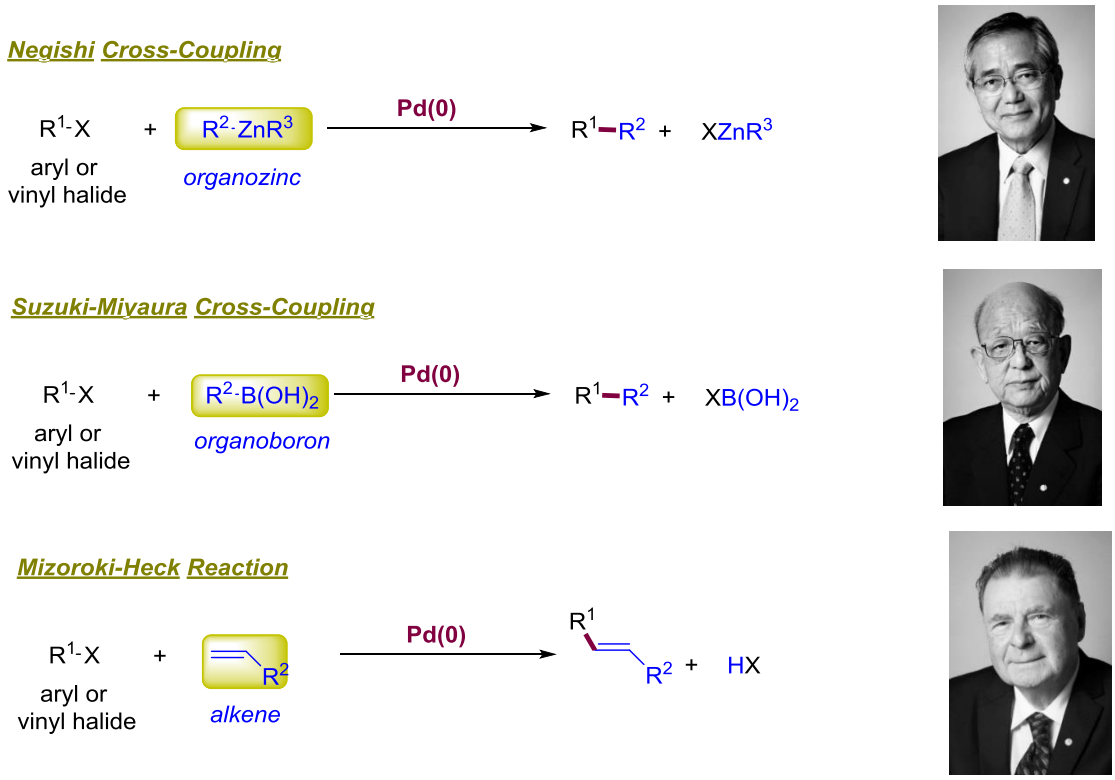

Scheme 8 Ei-ichi Negishi, Akira Suzuki and Richard F. Heck (Nobel Prize in Chemistry 2010) "Palladium-Catalyzed Cross-Couplings in Organic Synthesis".

[1] a) Baba, S.; Negishi, E. *J. Am. Chem. Soc.* **1976**, *98*, 6729. b) King, A. O.; Okukado, N.; Negishi, E. *J. Chem. Soc., Chem. Commun.***1977**, *19*, 683. c) Miyaura, N.; Yamada, K.; Suzuki, A. *Tetrahedron Lett.* **1979**, *20*, 3437. d) Miyaura, N.; Suzuki, A. *J. Chem. Soc. Chem. Commun.* **1979**, 866. e) Heck, R. F.; Nolley, J. P. *J. Org. Chem.* **1972**, *37*, 2320. f) Mizoroki, T.; Mori, K.; Ozaki, A. *Bull. Chem. Soc. Jpn.* **1971**, *44*, 581. For Nobel lectures, see: g) Seechurn, C. C. C. J.; Kitching, M. O.; Colacot, T. J.; Sniekus, V. *Angew. Chem. Int. Ed.* **2012**, *51*, 5062. h) Suzuki, A. *Angew. Chem. Int. Ed.* **2011**, *50*, 6722. i) Negishi, E.-I. *Angew. Chem. Int. Ed*. **2011**, *50*, 6738. j) Dieck, H. A.; Heck, R. F. *J. Am. Chem. Soc.* **1974**, *96*, 1133.

[2] a) Biffis, A.; Centomo, P.; Del Zotto, A.; Zecca, M. *Chem. Rev.* **2018**, *118*, 2249. b) Magano, J.; Dunetz, J. R. *Chem. Rev.* **2011**, *111*, 2177. c) Corbet, J.-P.; Mignani, G. *Chem. Rev.* **2006**, *106*, 2651.

In a "classical" metal-catalyzed cross-coupling reaction, it is suggested that nucleophiles react with electrophiles under the assistance of a transition metal (Scheme 9). In particular, the most common electrophiles are aryl or vinyl halides but alkyl halides can be also utilized. Concerning the nucleophilic counterpart, organometallic reagents are widely used for the formation of new C–C bonds and the challenging C–heteroatom bond formation often features the use of alcohols, amines and thiols, among others.[3]

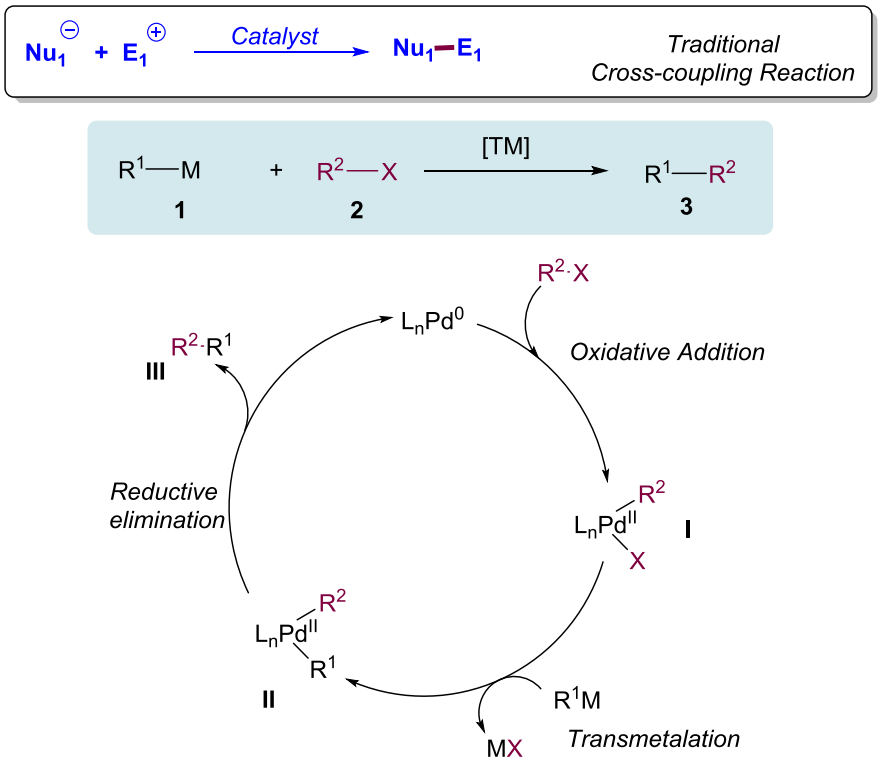

Scheme 9 Traditional Cross-Coupling Reaction.

Palladium and nickel are the most recurring transition metal catalysts for traditional cross-coupling reactions and the widely accepted mechanism is based on three elemental steps (Scheme 9): the oxidative addition of the commonly used (pseudo)halide electrophilic compound to the metal center oxidizes the latter in two units. Subsequently, the transmetalation with the nucleophilic reagent takes place for the formation of intermediate **II**, which undergoes a reductive elimination releasing the coupling product and generating the active catalyst.

However, this traditional strategy usually requires the use of an organometallic species. For this reason, chemists have searched for new techniques where more unconventional substrate combinations can take place increasing the organic synthesis portfolio as well as the sustainability of the process.

[3] a) Paul, F.; Patt, J.; Hartwig, J. F. *J. Am. Chem. Soc.* **1994**, *116*, 5969. b) Guram, A. S.; Buchwald, S. L. *J. Am. Chem. Soc.* **1994**, *116*, 7901. For a recent perspective: Dorel, R.; Grugel, C. P.; Haydl, A. M. *Angew. Chem. Int. Ed.* **2019**, *58*, 17118.

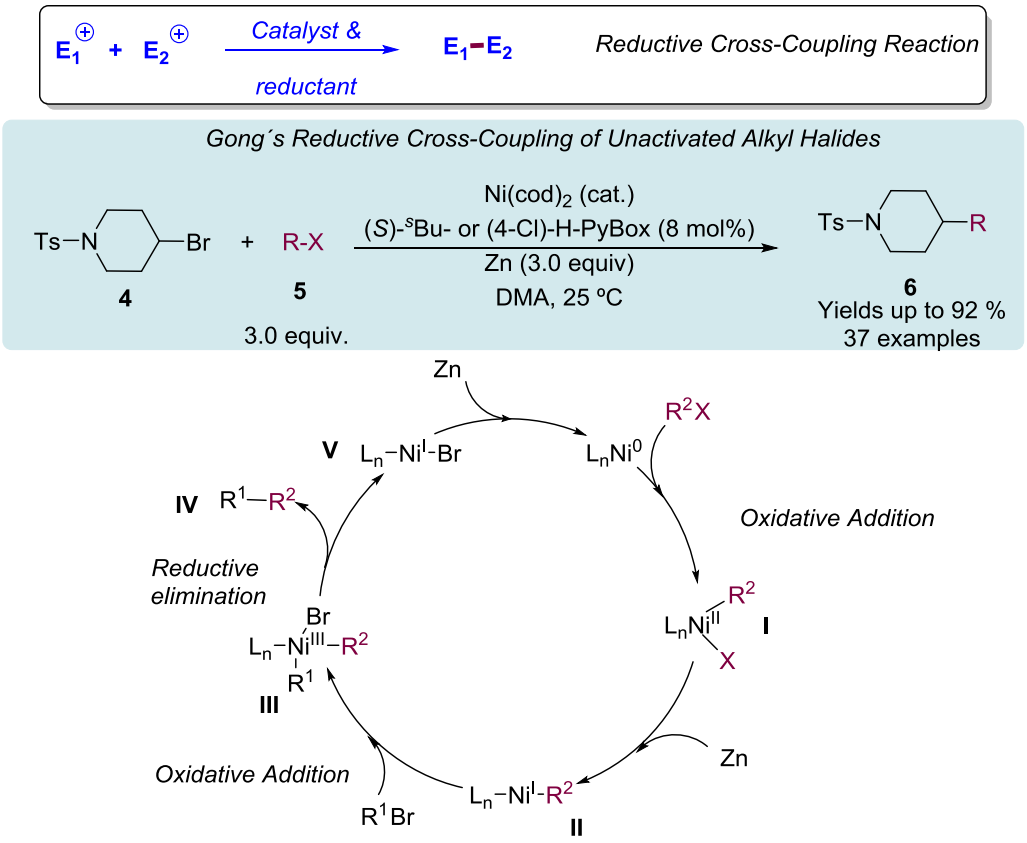

Scheme 10 Reductive Cross-Coupling Reaction.

A reductive cross-coupling reaction is one of those strategies in which two electrophiles can be coupled in the presence of a reducing agent and without the need for organometallic compounds.[4] As an example, in 2011 Gong and co-workers[5] developed a nickel-catalyzed cross-coupling reaction between two different electrophilic alkyl halides under reductive conditions. The reaction proceeds in the following manner (Scheme 10): it is proposed that firstly an oxidative addition occurs with the excess of the most reactive alkyl halide to obtain the intermediate **I**. Then, if a second oxidative addition of the less reactive alkyl halide occurred, a Ni^{IV} complex would be formed. However, this option is often discarded and the commonly accepted pathway features the reduction of intermediate **I** to the corresponding Ni^{I} complex **II** with the aid of Zn in order to allow the second oxidative addition and further formation of Ni^{III} complex **III**. In this way, the product **IV** is released by a reductive elimination and Ni^{I} complex **V** is eventually reduced to form the active catalytic species.

[4] a) Weix, D. J. *Acc. Chem. Res.* **2015**, *48*, 1767. b) Gu, J.; Wang, X.; Xue, W.; Gong, H. *Org. Chem Front.* **2015**, *2*, 1411. c) Everson, D. A.; Weix, D. J. *J. Org. Chem.* **2014**, *79*, 4793. d) Moragas, T.; Correa, A.; Martin, R. *Chem. Eur. J.* **2014**, *20*, 8242.
[5] Yu, X.; Yang, T.; Wang, S.; Xu, H.; Gong, H. *Org.Lett.* **2011**, *13*, 2138.

On the other hand, the coupling of two nucleophilic centers is possible under oxidative reaction conditions (Scheme 11). One of the main advantages of this strategy relies on the high atom-economy when employing non-functionalized C–H coupling partners.

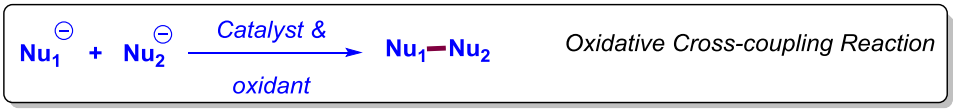

Scheme 11 Oxidative Cross-Coupling Reaction.

Besides some examples that appeared before 2000, the modern area of oxidative cross-couplings started with significant works from the groups of Murahashi[6] and Li[7]. In 2004, Li and co-workers termed to a specific example of oxidative cross-coupling reaction, '*Cross-Dehydrogenative Coupling*' (CDC).[8] In general terms, CDC type reactions enable the direct C–C/C–X bond formation from two different C–H or C–H/X–H bonds with the "formal" generation of H_2 in the presence of an oxidant (Scheme 12).

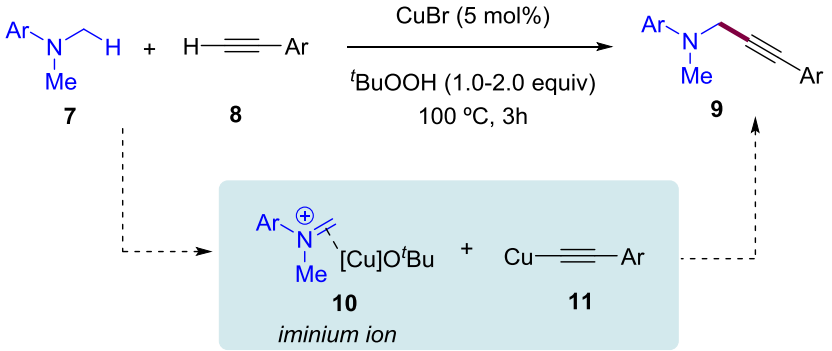

Scheme 12 Copper-Catalyzed CDC type Reaction between Dimethylanilines and Alkynes.

They managed to couple in a straightforward manner dimethylanilines and alkynes with copper catalysis and *tert*-butyl hydroperoxide as the oxidant. Generally, in CDC reactions two important intermediates are generated *in situ*, the nucleophilic anion and the electrophilic cation upon oxidative elemental steps.[9] In this particular case, the alkyne is converted into the nucleophilic copper acetylide which further attacks the electrophilic iminium derived from the starting dimethylaniline.

[6] Murahashi, S.-I.; Komiya, N.; Terai, H.; Nakae, T. *J. Am. Chem. Soc.* **2003**, *125*, 15312.
[7] Li, C.-J. *Tetrahedron* **1996**, *52*, 5643.
[8] Girard, S. A.; Knauber, T.; Li, C.-J. *Angew. Chem. Int. Ed*. **2014**, *53*, 74.
[9] Yi, H.; Zhang, G.; Wang, H.; Huang, Z.; Wang, J.; Singh, A. K.; Lei, A. *Chem. Rev*. **2017**, *117*, 9016.

Concerning the sustainability, while the lack of prefunctionalization could be a major advantage, it could limit the functional group tolerance and create the aid of directing groups to achieve high selectivity in the case of competing distinct C−H bonds. As the need for an external oxidant is often a drawback, the most ideal reaction conditions would imply a metal-free system where oxygen would act as the oxidant and consequently, water would be the only chemical waste.[10]

1.2. Metal-Catalyzed C–H Functionalization

Organic synthesis has largely involved the interconversion of pre-existing functional groups, while C–H bonds were considered inert entities for a long time owing to their high dissociation energy.[11] However, during the last decade C–H functionalization has emerged as a powerful tool for the construction of complex molecules in modern organic synthesis. This attractive bond forming strategy, where C–H bond is considered as a latent functional group, enables the use of readily available starting materials without the need of a prefunctionalization and it is a high atom- and step-economical process (Scheme 13).

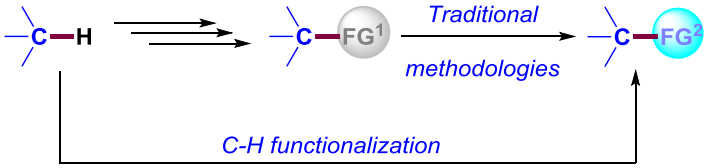

Scheme 13 Traditional Functional Group Interconversion vs C–H Functionalization.

The vast majority of C−H functionalizations have been limited to the widely use of cost-intensive transition metal catalysts like palladium,[12] iridium,[13] rhodium,[14] and ruthenium.[15] The reality of these precious metal

[10] Shi, Z.; Zhang, C.; Tang, C.; Jiao, N. *Chem. Soc. Rev.* **2012**, *41*, 3381.
[11] Gandeepan, P.; Müller, T.; Zell, D.; Cera, G.; Warratz, S.; Ackermann, L. *Chem. Rev.* **2019**, *119*, 2192.
[12] a) Choy, P. Y.; Wong, S. M.; Kapdi, A.; Kwong, F. Y. *Org. Chem. Front.* **2018**, *5*, 288. b) Le Bras, J.; Muzart, J. *Eur. J. Org. Chem.* **2018,** 1176. c) Baudoin, O. *Acc. Chem. Res.* **2017**, *50*, 1114. d) Kakiuchi, F.; Kochi, T. *Isr. J. Chem.* **2017**, *57*, 953. e) Della Ca', N.; Fontana, M.; Motti, E.; Catellani, M. *Acc. Chem. Res.* **2016**, *49*, 1389. f) Ye, J.; Lautens, M. *Nat. Chem.* **2015**, *7*, 863. g) Neufeldt, S. R.; Sanford, M. S. *Acc. Chem. Res.* **2012**, *45*, 936. h) Sun, C.-L.; Li, B.-J.; Shi, Z.-J. *Chem. Commun.* **2010**, *46*, 677. i) Chen, X.; Engle, K. M.; Wang, D.-H.; Yu, J.-Q. *Angew. Chem., Int. Ed.* **2009**, *48*, 5094.
[13] a) Yuan, C.; Liu, B. *Org. Chem. Front.* **2018**, *5*, 106. b) Haldar, C.; Emdadul Hoque, M.; Bisht, R.; Chattopadhyay, B. *Tetrahedron Lett.* **2018,** *59*, 1269. c) Nagamoto, M.; Nishimura, T. *ACS Catal.* **2017**, *7*, 833. d) Sharninghausen, L. S.; Crabtree, R. H. *Isr. J. Chem.* **2017**, *57*, 937. e) Kim, J.; Chang, S. *Angew. Chem. Int. Ed.* **2014**, *53*, 2203. f) Pan, S.; Shibata, T. *ACS Catal.* **2013**, *3*, 704. g) Suzuki, T. *Chem. Rev.* **2011**, *111*, 1825. h) Choi, J.; Goldman, A. S. *Top. Organomet. Chem.* 2**011**, *34*, 139. i) Satoh, T.; Ueura, K.; Miura, M. *Pure Appl. Chem.* **2008**, *80*, 1127.
[14] a) Piou, T.; Rovis, T. *Acc. Chem. Res.* **2018**, *51*, 170. b) Yang, Y.; Li, K.; Cheng, Y.; Wan, D.; Li, M.; You, J. *Chem. Commun.* **2016**, *52*, 2872. c) Ye, B.; Cramer, N. *Acc. Chem. Res.* **2015**, *48*, 1308. d) Wencel-Delord, J.; Patureau, F. W.; Glorius, F. *Top. Organomet. Chem.* **2015**, *55*, 1. e) Song, G.; Wang, F.; Li, X. *Chem. Soc. Rev.* **2012**, *41*, 3651. f) Colby, D. A.; Tsai, A. S.; Bergman, R. G.; Ellman, J. A. *Acc. Chem. Res.* **2012**, *45*, 81. g) Du Bois, J. *Org. Process Res. Dev.* **2011**, *15*, 758. h) Colby, D. A.; Bergman, R. G.; Ellman, J. A. *Chem. Rev.* **2010**, *110*, 624. i) Satoh, T.; Miura, M. *Chem. Eur. J.* **2010**, *16*, 11212.
[15] a) Nareddy, P.; Jordan, F.; Szostak, M. *ACS Catal.* **2017**, *7*, 5721. b) Leitch, J. A.; Frost, C. G. *Chem. Soc. Rev.* **2017**, *46*, 7145. c) Zha, G.-F.; Qin, H.-L.; Kantchev, E. A. B. *RSC Adv.* **2016**, *6*, 30875. d) Ruiz, S.; Villuendas, P.; Urriolabeitia,

catalysts has been the goal of several research groups and hence they present the advantage of exhibiting a broad substrate scope and well-studied mechanisms, where the putative organometallic intermediates are often predictable.[16] Nevertheless, the tolerance level of trace metal impurities in drugs and crop protecting agents is a fundamental aspect that must be taken into account. In this respect, the noble 4d and 5d transition metals not only are expensive, but they also exhibit a high level of toxicity which could be prejudicial for their further applications in agrochemical and pharmaceutical industries (Figure 1).[11]

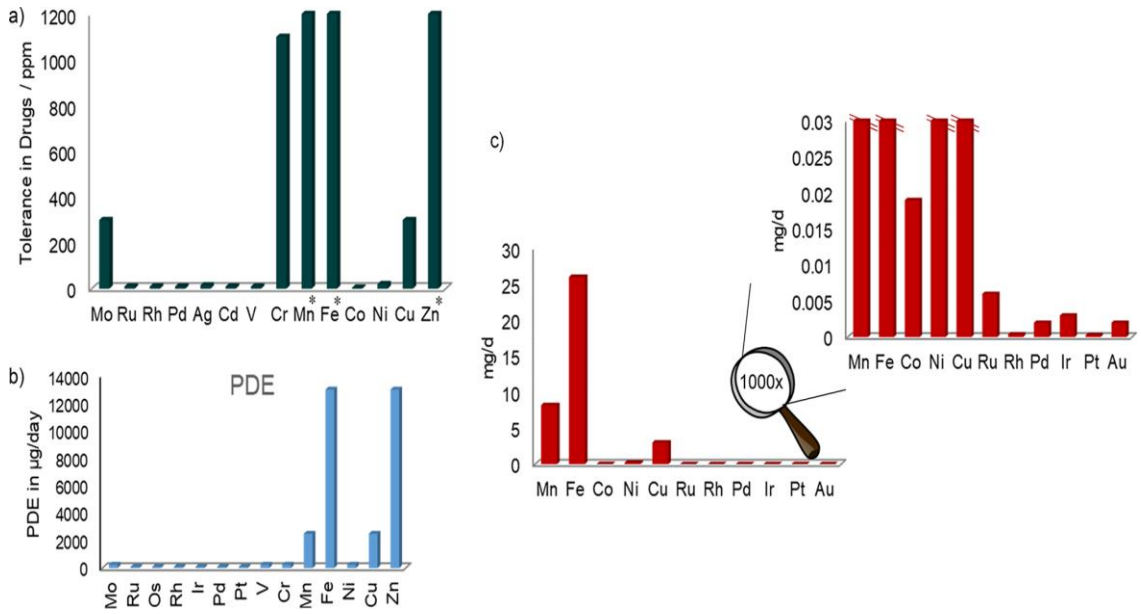

Figure 1: a) Tolerance of Transition Metals in Drugs. b) Permitted Daily Exposure. (PDE) c) Upper Range of Dietary Intake for Adults.

As a direct consequence, during the last decade first-row metal catalysts (e.g. Fe, Mn, Co, Cu, Ni) have represented an advantageous alternative for C−H activation reactions having similar or even better reactivity than precious metals.[17] 3*d* Transition metals have gained great interest due to their remarkable properties such as the high abundance in the Earth crust, the low-cost and the low level of toxicity.[11] Nonetheless, in comparison with the second-row transition metals' established mechanisms, the fact that they undergo easier ligand exchange and disproportionation, as well as their possible multiple oxidation states make more difficult the comprehension of the underlying reaction mechanisms.[16]

E. P. *Tetrahedron Lett*. **2016**, *57*, 3413. e) Manikandan, R.; Jeganmohan, M. *Org. Biomol. Chem*. **2015**, *13*, 10420. f) Thirunavukkarasu, V. S.; Kozhushkov, S. I.; Ackermann, L. *Chem. Commun*. **2014**, *50*, 29. g) Li, B.; Dixneuf, P. H. *Top. Organomet. Chem*. **2014**, *48*, 119. h) De Sarkar, S.; Liu, W.; Kozhushkov, S. I.; Ackermann, L. *Adv. Synth. Catal*. **2014**, *356*, 1461. i) Ackermann, L. *Acc. Chem. Res*. **2014**, *47*, 281. j) Kozhushkov, S. I.; Ackermann, L. *Chem. Sci.* **2013**, *4*, 886. k) Arockiam, P. B.; Bruneau, C.; Dixneuf, P. H. *Chem. Rev.* **2012**, *112*, 5879.

[16] Hayler, J. D.; Leahy, D. K; Simmons, E. M. *Organometallics* **2019** *38*, 36.

[17] Gallego, D.; Baquero, E. A. *Open Chem.* **2018**, *16*, 1001.

There are numerous the investigations that have contributed to the knowledge about elementary steps in late-transition metal-catalyzed C–H activation reactions. Among the well-established reaction mechanisms, steps such as oxidative addition (OA), electrophilic aromatic substitution (SEAr) and σ-bond metathesis (σBM) have been accepted to rationalize the activation of C–H bonds and their further functionalization (Figure 2).

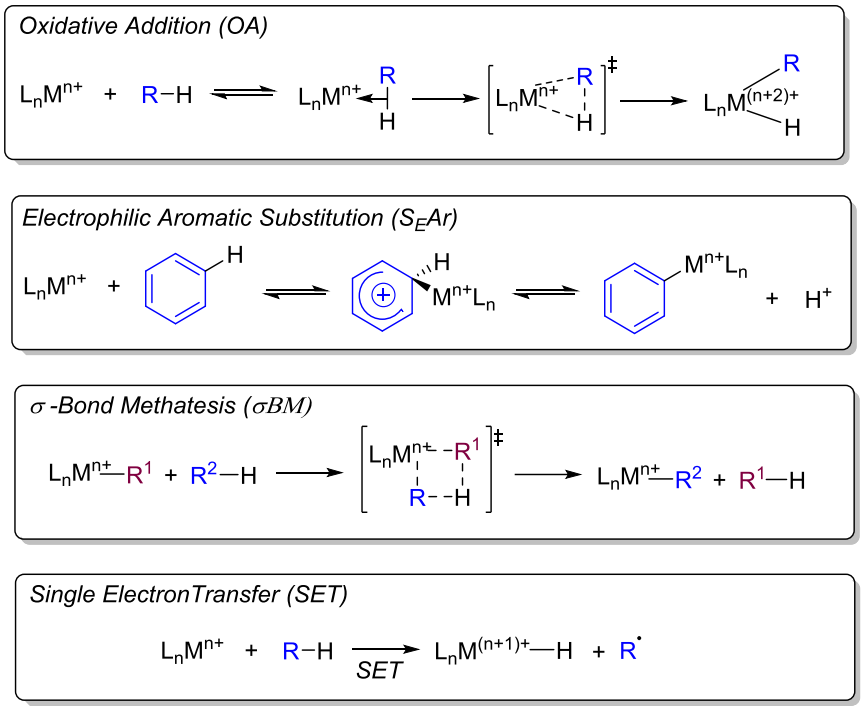

Figure 2 Different Fundamental Steps for C–H Activation by a Metal Complex.

An electron-rich metal center (M^{n+}) can coordinate with a given C–H bond lowering its energy barrier through a *dπ*-back donation and facilitating its cleavage. As a consequence, a [H–$M^{(n+2)+}$–(alkyl/aryl)] organometallic species is formed oxidizing the metal center in two units, terming this step *Oxidative Addition* (OA).

On the contrary, in an *Electrophilic Aromatic Substitution* (S_EAr) step no change in the metal oxidation state occurs despite the fact that the electrophilic metal center acts as a Lewis acid interacting with an aromatic substrate and generates a C(aryl)–M bond. Due to the C(aryl)–H acidity increase, the hydrogen atom could be released either as a proton or with the aid of a base, which is in the coordination sphere of the metal and it is known as a *Base Assisted Intramolecular Electrophilic-Type Substitution* (BIES).

A carbon-metal bond is also formed in a *σ-Bond Metathesis* (σ-BM). Metals with high oxidation states are more prone to undergo this step, which proceeds through a four-centered transition state with simultaneous bond cleavage and formation. Hence, a metal–ligand exchange takes place without changing the metal center oxidation number.

The C–H activation steps described above involved an organometallic species intermediate. However, a distinct pathway could involve a *Single Electron Transfer* (SET) event consisting in a redox process, where the metal and the substrate are not linked. The homolytic cleavage of the C–H bond leads to a metal-hydride species (with the metal center oxidation state one unit increased) and a carbon centered radical, which could couple with either an electrophile or with another radical species.

The installation of Lewis basic functional groups, known under the term of "directing group" (DG), is also one of the most common strategy that leads to the selective activation of a C–H bond in the presence of other multiple bonds within organic molecules. The coordination between the DG and the metal center results in the decrease of the energy barrier of the closest *ortho* C–H bond, which is cleaved forming a thermodynamically stable five- or six-membered metalacycle intermediate (Scheme 14).

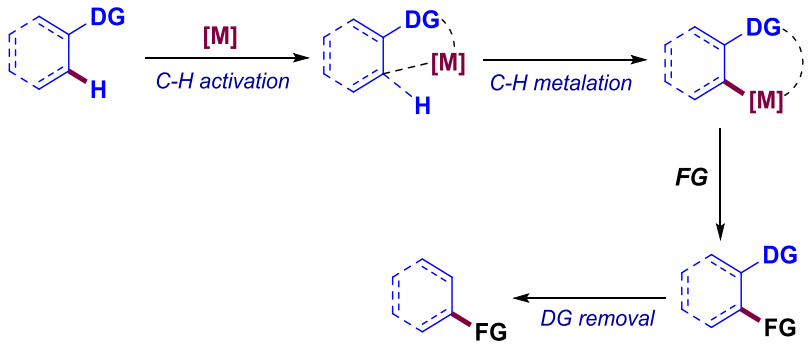

Scheme 14 DG-Assisted Metal-Catalyzed C–H Functionalization.

Nitrogen-containing heterocycles are among the most commonly used DGs owing to their high ability to form strong N–metal interactions. Additionally, the biological activity exhibited by some of these heterocycles such as pyridine make them privileged scaffolds according to the database of U.S. FDA approved drugs.[18]

The feasibility of the chelation assistance tactic is often diminished, as further steps to set up and to remove the DG are required, what makes the process less step-economical. Moreover, in some cases the cleavage of the directing groups turns out to be more complicate than expected. Therefore, if the DG itself has a significant role in further applications, its cleavage would not be necessary. This is the case of pyridine; this six-membered aromatic ring is recognized to be the second most utilized nitrogen heterocycle in drug discovery and hence, it has attracted much attention as a powerful DG for transition metal-catalyzed C–H activation (Figure 3).[19]

[18] Vitaku, E.; Smith, D. T.; Njardarson, N. T. *J. Med. Chem.* **2014**, *57*, 10257.
[19] Swamy, T.; Reddy, B. V. S.; Grée, R.; Ravinder, V. *ChemistrySelect* **2018**, *3*, 47.

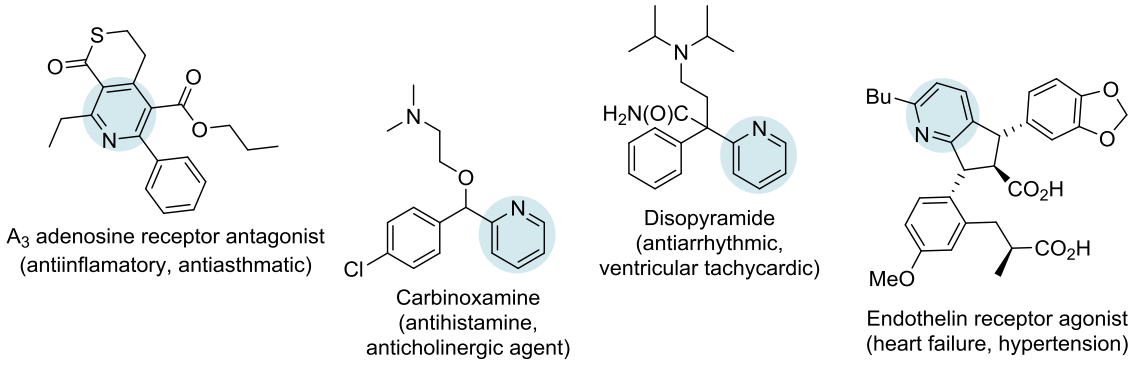

Figure 3 Pyridine-Containing Drugs.

Quinoline is also a Lewis basic heterocycle present in a large amount of pharmaceutical compounds. Thanks to its ability to coordinate with metal centers, Daugulis introduced this framework as a versatile DG for a wide variety of C–H functionalization processes, such as the cobalt-catalyzed C(sp^2)–H bond alkenylation with alkynes (Scheme 15).[20] The most usual strategy for the installation of quinoline is through an amide. In this regard, the DG behaves as a bidentate auxilliary with the metal, which leads to the formation of a more rigid metalacycle intermediate. As an advantage to the use of pyridines as DG, the cleavage of this scaffold has been described in several occasions under mild reactin conditions.[21]

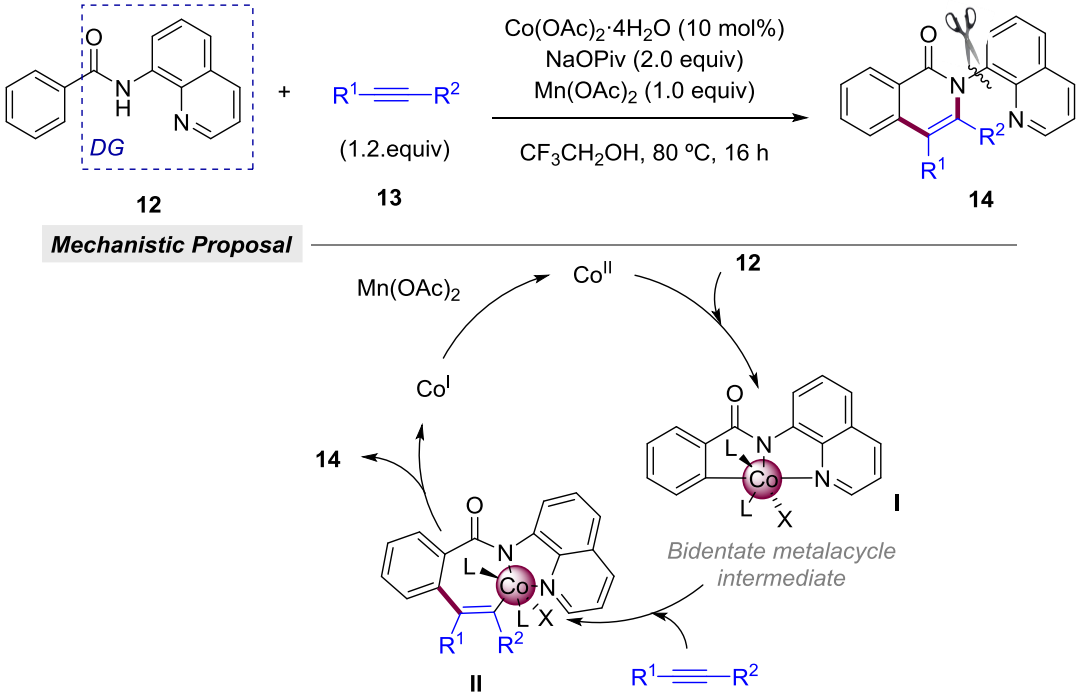

Scheme 15 Cobalt-Catalyzed C(sp^2)–H Bond Alkenylation with Alkynes.

[20] Grigorjeva, L.; Daugulis, O. *Angew. Chem. Int. Ed.* **2014**, *53*, 10209.
[21] a) Zhang, Z.; Li, X.; Song, M.; Wan, Y.; Zheng, D.; Zhang, G.; Chen, G. *J. Org. Chem*. **2019**, *84*, 12792. b) Yu. L.; Chen, X.; Liu, D.; Hu, L.; Yu, Y.; Huang, H.; Tan, Z.; Gui, Q. *Adv. Synth. Catal*. **2018**, *360*, 1346.

1.3. General Objectives of this Doctoral Thesis

The fundamental studies along this Doctoral Thesis will be conducted within the field of peptide chemistry and heterocyclic synthesis. Hence, we established the following main objectives:

- To develop new sustainable C(sp^3)–H functionalization reactions featuring base metal catalysts.
- To develop new late-stage peptide tagging techniques based on C–H functionalization processes.
- To exploit the use of 1,2,3-triazoles as practical DGs in the challenging and unexplored field of remote functionalization.

Chapter 2.

Base Metal-Catalyzed C(sp^3)–H Cross-Dehydrogenative-Coupling (CDC) of Glycine Derivatives

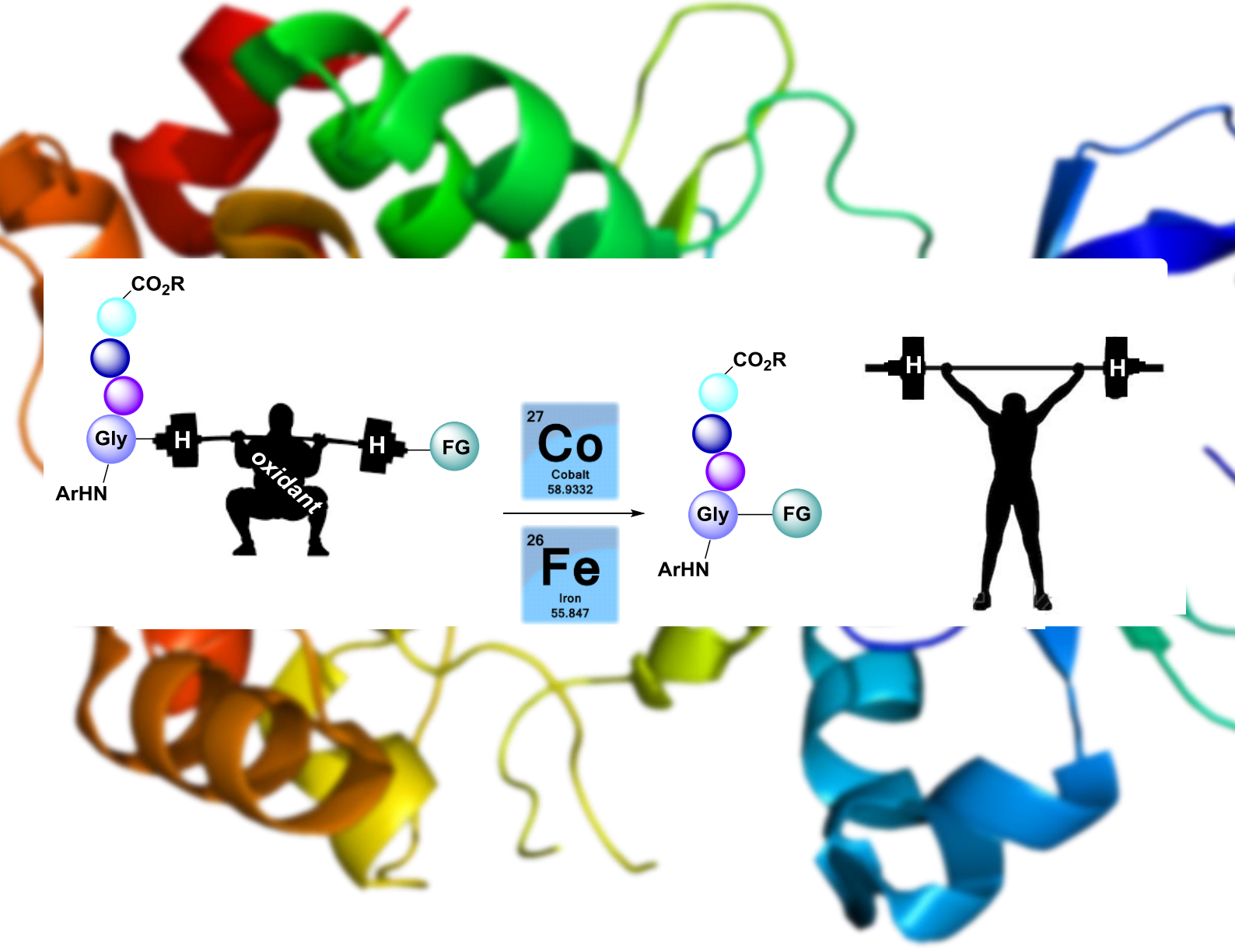

2.1. Introduction

2.1.1. α-C(sp^3)–H Functionalization at Peptide Backbone

Amino acids and peptides constitute the structure of a great amount of biologically relevant compounds, thus being versatile building blocks for organic synthesis and drug discovery. In this aspect, the development of efficient methodologies for the selective modification of protein subunits would result in a wide variety of relevant peptides and proteins incorporating non-proteinogenic amino acid residues. In the present days, modified amino acids and peptides have exhibited multiple applications such as intermediates in total synthesis, efficient ligands in enantioselective reactions, or drugs with improved pharmacological properties comparing with their parent natural derivatives.[22]

Strecker reaction,[23] Rh-catalyzed hydrogenation,[24] Petatesis reaction,[25] carbanion chemistry[26] or solid phase techniques[27] are among the diverse existing methodologies for the assembly of amino acids. Nonetheless, these strategies often demand a high excess of reagents like strong bases and due to the lack of enantioselectivity, asymmetric versions have to be often applied for the chiral center generation. In contrast to conventional methodologies, transition metal-catalyzed C–H functionalization approaches have turned out to be versatile alternative tools for the construction of unnatural amino acid and peptide derivatives. This atom-economical process allows for the use of cheap chiral starting materials with no protection/deprotection steps, which is excellent for the late-stage modification of more attractive and complex molecules like proteins.

Depending on the C–H bond within the α-amino acid or peptide sequence, either peptide backbone's α-C–H functionalization or side-chain modification could be distinguished (Figure 4).[28]

[22] a) Saladino, R.; Bottaa, G.; Crucianelli, M. *Mini-Rev. Med. Chem.* **2012**, *12*, 277. b) Perdih, A.; Dolenc, M. S. *Curr. Org. Chem.* **2007**, *11*, 801. c) Nájera, C.; Sansano, J. M. *Chem. Rev.* **2007**, *107*, 4584.
[23] Wang, J.; Liu, X.; Feng, X. *Chem. Rev.* **2011**, *111*, 6947.
[24] Tang, W.; Zhang, X. *Chem. Rev.* **2003**, *103*, 3029.
[25] Candeias, N. R.; Montalbano, F.; Cal, P. M. S. D.; Gois, P. M. P. *Chem. Rev.* **2010**, *110*, 6169.
[26] Shirakawa, S.; Maruoka, K. *Angew. Chem. Int. Ed*. **2013**, *52*, 4312.
[27] Bondalapati, S.; Jbara, M.; Brik, A. *Nat. Chem*. **2016**, *8*, 407.
[28] a) Brandhofer, T.; Mancheño, O. G. *Eur. J. Org. Chem*. **2018**, 6050. b) San Segundo, M.; Correa, A. *Synthesis* **2018**, *50*, 2853.

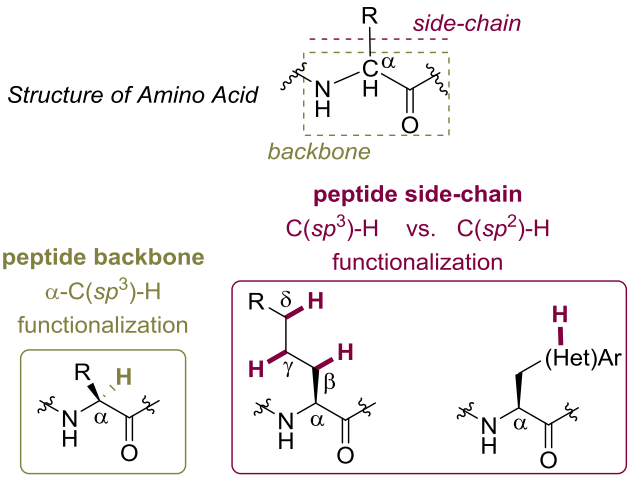

Figure 4 Different C–H bond Positions in Amino Acids.

C–H functionalization reactions can be classified into different categories: the so-called inner-sphere and outer-sphere mecanisms (Figure 5). An inner-sphere mechanism is considered when a bond between the carbon and the metal center is formed as a consequence of the C–H activation step. On the other hand, the outer-sphere mechanism consists on the oxidation of a C–H bond assisted by an oxidant, which provides a cationic or radical intermediate. The latter could be trapped by a suitable nucleophile and no carbon-metal bond containing-intermediate would be involved.[28] Accordingly, if a metal-catalyst is employed when an outer-sphere pathway is operative, it played a redox-role within the process.

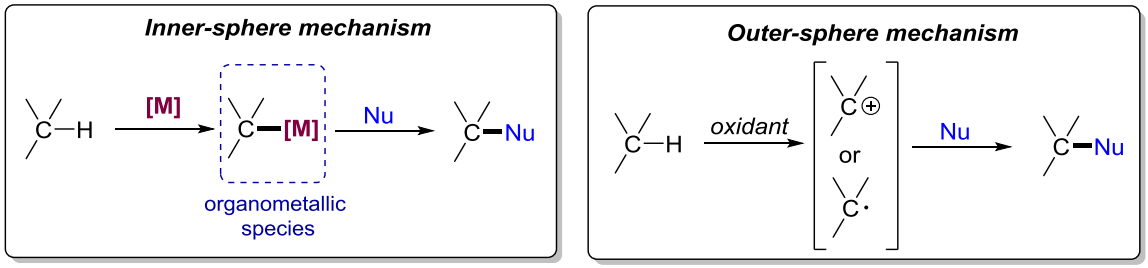

Figure 5 Inner- and Outer-Sphere Mechanisms for C–H Functionalization.

The latter strategy is a commonly accepted mechanism for the α-C(sp^3)–H functionalization of the amino acid backbone. As a result of being adjacent to the nitrogen atom of the amino group, this specific C–H bond is prone to undergo an easy oxidation step. A hydrogen abstraction (HAT) of the α-amino acid leads to the **Int-A**, which can either undergo a second HAT to provide an imine (**Int-B**) or a single electron transfer (SET) to provide an

iminium intermediate (**Int-D**). Both electrophilic species could eventually undergo further coupling with the corresponding nucleophile (Scheme 16).

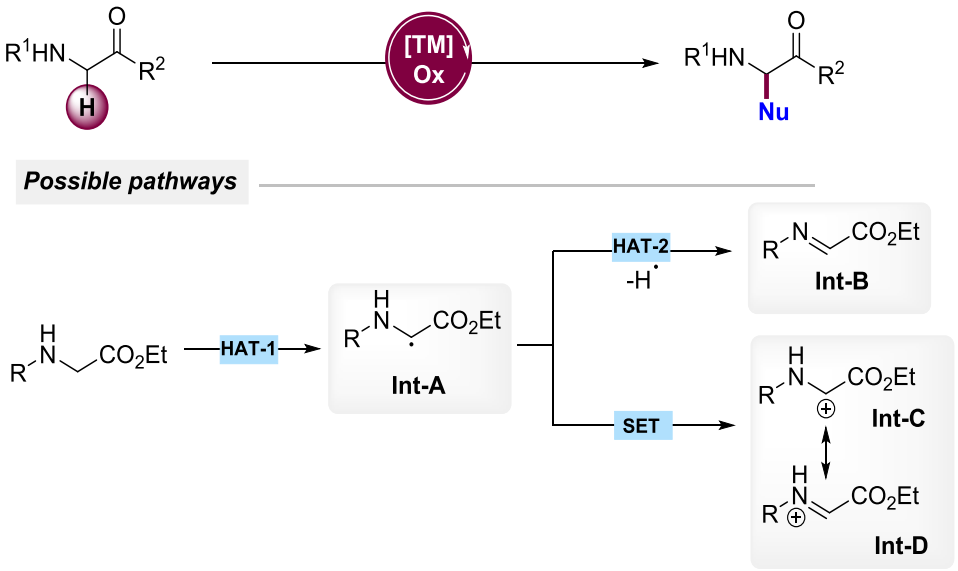

Scheme 16 α-C(sp^3)–H Functionalization of α-Amino Carbonyl Compounds.

In the next section, the state-of-the-art in the realm of glycine-containing compounds upon CDC processes will be briefly described, thereby including key breakthroughs in the field to illustrate the high utility of this oxidative technique for the manipulation of peptides.

2.1.1.1. Glycine C–H Functionalization

Glycine is a major protein component and one of the most important natural amino acids in living organisms. It has a wide range of biological and physiological properties.[29] As a consequence of being the simplest and the most inexpensive natural amino acid, a tremendous interest for its modification upon α-C(sp^3)-H functionalization techniques has been created among chemists. In this regard, the strategy is an ideal route for the coupling of glycine derivatives with different nucleophiles. Recently, CDC reactions of α-amino acid derivatives with the C–H bonds of various nucleophiles have demonstrated considerable importance for the synthesis of versatile α-substituted α-amino acid derivatives.[28]

In 2008, the group of Li developed a methodology for the efficient installation of malonates into the C–H bond adjacent to the amino group in *N*-acetylglycine derivatives (Scheme 17).[30] However, stoichiometric amounts of a copper source and high temperatures were required, which made this protocol ineffective from a sustainable and practical point of view. The use of harsh reaction conditions to afford the desired product was attributed to the difficult formation of *N*-Ac-Gly electrophilic intermediates, which are unstable in comparison with their parent ones derived from *N*-aryl compounds used shortly thereafter.

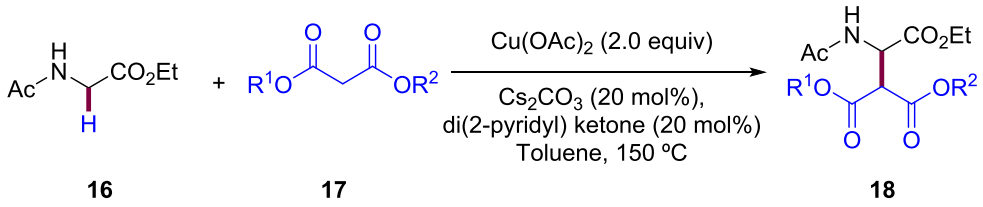

16 **17** **18**

Scheme 17 Copper-Mediated α-C(sp^3)–H Functionalization with Malonates.

In this pioneering work, they also reported the first CDC reaction on a secondary amine substrate with the coupling between the more active *p*-methoxyphenyl glycine amides and alkynes with a combination of a catalytic copper bromide and *tert*-butyl hydroperoxide as the oxidant.[30] With similar conditions, the same group made possible the arylation of glycine derivatives and short peptides utilizing boronic acids and other nucleophiles as coupling partners (Scheme 18).[31] However, in all cases the aromatic ring of the terminal glycine was required for the process to occur.

[29] Gundersen, R. Y.; Vaagenes, P.; Breivik, T.; Fonnum, F.; Opstad, P. K. *Acta Anaesthesiol. Scand.* **2005**, *49*, 1108.
[30] Zhao, L.; Li, C.-J. *Angew. Chem. Int. Ed*. **2008**, *47*, 7075.
[31] Zhao, L.; Baslé, O.; Li, C.-J. *Proc. Nat. Ac. Sci. U.S.A.* **2009**, *106*, 4106.

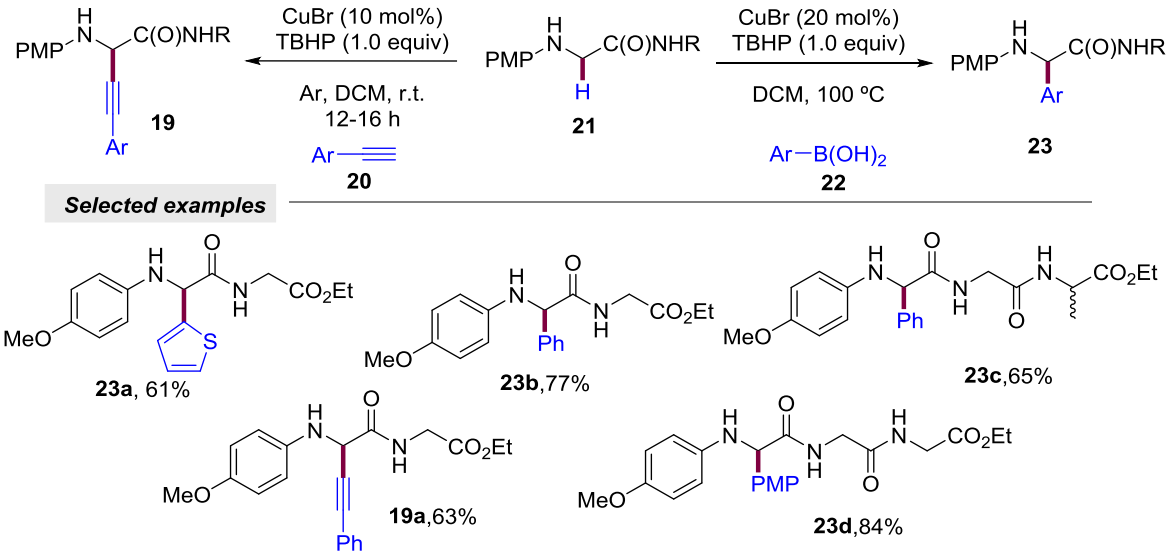

Scheme 18 Copper-Catalyzed C(sp^3)–H Alkynylation and Arylation of p-Methoxyphenyl Glycine derivatives.

It was not until 2015 when Yang and co-workers went further with the use of boronic acids to developed an asymmetric palladium-catalyzed α-C(sp^3)-H arylation process for aryl glycine ester derivatives (Scheme 19).[32] The enantioselectivity was attributed to the chiral dihydroxazole type ligand, which by coordination with the metal center formed the active chiral palladium catalyst **I**. Then, a transmetallation with the aryl boronic acid provided intermediate **II**, which coordinated with the *in situ* formed imine. In this way the addition of the aryl group was favored (**III**) as the substituent of the ligand blocked the other side.

[32] Wei, X.-H. ; Wang, G.-W.; Yang, S.-D. *Chem. Commun.* **2015**, *51*, 832.

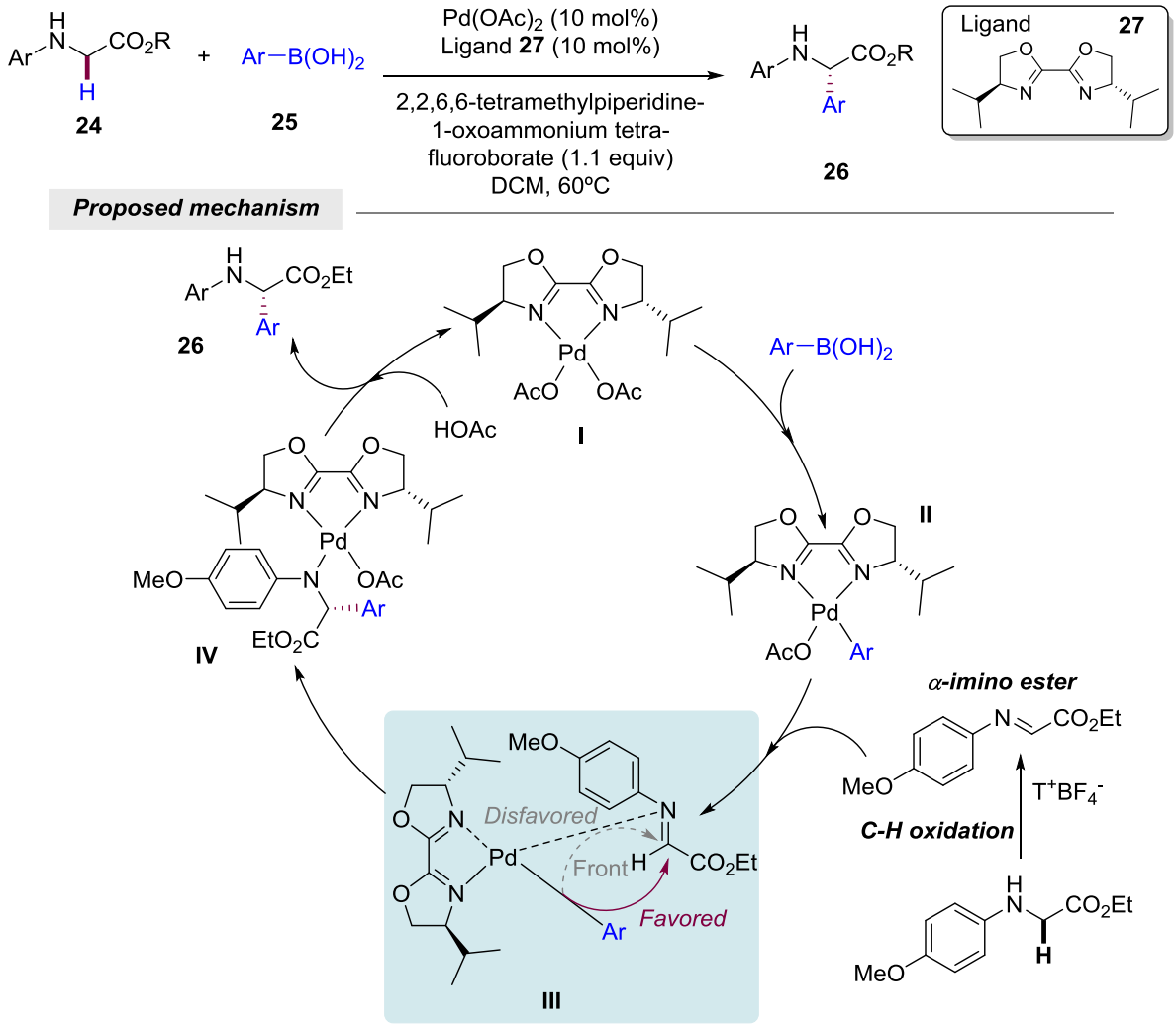

Scheme 19 Palladium-Catalyzed Enantioselective Direct C–H Arylation Reaction.

Nevertheless, in comparison with the former methodology, an expensive and more toxic palladium catalyst was needed and a single example of a dipeptide compound was submitted to the reaction conditions. Regarding more sustainable first-row transition metals, copper has been the most employed one as far as glycine C–H functionalization is concerned. Among different coupling partners, ketones,[33] α-substituted β-ketoesters,[34] ethers[35] and imidazoheterocycles[36] have been installed in the α-amino acid. Alkylation processes have been also carried out with iron catalysis[37] and a metal-free system[38] for both aryl glycine ester and amides. On the other hand, the low-cost and easily available nickel catalysis was applied by You's group for an oxidative C(sp^3)-H

[33] Xie, J.; Huang, Z.-Z. *Angew. Chem. Int. Ed.* **2010**, *49*, 10181.
[34] Zhang, G.; Zhang, Y.; Wang, R. *Angew. Chem. Int. Ed.* **2011**, *50*, 10429.
[35] Wei, W.-T.; Song, R.-J.; Li, J.-H. *Adv. Synth. Catal.* **2014**, *356*, 1703.
[36] Jiao, J.; Zhang, J.-R.; Liao, Y.-Y.; Xu, L.; Hu, M.; Tang, R.-Y. *RSC Adv.* **2017**, *7*, 30152.
[37] Liu, P.; Wang, Z.; Lin, J.; Hu, X. *Eur. J. Org. Chem.* **2012**, 1583.
[38] Peng, H.; Yu, J.-T.; Jiang, Y.; Yang, H.; Cheng, J. *J. Org. Chem.* **2014**, *79*, 9847.

backbone benzylation reaction of phenylalanine and glycine derivatives, which stands out among the scarce methodologies for the access to α-quaternary centers in amino acids. (Scheme 20).[39a]

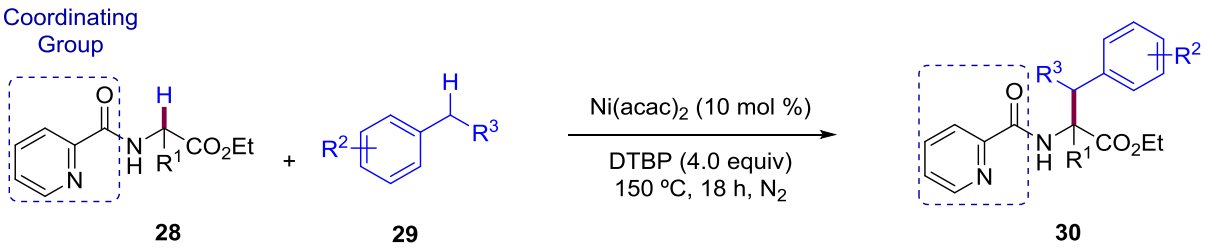

Scheme 20 Nickel-Catalyzed Directed C(sp^3)-H Benzylation Reaction of Phe and Gly Derivatives

Despite the use of environmentally appealing base metal-catalysis, the additional steps for installing and removing the directing group represented a clear drawback. Moreover, most of the methodologies described so far were limited to the single unit of *N*-aryl glycine derivatives and were not applied in longer peptide sequences.

2.1.1.2. Glycine C–H Heteroarylation with Indole Derivatives

Within different heteroaryl compounds existing in nature, indoles are of fundamental interest and present in pharmacologically active natural products with a wide variety of applications such as antitumor agents.[40] In light of its remarkable bioactivity, this heteroaromatic scaffold can be found in many agrochemicals and drugs against various diseases (Figure 6). Accordingly, the installation of such a privileged heterocycle into peptide derivatives has gained a lot of attention among synthetic chemists.

[39] a) Li, K.; Wu, Q.; Lan, J.; You, J. *Nat. Chem.* **2015**, *6*, 8404. b) Li, K.; Tang, G.; Huang, J.; Song, F.; You, J. *Angew. Chem. Int. Ed*. **2013**, *52*, 12942.
[40] a) Jagtap, R. A.; Punji, B. *Asian J. Org. Chem.* **2020**, *9*, 326. b) Zenkov, R. G.; Ektova, L. V.; Vlasova, O. A.; Belitskiy, G. A.; Yakubovskaya, M. G.; Kirsanov, K. I. *Chem. Heterocycl. Compd.* **2020**, *56*, 644.

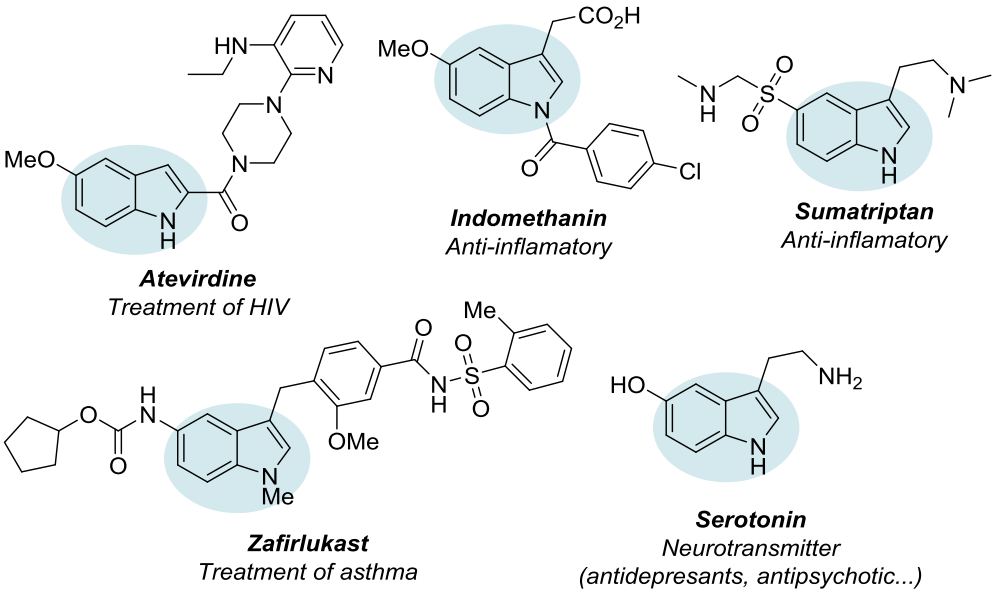

Figure 6 Indole Scaffold Containing Drugs and Natural Products.

In this respect, metal catalysis has been an essential tool for the selective introduction of the indole motif into glycine derivatives. Li and co-workers, with the previously mentioned copper-catalyzed arylation, prepared the first and unique metal-catalyzed indolylglycine tripeptide **32** with 89% yield (Scheme 21).[31]

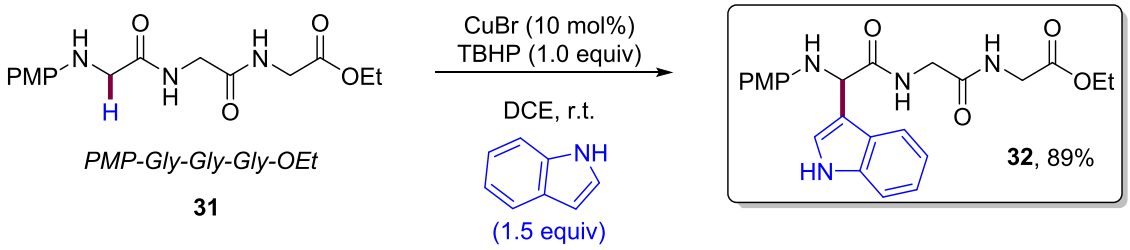

Scheme 21 First Example of Copper-Catalyzed Heteroarylation of Short Peptides.

In 2012, switching from inert atmosphere to air 2-(1*H*-indol-3yl)-2-imino carbonyl **33** and 2-(1*H*-indol-3yl)-2-oxo carbonyl **36** were obtained (Scheme 22).[41] It was proposed that the oxidative deprotonation of *N*-Ph-Gly-OEt by TBHP provided the imine intermediate[42] and the further Friedel-Crafts alkylation led to the imine product **33**. On the other hand, the hydrolysis of **33** by H_2O with the aid of $CuCl_2$, TBHP, and O_2 resulted in product **36**.

[41] Wu, J.-C.; Song, R.-J.; Wang, Z.-Q.; Huang, X.-C.; Xie, Y.-X.; Li, J.-H. *Angew. Chem. Int. Ed*. **2012**, *51*, 3453.
[42] a) Patila, R. D.; Adimurthy, S. *Adv. Synth. Catal*. **2011**, *353*, 1695. b) Gommermann, N.; Koradin, C.; Polborn, K.; Knochel, P. *Angew. Chem. Int. Ed.* **2003**, *42*, 5763. c) Koradin, C.; Gommermann, N.; Polborn, K.; Knochel, P. *Chem. Eur. J.* **2003**, *9*, 2797. d) Wei, C.; Li, C. J. *J. Am. Chem. Soc.* **2002**, *124*, 5638.

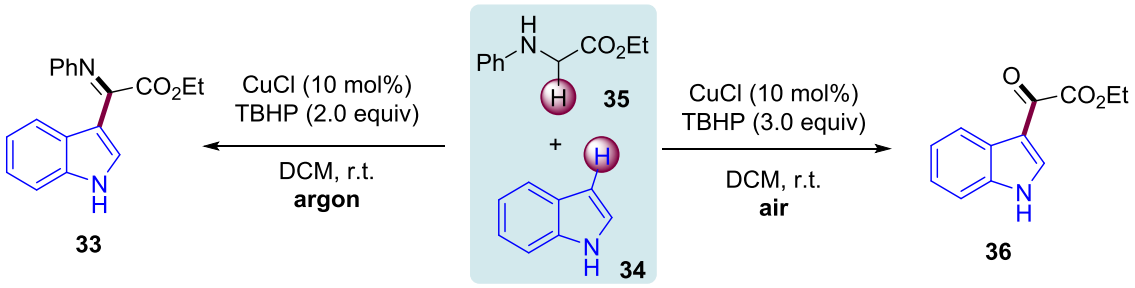

Scheme 22 Copper-Catalyzed C–H Oxidation/Cross-Coupling of N-Ph-Gly-OEt.

The same year, Rueping and his group developed a visible-light photoredox-catalyzed methodology for the introduction of indoles into *N*-arylglycine ester derivatives (Scheme 23).[43] Although they were able to extend the method to short dipeptides, the scope was limited to *N*-(*p*-tolyl)glycine derivatives and an expensive iridium catalyst was required.

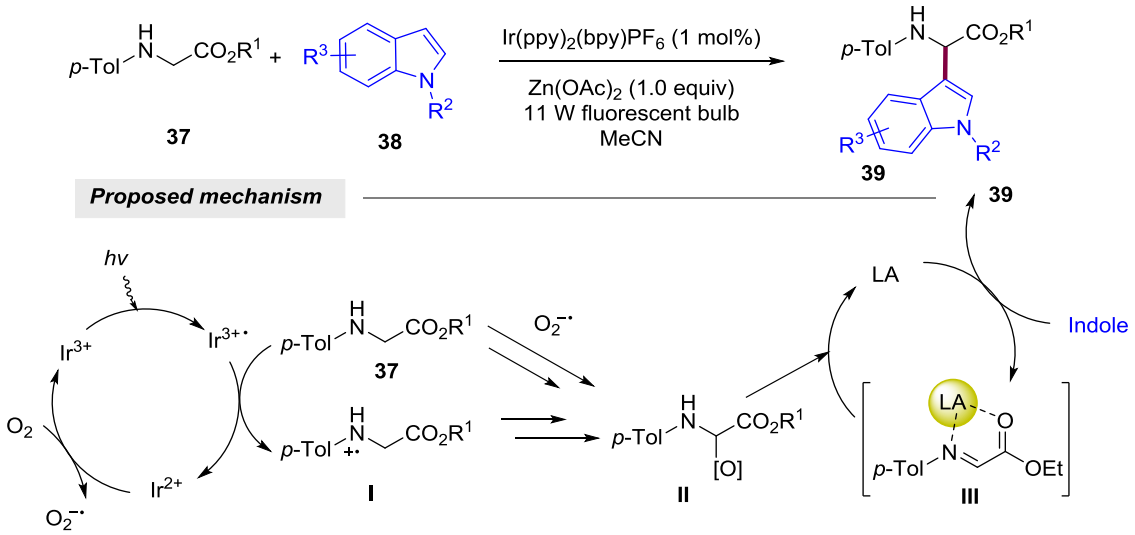

Scheme 23 Visible-Light Photoredox and Lewis Acid Catalysis for Gly-Containing Peptides Indolation.

The catalytic cycle begins with the irradiation of Ir^{3+} to be excited to $Ir^{3+\bullet}$ species, which upon SET would be reduced to Ir^{2+} and radical cation **I** would be formed. The latter is further oxidized to α-carbon hydroperoxide or hemi aminal **II**. On the other hand, the active catalyst is then regenerated with molecular oxygen leading to the formation of a superoxide anion. The latter species could also react with the starting material giving directly intermediate **II**. In the absence of the Lewis acid no reaction took place, thus demonstrating the crucial role of

[43] Zhu, S.; Rueping, M. *Chem. Commun.* **2012**, *48*, 11960.

$Zn(OAc)_2$ in the substrate activation (**III**). Ru-catalyzed photoredox chemistry also provided a single example of the introduction of the heteroaromatic scaffold into *N*-(*p*-methoxy)phenyl glycine ethyl ester in 50% yield.[44]

In 2013 and 2016, You and Feng, respectively, developed iron-catalyzed CDC methodologies using peroxides as oxidant. The former carried out a coordinating activation strategy to furnish α-quaternary α-amino acids through the iron(III)-catalyzed oxidative functionalization of α-C(sp^3)–H bonds of α-tertiary α-amino acid esters (Scheme 24).[39b] Despite the introduction of different nucleophiles besides indole derivatives, the method was restricted to simple amino acids and to high temperatures which apparently difficult the manipulation of peptides.

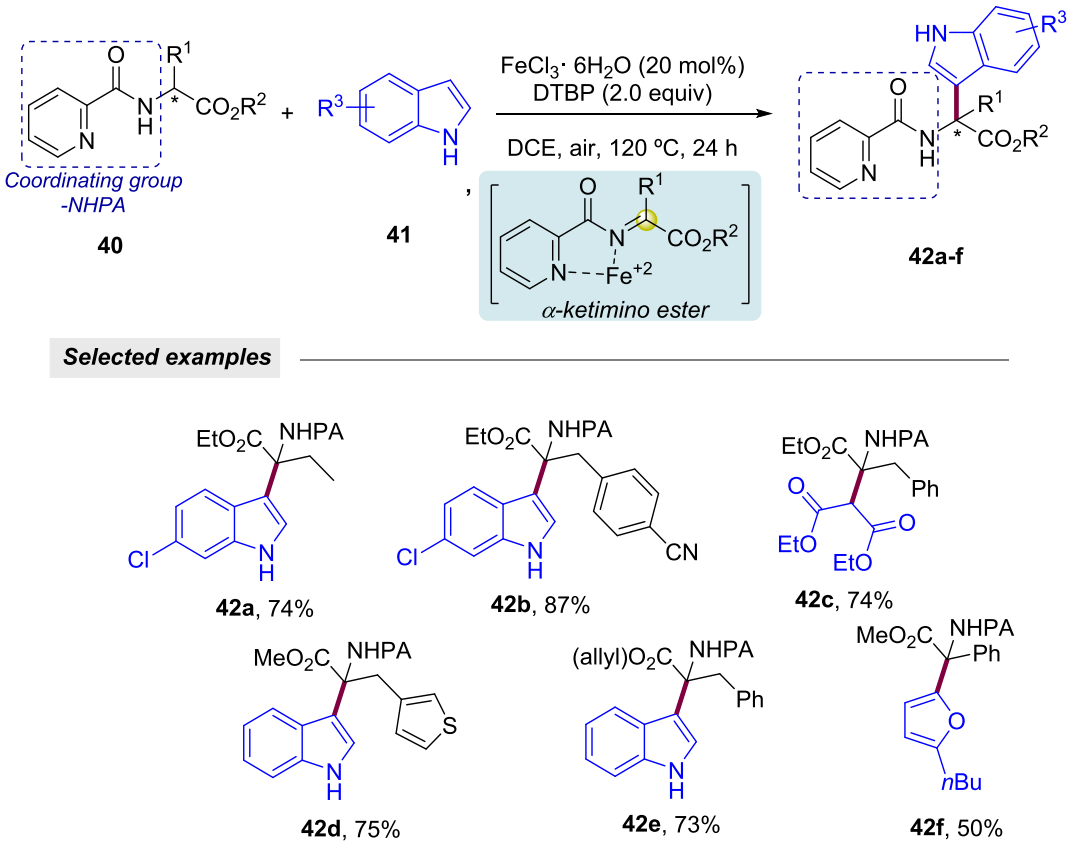

Scheme 24 Iron(III)-Catalyzed Functionalization of α-C(sp^3)–H Bonds of α-Tertiary α-Amino Esters.

[44] Wang, Z.-Q.; Hu, M.; Huang, X.-C.; Gong, L.-B.; Xie, Y.-X.; Li, J.-H. *J. Org. Chem*. **2012**, *77*, 8705.

On the other hand, with Feng's method,[45] the product could be obtained at room temperature but few examples of glycine esters could be observed as the approach was optimized for α-amino ketone compounds.

Despite the advances realized, new and sustainable methods are in high demand. Extension of the substrate scope to short-to-medium peptides, high operational simplicity and the use of alternative first-row transition metals like cobalt, which has been rarely used in these endeavors are important issues to address on the field.

2.1.2. Cobalt Catalysis

Cobalt belongs to the cost-efficient 3d transition metals and, despite the fact that its abundance in the Earth's crust is not as high as copper's or iron's ones, it is still 1000 times more common than palladium. Because of its lower toxicity and its essential role in biologically appealing compounds such as vitamin B12, cobalt represents a particularly attractive option for C–H functionalization.[46] Delving into the literature, the first Co-catalyzed C–H activation reaction was carried out in 1955 by Murahashi and co-workers, when they described the reaction of (*E*)-*N*,1-diphenylmethanimine under 100–200 bar of CO with the use of $[Co_2(CO)_8]$ as catalyst to obtain 2-phenylphthalimidine.[47] Since that moment on, a great number of reports have been published regarding the application of cobalt catalysis in C–H activation and the field has been summed up in several recent reviews.[48] With the beginning of this decade, the interest for new cobalt-catalyzed methodologies has become more frequent.

Low- and high-valent cobalt catalysis has enabled C–C and C–X bond forming processes upon C–H functionalization events. The group of Nakamura, Yoshikai and Ackermann among others were pioneers in C–H modification upon low-valent cobalt catalysis.[49] The unique reactivity of these type of methodologies was demonstrated with transformations like hydroarylation of alkynes and olefins, and *ortho*-alkylation of (hetero)aromatics. Two representative examples are described in Scheme 25: directed cobalt(II)-catalyzed alkynylation[50] and alkylation[51] reaction of indole derivatives.

Together with cobalt(II) catalyst, electron-rich ligands and the addition of stoichiometric reductive reagents, like Grignard species, are known to be the key general features for a high activity and regeneration of the low-valent active catalyst. However, the use of Grignard reagents represents a disadvantage from a chemoselectivity and sustainability point of view.

---

[45] Zhang, Y.; Ni, M.; Feng, B. *Org. Biomol. Chem*. **2016**, *14*, 1554.
[46] Leyssens, L.; Vinck, B.; Van Der Straeten, C.; Wuyts, F.; Maes, L. *Toxicology* **2017**, *387*, 43.
[47] Murahashi, S. *J. Am. Chem. Soc.* **1955**, *77*, 6403.
[48] a) Yoshino, T.; Matsunaga, S. *Asian J. Org. Chem.* **2018**, *7*, 1193. b) Pototschnig, G.; Maulide, N.; Schnürch, M. *Chem. Eur. J.* **2017**, *23*, 9206. c) Hammann, J. M.; Hofmayer, M. S.; Lutter, F. H.; Thomas, L.; Knochel, P. *Synthesis* **2017**, *49*, 3887. d) Moselage, M.; Li, J.; Ackermann, L. *ACS Catal*. **2016**, *6*, 498.
[49] Gao, K.; Yoshikai, N. *Acc. Chem. Res*. **2014**, *47*, 1208.
[50] Ding, Z.; Yoshikai, N. *Angew. Chem. Int. Ed*. **2012**, *51*, 4698.
[51] Punji, B.; Song, W.; Shevchenko, G. A.; Ackermann, L. *Chem. Eur. J.* **2013**, *19*, 10605.

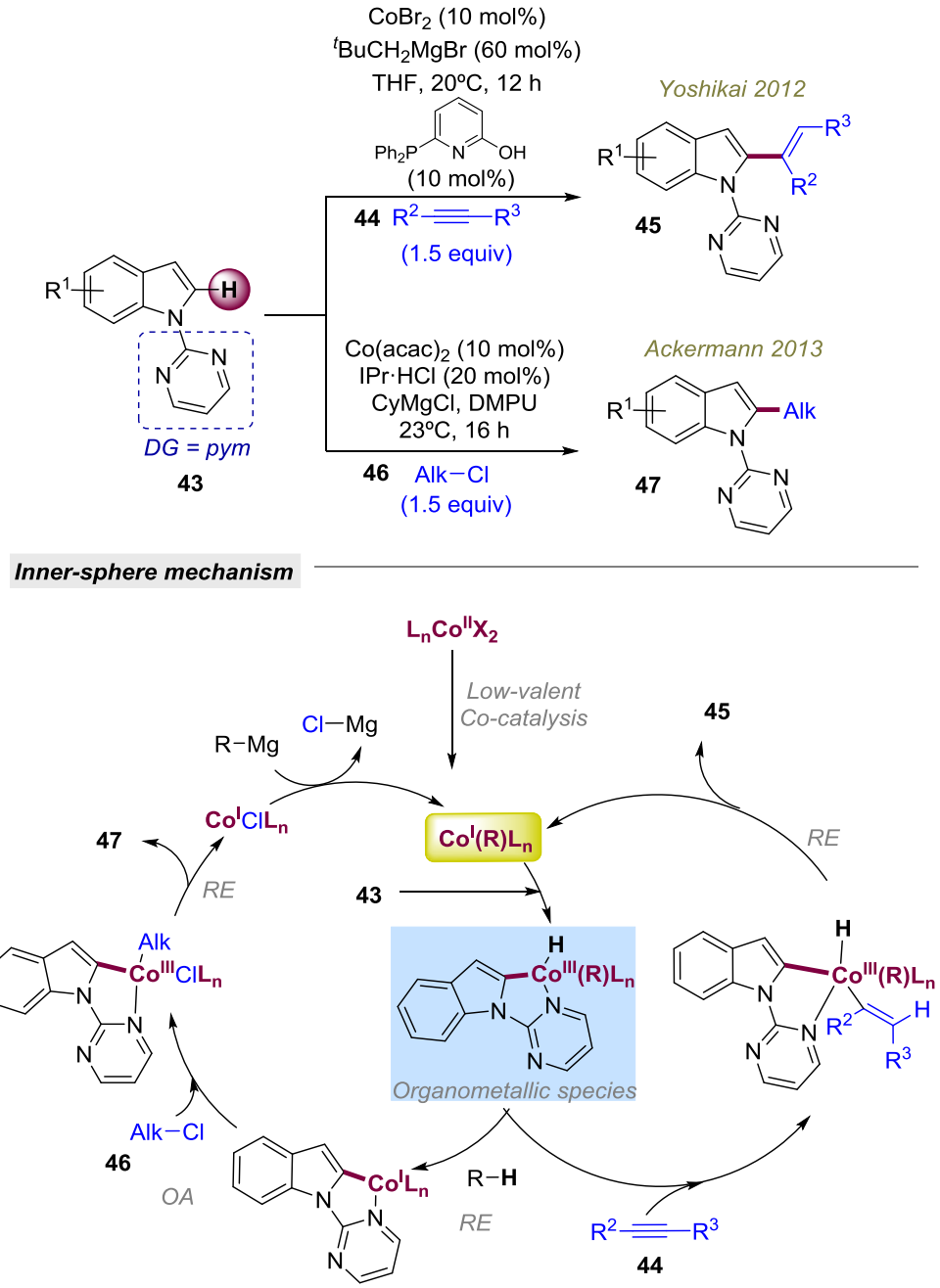

Scheme 25 Pyrimidine-Directed Cobalt-Catalyzed Alkynylation and Alkylation Reaction of Indole Derivatives.

In contrast to the low-valent cobalt catalysis, high-valent Co(III)-catalyzed protocols for C–H diversifications have increased in recent years. In 2013, Matsunaga and Kanai disclosed a significant advance in high-valent cobalt-catalyzed C–H activation.[52] The addition of 2-arylpyridines to *N*-sulfonylimines and enones was found possible with the efficient cationic Co^{III} catalyst [{Cp*Co(C_6H_6)}(PF_6)$_2$]. The employment of Cp*Co(III)

[52] a) Yoshino, T.; Ikemoto, H.; Matsunaga, S.; Kanai, M. *Angew. Chem. Int. Ed.* **2013**, *52*, 2207. b) Yoshino, T.; Ikemoto, H.; Matsunaga, S.; Kanai, M. *Chem. Eur. J.* **2013**, *19*, 9142.

complexes as catalyst promoted a reactivity pattern similar to that of Cp*Rh^{III} catalysts, being even more reactive in some cases and tolerating a wide variety of functional groups.[53,54]

One year later, Daugulis and co-workers developed a novel $Co(OAc)_2 \cdot 4H_2O$ catalyzed 8-aminoquinoline (AQ) C(sp^2)–H alkenylation/annulation with Mn or Ag salts as co-catalyst (Scheme 26).[55] They proposed a reaction pathway in which Co^{II} is oxidized to Co^{III} with the aid of an oxidant such such as a Mn or Ag-based source. Then, the catalytic cycle is initiated by a non-oxidative C–H activation concerted metalation–deprotonation (CMD) mechanism or an intermolecular SET pathway. Remarkably, this type of reaction mechanisms did not require any reductants such as Grignard reagents or Zn powder.

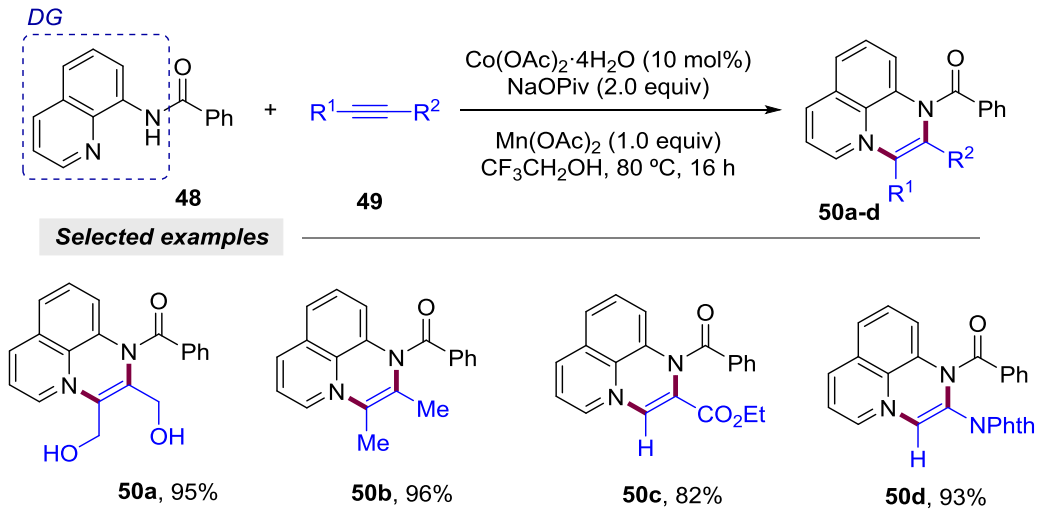

Scheme 26 Cobalt(II)-Catalyzed Aminoquinoline-Directed C(sp^2)–H Bond Alkenylation with Alkynes.

Due to its unique catalytic behavior, cobalt catalysis has sparked interest between different research groups for the design of novel cross-dehydrogenative coupling reactions.[56] In 2010, Chang and co-workers described the amination of azole derivatives using cobalt(II) acetate as catalyst and mild reaction conditions (Scheme 27).[57] Concerning the scope, only secondary amines were applicable, while primary amines could be assembled with manganese catalysis.

[53] Wang, S.; Chen, S.-Y.; Yu, X.-Q. *Chem. Commun.* **2017**, *53*, 3165.
[54] Wei, D.; Zhu, X.; Niu, J.-L.; Song, M.-P. *ChemCatChem* **2016**, *8*, 1242.
[55] Grigorjeva, L.; Daugulis, O. *Angew. Chem. Int. Ed.* **2014**, *53*, 10209.
[56] Phillips, A. M. F.; Pombeiro, A. J. L. *ChemCatChem* **2018**, *10*, 3354.
[57] Kim, J. Y.; Cho, S. H.; Joseph, J.; Chang, S. *Angew. Chem. Int. Ed.* **2010**, *49*, 9899.

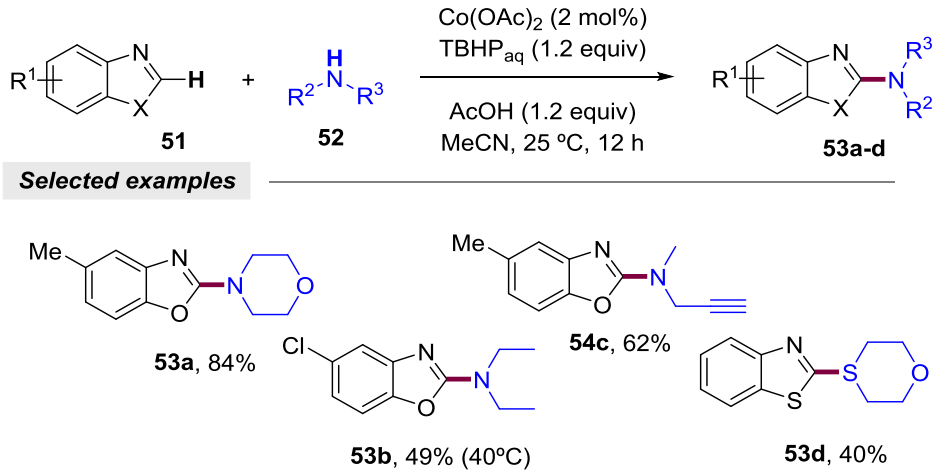

Scheme 27 Cobalt(II)-Catalyzed Amination of Azoles.

Interestingly, Ge and co-workers came up with the conditions for the first unactivated C(sp^3)–H bond amination of aliphatic amides by a cobalt-catalyzed intermolecular dehydrogenative coupling[58] to obtain monocyclic and spiro β- or γ-lactams (Scheme 28).

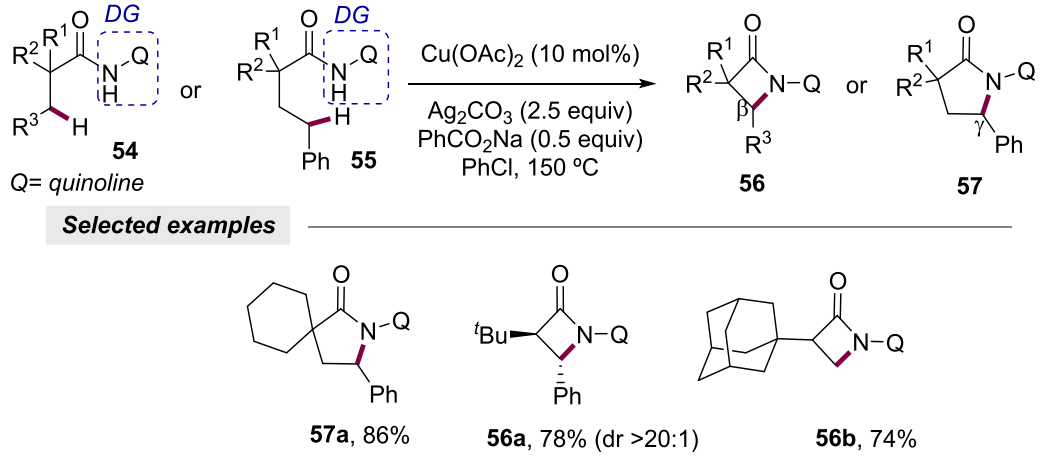

Scheme 28 β- and γ-Lactams Synthesis Through a Quinolone-Directed Cobalt-Catalyzed C(sp^3)–H Bond Amination of Aliphatic Amides.

You and co-workers managed to couple (benzo)oxazole derivatives with other (hetero)aromatics using the same cobalt source as the catalyst, silver carbonate in stoichiometric amount as the oxidant and pivalic acid as additive in toluene at 120 ^{0}C.[59] In this case, the quinoline scaffold was also installed as a DG enabling the process to

[58] Wu, X.; Yang, K.; Zhao, Y.; Sun, H.; Li, G.; Ge, H. *Nat. Commun*. **2015**, *6*, 6462.
[59] Tan, G.; He, S.; Huang, X.; Liao, X.; Cheng, Y.; You, J. *Angew. Chem. Int. Ed.* **2016**, *55*, 10414.

occur upon a selective inner-sphere mechanism. Not only quinoline but other directing groups have been also utilized for thiolation[60] or allylic selective alkenylation[61] of indoles together with cobalt catalysts.

High-valent cobalt catalysis has exhibited high reactivity in combination with peroxides, enabling the coupling of (thio)ethers with different (hetero)aromatic compounds[62] such as (benzo)oxazoles,[62a] thiazoles,[62b] or coumarins.[62c] *Tert*-butyl hydroperoxide is often utilized as the oxidant, whose decomposition is known to be induced by a Co^{II}/Co^{III} system.[63] This decomposition process leads to a sequence of radical reactions, which enable the hydrogen abstraction of the corresponding alkane/ether. The latter is converted *in situ* into a nucleophilic radical species able to couple with the other partner upon an outer-sphere type mechanism where no metal-carbon bond containing intermediate is involved (Scheme 29).

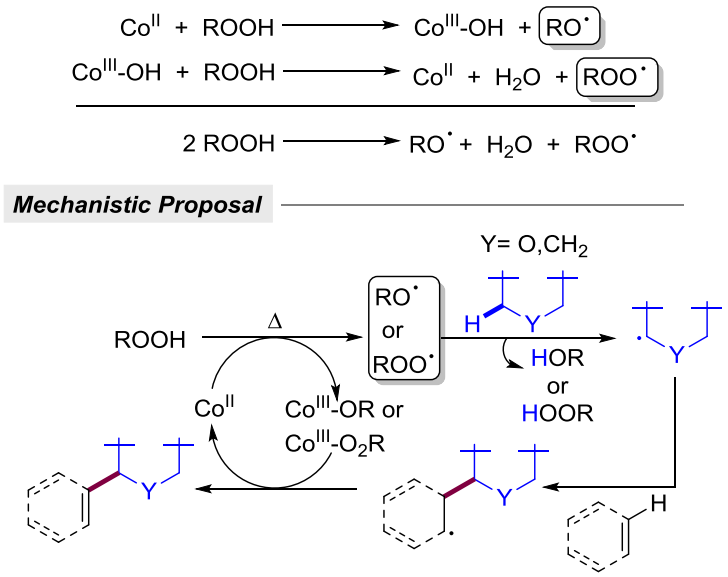

Scheme 29 Mechanistic Proposal for a Co(II)/THBP System-mediated CDC Reaction.

In 2015, the cobalt-catalyzed CDC reaction between tetrahydroisoquinolines and indole derivatives was established by Wu and co-workers.[64] Combining $CoCl_2$ and dmgH (dimethylglyoxime) as ligand, a photosensitizer **I** is formed *in situ*. Upon its irradiation, species **I** is excited to species **II** which induces a catalytic cycle that enables the abstraction of the hydrogen atom of the C–H bond adjacent to the nitrogen in tetrahydroisoquinolines **58** by a SET pathway described earlier in Scheme 16. The active photosensitizer is

[60] Gensch, T.; Klauck, F. J. R.; Glorius, F. *Angew. Chem. Int. Ed*. **2016**, *55*, 11287.
[61] Maity, S.; Dolui, P.; Kancherla, R.; Maiti, D. *Chem. Sci.* **2017**, *8*, 5181.
[62] a) Li, Y.; Wang, M.; Fan, W.; Qian, F.; Li, G.; Lu, H. *J. Org. Chem.* **2016**, *81*, 11743. b) Wang, X.; Lei, B.; Ma, L.; Zhu, L.; Zhang, X.; Zuo, H.; Zhuang, D.; Li, Z. *Chem. Asian J.* **2017**, *12*, 2799. c) Dian, L.; Zhao, H.; Zhan-Negrerie, D.; Du, Y. *Adv. Synth. Catal.* **2016**, *358*, 2422. d) Li, Q.; Hu, W.; Hu, R.; Lu, H.; Li, G. *Org. Lett.* **2017**, *19*, 4676.
[63] Turrà, N.; Neuenschwander, U.; Baiker, A.; Peeters, J.; Hermans, I. *Chem. Eur. J.* **2010**, *16*, 13226.
[64] Wu, C.-J.; Zhong, J.-J.; Meng, Q.-Y.; Lei, T.; Gao, X.-W.; Tung, C.-H.; Wu, L.-Z. *Org. Lett.* **2015**, *17*, 884.

regenerated by reaction with molecular oxygen. The resulting superoxide anion reduces intermediate **IV** to **V** radical species, which is further oxidized to the iminium intermediate by the previously mentioned HAT process. The iminium cation intermediate then is attacked by the most nucleophilic C3 position of the indole to yield the desired product **60**.

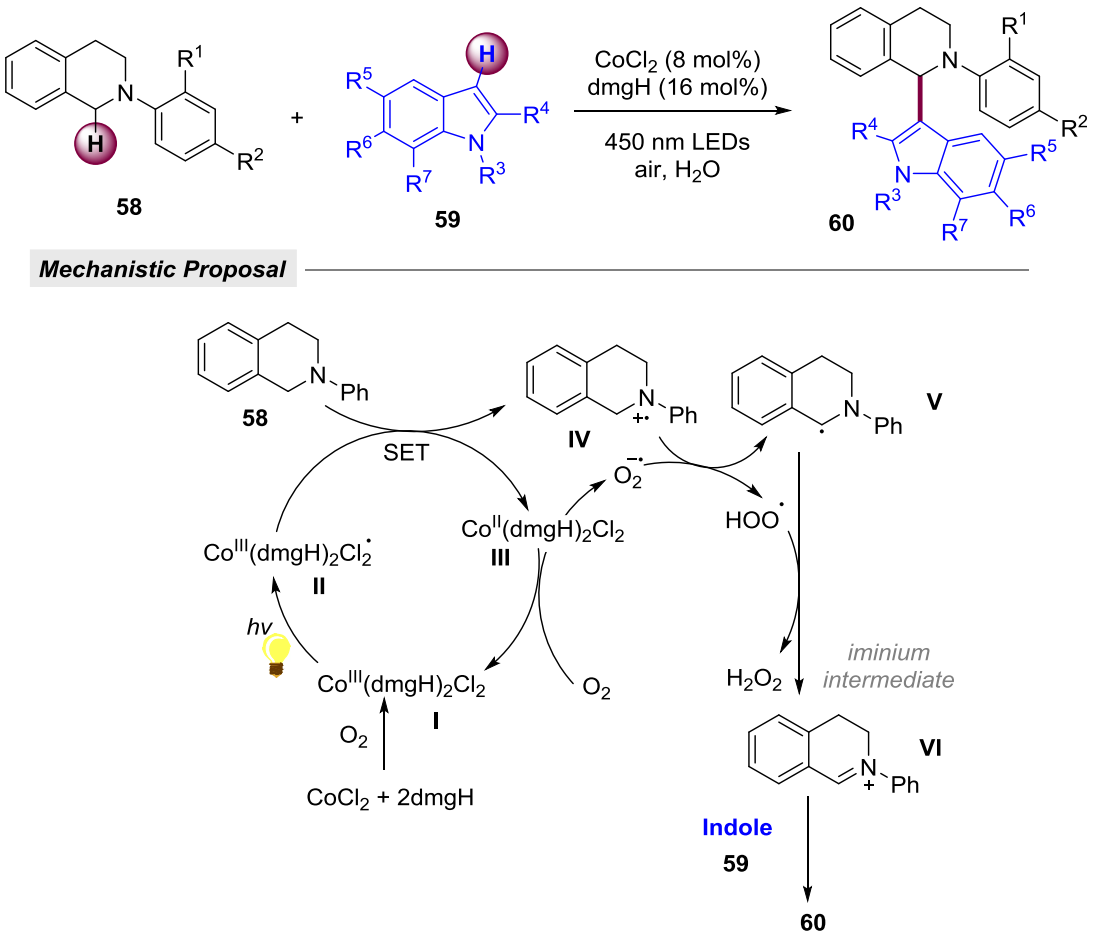

Scheme 30 Cobalt-Catalyzed CDC between Tetrahydroisoquinolines and Indoles.

These selected examples illustrated the ample opportunities of cobalt catalysis in the field of C–H functionalization, and hence inspired us to implement this cost-efficient base metal catalyst in the field of peptide chemistry.

2.2. Objective

Owing to their many opportunities in proteomics, several protocols have been developed for the α-C–H functionalization of α-amino carbonyl compounds. Based on oxidative cross-coupling reaction conditions, the methodologies described above found the solution for previous disadvantages such as the requirement of a strong base for the classical enolate chemistry, which sometimes induced racemization when using peptide settings, or the lack of site-selectivity. Despite the remarkable importance of these processes, their scope was often limited to the specific use of *p*-methoxyphenyl glycine amides while α-amino esters were often found unreactive and rare examples of peptides could be observed.

On the other hand, in the last decades metal-catalysis has gained a lot of interest in organic synthesis as it provides an ideal tool for the selective C–H functionalization of a wide variety of unactivated compounds. Furthermore, 3*d* transition metals such as cobalt have demonstrated to exhibit similar activity to that of precious noble metals like Pd, Rh and Ru. Hence, we envisioned that cobalt catalysis could provide an ideal alternative for a more economical and sustainable late-stage C–H peptide diversification.

In this chapter we will describe our results dealing with the development of novel cobalt-catalyzed α-C(sp^3)–H heteroarylation and aminocarbonylation protocols of glycine containing amino acid and peptide derivatives with indoles and formamides, respectively (Scheme 31).

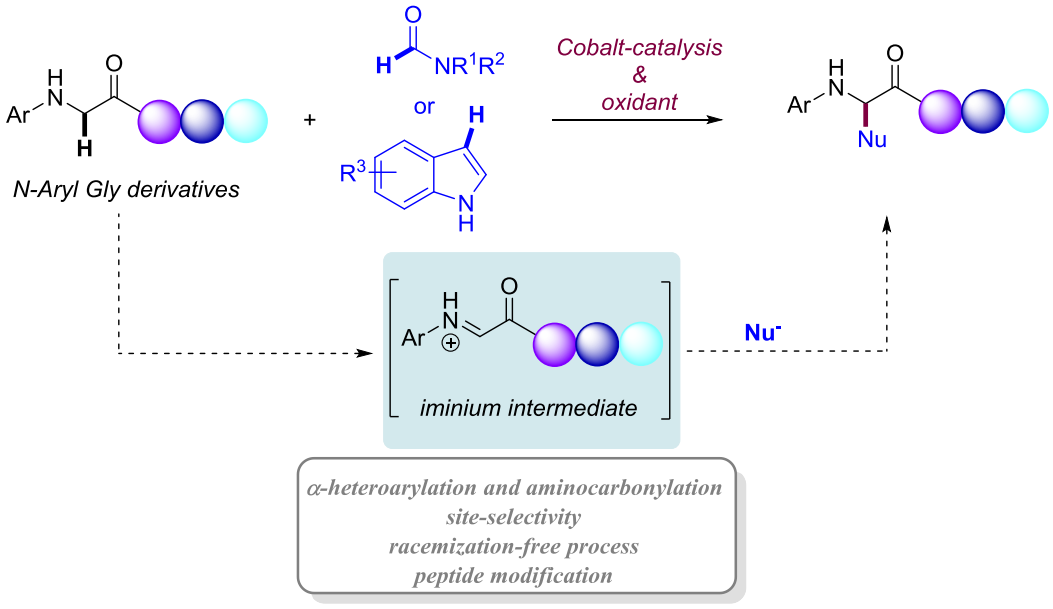

Scheme 31 Cobalt-Catalyzed α-C(sp^3)–H Heteroarylation and Aminocarbonyaltion of N-Aryl Glycine Derivatives.

2.3. Co-Catalyzed C(sp^3)–H Heteroarylation of Glycine and Peptide Derivatives

Metal-catalyzed C–H functionalization is a hot topic in modern organic synthesis. Among these chemical processes, the modification of α-C(sp^3)–H bonds of amino acid derivatives has been extensively studied owing to the wide presence of the resulting modified amino carbonyl units in many structures of natural products and biomolecules. In particular, the α-arylation of glycine derivatives with indoles has been recently explored upon transition-metal catalysis (Ru, Fe and Cu).[28] In this section, an alternative yet novel, mild route to the C–H oxidative cross-coupling of α-amino ester compounds with indoles catalyzed by cost efficient cobalt-salts will be disclosed.

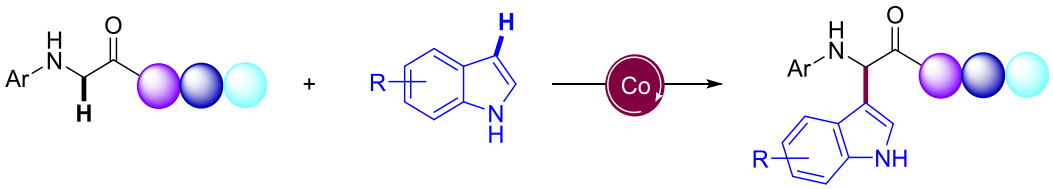

Scheme 32 Cobalt-Catalyzed C(sp^3)–H Indolation of Glycine-Containing Peptides.

2.3.1. Optimization of the Reaction Conditions

We began our study by selecting the model cross-coupling reaction between *N*-phenyl glycine ethyl ester **61a** and indole **62a**, where both substrates lacked substituents that could influence on the reactivity. Given the positive results of $Co(acac)_2 \cdot H_2O$ obtained for the alkylation reaction of glycine derivatives in our group,[65] we started our investigation by evaluating the influence of oxidants. Hence, the starting materials were submited to cobalt catalysis in anhydrous acetonitrile at room temperature for 24 hours.

Along these early experiments, only peroxides were tested as they are known to enable the SET step followed by the hydrogen abstraction in α-amino carbonyl compounds (Scheme 29).[63] As disclosed on Table 1, a variety of peroxides turned out to be almost unreactive giving traces or none desired product (Table 1, entry 3,4,5), whereas the use of *tert*-butyl hydroperoxide, in both aqueous (Table 1, entry 2) and decane media (Table 1, entry 1), enabled the coupling between the amino acid and indole in promising yields, 31 % and 32 %, respectively. Surprisingly, the reaction could be carried out with the most convenient molecular oxygen although in a comparatively lower 18 % yield (Table 1, entry 6). Given its lower price and higher sustainability, we continued our screening studies using an aqueous solution of TBHP.

[65] PhD Thesis by Marcos San Segundo, UPV-EHU 2020.

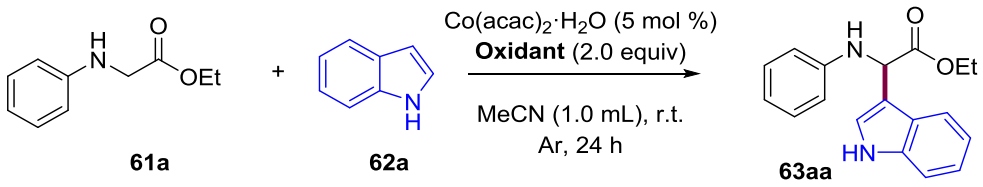

Entry	Oxidant	Yield (%)[a]
1	TBHPdec	32
2	TBHPaq	31
3	DTBP	n.r.
4	CHP	traces
5	DCP	n.r.
6	O_2 (1 atm)	18

Reaction conditions: **61a** (0.5 mmol), **62a** (0.5 mmol), $Co(acac)_2 \cdot H_2O$ (5 mol %), MeCN (1.0 mL), r.t., 24 h, under Ar. TBHPaq = *tert*-butyl hydroperoxide (70 wt. % in H_2O), TBHPdec = *tert*-butyl hydroperoxide (5.0-6.0 M in decane), DTBP = di-*tert*-butyl peroxide, DCP = dicumyl peroxide, CHP = cumene hydroperoxide.
[a] Isolated yield after purification by column chromatography.

Table 1 Screening of Oxidants.

Interestingly, upon exposure of **61a** to 10 mol % of different cobalt catalysts with an aqueous solution of *tert*-butyl hydroperoxide in acetonitrile as solvent at room temperature, we observed a slightly higher yield of the product with the initial $Co(acac)_2 \cdot H_2O$ (Table 2, entry 2). In stark contrast, the rest of the Co(II) and Co(III) sources either shown to be unreactive toward the cross-coupling reaction or provided very little conversion of the starting material into product **63aa**, thus the yields were not determined (Table 2).

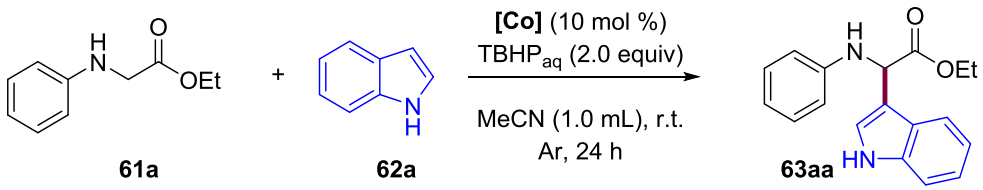

Entry	[Co]	Yield (%)[a]
1	$Co(OAc)_2 \cdot 4H_2O$	traces
2	$Co(acac)_2 \cdot H_2O$	39
3	$Co(acac)_3$	traces
4	$CoCl_2$	traces
5	CoF_2	n.d.
6	CoF_3	n.d.
7	$Co(NO_3)_2 \cdot 6H_2O$	traces

Reaction conditions: **61a** (0.5 mmol), **62a** (0.5 mmol), [Co] (10 mol %), TBHPaq (2.0 equiv), MeCN (1.0 mL), r.t., 24 h, under Ar. [a] Isolated yield after purification by column chromatography.

Table 2 Screening of Cobalt Catalysts.

At this point, in order to appropriately judge the role of the metal and the oxidant, blank experiments were carried out (Table 3). As expected, when Co catalyst and peroxide were omitted, the reaction resulted in no product formation. Hence, these control experiments underpinned the key role that both the cobalt catalyst and oxidant played in the reaction outcome.

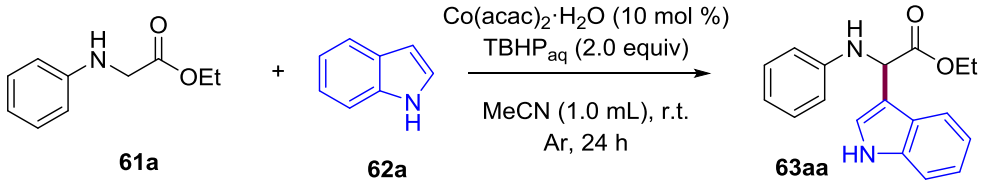

Entry	[Co]	Oxidant	Yield (%)
1	***x***	$TBHP_{aq}$	0
2	$Co(acac)_2 \cdot H_2O$	***x***	0

Reaction conditions: **61a** (0.5 mmol), **62a** (0.5 mmol), $Co(acac)_2 \cdot H_2O$ (10 mol %), MeCN (1.0 mL), TBHPaq (2.0 equiv), r.t., 24 h, under Ar.

Table 3 Blank Experiments.

Next, we investigated the effect of the solvent. In spite of the low yields, halogenated dichloroethane and tetrachloroethylene together with acetone were the only solvents that provided product **63aa** (Table 4, entry 2, 6 and 7). No desired product or trace amounts of **63aa** were observed with other solvents such as DMF, PhCl or toluene. In those cases, oxidation of starting glycine derivative **61a** to its corresponding imine was mostly detected in our attempts. Therefore, acetonitrile was selected as the optimal solvent providing the α-indole *N*-phenyl glycine ethyl ester **63aa** in 42 % yield (Table 4, entry 1).

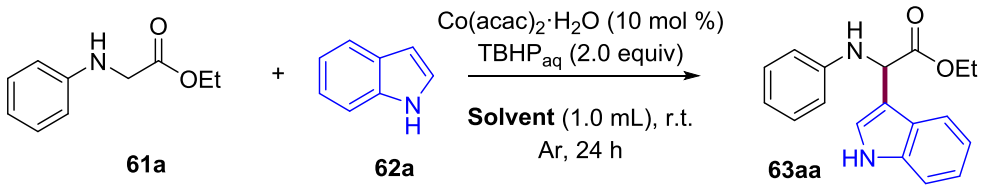

Entry	Solvent	Yield (%)[a]
1	MeCN	42
2	DCE	12
3	DMF	n.d.
4	PhCl	traces
5	toluene	n.d.
6	acetone	12
7	tetrachloroethylene	10

Reaction conditions: **61a** (0.5 mmol), **62a** (0.5 mmol), $Co(acac)_2 \cdot H_2O$ (10 mol %), solvent (1.0 mL), TBHPaq (2.0 equiv), r.t., 24 h, under Ar. [a] Isolated yield after purification by column chromatography.

Table 4 Screening of Solvents.

In order to further improve the yield, we performed other experiments to evaluate the influence of the temperature as well as the ratio of both coupling partners in the reaction outcome. Remarkably, higher yields were found upon raising the reaction temperature to 40 ^{0}C (Table 5, entry 1) while decomposition of the starting material occurred up to this temperature. Importantly, the use of two equivalents of **61a** toward one of the indole shown to be beneficial leading to 65 % yield of **63aa** (Table 5, entry 3). Nevertheless, a bigger excess of the amino ester derivative did not exhibit any higher reactivity (Table 5, entry 4). When the suitable rate of starting material was applied to the reaction conditions using DCE as solvent a considerable decrease of the yield was

observed (Table 5, entry 5). Similar results were obtained when we performed the reaction under air and during a larger period of time (Table 5, entry 6 and 7).

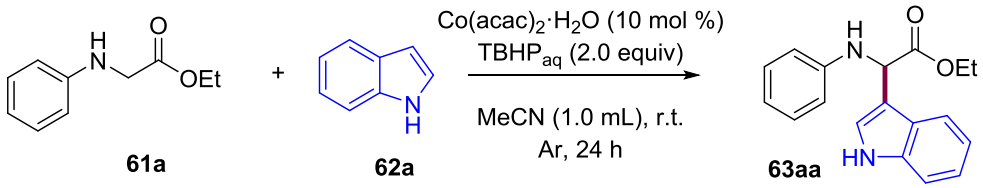

Entry	Change from standard conditions	Yield (%)[a]
1	40 ºC instead of r.t.	55
2	Ratio **61a**:**62a** (1:2)	60
3	Ratio **61a**:**62a** (2:1)	65
4	Ratio **61a**:**62a** (3:1)	67
5	Ratio **61a**:**62a** (3:1), DCE instead of MeCN	53
6	Under air	56
7	48 h	58

Reaction conditions: **61a** (0.5 mmol), **62a** (0.5 mmol), $Co(acac)_2 \cdot H_2O$ (10 mol %), MeCN (1.0 mL), TBHPaq (2.0 equiv), r.t., 24 h, under Ar. [a] Isolated yield after purification by column chromatography

Table 5 Screening of Substrate Equivalents.

After this set of screening experiments, we determined that the use of catalytic amounts of $Co(acac)_2 \cdot H_2O$ in combination with an aqueous solution of TBHP in acetonitrile at 40 ºC provided the desired product **63aa** in 65 % yield. Remarkably, the addition of no additive was required to couple *N*-Ph-Gly-OEt with the indole moiety, which together with the mild temperature and avoidance of a toxic chlorinated solvent leads to an atom-economical and sustainable system which complements existing heteroarylation protocols.

2.3.2. Scope of N-Aryl Glycine Derivatives and Indoles

With a set of easily prepared *N*-Ar-Gly-OEt compounds and commercially available indoles in hand, we tested our optimized reaction conditions for the formation of a variety of α-amino amides. The combination of $Co(acac)_2 \cdot H_2O$ and an aqueous solution of TBHP in acetronitrile at 40 ºC provided yields up to 78 % with high operational simplicity and selectivity. Moreover, unlike the method by Li, which was restricted to the use of highly activated PMP-Gly-amides,[22] our method was compatible with non-activated *N*-aryl glycine esters (Scheme 33).

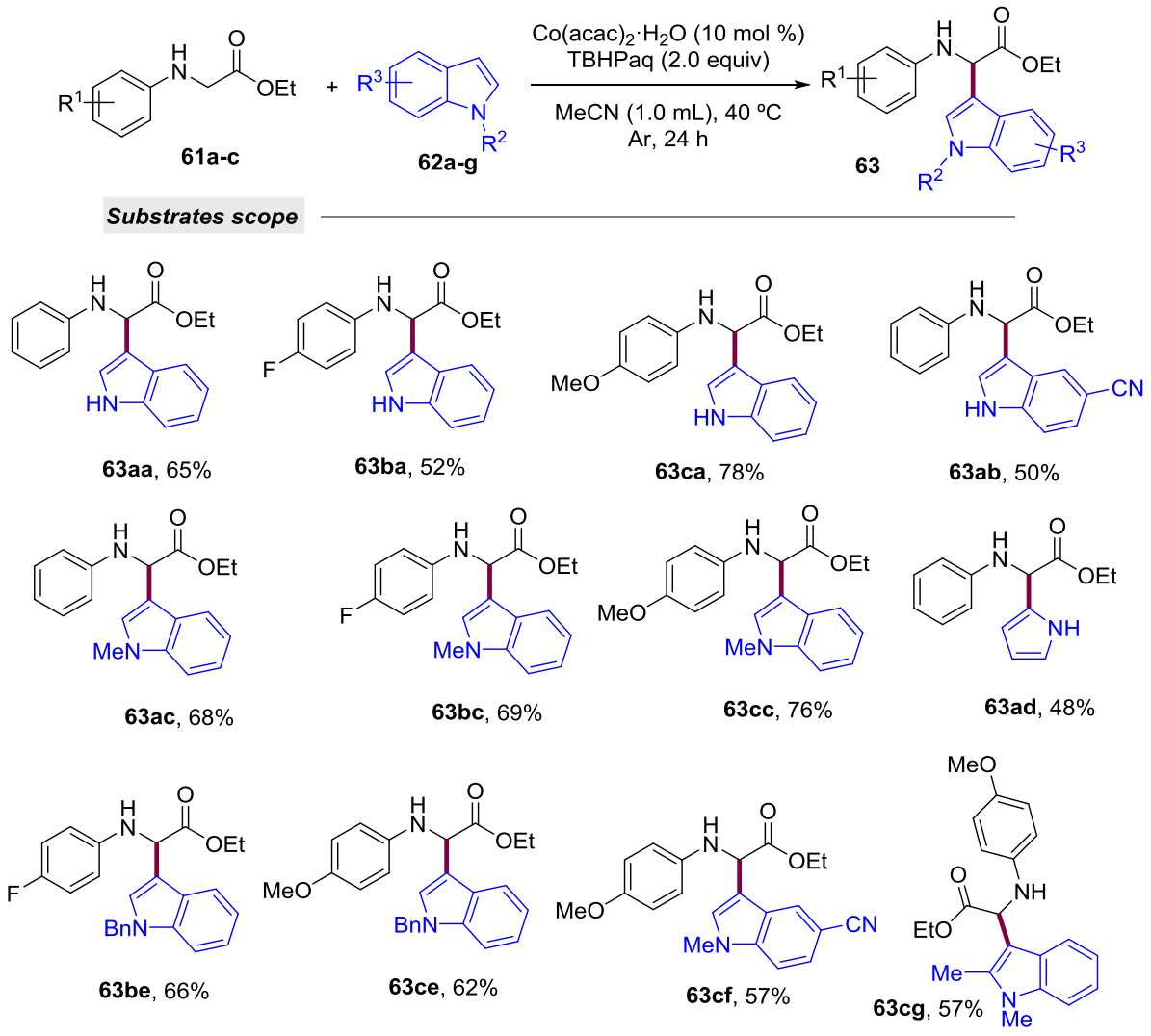

Reaction conditions: **61a-c** (1.0 mmol), **62a-g** (0.5 mmol), $Co(acac)_2$ H_2O (10 mol %), TBHPaq (2.0 equiv), MeCN (1.0 mL), 40 ºC, 24 h, under Ar. Yields of isolated products after column chromatography; average of at least two independent runs.

Scheme 33 Scope of N-Aryl Glycine Derivatives and Indoles.

When coupling indole derivatives with the electron-rich PMP-Gly-OEt (**61c**), higher yields were obtained in comparison with the ones obtained when using with *N*-Ar-Gly-OEt containing an electron-withdrawing substituent such as a fluorine atom, probably due its higher ability to stabilize the corresponding electrophilic imine or iminium-type intermediate. It must be highlighted that free N–H indoles provided in good yields, thus evidencing that a protecting group was not required (**63aa**, **63ba**, **63ca**, **63ad**). Regarding the heterocyclic partners, both *N*-methyl and *N*-benzyl indoles were shown to give the targeted products in an interval of 57-69 % yield (**63ac**, **63bc**, **63cc**, **63be**, **63ce**). Moreover, substituted indoles with different electronic properties were tolerated. Less nucleophilic 5-cyano indole provided the desired products in 50-57 % yield. Likewise, sterically demanding 2-methyl-indole was perfectly accommodated giving rise **63cg** in 57 % yield. Interestingly, the use of less reactive pyrrole resulted in the formation of product **63ad** with a moderate 48 % yield, and the process occurred at its most reactive C-2 site.

2.3.3. Unsuccessful Scope

During the study of the scope of our heteroarylation procedure, we found that a variety of substrates showed a lower or even no reactivity to afford the targeted products (Figure 7). Whereas F-containing aryl glycinates were proven efficient coupling partners, chlorine-analogues afforded the products **63da** and **63fa** in low yields. Likewise, the use of *meta*-OMe-aryl derivative **63ea** was found less reactive than its *para*-substituted isomer, thus evidencing the high importance of the stability of the transient electrophilic species.

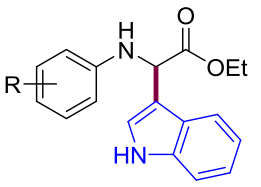

63da, R=4-Cl, 27%
63ea, R=3-OMe, 30%
63fa, R=3-Cl, 18%

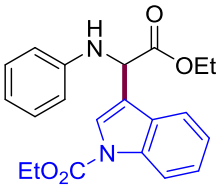

63ah, n.r.

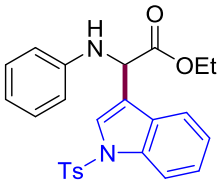

63ai, n.r.

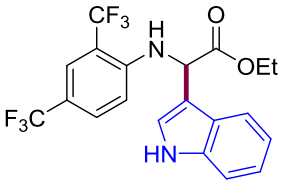

63ga, n.r

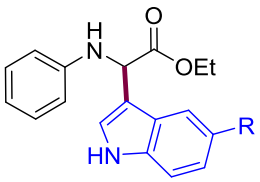

63aj, R=Br, 23% (80 ºC)
63ak, R=OMe, 30% (80 ºC)

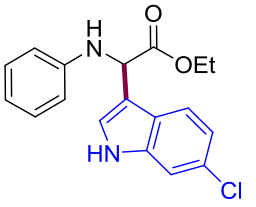

63al, 26% (80 ºC)

Reaction conditions: **61a-c** (1.0 mmol), **62a-gl** (0.5 mmol), $Co(acac)_2$ H_2O (10 mol %), TBHPaq (2.0 equiv), MeCN (1.0 mL), 40 ºC, 24 h, under Ar. Yields of isolated products after column chromatography; average of at least two independent runs.

Figure 7 Unsuccessful Substrates.

Concerning the heterocyclic coupling partner, indoles **62j**, **62l** and **62k** provided product **63aj**, **63al** and **63ak** in low yields, in spite of raising the reaction temperature up to 80 ºC. The electron-withdrawing chlorine and bromine atoms and the position of methoxy group deeply affected the nucleophilicity of the C3 position in the heterocyclic coupling partner, thereby resulting in the reactivity decrease. As expected, when indoles were *N*-protected with electron-withdrawing substituents such as a carbamate (**63ah**) and tosyl (**63ai**) group no reaction took place, reinforcing the key role of the indole as the nucleophile of the process.

Additionally, the low or even the lack of reactivity exhibited by other tested nucleophiles evidenced the higher selectivity of this cobalt-catalyzed functionalization of *N*-aryl glycine esters towards indole scaffold (Scheme 34). Owing to the similarity with pyrrole structure, which pleasingly resulted in the desired substituted α-amino amide, *N*-methyl pyrrole (**64a**), furan (**64c**), benzimidazole (**64af**) and thiophene derivatives (**64b**, **64g**) were submited to the optimal reaction conditions. However, the reaction conditions were only suitable for the coupling of **61a** with thiophene leading to the formation of **65ab** in 33% yield. Despite the presence of methyl group, N-methylpyrrole did not react under the optimal reaction conditions. Likewise, benzimidazole **64f**, which upon deprotonation has demonstrated in previous reports that could couple with radical intermediates turned out to be unreactive. On the other side, no product was observed when the amide and the α-amino acid alkene derivatives **64d** and **64e** were tested. Interestingly, the activated 1,3,5-trimethoxybenzene provided the highest yield among this family of nucleophiles, which after a fast rescreening of parameters like temperature and catalyst source, resulted in a promising 51 % yield utilizing $CoCl_2$ as the catalyst at 80 ºC. These results evidenced that slight modifications on the reaction conditions could open up the possibility of coupling other (hetero)arenes with *N*-aryl glycine esters.

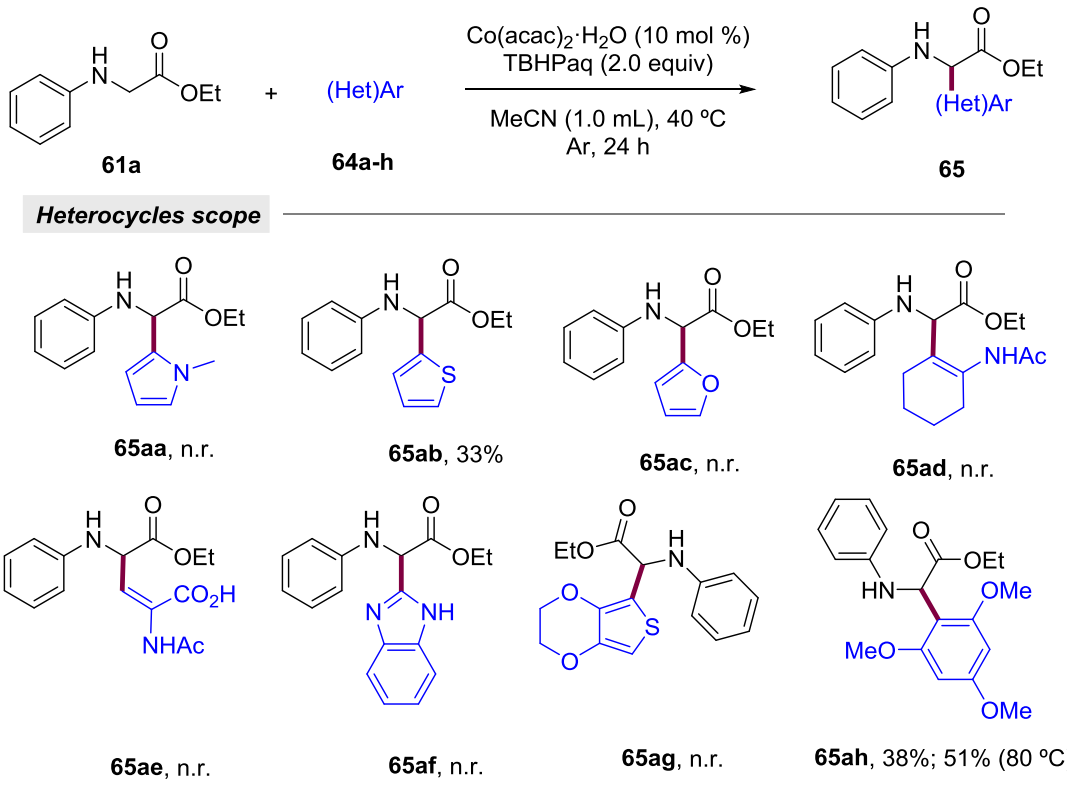

Reaction conditions: **61a** (1.0 mmol), **64a-h** (0.5 mmol), $Co(acac)_2 \cdot H_2O$ (10 mol %), TBHPaq (2.0 equiv), MeCN (1.0 mL), 40 ºC, 24 h, under Ar. Yields of isolated products after column chromatography; average of at least two independent runs.

Scheme 34 Unsuccessful Other Heterocycles.

2.3.4. Scope of Dipeptides and Tripeptides

Subsequently, we were encouraged to test short peptides, which often tend to suffer from oxidative cleavage making sometimes their manipulation a difficult task.[66] Nevertheless, the corresponding products of some easily prepared di- and tripeptides were obtained in moderate to excellent yields (Scheme 35). Dipeptides bearing valine and proline units underwent the heteroarylation providing product **67a** and **67c** in 92 % and 63 % yield, respectively. On the other side, the reaction was found entirely selective and the developed CDC protocol ensured the functionalization at the terminal glycine unit exclusively even when other glycine residues were present (**67b**, **67d**, **67e**). This result would be in agreement with previous methodologies where the aryl ring in the *N*-terminal of the glycine unit was essential for the formation and stabilization of the electrophilic intermediate, thus providing substrate-controlled selectivity.

[66] Dean, R. T.; Fu, S.; Stocker, R.; Davies, M. J. *Biochem. J.* **1997**, *324*, 1.

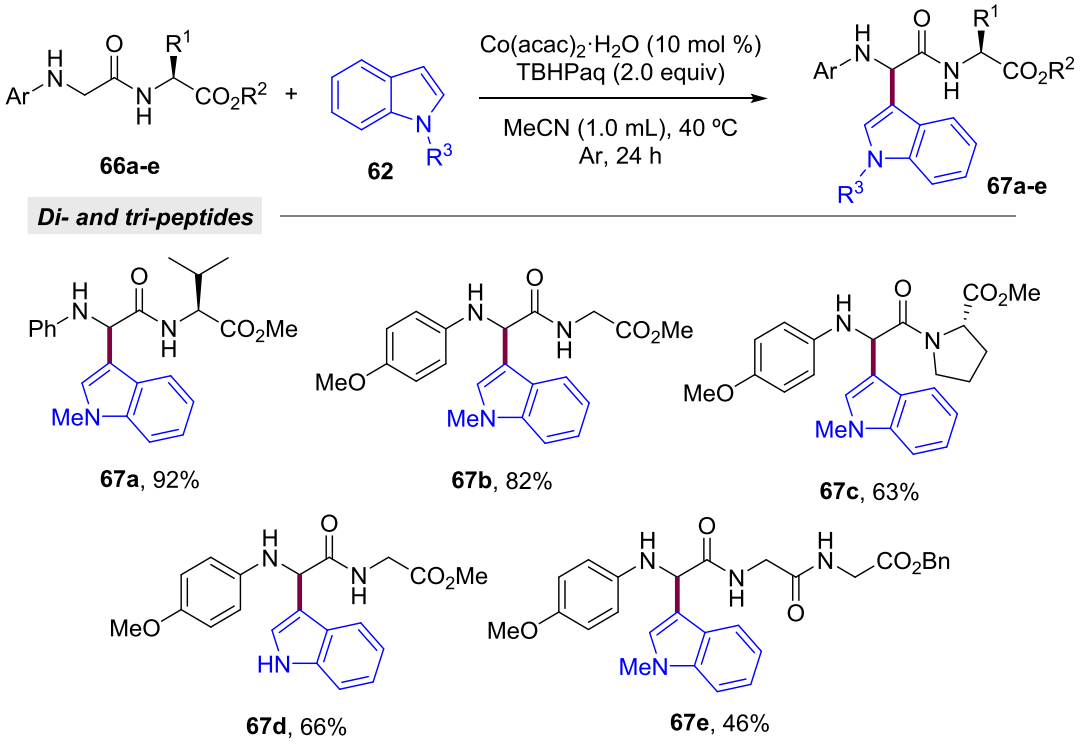

Reaction conditions: **66a-e** (1.0 mmol), **62** (0.5 mmol), $Co(acac)_2 \cdot H_2O$ (10 mol %), TBHPaq (2.0 equiv), MeCN (1.0 mL), 40 ºC, 24 h, under Ar. Yields of isolated products after column chromatography; average of at least two independent runs.

Scheme 35 Scope of Glycine-Containing Dipeptides and Tripeptides.

This alternative Co-catalyzed methodology represents a solution to the downsides usually observed in enolate chemistry for the modification of α-amino carbonyl compounds. Owing to the utilized strong bases, peptide substrates often experience lack of regioselectivity in the presence of more than one glycine unit and the preservation of the existing stereocenters is usually lost. Conversely, we verified by HPLC analysis that the existing stereocenters within dipeptides **67a** and **67c** remained intact, thereby resulting in a racemization-free protocol which outscores other traditional approaches in peptide chemistry.

2.3.5. Mechanistic Proposal

To gain some insights into the mechanism, we performed some control experiments. First of all, we carried out the reaction between **61a** and **62a** in the presence of radical traps such as TEMPO, 1,1-diphenylethene and butylated hydroxytoluene (BHT) (Scheme 36). We suggested that a radical pathway could be operative as the addition of the three of them resulted in the inhibition of the reaction with no product formation.

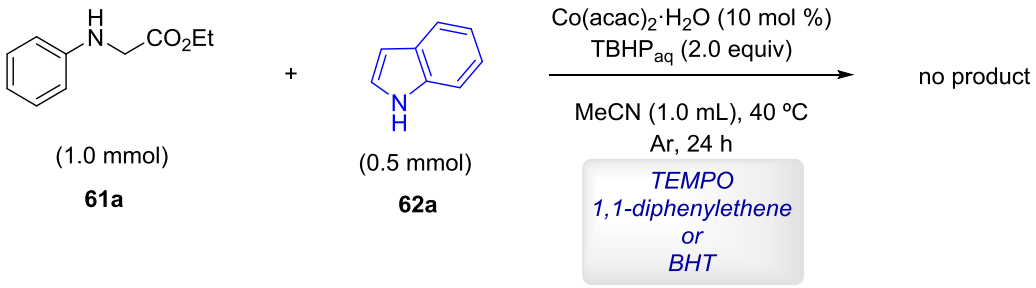

Scheme 36 Control Experiments with Radical Traps.

On the basis of previously mentioned reports,[28] it has been suggested that oxidative reaction conditions enable the *in situ* formation of an imine or an iminium-type intermediate from the corresponding α-amino ester. In order to have more insights into the reaction mechanism, we synthesized imine **68c** and performed a series of experiments. When the imine was submitted to the optimal reaction conditions full conversion of the starting material into product **68ca** was observed. Nevertheless, the most highlighting finding was that full conversion was also obtained when the same reaction was performed in the absence of both the metal and the oxidant, proving that an imine intermediate might be operative (Scheme 37, a). Furthermore, the latter result suggested that cobalt catalyst together with the peroxide were crucial for the formation of an imine or iminium intermediate but not for the nucleophilic attack.

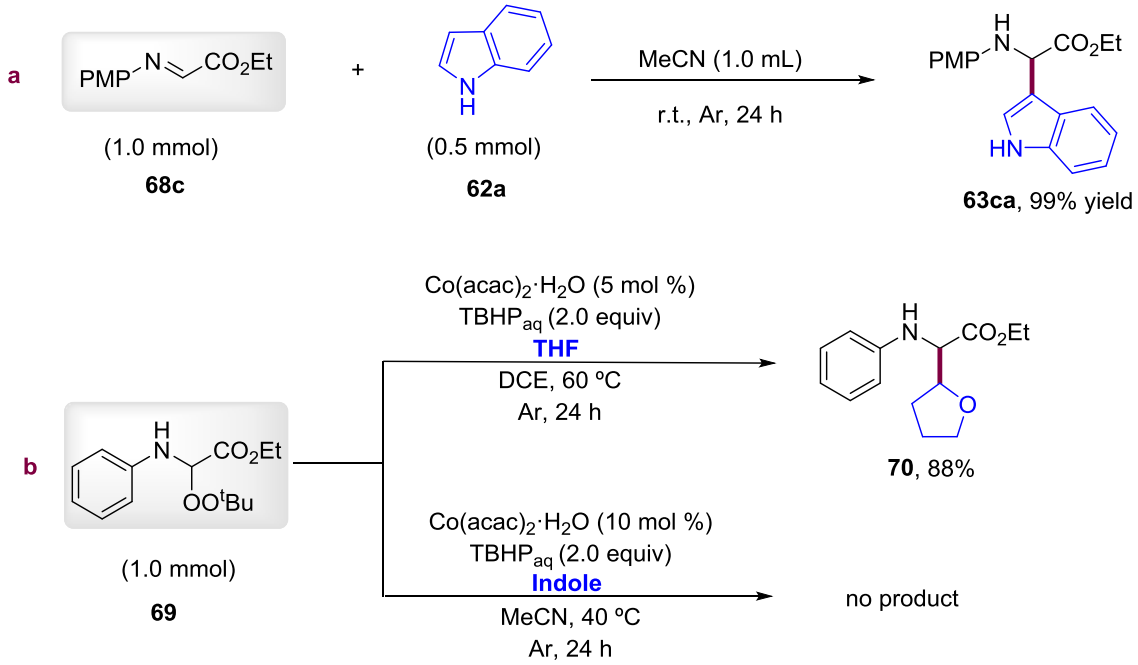

Scheme 37 Control Experiments.

In the concurrent cobalt-catalyzed alkylation of α-amino esters which was under study at the same time in our group, α-*tert*-butyldioxyl intermediate **69** was isolated[67] when the reaction was performed in the absence of the alkylating reagent. Moreover, compound **69** led to the corresponding alkylated product **70** under optimized conditions, evidencing its reasonable intermediacy along the CDC alkylation process. On the contrary, our heteroarylation did not occur when submitting such a peroxide species **69** to the optimized reaction conditions which evindences the distinct electronic features of the highly nucleophilic indole in comparison with the soft nucleophilic alkyl radical species (Scheme 37, b). Additionally, control experiment shown the crucial role of the free amino group in the amino acid since compound **71** bearing a tertiary amine did not provide the desired product under the cobalt/TBHP system **(**Scheme 38**)**.

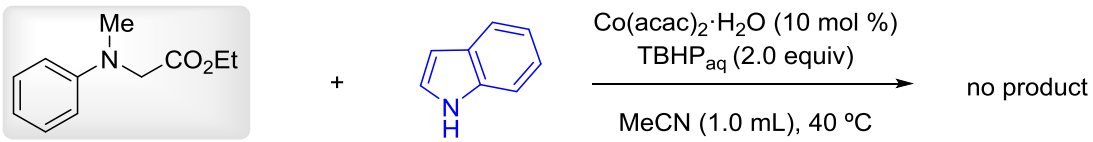

Scheme 38 Cobalt-Catalyzed C–H Functionalization of a Tertiary Amine.

Based on the results so far, a mechanistic proposal is depicted in Scheme 39

Scheme 39. We assume that the reaction is initiated by the cleavage of ^{t}BuOOH, induced by Co^{II} which is oxidized to Co^{III} forming *tert*-butoxy radical **A**.[63] The latter radical species is responsible of the Hydrogen Atom Transfer (HAT) radical intermediate **B**. Subsequently, this carbon-centered radical is further oxidized to carbocation **C** by a Single Electron Transfer (SET) regenerating the active $cobalt^{II}$ catalyst. The latter electrophilic species **C** would be trapped to furnish product **63**.

[67] Xia, Q.; Wang, Q.; Yan, C.; Dong, J.; Song, H.; Li, L.; Liu, Y.; Wang, Q.; Liu, X.; Song, H. *Chem. Eur. J.* **2017**, *23*, 10871.

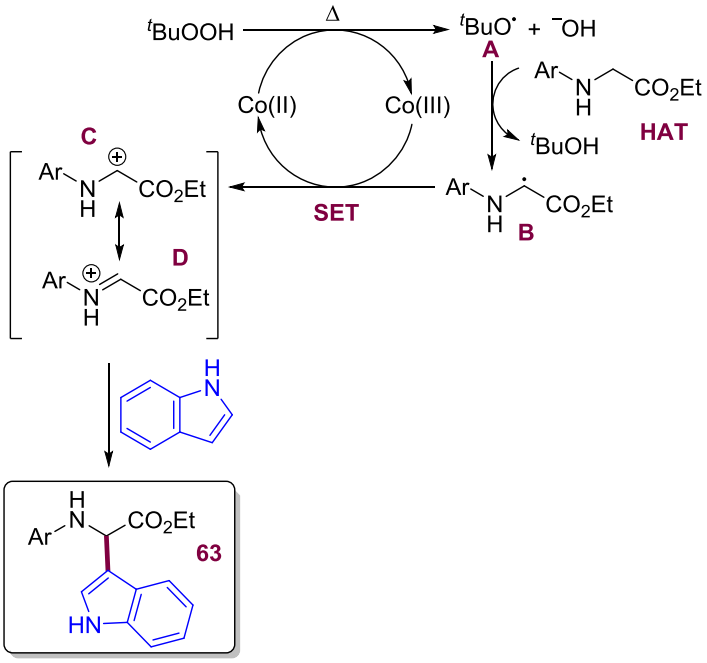

Scheme 39 Proposed Mechanism.

Nevertheless, our group has recently performed a computational study of the CDC between *N*-aryl glycinates and indoles in the presence of a Co(II)/TBHP catalytic system.[68] Interestingly, despite the fact that existing reports suggested both imine and iminium-type intermediates, DFT studies revealed that the former species is the most favorable one for our cobalt-catalyzed heteroarylation reaction. Likewise, *N*-aryl substituted derivatives and secondary amines seemed to favor the process as well. These conclusions were in agreement with our experimental results and justified the full conversion of the synthesized imine intermediate into the desired product.

[68] Andrade-Sampedro, P.; Correa, A.; Matxain, J. M. *J. Org. Chem.* **2020**, DOI: 10.1021/acs.joc.0c01816

2.4. Co-Catalyzed C(sp^3)–H Aminocarbonylation of Glycine Derivatives

First-row transition metals have demonstrated to be efficient tools for the modification of α-amino acid compounds overcoming previous existing limitations, such as the need of prefunctionalized substrates or the racemization of the existing chiral centers. For this reason, we seek for new sustainable methodologies to carry out other C–H bond functionalizations of amino acids involving unprecedented coupling partners.

At the time this thesis was in progress, our group disclosed a cobalt-catalyzed alkylation of *N*-aryl glycine derivatives with cyclic ethers like THF. Inspired by the idea of using a solvent as the coupling partner, we turned our attention to *N*,*N*-dimethylformamide (DMF) in the modification of peptides.[69] DMF is a multipurpose reagent and owing to its structure, this solvent has acted as a versatile building block.[70] In this regard, DMF has served as a precursor in reactions such as formylation, amination, cyanation and aminocarbonylation. In particular, the latter transformation into glycine derivatives would result in the formation of interesting α-amido-α-amino acid compounds.

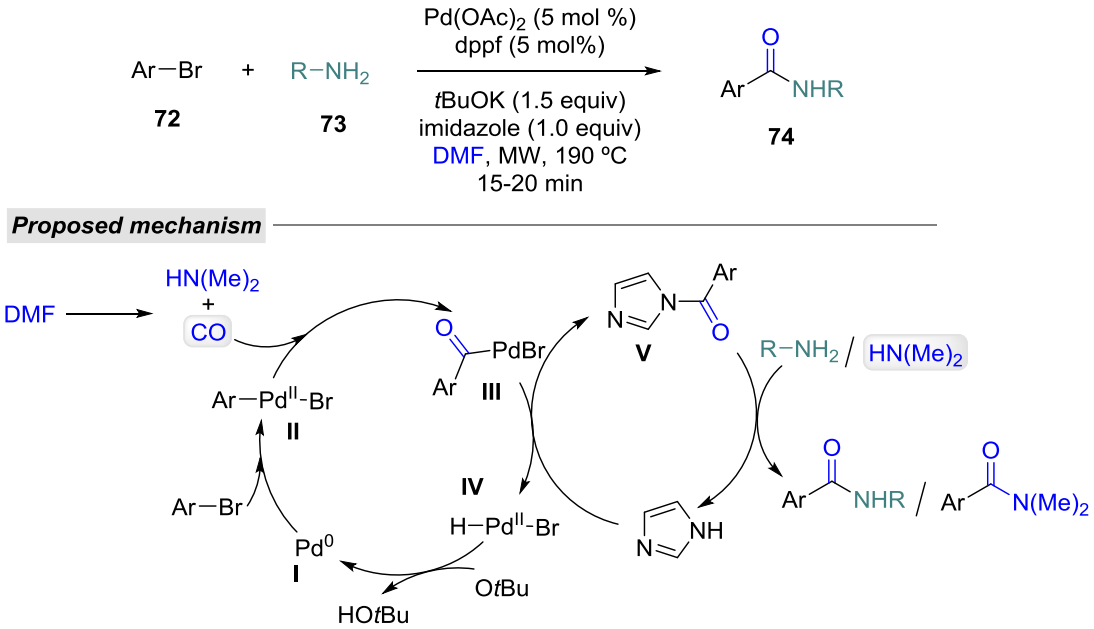

Scheme 40 DMF as –CO and –N(Me)$_2$ source.

In 2002, Hallberg and co-workers reported a palladium-catalyzed aminocarbonylation of aryl bromides under microwave irradiation where DMF served as a source of CO with an excess of amines, such as benzylamine and aniline (Scheme 40).[71] The use of imidazole, which acts as a powerful Lewis base and acylating catalyst,

[69] Heravi, M. M.; Ghavidel, M.; Mohammadkhani, L. *RSC Adv.* **2018**, *8*, 27832.
[70] a) Ding, S.; Jiao, N. *Angew. Chem. Int. Ed*. **2012**, *51*, 9226. b) Muzart, J. *Tetrahedron* **2009**, *65*, 8313.
[71] Wan, Y.; Alterman, M.; Larhed, M.; Hallberg, A. *J. Org. Chem.* **2002**, *67*, 6232.

enables the formation of species **V** and its further coupling with the corresponding amine. In the absence of the latter, the dimethylamine generated from the decomposition of DMF reacted with intermediate **V**, thus serving as a $-NMe_2$ source.[72]

Additionally, Vilsmeier reagent, which is achieved from *N*,*N*-disubstituted formamides and acid chlorides, is a common intermediates in transformations involving DMF. As an example, Hiyama reported the palladium-catalyzed direct aminocarbonylation of aryl iodides utilizing DMF as an amide source (Scheme 41).[73] The reaction proceeded through a Heck-type addition of aryl halides to the *in situ* formed Vilsmeier reagent from DMF and $POCl_3$.

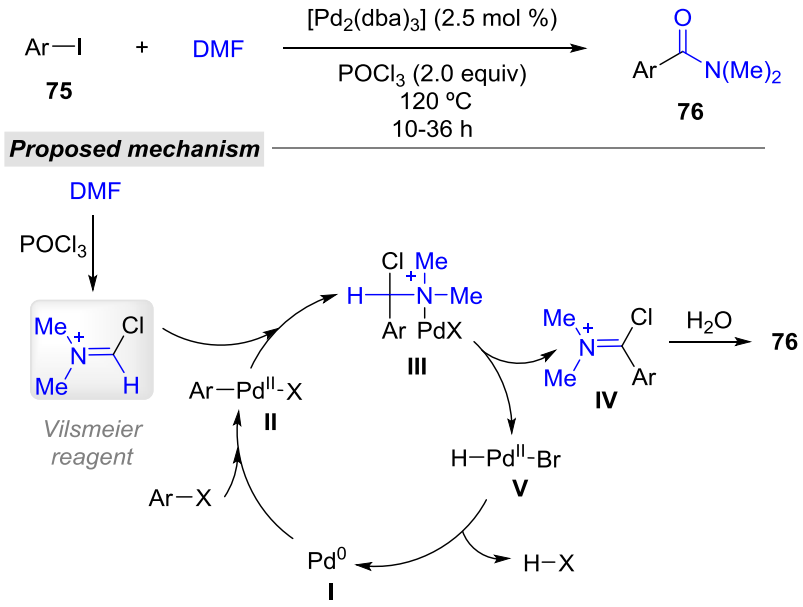

Scheme 41 Palladium-Catalyzed Direct Aminocarbonylation of Aryl Iodides with DMF.

In contrast to the requirement of additives and the use of expensive transition metals observed in the described aminocarbonylation transformations, Wang and co-workers reported a practical metal-free CDC reaction between azoles and DMF to deliver the aminocarbonylated products (Scheme 42).[74] The authors suggested that the homolytic cleavage of the oxidant *tert*-butyl peroxybenzoate (TBPB) forming the corresponding radical species was responsible for the following hydrogen atom abstraction of both substrates. Thus, the amidation product was proposed to be generated as a consequence of a radical-radical coupling.

[72] Schnyder, A.; Beller, M.; Mehltretter, G.; Nsenda, T.; Studer, M.; Indolese, A. F. *J. Org. Chem.* **2001**, *66*, 4311.
[73] Hosoi, K.; Nozaki, K.; Hiyama, T. *Org. Lett.* **2002**, *4*, 2849.
[74] Tao, H.; Li, H.; Li, P.; Wang, L. *Chem. Commun*. **2011**, *47*, 8946.

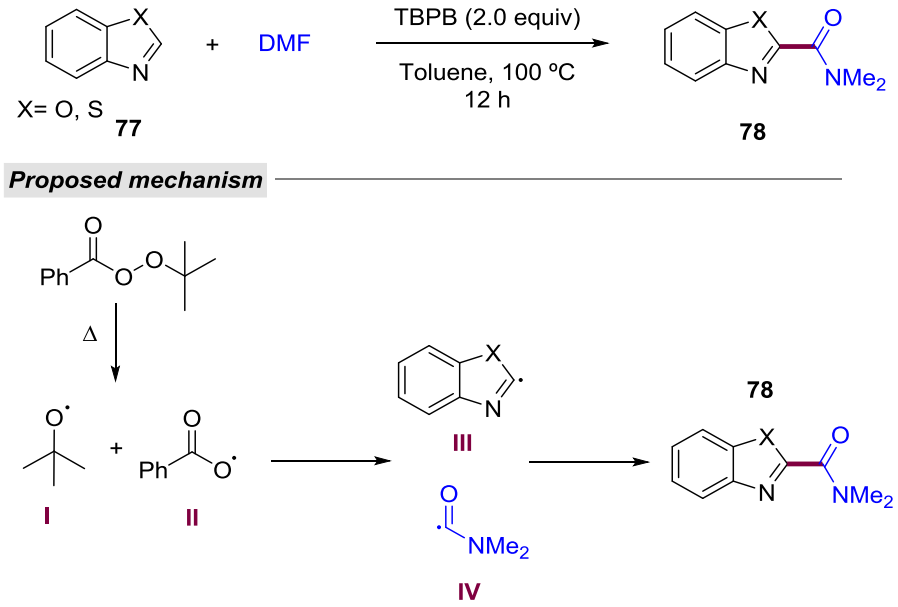

Scheme 42 CDC Amidation of Azoles with DMF.

We believe that the full potential of DMF as a versatile building block has not been fully explored. Accordingly, we envisioned its use as a novel coupling partner in the modification of amino acids and peptides upon an unprecedented CDC reaction.

2.4.1. Optimization of the Reaction Conditions

We initiated our investigation by analyzing the aminocarbonylation of *N*-Ph-Gly-OEt **61a** with DMF. As a preliminary study, we performed numerous reactions varying the metal source using $TBHP_{dec}$ and DMF as solvent (Table 6), and mostly first-row transition metal salts like Co, Cu and Fe were tested. To our delight, early attempts supported the feasibility of our approach and the targeted product **79a** was obtained in 50 % yield with a combination of $FeCl_2$ (10 mol %) and a decane solution of TBHP at 60 ºC in DMF (Table 6, entry 3). We have demonstrated above the ability of cobalt catalysts to perform CDC reactions and we were interested in the development of a cobalt-catalyzed aminocarbonylation of glycine derivatives. For that reason, our first attempts were carried out with a wide set of Co salts which unfortunately turned out to be inactive with the exceptions of $CoCl_2$ and $CoCl_3$ (Table 6, entry 1, 2). The rest of the tested Co- and Cu-catalyzed reactions resulted in no product formation or just traces. However, $FeCl_2$ shown comparatively higher reactivity for the aminocarbonylation reaction, which represents an ideal alternative to colbalt catalyst is owing to its low toxicity and price. In this manner, other halogen-containing iron sources such as $FeCl_3$ and $FeBr_3$ also provided the desired product although in lower yields (Table 6, entry 4, 5) and $Fe(OAc)_2$ and Fe_2O_3 resulted in traces of **79a** (Table 6, entry 6, 7).

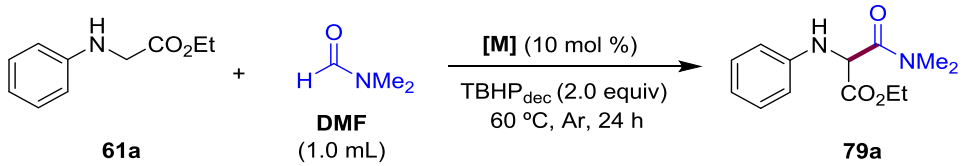

Entry	[M]	Yield (%)[a]
1	$CoCl_2$	25
2	$CoCl_3$	16
3	$FeCl_2$	50
4	$FeCl_3$	37
5	$FeBr_3$	21
6	$Fe(OAc)_2$	traces
7	Fe_2O_3	traces

Reaction conditions: **61a** (0.5 mmol), DMF (1.0 mL), [M] (10 mol %), TBHPdec (2.0 equiv), 60 ºC, 24 h, under Ar. [a] Isolated yield after purification by column chromatography.

Table 6 Screening of Metal Catalysts.

After establishing $FeCl_2$ as the optimal catalyst, we turned our attention to find an appropriate oxidant. Seeking for the most sustainable protocol as possible, we tested inorganic oxidants such as $K_2S_2O_8$ and $(NH_4)_2S_2O_8$ as well as molecular oxygen and hydrogen peroxide together with some others. Nevertheless, TBHP proved to be the most efficient oxidant, which provided 45 % yield in an aqueous solution and 52 % yield in a decane solution.

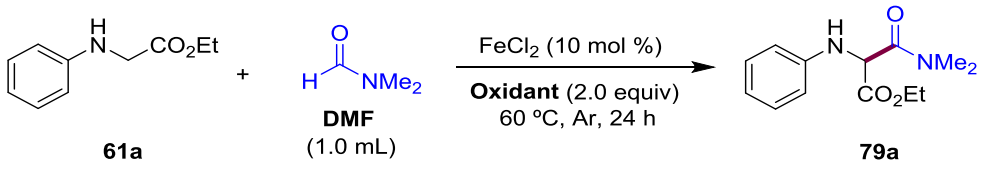

Entry	Oxidant	Yield (%)[a]
1	$TBHP_{aq}$	45
2	$TBHP_{dec}$	52
3	O_2	n.r.
4	$K_2S_2O_8$	traces
5	$(NH_4)_2S_2O_8$	n.d.
6	H_2O_2	n.d.
7	Oxone	n.d.
8	Selecfluor	n.d.
9	DCP	n.d.
10	BzO	n.d.
11	DTBP	n.d.
12	TBPB	n.d.

Reaction conditions: **61a** (0.5 mmol), DMF (1.0 mL), $FeCl_2$ (10 mol %), oxidant (2.0 equiv), 60 °C, 24 h, under Ar. [a] Isolated yield after purification by column chromatography. n.d.= not determined.

Table 7 Screening of Oxidants.

With a Fe catalytic system in hand, we next decided to have a close look at the catalyst and reagents loading. As shown in Table 8, the best conditions were found at 60 °C and with a more diluted solution of DMF (0.25 M), with a 59 % isolated yield of **79a**. In general, the decrease in the reagent load resulted in traces of the product

while the increase of iron catalyst and $TBHP_{dec}$ were determined by TLC to generate a higher amount of side-products like the oxidized glycine derivative and less conversion of the starting material (entry 4 and 8). Additionally, an inert atmosphere seemed to be crucial as well as the use of anhydrous DMF, otherwise lower yields were obtained (entry 1 and 2). Nonetheless, the addition of molecular sieves into the reaction mixture for the removal of water had also a negative effect (entry 7).

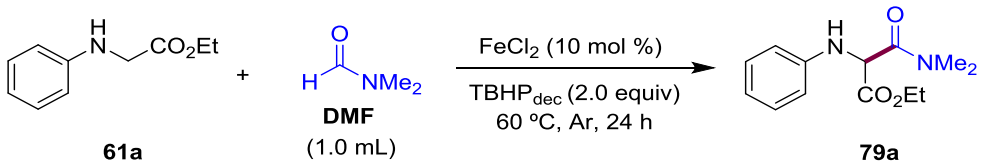

Entry	Change from standard conditions	Yield (%)[a]
1	No argon	traces
2	DMF wet	42
3	$FeCl_2$ (5 mol%)	traces
4	$FeCl_2$ (15 mol%)	n.d.
5	DMF (0.5 mL)	traces
6	DMF (2 mL)	59
7	Molecular sieves	43
8	$TBHP_{dec}$ (3 equiv)	n.d.
9	$ZnCl_2$ (1.0 equiv)	42
10	$Bi(OTf)_3$ (1.0 equiv)	37

Reaction conditions: **61a** (0.5 mmol), DMF (1.0 mL), $FeCl_2$ (10 mol %), $TBHP_{dec}$ (2.0 equiv), 60 °C, 24 h, under Ar. [a] Isolated yield after purification by column chromatography. n.d.= not determined.

Table 8 Changes from the Standard Conditions.

Based on previous reports,[43] we wondered if the addition of Lewis acids could activate and stabilize the proposed imine intermediate (Figure 8). However, after screening a number of Lewis acids, no positive effect was observed. For instance, the addition of $ZnCl_2$ and $Bi(OTf)_3$ resulted in lower yields y (Table 8, entry 9, 10).

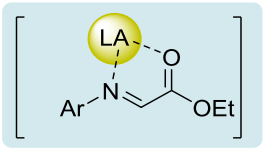

Figure 8 Imine Intermediate Stabilized by a Lewis Acid.

In order to improve the yield, other salts of Ag, Cu and Mn were added to the reaction system as co-catalysts. Unfortunately, in all cases the process was entirely inhibited. Moreover, owing to the reproducibility issues, further screening was conducted to obtain a reliable protocol. Given that the use of a chlorinated solvent in alkylation reactions with THF was found beneficial[75] and trying to minimize the amount of DMF, we evaluated the influence of co-solvents. Among all the tested co-solvents, tBuOH was found to have a positive effect resulting in a higher yield (Table 9, entry 7). In contrast, the variation of the temperature led to comparatively lower yields.

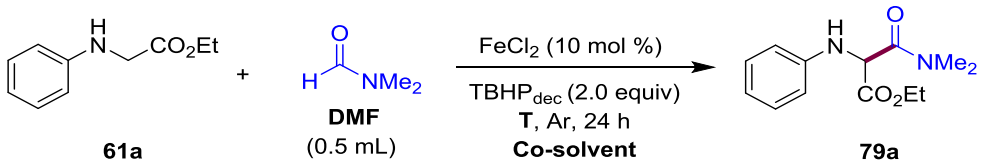

Entry	Co-solvent	T (ºC)	Yield (%)[a]
1	Toluene	60	29
2	MeCN	60	29
3	DCE	60	n.d.
4	DMA	60	n.d.
5	PhCl	60	n.d.
6	Acetone	60	n.d.
7	^{t}BuOH	60	67
8	none	r.t.	traces
9	none	40	27
10	none	80	38
11	none	60	59

Reaction conditions: **61a** (0.5 mmol), DMF (1.0 mL), co-solvent (0.5 mL) $FeCl_2$ (10 mol %), TBHPdec (2.0 equiv), 24 h, under Ar. [a] Isolated yield after purification by column chromatography. n.d.= not determined.

Table 9 Screening of Co-solvent and Temperature.

[75] San Segundo, M.; Guerrero, I. Correa, A. *Org. Lett*. **2017**, *19*, 5288.

Next, we investigated the influence of a variety of commonly used additives in the formation of product **79a** (Table 10). Additives such as carboxylic acids, phosphines, amine, and phase transfer agents (Table 10, entry 14-16) were tested in catalytic amounts because of their observed positive effect on the reactivity in a plethora of related methodologies. However, in the aminocarbonylation of *N*-aryl glycinate **61a** did not have any impact. On the one hand, chelating-ligands that could attach to the metal center modifying its reactivity, like phosphines (Table 10, entry 2-8) and amines (Table 10, entry 9-13), seemed to have no effect on the reaction outcome with the exception of dppf and phenanthroline which led to a considerable decrease in yield (Table 10, entry 6 and 10).

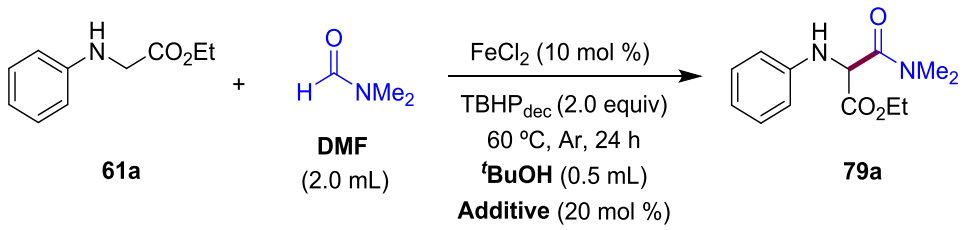

Entry	Change from standard conditions	Yield (%)[a]
1	none	65
2	JohnPhos	64
3	XPhos	69
4	^{t}BuPhos	59
5	PPh_3	63
6	dppf	21
7	$PCy_3 \cdot HBF_4$	60
8	$^{t}Bu_3P$	63
9	Neocuproine	56
10	Phenanthroline	37
11	Lutidine	63
12	Pyridine	58
13	DMAP	67
14	TBAB (50 mol%)	45
15	Me_4NCl (50 mol%)	52
16	NH_4Cl (50 mol%)	18

Reaction conditions: **61a** (0.5 mmol), DMF (1.0 mL), $FeCl_2$ (10 mol %), $TBHP_{dec}$ (2.0 equiv), ^{t}BuOH (0.5 mL), 60 °C, 24 h, under Ar. [a] Isolated yield after purification by column chromatography.

Table 10 Screening of Additives.

Despite all of our attempts, the use of additives did not result in higher yields. Accordingly, the best results involved the use of $FeCl_2$ in combination with TBHP in DMF as solvent (Table 10, entry 1). Moreover, X-Ray analysis of **79a** confirmed the structre of the aminocarbonylated product (Figure 9).

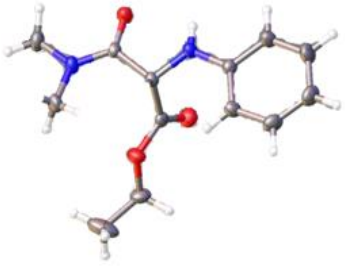

*Figure 9. X-Ray Chrystallography of **79a***

2.4.2. Scope of N-Aryl Glycine Derivatives

With the optimal reaction conditions in hand, a short family of glycine derivatives were tested (Scheme 43). In stark contrast to the model reaction, most of the substrates utilized in the prior cobalt-catalyzed heteroarylation of glycine derivatives,[75] resulted unreactive with no conversion of the starting material. Furthermore, the ones which underwent the targeted CDC reaction provided moderate yields up to 45 %. In this regard, electron donating groups such as benzyl ether and acetamide (**79b**, **79e**) resulted in similar yields than those achieved with halogenated substituents-containing aryl glycine esters (**79c**, **79d**). Interestingly, slightly better results were obtained when Gly-containing dipeptides were submited to the reaction conditions. Among a set of dipeptides, the aminocarbonylated product of Ph-Gly-Gly-OEt, Ph-Gly-Pro-OMe and (*p*-OMe-Ph)-Gly-Pro-OMe were obtained in moderate yields (**79f**, **79g**, **79h**). Despite the limited success, the obtained products verified the high site-selectivity of the process driven by the terminal *N*-aryl group.

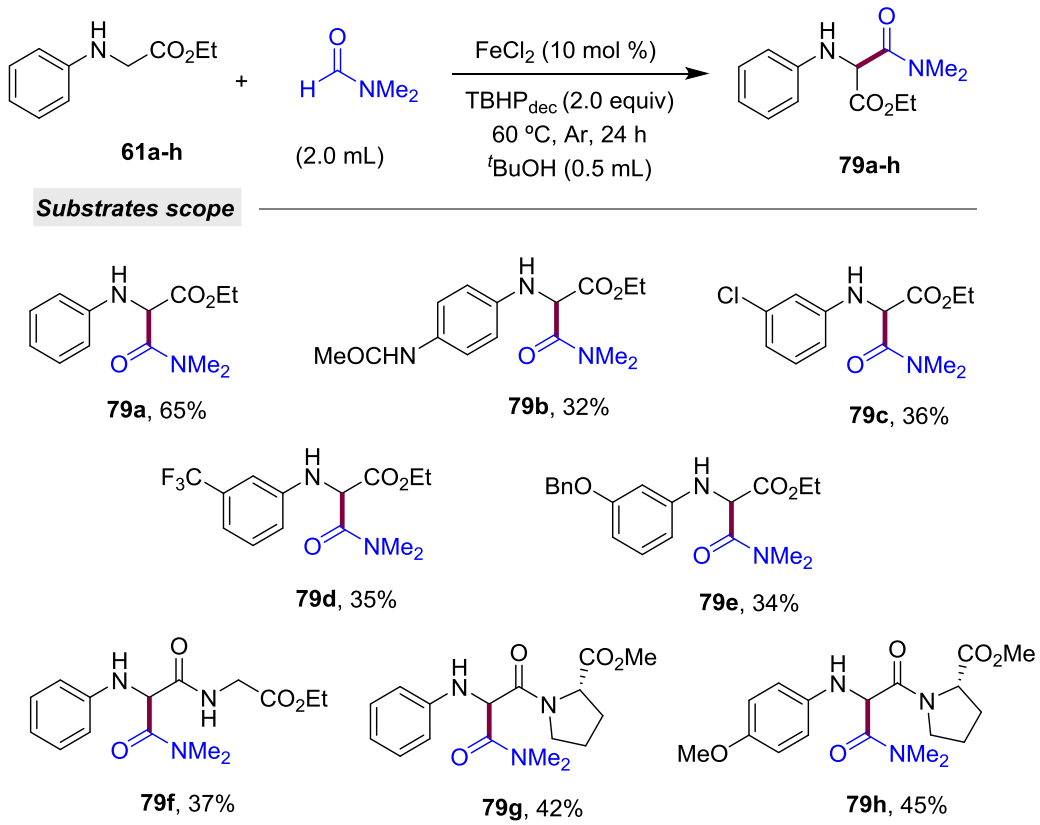

Reaction conditions: **61a** (0.5 mmol), DMF (1.0 mL), $FeCl_2$ (10 mol %), $TBHP_{dec}$ (2.0 equiv), ^tBuOH (0.5 mL), 60 °C, 24 h, under Ar. Isolated yield after purification by column chromatography.

Scheme 43 Scope of N-Aryl Glycine Derivatives.

On the other hand, we evaluated the feasibility of performing the process with other formamides different to DMF. Unfortunately, most of the tested formamides were found unreactive or exhibited low conversion under the standard conditions. In this respect, several additional studies should be conducted to broaden the synthetic scope and increase the utility of this Fe-catalyzed CDC technique.

2.4. Conclusion

In conclusion, we have developed an alternative C(sp^3)−H heteroarylation of *N*-aryl glycine derivatives with the use of the cost-efficient cobalt catalysis.[75] Notably, our method enabled the selective installation of indole derivatives into α-amino carbonyl compounds including a set of short-peptides of utmost proteomic importance under mild reaction conditions and with total preservation of the chirality of the existing stereocenters. Likewise, an unprecedented CDC of glycine derivatives with DMF featuring environmentally friendly iron catalysis has been studied. However, the latter protocol has shown so far a limited scope and further investigation is clearly required to obtained a robust and reliable method.

2.5. Experimental Procedures

In this section, the general procedures of the processes developed along this chapter will be detailed and a selection of representative products is included. For the full characterization data, please see the SI of the published article.[75]

2.6.1. General Procedure: Co-Catalyzed C(sp^3)−H Heteroarylation

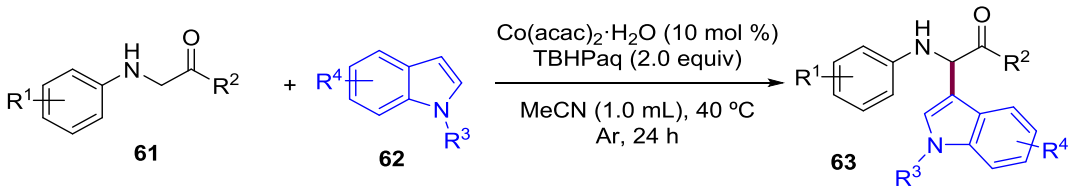

A reaction tube containing a stirring bar was charged with the corresponding α-amino carbonyl compound **61** (1.0 mmol, 2.0 equiv), the corresponding indole (0.50 mmol, 1.0 equiv) (if solid) and $Co(acac)_2{\cdot}H_2O$ (10 mol %). The reaction tube was then evacuated and back-filled with dry argon (this sequence was repeated up to three times). The corresponding indole (0.50 mmol, 1.0 equiv) (if liquid), MeCN (1 mL) and an aqueous solution of TBHP (70 wt. % in H_2O) (2.0 equiv) were then added under argon atmosphere. The reaction tube was next warmed up to 40 ºC and stirred for 24 hours. The mixture was then allowed to warm to room temperature, concentrated under reduced pressure and the corresponding product was purified by flash chromatography (DCM/Hexane 3/1).

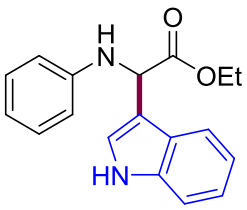

(63aa)

Ethyl 2-(1*H*-indol-3-yl)-2-(phenylamino)acetate (63aa). Following the general procedure, using *N*-phenylglycine ethyl ester (**61a**) (1.00 mmol, 179.1 mg) and indole (0.50 mmol, 58.6 mg) provided 96 mg (65% yield) of **63aa** as a yellow oil. The spectroscopic data correspond to those previously reported in the literature.[76] ^{1}H NMR (400 MHz, $CDCl_3$) δ 8.17 (br s, 1H), 7.84 (d, J = 7.8 Hz, 1H), 7.30 (d, J = 7.9 Hz, 1H), 7.26 – 7.09 (m, 5H), 6.74 (t, J = 7.3 Hz, 1H), 6.65 (d, J = 7.8 Hz, 2H), 5.40 (s, 1H), 4.69 (br s, 1H) 4.32 – 4.07 (m, 2H), 1.21 (t, J = 7.1 Hz, 3H).^{13}C NMR (101 MHz, $CDCl_3$) δ 172.7, 146.5, 136.5, 129.2, 125.7, 123.2, 122.4, 119.9, 119.5,

[76] Jiang, B.; Huang, Z.-G. *Synthesis* **2005**, *13*, 2198.

118.1, 113.4, 112.3, 111.4, 61.6, 54.3, 14.1.

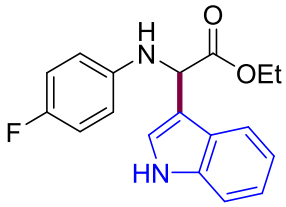

(63ba)

Ethyl 2-[(4-fluorophenyl)amino]-2-(1*H*-indol-3-yl)acetate (63ba). Following the general procedure, using *N*-(4-fluorophenyl)glycine ethyl ester (1.0 mmol, 197.1 mg) and indole (0.50 mmol, 58.6 mg) provided 82 mg (52% yield) of **63ba** as a white solid. (hexanes/EtOAc 9/1). Mp 122 ºC, (Lit. 128-130 ºC). The spectroscopic data correspond to those previously reported in the literature.[77] ^{1}H NMR (400 MHz, $CDCl_3$) δ 8.25 (br s, 1H), 7.89 (d, J = 7.8 Hz, 1H), 7.42 (d, J = 7.9 Hz, 1H), 7.27 (dq, J = 14.7, 7.7, 7.2 Hz, 2H), 6.92 (t, J = 8.7 Hz, 2H), 6.64 (dd, J = 8.9, 4.3 Hz, 2H), 5.40 (s, 1H), 4.66 (br s, 1H), 4.39 – 4.14 (m, 2H), 1.28 (t, J = 7.1 Hz, 3H). ^{13}C NMR (101 MHz, $CDCl_3$) δ 172.5, 155.8 (d, J = 242.4 Hz), 142.8, 136.4, 125.7, 123.0, 122.6, 120.0, 119.5, 115.6 (d, J = 23.2 Hz), 114.3 (d, J = 5.0 Hz), 112.4, 111.4, 61.6, 54.8, 14.1.

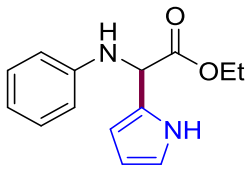

(63ad)

Ethyl 2-(phenylamino)-2-(1*H*-pyrrol-2-yl)acetate (63ad). Following the general procedure, using *N*-phenylglycine ethyl ester (1.00 mmol, 179.1 mg) and pyrrole (0.50 mmol, 35 µL) provided 58 mg (48 % yield) of **63ad** as a colorless oil. (hexanes/EtOAc 9/1). ^{1}H NMR (400 MHz, MeCN-d_3) δ 9.10 (br s, 1H), 6.92 (t, J = 7.9 Hz, 2H), 6.57 – 6.39 (m, 4H), 5.92 (s, 1H), 5.85 (q, J = 2.8 Hz, 1H), 4.99 (d, J = 7.4 Hz, 1H), 4.82 (s, 1H), 4.06 – 3.83 (m, 2H), 0.99 (t, J = 7.1 Hz, 3H).^{13}C NMR (101 MHz, MeCN-d_3) δ 172.8, 148.4, 130.5, 128.4, 119.7, 119.4, 114.8, 109.5, 108.3, 62.9, 56.2, 14.9. IR (neat, cm^{-1}): 3388, 2980, 1724, 1601, 1502, 1307, 1179, 1021, 722, 691. MS (ESI$^-$) *m/z* (%) 319 (M+HCO_2H-H). HRMS *calcd.* for ($C_{15}H_{17}N_2O_3$): 319.1294, *found* 319.1294 (formic acid comes from the mobile phase).

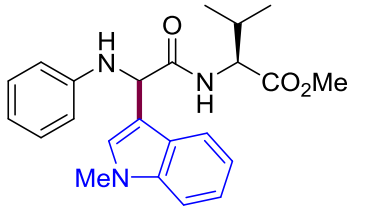

(67a)

[77] Jadhav, S. D.; Singh, A. *J. Org. Chem.* **2016**, *81*, 522.

Methyl [2-(1-methyl-1*H*-indol-3-yl)-2-(phenylamino)acetyl]-*L*-valinate (67a). Following the general procedure, using peptide **66a** (0.50 mmol, 132 mg) and *N*-methyl indole (0.50 mmol, 62 µL) provided 91 mg (92% yield) of **67a** as a white solid. Mp = 149-150°C. (dr = 2:1). ^{1}H NMR (400 MHz, $CDCl_3$) δ 7.74 – 7.66 (m, 1H), 7.62 – 7.50 (m, 1H), 7.40 – 7.13 (m, 6H), 6.87 (t, *J* = 7.4 Hz, 1H), 6.74 (d, *J* = 8.0 Hz, 2H), 5.14 (s, 1H), 4.69 – 4.58 (m, 1H), 3.81 (s, 3H), 3.77 (s, 2H), 3.63 (s, 1H), 2.30 – 2.16 (m, 1H), 0.94 (dd, *J* = 12.8, 6.9 Hz, 2H), 0.87 (d, *J* = 6.9 Hz, 2H), 0.75 (d, *J* = 6.9 Hz, 2H).^{13}C NMR (101 MHz, $CDCl_3$) δ 172.6, 172.4, 172.1, 171.9, 147.4, 147.1, 137.6, 137.4, 129.6, 129.5, 128.1, 127.9, 126.5, 126.2, 122.5, 122.4, 120.0, 119.5, 119.5, 119.4, 119.3, 114.5, 114.1, 112.0, 111.8, 110.0, 109.9, 58.3, 57.7, 57.5, 57.2, 52.4, 52.2, 33.1, 31.3, 31.2, 19.3, 18.2, 17.6. IR (neat, cm^{-1}): 3360, 2962, 1738, 1655, 1602, 1506, 1206, 741. MS (ESI^{+}) *m/z* (%) 394 (M+H). HRMS *calcd.* for ($C_{23}H_{28}N_3O_3$): 394.2131, *found* 394.2128. HPLC for the compounds (D, L) and (L, L) configurations (Chiralpak IC; 80:20 Hexane: isopropanol; 1 mL/min, λ = 210 nm). t_R =18.8 min, t_R = 37.6 min.

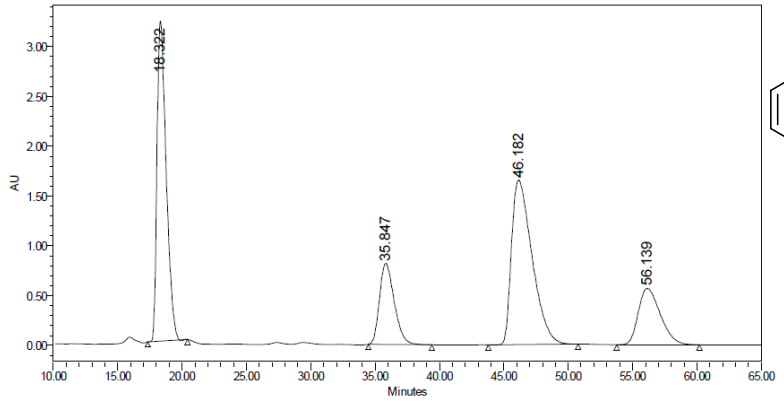

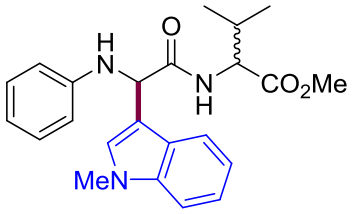

	RT	Area	% Area	Height
1	18.322	159306519	33.58	3208629
2	35.847	64649562	13.63	812235
3	46.182	183335796	38.65	1649760
4	56.139	67052046	14.14	565731

Chiralpak IC; 80:20 Hexane: isopropanol; 1 mL/min, λ = 210 nm)

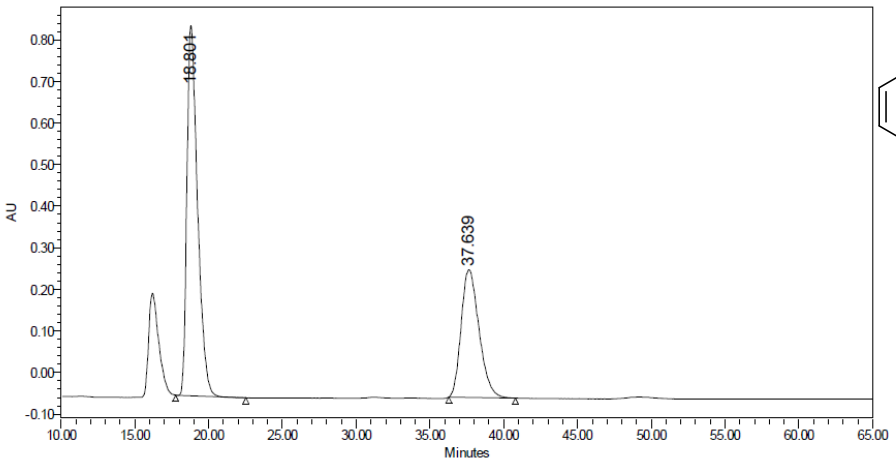

	RT	Area	% Area	Height
1	18.801	44644028	63.32	889487
2	37.639	25860929	36.68	307025

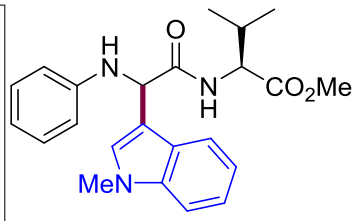

(67a)

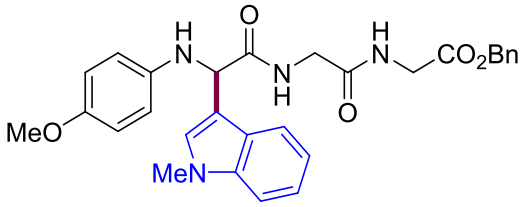

(67e)

Benzyl [2-((4-methoxyphenyl)amino)-2-(1-methyl-1*H*-indol-3-yl)acetyl]glycylglycinate (67e). Following the general procedure, using peptide **66e** (0.50 mmol, 193 mg) and *N*-methyl indole (0.50 mmol, 62 µL) provided 59 mg (46%) of **67e** as a brown solid. Mp = 48 °C. ^{1}H NMR (400 MHz, $CDCl_3$) δ 7.84 (t, J = 6.0 Hz, 1H), 7.67 (d, J = 7.8 Hz, 1H), 7.46 – 7.22 (m, 7H), 7.13 (t, J = 7.5 Hz, 1H), 6.82 (d, J = 8.8 Hz, 2H), 6.67 (d, J = 8.8 Hz, 2H), 5.18 (s, 2H), 5.10 (s, 1H), 4.22 – 4.06 (m, 1H), 4.03 – 3.83 (m, 4H), 3.76 (s, 3H), 3.75 (s, 3H).^{13}C NMR (101 MHz, $CDCl_3$) δ 173.5, 169.5, 169.3, 153.4, 141.1, 137.3, 135.3, 128.8, 128.7, 128.4, 127.8, 126.2, 122.4, 120.0, 119.0, 115.1, 115.0, 111.7, 109.8, 67.3, 58.1, 55.8, 43.2, 41.2, 32.9 ppm. IR (neat, cm^{-1}): 3349, 3041, 2932, 2831, 1745, 1662, 1510, 1238, 1191, 743. HRMS *calcd.* for ($C_{29}H_{30}N_4O_5$): 515.2216, *found* 515.2213.

2.6.2. General Procedure: Fe-Catalyzed C(sp^3)–H Aminocarbonylation

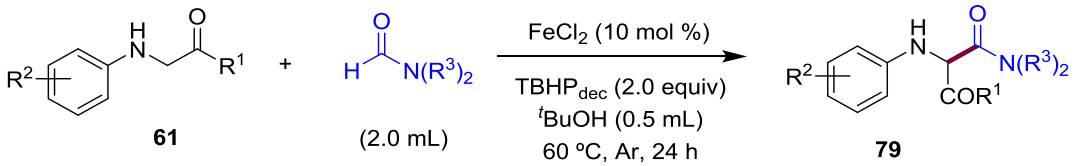

A reaction tube containing a stirring bar was charged with the corresponding α-amino carbonyl compound **61** (if solid) (0.5 mmol, 1.0 equiv) and $FeCl_2$ (10 mol %). The reaction tube was then evacuated and back-filled with dry argon (this sequence was repeated up to three times). The corresponding α-amino carbonyl compound **61** (if liquid) (0.5 mmol, 1.0 equiv), a solution of TBHP in decane (5.0-6.0 M in decane) (2.0 equiv.), the corresponding formamide (2.0 mL) and *tert*-butanol (0.5 mL) were then added under argon atmosphere. The reaction tube was next warmed up to 60 ºC and stirred for 24 hours. The mixture was then allowed to warm to room temperature, concentrated under reduced pressure and the corresponding product was purified by flash chromatography (hexanes/AcOEt 7/3), unless otherwise indicated.

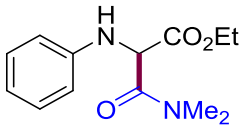

79a

Ethyl (R)-3-(dimethylamino)-3-oxo-2-(phenylamino)propanoate (79a). Following the general procedure, using *N*-phenylglycine ethyl ester (**61a**) (0.5 mmol, 89.6 mg) provided 81 mg (65 % yield) of **79a** as white solid. ^{1}H NMR (400 MHz, $CDCl_3$) δ 7.27 – 7.12 (m, 1H), 6.78 (t, *J* = 7.3 Hz, 1H), 6.69 (d, *J* = 7.7 Hz, 1H), 5.03 (s, 1H), 4.22 (qq, *J* = 7.6, 3.6 Hz, 1H), 3.21 (s, 11H), 3.04 (s, 2H), 1.22 (t, *J* = 7.1 Hz, 2H). ^{13}C NMR (101 MHz, $CDCl_3$) *δ* 168.7, 166.2, 145.9, 129.3, 118.7, 113.7, 62.1, 58.6, 37.3, 36.4, 14.1. HRMS *calcd.* for ($C_{13}H_{18}N_2O_3$): 250.1317, *found* 250.1307.

2.6.3. NMR spectra

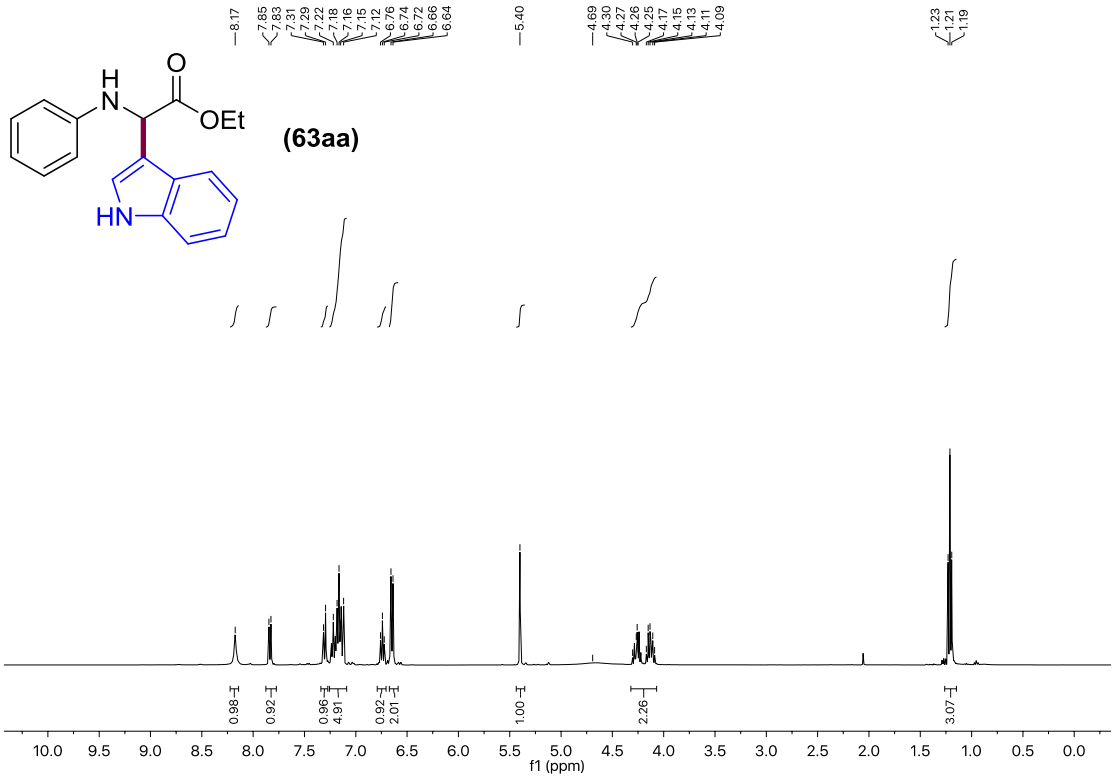

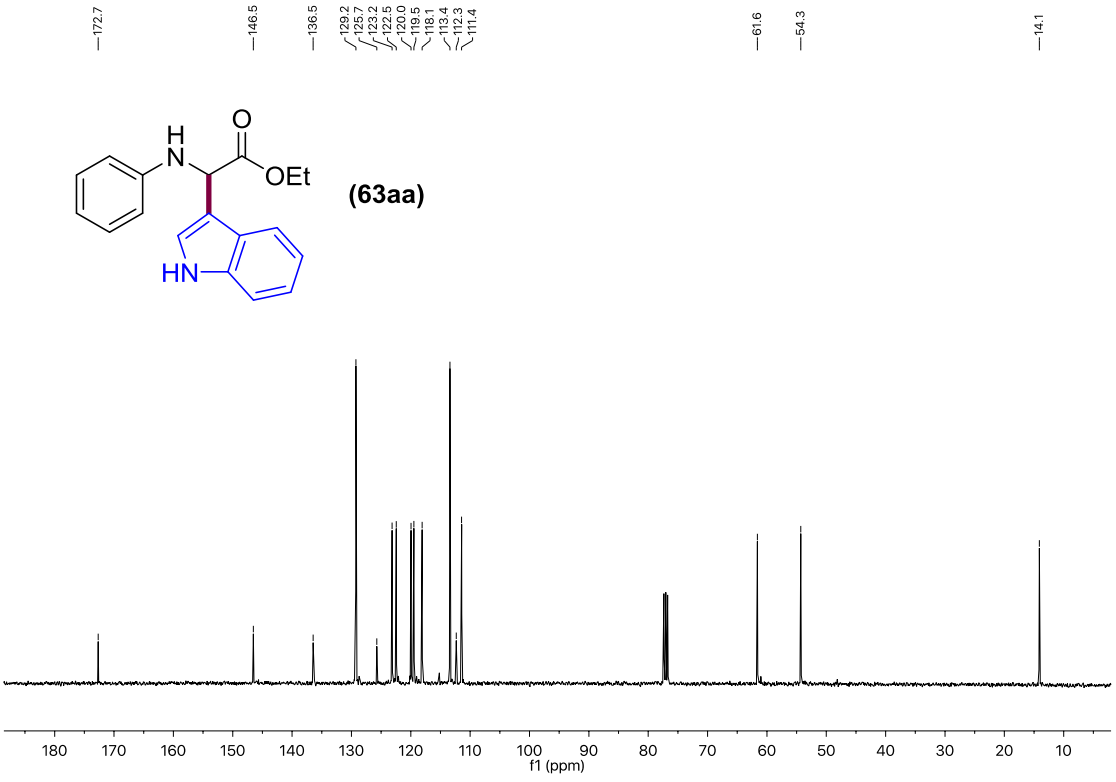

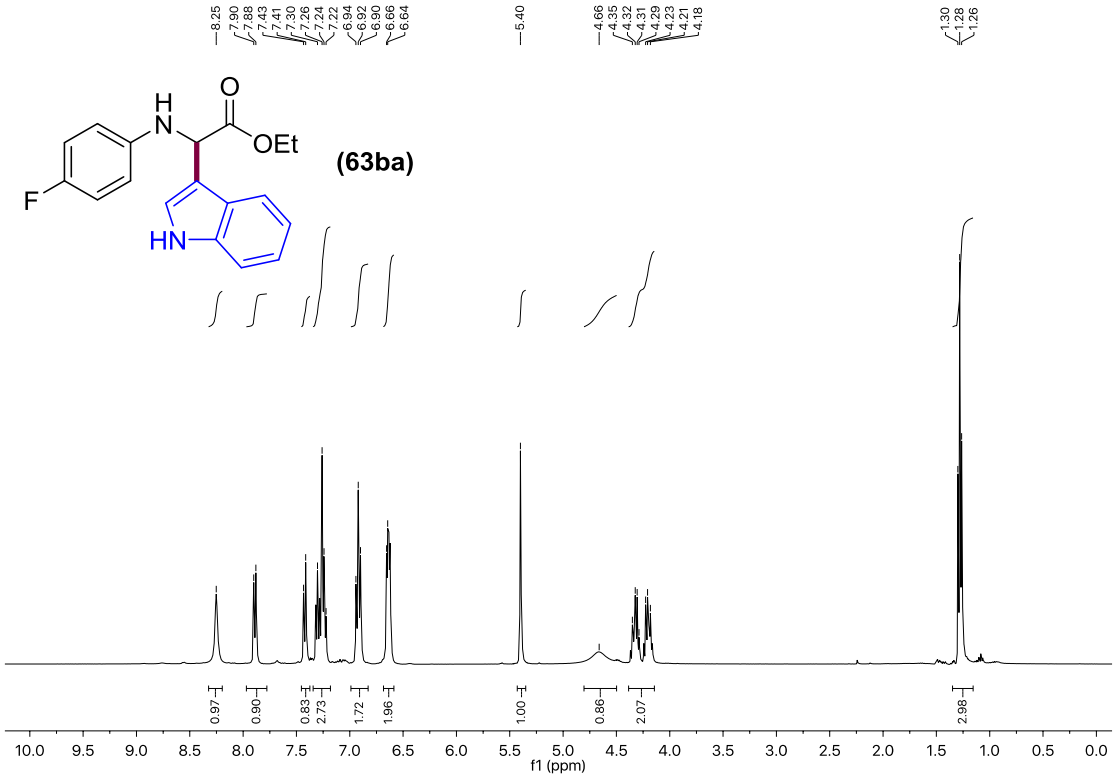
8.25
7.90
7.88
7.43
7.41
7.30
7.26
7.24
7.22
6.94
6.92
6.90
6.66
6.64
5.40
4.66
4.35
4.32
4.31
4.29
4.23
4.21
4.18
1.30
1.28
1.26
H
N
O
OEt
F
HN
(63ba)
0.97
0.90
0.83
2.73
1.72
1.96
1.00
0.86
2.07
2.98
10.0
9.5
9.0
8.5
8.0
7.5
7.0
6.5
6.0
5.5
5.0
4.5
4.0
3.5
3.0
2.5
2.0
1.5
1.0
0.5
0.0
f1 (ppm)

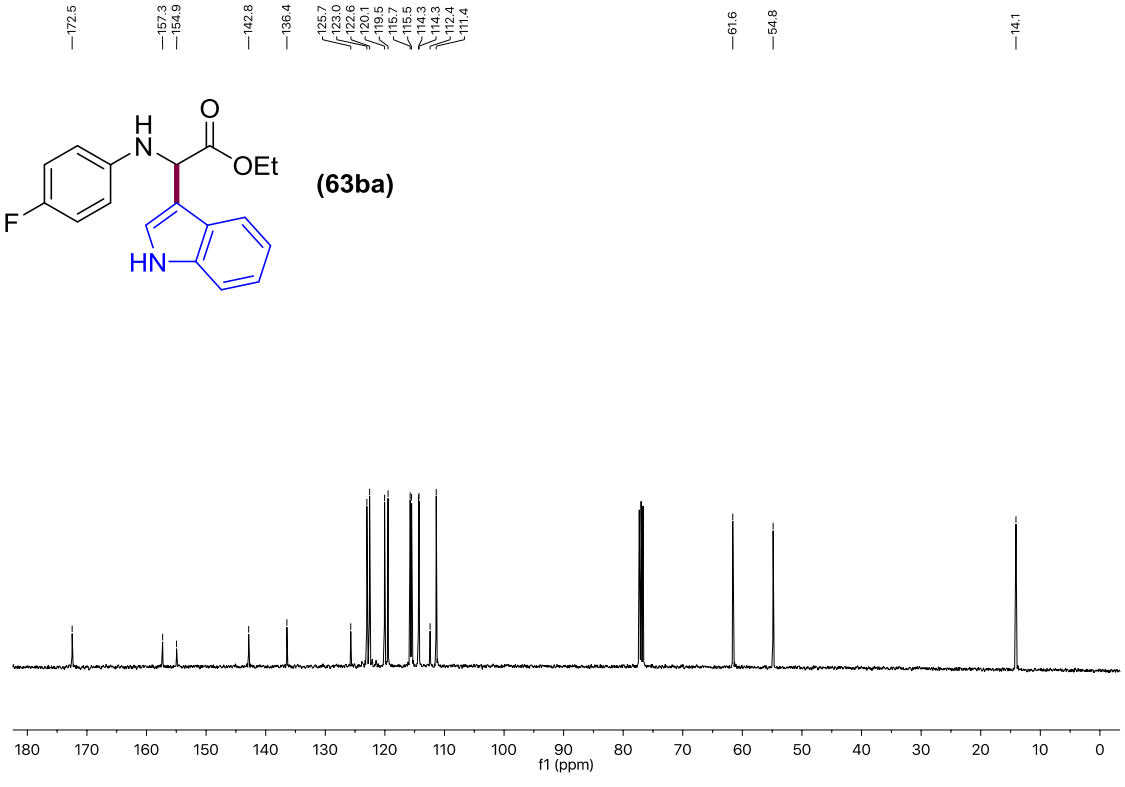
172.5
157.3
154.9
142.8
136.4
125.7
123.0
122.6
120.1
119.5
115.7
115.5
114.3
114.3
112.4
111.4
61.6
54.8
14.1
H
N
O
OEt
F
HN
(63ba)
180
170
160
150
140
130
120
110
100
90
80
70
60
50
40
30
20
10
0
f1 (ppm)

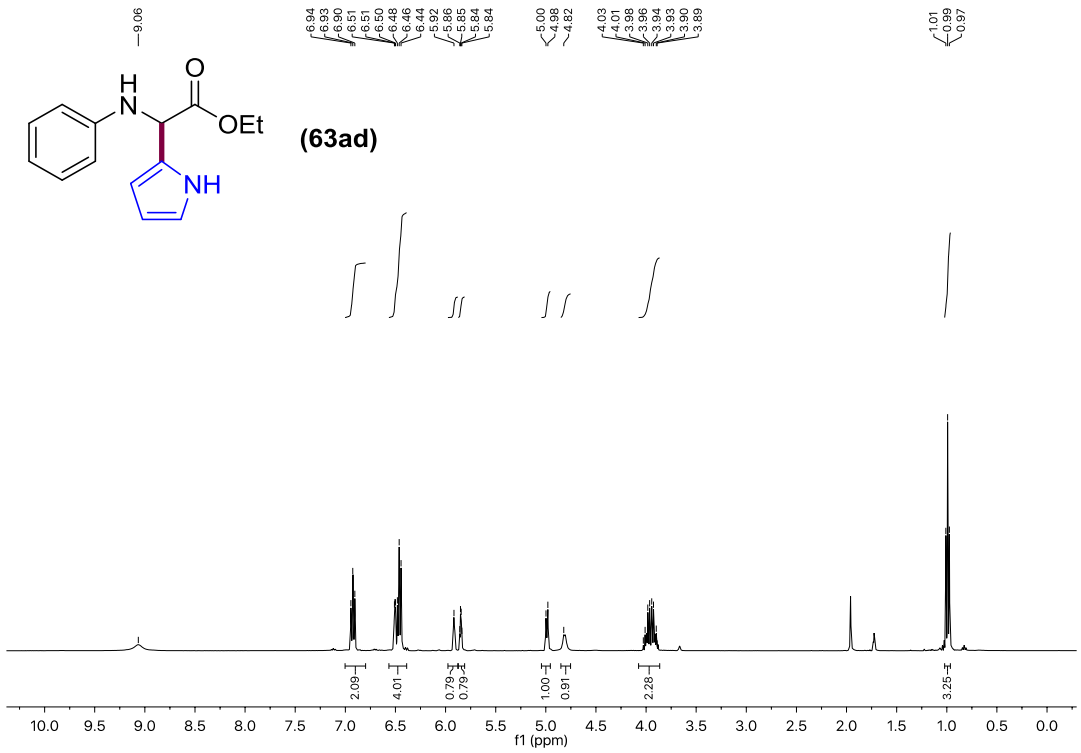
9.06
6.94
6.93
6.90
6.51
6.51
6.50
6.48
6.46
6.44
5.92
5.86
5.85
5.84
5.84
5.00
4.98
4.82
4.03
4.01
3.98
3.96
3.94
3.93
3.90
3.89
1.01
0.99
0.97
H
N
O
OEt
NH
(63ad)
2.09
4.01
0.79
0.79
1.00
0.91
2.28
3.25
10.0 9.5 9.0 8.5 8.0 7.5 7.0 6.5 6.0 5.5 5.0 4.5 4.0 3.5 3.0 2.5 2.0 1.5 1.0 0.5 0.0
f1 (ppm)

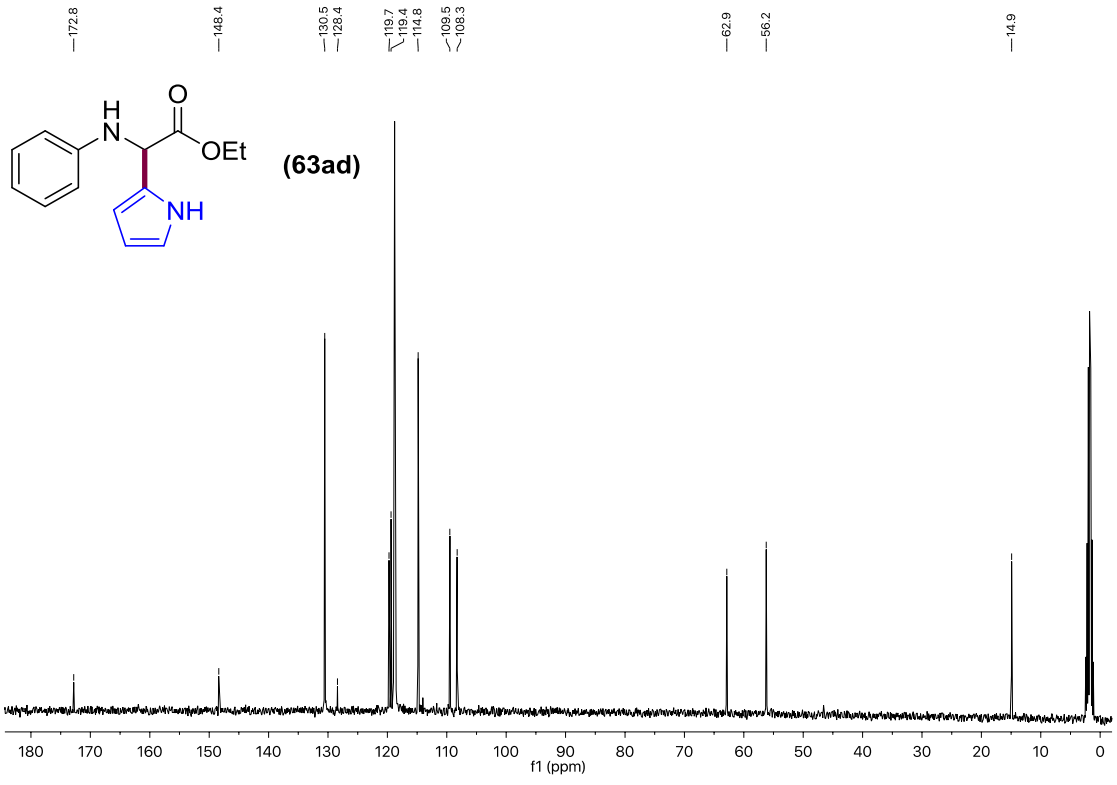
172.8
148.4
130.5
128.4
119.7
119.4
114.8
109.5
108.3
62.9
56.2
14.9
H
N
O
OEt
NH
(63ad)
180 170 160 150 140 130 120 110 100 90 80 70 60 50 40 30 20 10 0
f1 (ppm)

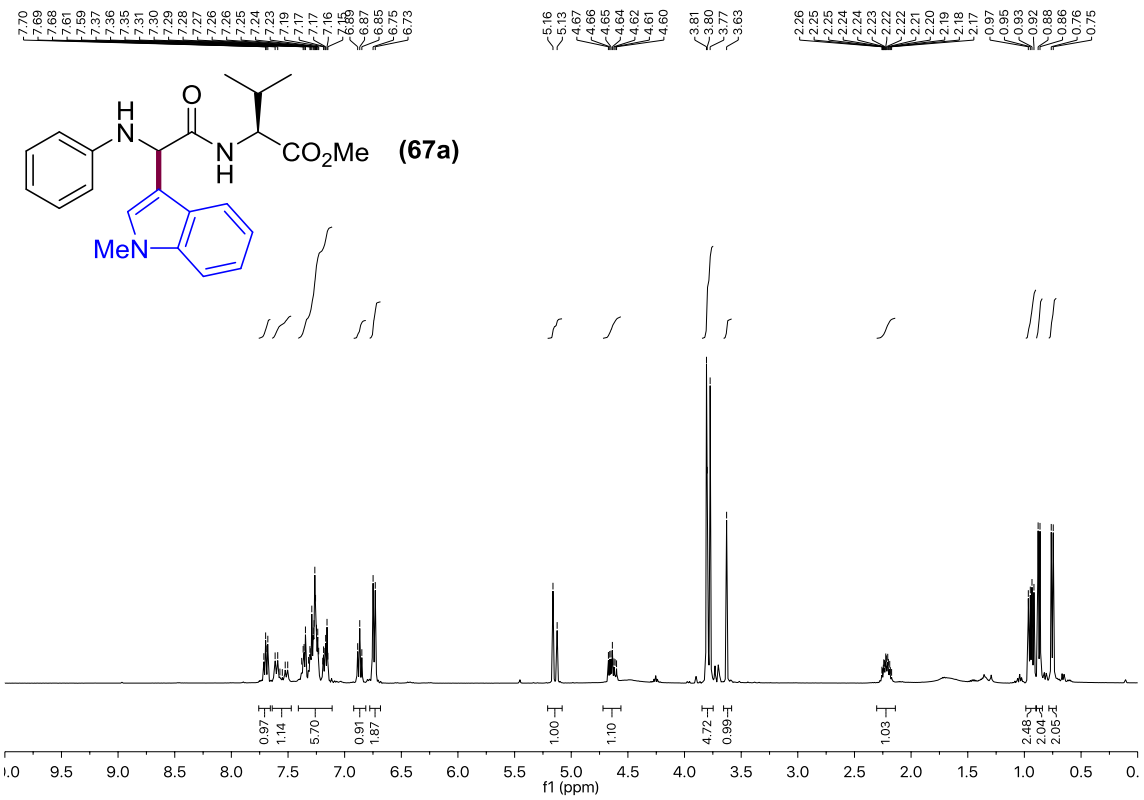
7.70 7.69 7.68 7.61 7.59 7.37 7.36 7.35 7.31 7.30 7.29 7.28 7.27 7.26 7.26 7.25 7.24 7.23 7.19 7.17 7.17 7.16 6.88 6.87 6.85 6.75 6.73
5.16 5.13 4.67 4.66 4.65 4.64 4.62 4.61 4.60
3.81 3.80 3.77 3.63
2.26 2.25 2.25 2.24 2.24 2.23 2.22 2.22 2.21 2.20 2.19 2.18 2.17
0.97 0.95 0.93 0.92 0.88 0.86 0.76 0.75
H N O N H CO2Me (67a)
MeN
0.97 1.14 5.70 0.91 1.87 1.00 1.10 4.72 0.99 1.03 2.48 2.04 2.05
f1 (ppm)

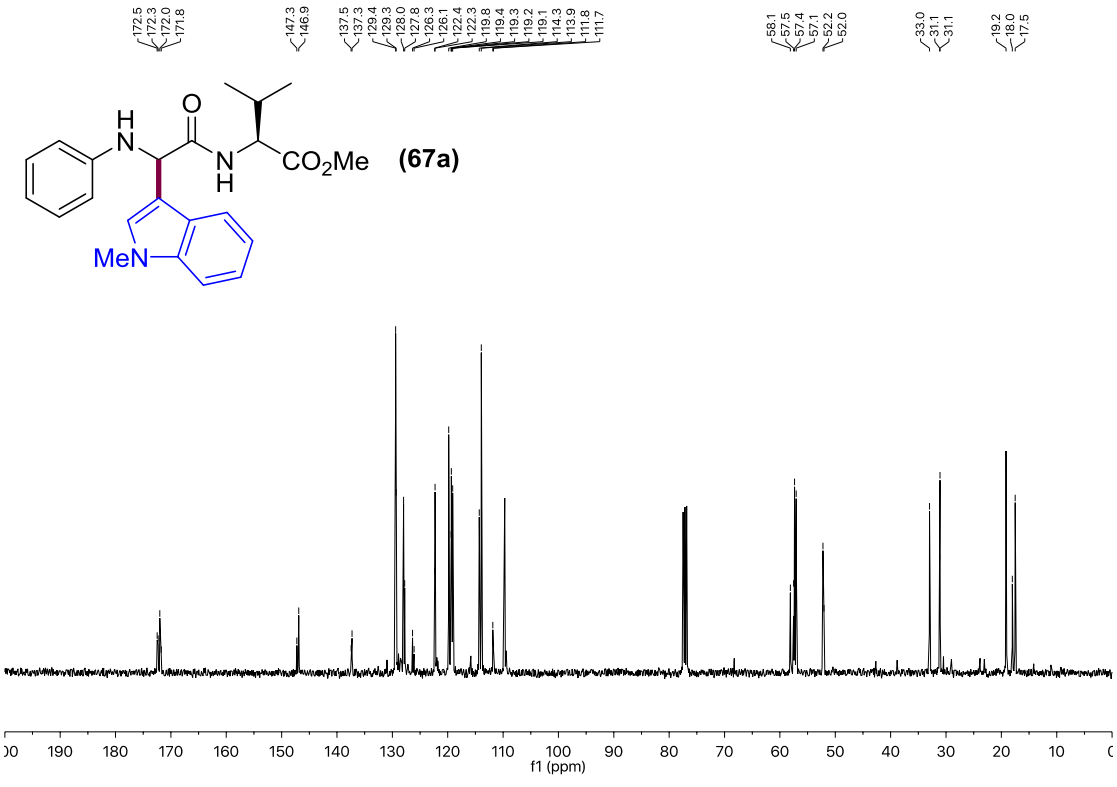
172.5 172.3 172.0 171.8
147.3 146.9
137.5 137.3 129.4 129.3 128.0 127.8 126.3 126.1 122.4 122.3 119.8 119.4 119.3 119.2 119.1 114.3 113.9 111.8 111.7
58.1 57.5 57.4 57.1 52.2 52.0
33.0 31.1 31.1
19.2 18.0 17.5
H N O N H CO2Me (67a)
MeN
f1 (ppm)

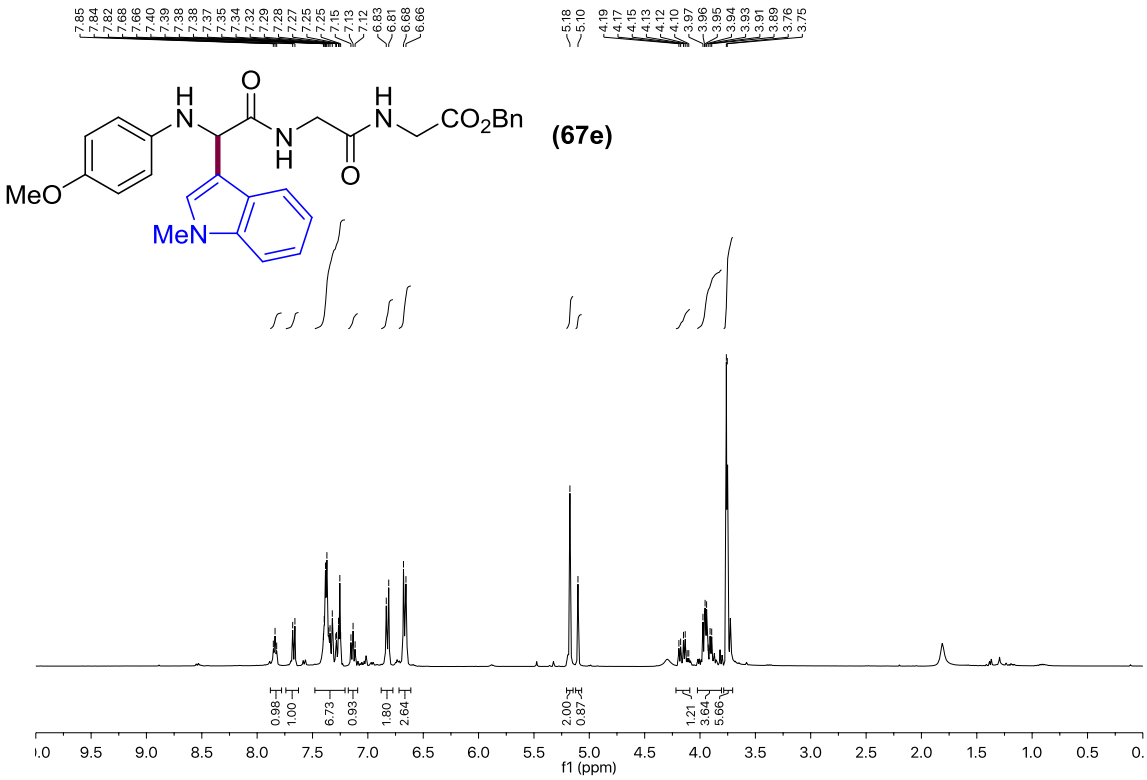
7.85
7.84
7.82
7.68
7.66
7.40
7.39
7.38
7.38
7.37
7.35
7.34
7.32
7.29
7.28
7.27
7.25
7.25
7.15
7.13
7.12
6.83
6.81
6.68
6.66
5.18
5.10
4.19
4.17
4.15
4.13
4.12
4.10
3.97
3.96
3.95
3.94
3.93
3.91
3.89
3.76
3.75
H
N
O
N
H
H
N
O
CO2Bn
MeO
MeN
(67e)
0.98
1.00
6.73
0.93
1.80
2.64
2.00
0.87
1.21
3.64
5.66
f1 (ppm)

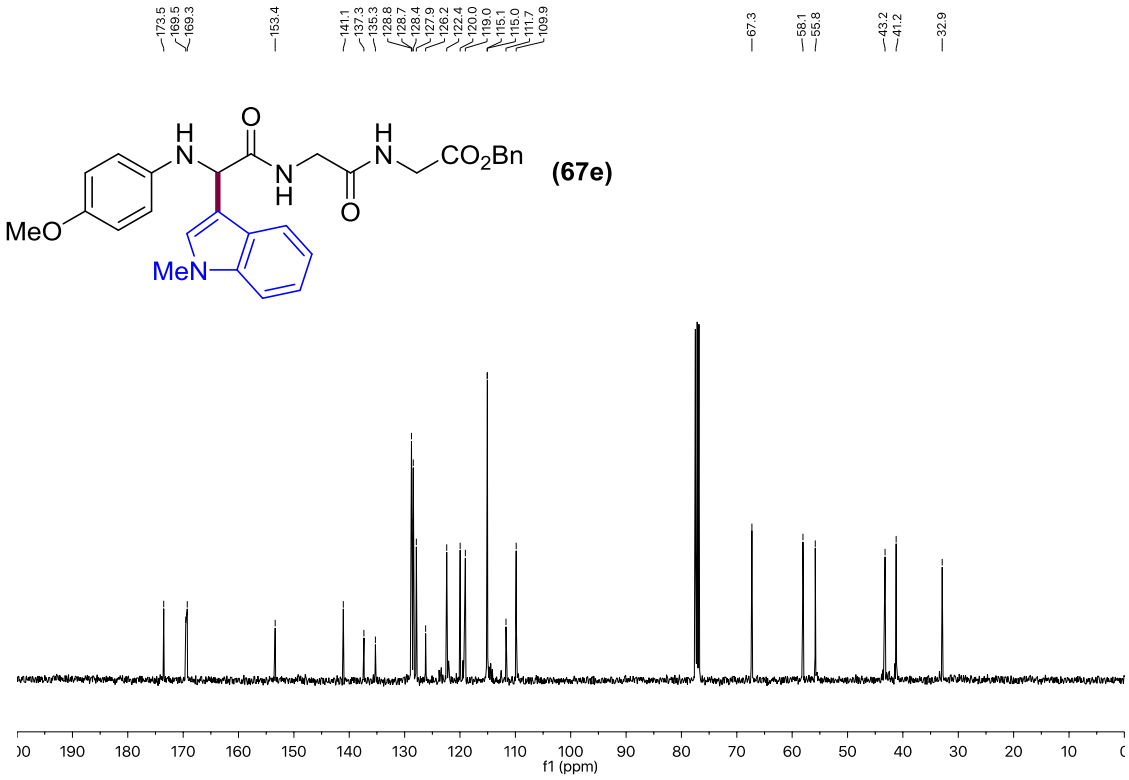
173.5
169.5
169.3
153.4
141.1
137.3
135.3
128.8
128.7
128.4
127.9
126.2
122.4
120.0
119.0
115.1
115.0
111.7
109.9
67.3
58.1
55.8
43.2
41.2
32.9
H
N
O
N
H
H
N
O
CO2Bn
MeO
MeN
(67e)
f1 (ppm)

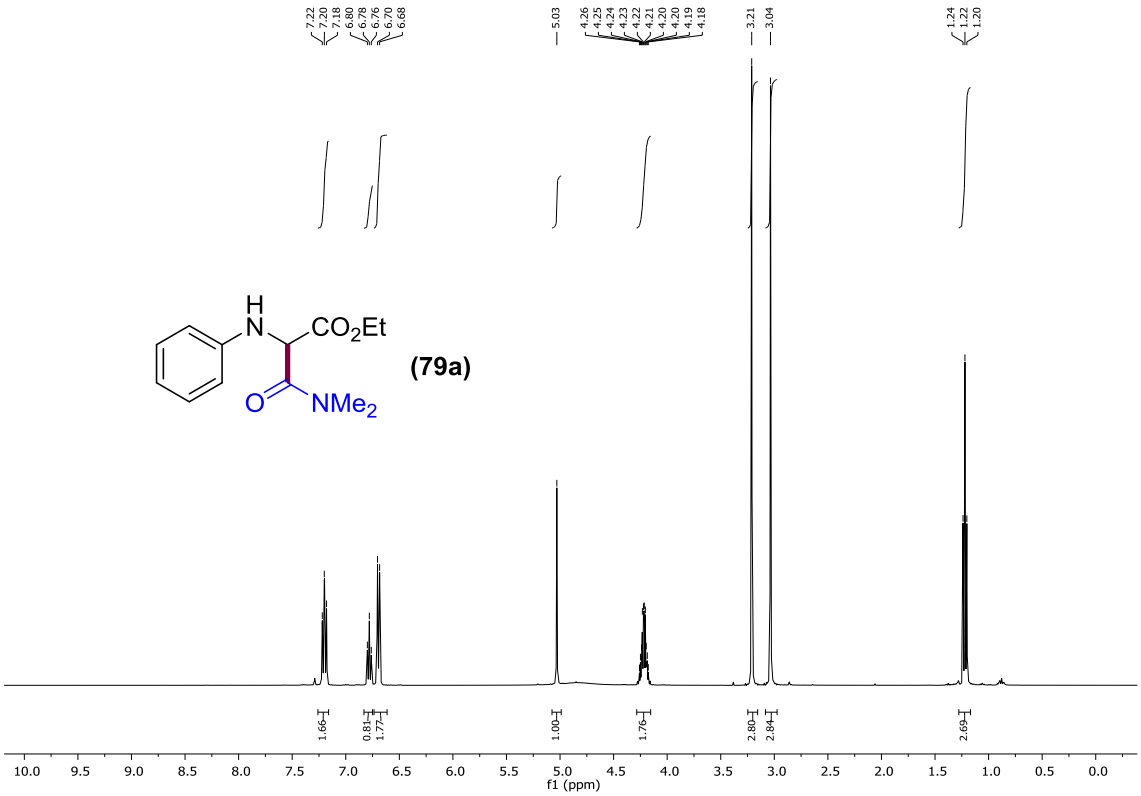
7.22
7.20
7.18
6.80
6.78
6.76
6.70
6.68
5.03
4.26
4.25
4.24
4.23
4.22
4.21
4.20
4.20
4.19
4.18
3.21
3.04
1.24
1.22
1.20
H
N
CO2Et
O
NMe2
(79a)
1.66
0.81
1.77
1.00
1.76
2.80
2.84
2.69
10.0 9.5 9.0 8.5 8.0 7.5 7.0 6.5 6.0 5.5 5.0 4.5 4.0 3.5 3.0 2.5 2.0 1.5 1.0 0.5 0.0
f1 (ppm)

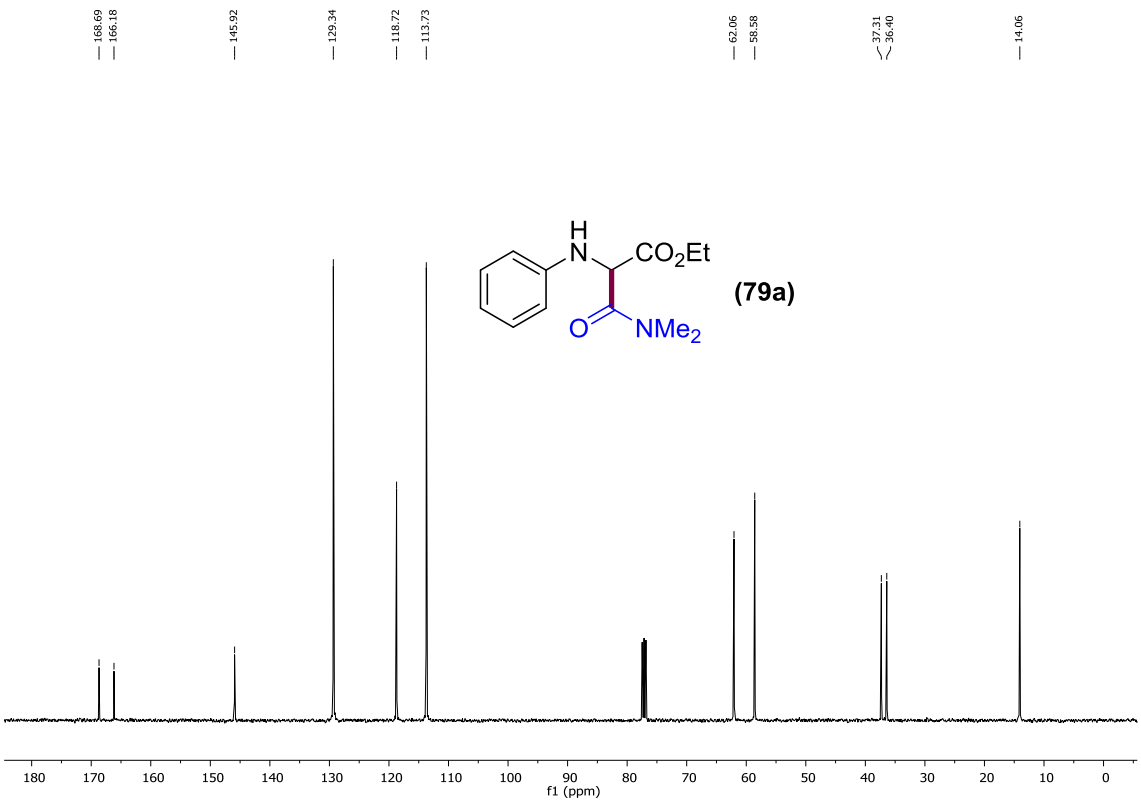
168.69
166.18
145.92
129.34
118.72
113.73
62.06
58.58
37.31
36.40
14.06
H
N
CO2Et
O
NMe2
(79a)
180 170 160 150 140 130 120 110 100 90 80 70 60 50 40 30 20 10 0
f1 (ppm)

Chapter 3.

Iron-Catalyzed C(sp^3)–H Functionalization of *N,N*-Dimethylanilines with Isocyanides

3.1 Introduction

3.1.1. Multicomponent reactions for molecular diversity: Ugi reaction

Convergent reactions with the combination of three or more starting materials leading to a single new multi-substituted product are termed multicomponent reactions (MCRs). The development of these one-pot protocols for the creation of biologically active molecules' libraries increases steadily as they provide processes where multiple bonds are formed simultaneously omitting the isolation of intermediates. Hence, being highly convergent and atom- and step-efficient reactions.[78]

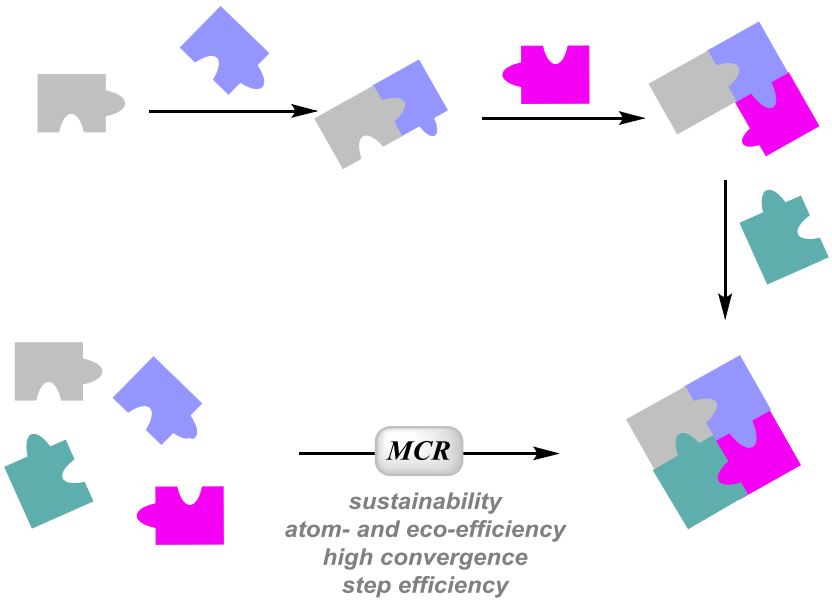

Scheme 44 Multicomponent Reactions (MCR).

After the pioneering discovery of the Strecker reaction (1850),[79] which allowed the formation of α-aminonitrile and its further transformation to α-amino acids by hydrolysis, Hantzsch 3- and 4-component reactions (1882),[80] the Biginelli-3CR (1893),[81] the Mannich-3CR (1912),[82] the Passerini-3CR (1921)[83] and the Ugi-4CR (1959)[84] have been among the most influential multicomponent reactions (Scheme 45). Over the past decades, the

[78] a) Rotstein, B. H.; Zaretsky, S.; Rai, V.; Yudin, A. K. *Chem. Rev*. **2014**, *114*, 8323. b) Brauch, S.; Van Berkel, S. S.; Westermann, B. *Chem. Soc. Rev*. **2013**, *42*, 4948.
[79] Strecker, A. *Ann. Chem. Pharm.* **1850**, *75*, 27.
[80] Hantzsch, A. *Justus Liebigs Ann. Chem*. **1882**, *215*, 1.
[81] Biginalli, P. *Ber. Dtsch. Chem. Ges*. **1891**, *24*, 1317.
[82] Mannich, C.; Krosche, W. *Arch. Pharm.* **1912**, *250*, 647.
[83] Passerini, M.; Simone, L. *Gazz. Chim. Ital.* **1921**, *51*, 126.
[84] Ugi, I. *Angew. Chem. Int. Ed. Engl.* **1962**, *1*, 8.

advancement of these reactions has gained great significance as they supply the access to very important organic compounds of high demand in the domain of drug discovery such as substituted pyridines, dihydropyrimidinones or β-amino carbonyl compounds.

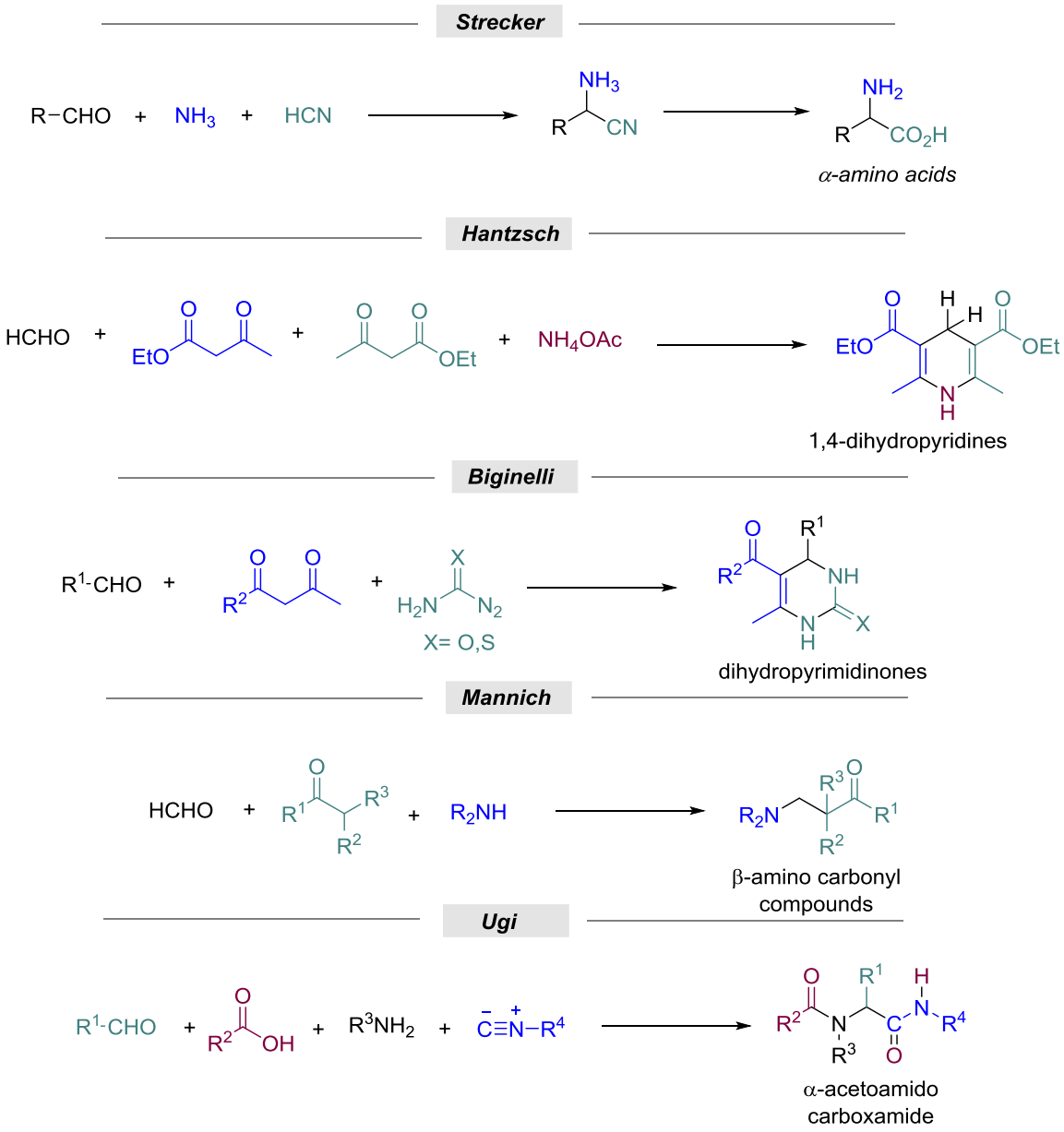

Scheme 45 Different Multicomponent Reactions.

In particular, the last mentioned Ugi multicomponent reaction is a versatile protocol to afford α-acetoamido carboxamide derivatives by the combination of an aldehyde, an amine, an isocyanide and a carboxylic acid. This 4-CR is a well-stablished method with a wide variety of applications like the synthesis of relevant *N*-

heterocycles,[85] functional chromophores or agrochemicals,[86] among many other usages of Ugi adducts, also referred to as peptoids in the field of organic chemistry.[87] In Scheme 46, a recent methodology developed by Cheibas *et al.* is depicted, which proved the still current interest for a practical synthesis of bis-β-lactam derivatives **5** afforded via Ugi MCR.[88] Albeit in moderate yields, an ample range of starting materials resulted compatible with the protocol to end up in bioactive products bearing functional groups such as halogens (**5a**), pyridine ring (**5b**) or even allylic groups (**5a**) that could take part in a further Diels-Alder reaction.

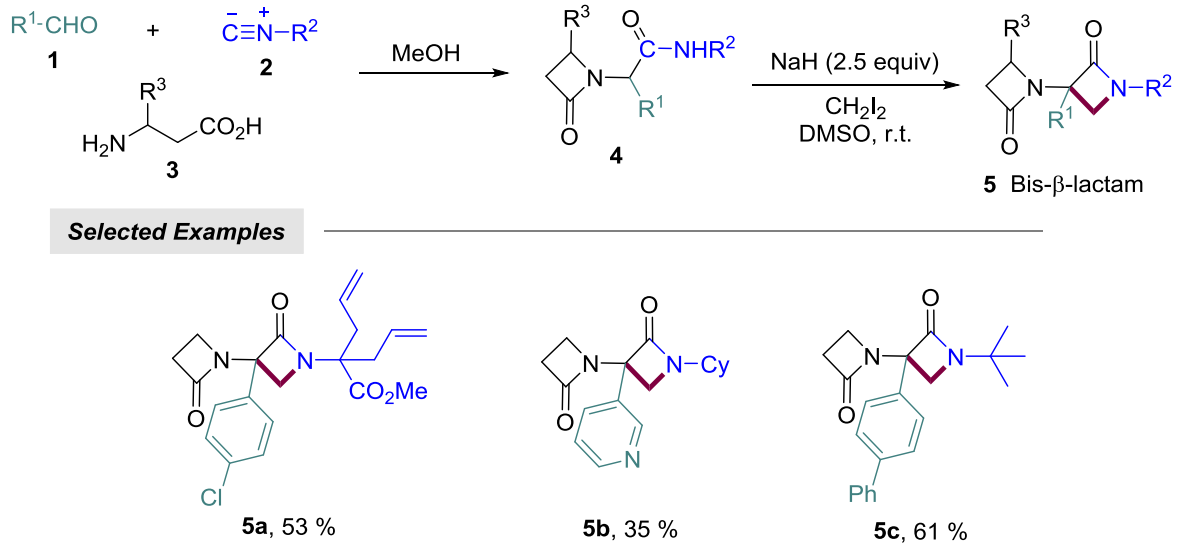

Scheme 46 Synthesis of Bis- β-Lactam Derivatives through Ugi Reaction.

Those post-Ugi transformations have become functional strategies for the diversification of complex molecules with often biomedical applications. Hence, secondary functional groups in Ugi substrates are crucial for the extension of the versatile multicomponent reaction to additional steps for the synthesis of more complex molecular libraries.[89] As an example, the use of alkyne-containing starting materials could open the way for cascade cyclizations. Van der Eycken and co-workers reported an efficient approach to convert Ugi-4CR adducts (**10**) into triazolo[1,5-*a*][1,4]benzodiazepinones (**11**) by a copper-catalyzed azide-alkyne cycloaddtion/Ullmann coupling (Scheme 47).[90] In particular, the use of a Cu(I) salt and sodium azide with the alkyne housed in compound **10**, provided the triazole-Cu species **12** through a Cu-catalyzed [3+2] cycloaddition. Then, an oxidative addition ocurred with the aryl bromide to achieve metallacycle **13**, which upon reductive

[85] Mohammadkhani, L.; Heravi, M. M. *ChemistrySelect* **2019**, *4*, 10187.
[86] Lamberth, C. *Bioorg. Med. Chem.* **2020**, *28*, 115471.
[87] Tron, G. C. *Eur. J. Org. Chem.* **2013**, 1849.
[88] Cheibas, C.; Cordier, M.; Li, Y.; El Kaïm, L. *Eur. J. Org. Chem.* **2019**, 4457.
[89] a) Cioc, R. C.; Ruijter, E.; Orru, R. V. A. *Green Chem.* **2014**, *16*, 2958. b) Dömling, A.; Wang, W.; Wang, K. *Chem. Rev.* **2012**, *112*, 3083.
[90] Vachhani, D. D.; Kumar, A.; Modha, S. G.; Sharma, S. K.; Parmar, V. S.; Van der Eycken, E. V. *Eur. J. Org. Chem.* **2013**, 1223.

elimination resulted in the formation of triazolo[1,5-*a*][1,4]benzodiazepinone **11** and the recovery of Cu(I) active catalyst.[91] More recently, a related Ugi-4CR analogue has been also described using azides instead of carboxylic acids to render in Ugi-tetrazole adducts, which are converted in a straightforward manner into 1,3,4-oxadiazoles by a Huisgen reaction.[92]

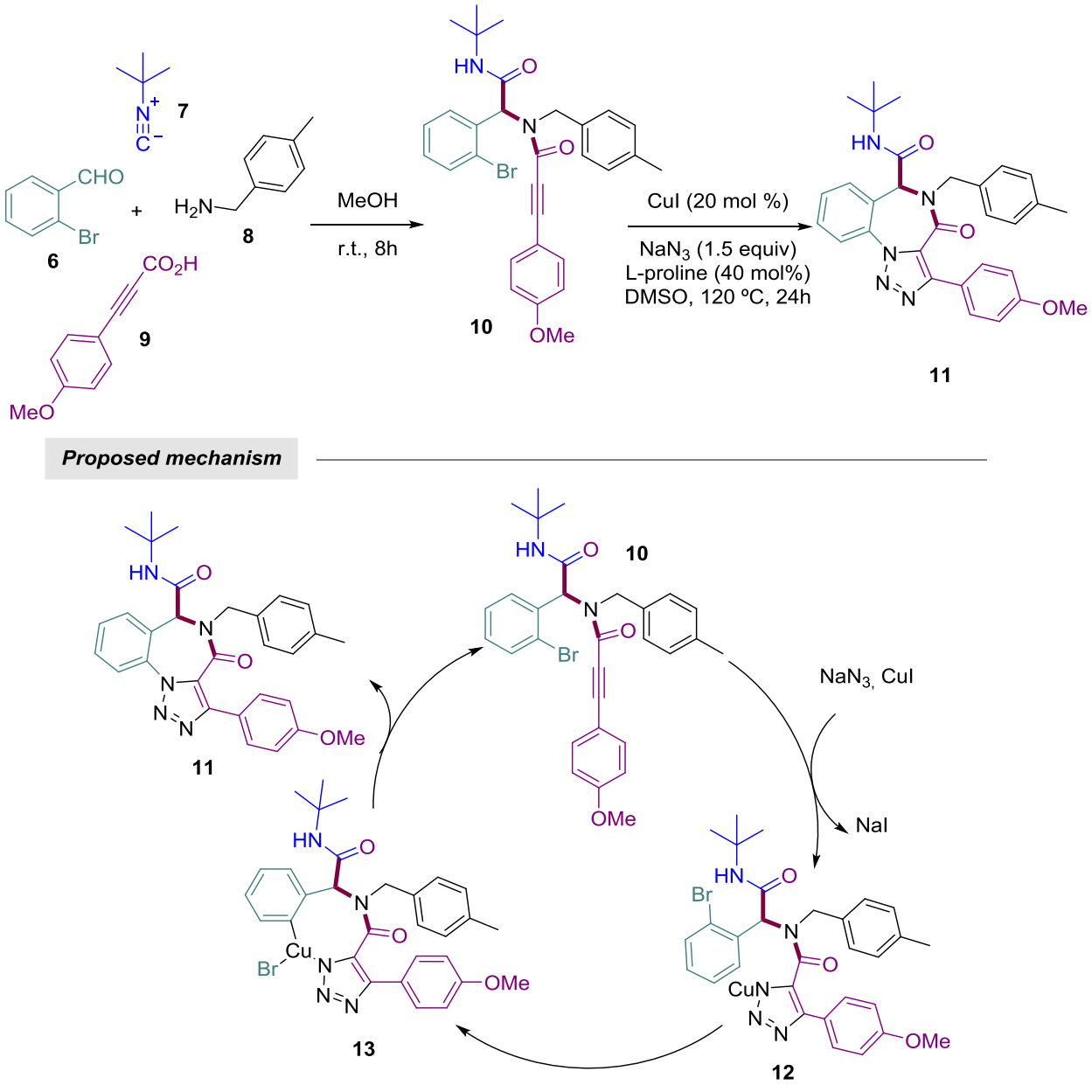

Scheme 47 Post Ugi Transformation.

[91] Yan, J.; Zhou, F.; Qin, D.; Cai, T.; Ding, K.; Cai, Q. *Org. Lett.* **2012**, *14*, 1262.
[92] Wang, Q.; Mgimpatsang, K. C.; Konstantinidou, M.; Shishkina, S. V.; Dömling, A. *Org. Lett.* **2019**, *21*, 7320.

As far as the multicomponent reactions are concerned, two (or more) convergent pathways usually exist for the formation of the same product. According to the most advanced information about the Ugi MCR mechanistic knowledge, two competitive pathways are under debate now (Scheme 48).[93]

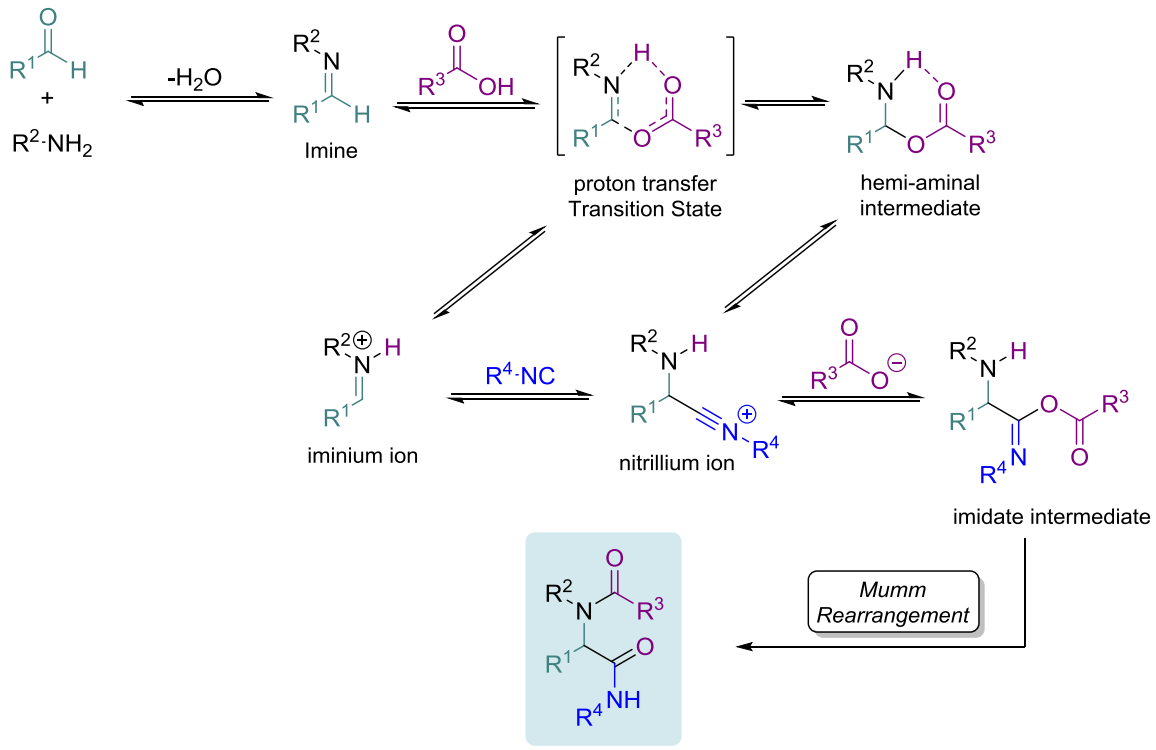

Scheme 48 Mechanistic Proposal for Ugi Reaction.

The MCR that gives access to peptide-like adducts begins with the *in situ* formation of the corresponding electrophilic imine between an amine and an aldehyde. Then, the latter reacts with the carboxylic acid to obtain a very reactive iminium ion by proton transfer, which is attacked by the isocyanide to give the nitrilium ion intermediate. This mechanistic proposal is considered the classical view of Ugi reaction. On the other hand, Fleurat-Lessard and co-workers[94] proposed a hemi-aminal alternative intermediate formed by the insertion of the carboxylic acid, which could be later on trapped by the isocyanide to reach the corresponding nitrilium ion. This cation reacts with the carboxylate ion to give an unstable imidate intermediate, which undergoes a Mumm rearrangement to afford the desired α-acetoamido carboxamide derivative. All studies agree that the reaction is more likely to occur with polar protic solvents because the intermediates are prone to form hydrogen bonds. However, while intermediates from the first mechanism were detected including the iminium ion, no hemi-aminal intermediate has been detected in mechanistic investigations carried out by ESI-MS(/MS) and charge

[93] a) Rocha, R. O.; Rodrigues, M. O.; Neto, B. A. D. *ACS Omega* **2020**, *5*, 972. b) Alvim, H. G. O.; Da Silva Júnior, E. N.; Neto, B. A. D. *RSC Adv.* **2014**, *4*, 54282.
[94] Chéron, N.; Ramozzi, R.; El Kaïm, L.; Grimaud, L.; Fleurat-Lessard, P. *J. Org. Chem*. **2012**, *77*, 1361.

tag strategy.[95] Therefore, the formation of a transient hemiaminal species has not been experimentally demonstrated.

The imine intermediate is also commonly referred to as Schiff base due to its ability to form hydrogen bonds, and could be chiral depending on the starting aldehyde or ketone applied for the Ugi reaction providing a new stereocenter. The synthesis of many natural products and potent drugs has been possible thanks to Ugi MCR, whose active isomer had to be separated by tedious and expensive procedures.[96] After the failure of several research groups, more recently, Houk and Tan developed the enantioselective phosphoric acid-catalyzed Ugi-4CR, thus overcoming the prior stereocontrol limitations (Scheme 49).[97]

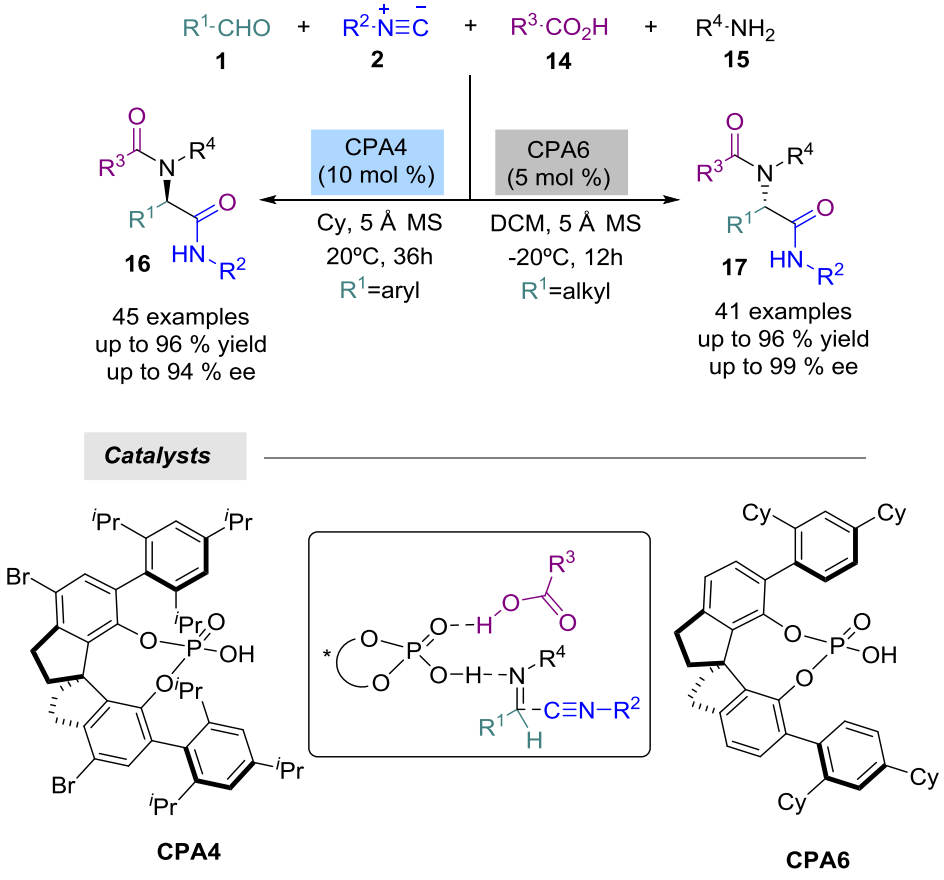

Scheme 49 Catalytic Enantioselective Ugi-4CR Reaction.

[95] a) Medeiros, G. A.; Da Silva, W. A.; Bataglion, G. A.; Ferreira, D. A. C.; de Oliveira, H. C. B.; Eberlin, M. N.; Neto, B. A. D. *Chem. Commun.* **2014**, *50*, 338. b) Iacobucci, C.; Reale, S.; Gal, J.-F.; De Angelis, F. *Eur. J. Org. Chem.* **2014**, 7087.
[96] Huang, Y.; Wolf, S.; Koes, D.; Popowicz, G. M.; Camacho, C. J.; Holak, T. A.; Dömling, A. *ChemMedChem* **2012**, *7*, 49.
[97] a) Zhang, J.; Yu, P.; Li, S.-Y.; Sun, H.; Xiang, S.-H.; Wang, J.; Houk, K. N.; Tan, B. *Science* **2018**, *361*, eaas8707. b) Shaabani, S.; Dömling, A. *Angew. Chem. Int. Ed.* **2018**, *57*, 16266.

Based on the step where imine activation through protonation leads to the generation of the iminium ion followed by nucleophilic attack of the corresponding isocyanide, they found that two chiral phosphoric acids could act as efficient organocatalysts resulting in excellent yields and *ee* values between 96-99%. The receptor side in the chiral catalyst would activate the Schiff base and facilitate the nucleophilic attack by hydrogen-bond stabilization. In this manner, **CPA4** catalyst was efficient towards aromatic aldehydes whereas **CPA6** was more suitable for aliphatic ones. Unexpectedly, no polar-protic solvent was utilized in any of the cases, which are known to stabilize iminium intermediates.[97] Without a doubt, this enantioselective methodology has supposed a major breakthrough in the realm of multicomponent reactions and it could be a guide for the development of other important assymmetric U-4CR variations such as three-component or intramolecular cyclization processes.

3.1.2. Oxidative Ugi-Type Reaction

Last years have witnessed numerous studies where the α-C–H bond adjacent to a heteroatom has been functionalized via oxidative cross-coupling reactions (as previously observed in Chapter 2). Consequently, new C–C bond-forming protocols for MCR like Mannich, Strecker or Aza-Henry are now possible thanks to this type of strategy. Likewise, oxidative cross-coupling reactions could offer some advantages to MCR such as the reduction of substrates being an atom-economical process, broadening the synthetic scope or allowing the use of milder conditions.

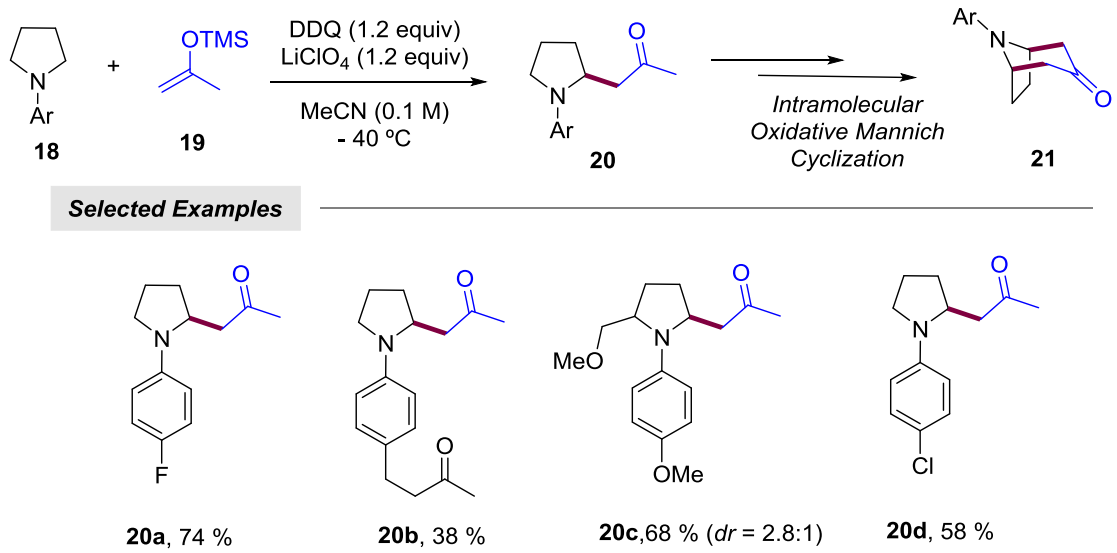

Scheme 50 Oxidative Mannich Reaction.

As a particular example, in an oxidative Mannich reaction the electrophilic imine is formed *in situ* from the corresponding *N*-alkyl amine **18**, which would avoid the intermediates' mixture resulting from having two different enolizable carbonyl compounds (Scheme 50).

As well as Mannich reaction, Ugi four-component reaction (U-4CRs) requires the condensation of an amine and an aldehyde for the *in situ* formation of the electrophilic intermediate. However, a more atom-economical oxidative multicomponent reaction wherein the iminium is generated directly from the oxidation of an amine has gained a lot of interest (Scheme 51). In this manner, the scope could be extended to other amines than primary ones.

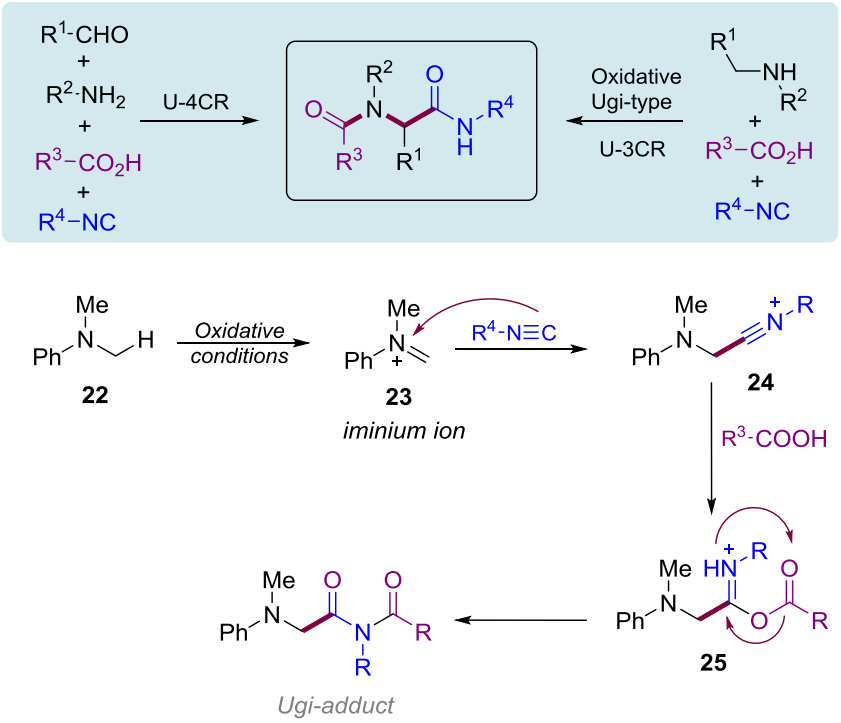

Scheme 51 Oxidative Ugi-type Reaction Mechanism.

In 2007, Zhu and Ngouansavanh reported the first oxidative *o*-iodoxybenzoic acid (IBX)-mediated three-component Ugi-type reactions for the dual acylation of tetrahydroisoquinolines **26** (Scheme 52).[98] The curiosity for organocatalytic oxidations with hypervalent iodine reagents has increased owing to their low cost, mild reaction conditions and their exceptional reactivity alternative to that of transition metal catalysts.[99] Hence, this metal-free methodology provided a short family of functionalized tetrahydroisoquinolines with a high functional group tolerance and with excellent yields. The synthesis of isoquinoline structure containing tripeptide **27b** must be highlighted.

[98] Ngouansavanh, T.; Zhu, J. *Angew. Chem. Int. Ed.* **2007**, *46*, 5775.
[99] Yoshimura, A.; Zhdankin, V. V. *Chem. Rev.* **2016**, *116*, 3328.

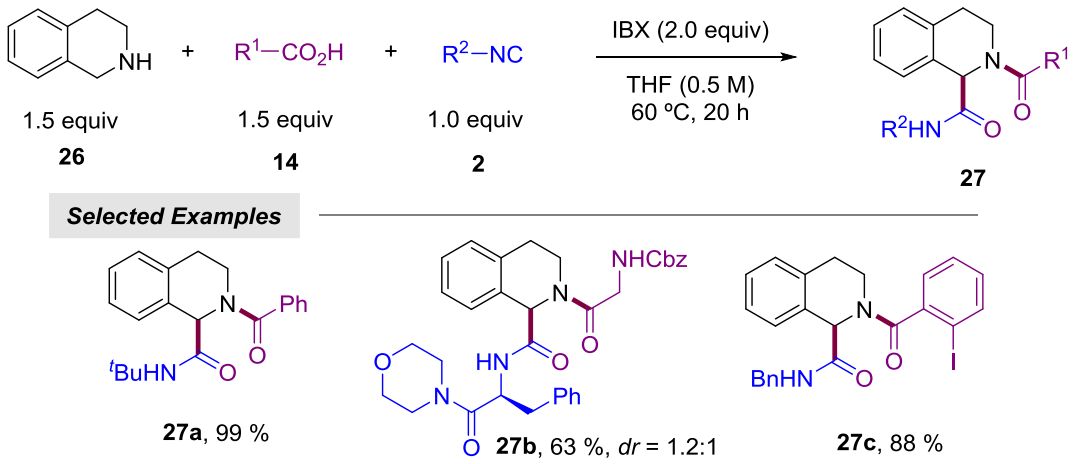

Scheme 52 IBX-Mediated Oxidative Ugi-Type Reaction to Functionalize Tetrahydroisoquinolines.

Almost a decade later, λ^5-iodane reagents were found suitable by González-Zamora and co-workers to synthesize nuevamine aza-analogues through an oxidative Ugi type 3CR followed by an aza-Diels–Alder cycloaddition.[100] There IBX was once again utilized for the oxidation of primary amines **28** to imine intermediates **29**, which after aqueous hydrolysis furnished aldehydes **31**. Further dehydration with the starting amine in the acidic medium resulted in the formation of the Schiff base **29**. The latter was isolated and reacted with the rest of Ugi reaction components, thus it was not be a one-pot multicomponent reaction as two steps were required (Scheme 53).[101]

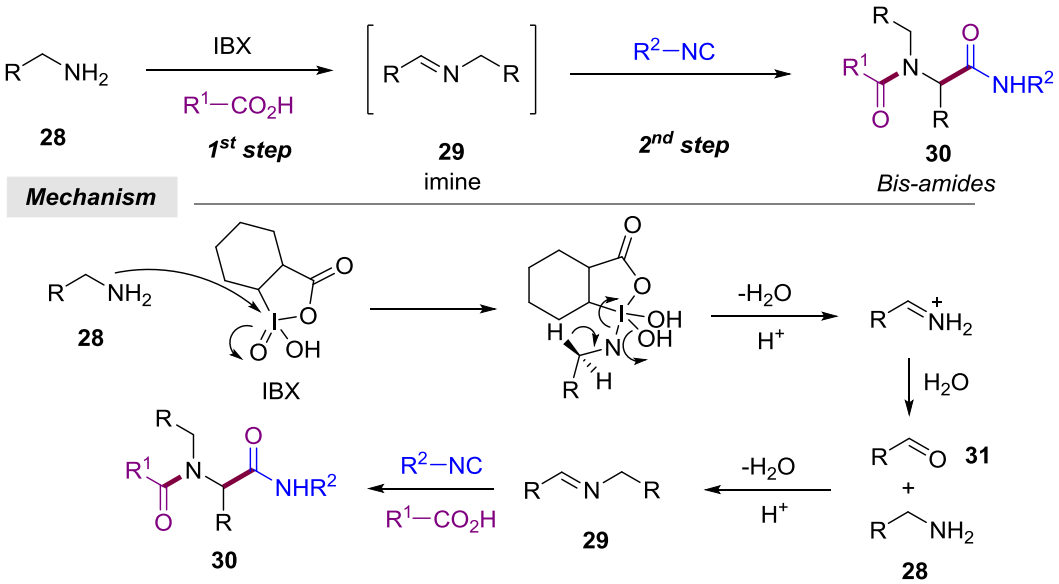

Scheme 53 IBX-Promoted Two-Step α-Amino Imide Synthesis.

[100] Islas-Jácome, A.; Gutiérrez-Carrilo, A.; García-Garibay, M. A.; González-Zamora, E. *Synlett* **2014**, *25*, 403.
[101] Singh, K.; Kaur, A.; Mithu, V. S.; Sharma, S. *J. Org. Chem.* **2017**, *82*, 5285.

In 2010, Xie and co-workers developed a U-3CR with copper catalysis and TBHP for the oxidation of *N*,*N*-dimethylanilines **22** and the assembly of α-amino imides **32** (Scheme 54).[102] Aromatic *N*-alkyl amines were chosen as starting material on account of the stabilization of the iminium intermediate by resonance.

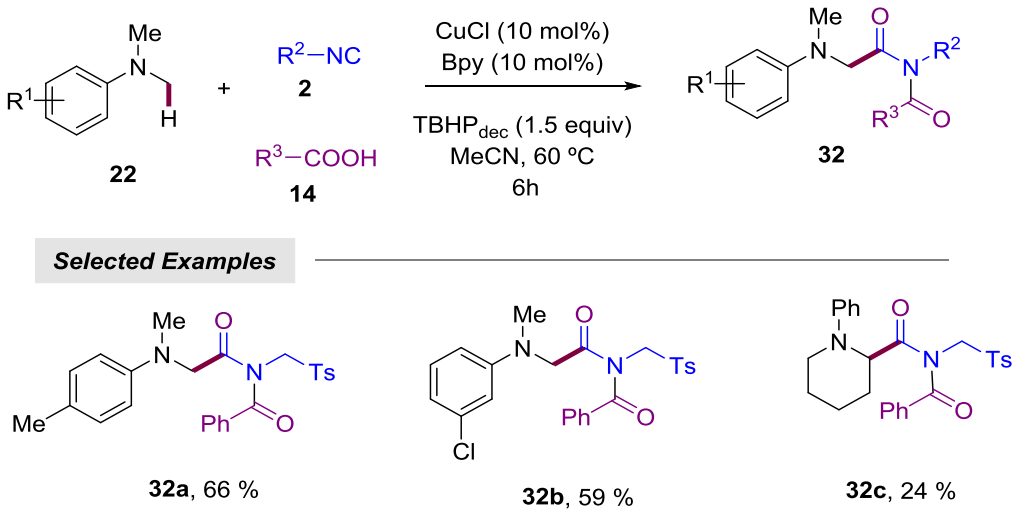

Scheme 54 Copper-Catalyzed Coupling of N,N-Dimethylanilines with Isocyanides and Carboxylic Acids.

The reaction conditions were selective to the use of bpy as supporting ligand and in most of the cases restricted to *p*-toluenesulfonylmethyl isocyanide and benzoic acids as nucleophiles. Liu and Han developed a similar copper/peroxide system to oxidize tertiary amines **33**.[103] The mixture of 20 mol % of copper(I) chloride, triphenylphosphine, TBHP, sodium dodecyl sulfate (SDS) at 70 ºC in water resulted in a short family of Ugi adducts **34** in moderate yields. The reaction was performed in the absence of carboxylic acids, so water had the double role of solvent and source of oxygen for the carbonyl formation resulting in a U-3CR with α-amino amides as the products (Scheme 55).

[102] Ye, X.; Xie, C.; Pan, Y.; Han, L.; Xie, T. *Org. Lett.* **2010**, *12*, 4240.
[103] a) Xie, C.; Han, L. *Tetrahedron Lett*. **2014**, *55*, 240. b) Ye, X.; Xie, C.; Huang, R.; Liu, J. *Synlett* **2012**, *23*, 409.

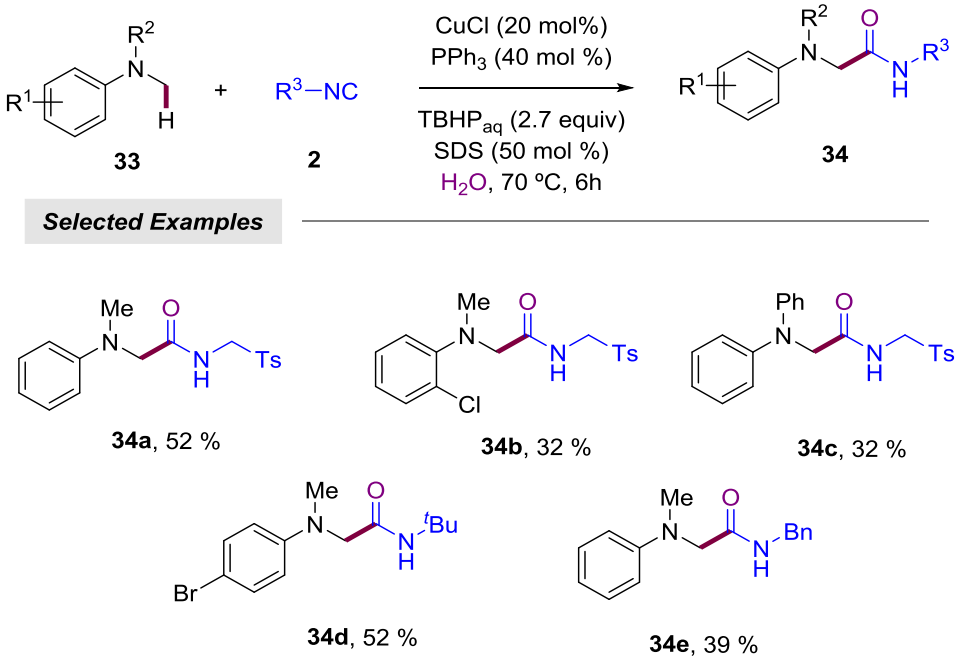

Scheme 55 Copper-Catalyzed Functionalization of N,N-Dimethylanilines with Isocyanides.

Rueping and co-workers also contributed to this field reporting three visible-light mediated oxidative multi-component reaction protocols of U-3CR (Scheme 56).[104] A stunning continuous flow protocol for the metal-free α-modification of aromatic tertiary amines **35** with isocyanides **2** was achieved as depicted in *method A*, whereas iridium and titanium catalysis (*method B* and *C*) were also applied for the formation of either α-amino amides **36** or imides **37**. Regarding *method C*, owing to its excellent stability and low toxicity, TiO_2 represents an ideal photocatalyst for sustainable development.[105] However, the three methodologies presented a scarce scope often limited to the use of *N,N*-dimethylaniline unit. Similar photoredox mediated Ugi reactions were also developed a couple of years later for both *N,N*-dimethylaniline derivatives and tetrahydroisoqunolines with rose Bengal catalyst, and Ru-catalyst, respectively.[106]

[104] a) Rueping, M.; Vila, C.; Bootwicha, T. *ACS Catal.* **2013**, *3*, 1676. b) Rueping, M.; Vila, C. *Org. Lett.* **2013**, *15*, 2092. c) Vila, C.; Rueping, M. *Green. Chem.* **2013**, *15*, 2056.
[105] a) Shiraishi, Y.; Hirai, T. *J. Photochem. Photobiol. C.* **2008**, *9*, 157. b) Chen, X.; Mao, S. S. *Chem. Rev.* **2007**, *107*, 2891.
[106] a) Gandy, M. N.; Raston, C. L.; Stubbs, K. A. *Chem. Commun.* **2015**, *51*, 11041. b) Cheng, Y.; Feng, G. *Org. Biomol. Chem.* **2015**, *13*, 4260.

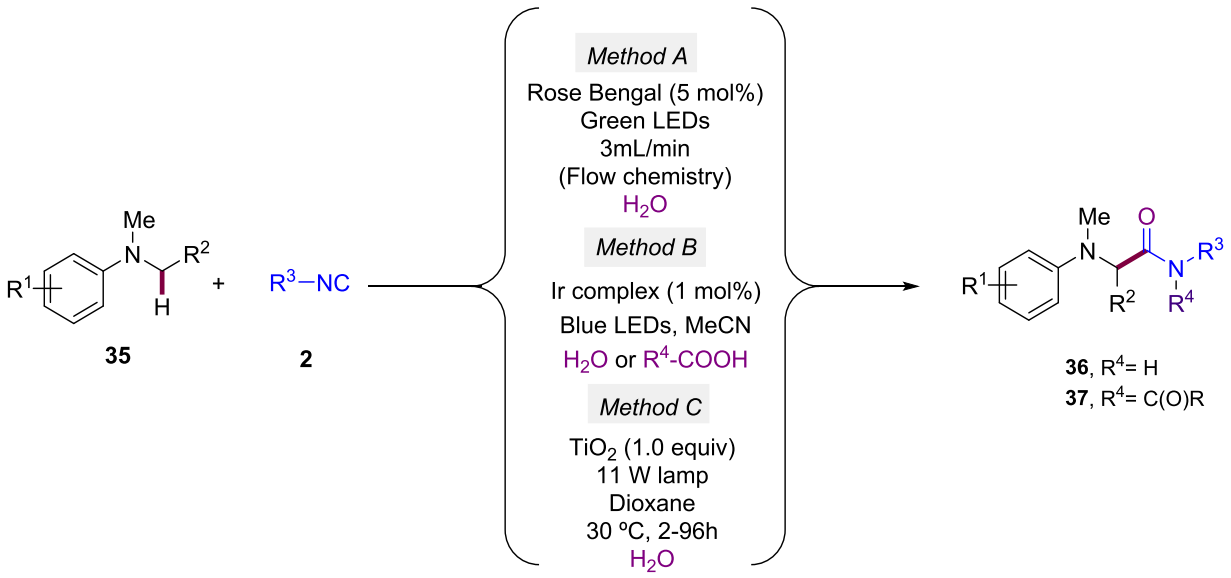

Scheme 56 Photoredox-Catalyzed Oxidative Ugi-Type Reactions.

As commented above, copper catalysis, hypervalent iodine reagents and visible light-mediated protocols have demonstrated their effectiveness towards one-pot Ugi-3CR variations with the use of secondary and tertiary amines. Nevertheless, primary amines were not tested in previous protocols besides the two-step α-amino imide formation of Sharma and co-workers.[101] Lately, an $Fe(NO_3)_3 \cdot 9H_2O$/TEMPO-catalyzed Ugi-type three-component reaction involving the oxidation of primary (arylmethyl)amines **38** to the corresponding imides **39** in the presence of air was reported by Batra and co-workers (Scheme 57).[107] A broad substrate scope with respect to aromatic amines **38** and carboxylic acids **14** was an appealing attribute of this work as well as the use of cost-efficient iron salts. Concerning the oxidant, TEMPO has shown valuable redox behavior leading to its extensive use as a reagent and/or catalyst in a broad range of both homogeneous and heterogeneous synthetic transformations. Moreover, from the green chemistry point of view, some traditional, stoichiometric quantities of hazardous metals and oxidants have been replaced by catalytic amounts of the environmentally benign, user-friendly TEMPO, thus mitigating the toxic effects of other oxidation systems. Nevertheless, its recovery and further reuse is a highly desirable issue as it is considerably expensive.[108]

[107] Dighe, S. U.; Kolle, S.; Batra, S. *Eur. J. Org. Chem*. **2015**, 4238.
[108] Beejapur, H. A.; Zhang, Q.; Hu, K.; Zhu, L.; Wang, J.; Ye, Z. *ACS Catal.* **2019**, *9*, 2777.

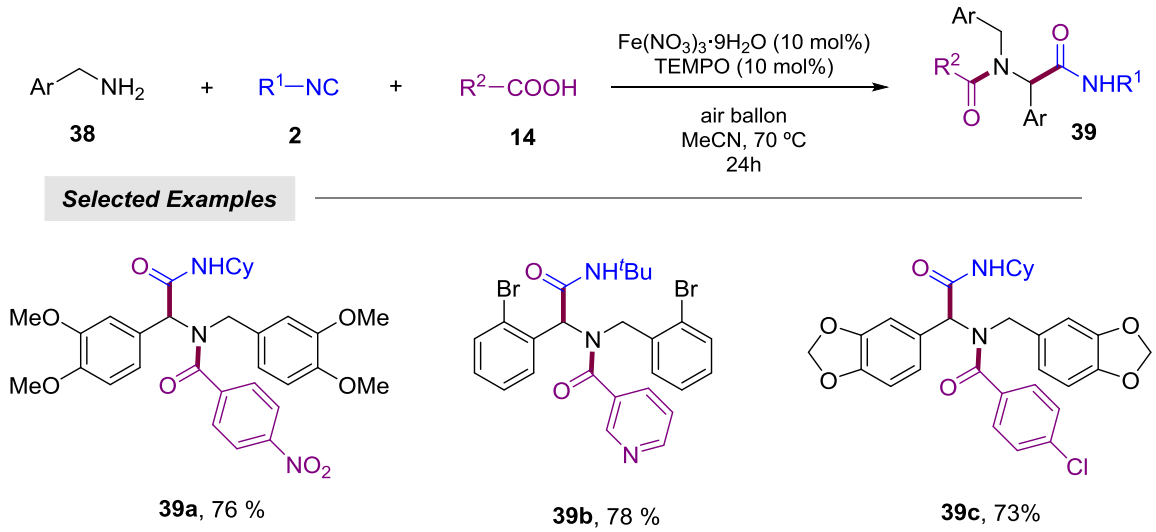

Scheme 57 Oxidative Ugi-Type MCR Using (Arylmethyl)amines as Imine Precursors.

Despite the wealth of reports in the field, most of the existing protocols still have several drawbacks such as limited synthetic scope or require the use of expensive catalysts. Accordingly, the assembly of α-amino amides through alternative oxidative Ugi-type reactions is still a challenging field of research.

3.2. Objective

Driven by the rapid growth in treatment of metabolic diseases and oncology, peptide chemistry has become a field of utmost importance.[109] The oxidative Ugi-type multicomponent reaction has demonstrated to be a potential tool to assemble unnatural α-amino amides, which are required precursors in the stabilization of peptide conformation by stapling techniques.

As part of our interest in sustainable C–H functionalization events for constructing amino acid derivatives, we decided to overcome the limited scope and the use of expensive photocatalysts and seek for a more sustainable alternative for the functionalization of (dialkyl)anilines through a U-3CR. On the basis of the well-known ability of iron catalysis for the activation of α-C(sp^3)–H bonds adjacent to amino groups, we were determined to come up with an alternative environmentally friendly and procedure that would offer the combination of a wider variety of substrates with the aid of less toxic and abundant iron catalysts.

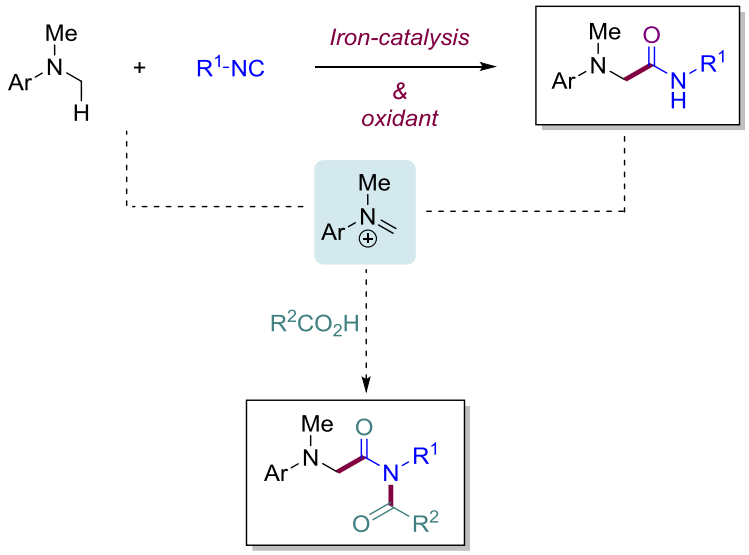

Scheme 58 Sustainable Ugi-Type Reaction through Iron-Catalyzed C–H Functionalization.

[109] Schwieter, K. E.; Johnston, J. N. *J. Am. Chem. Soc*. **2016**, *138*, 14160.

3.3. Sustainable Ugi-type Oxidative Reactions Through Iron-Catalyzed C(sp^3)–H Functionalization of *N,N*-Dimethylanilines

3.3.1. Optimization of Reaction Conditions

In the following section, the optimization of an unprecedented and practical Ugi-type reaction upon *N,N*-dimethylaniline derivatives and isocyanides catalyzed by cost-efficient iron salts is described. In order to initiate the optimization of the reaction conditions, *N,N*-dimethylaniline **22a** and the easy-to-handle white solid *p*-toluenesulfonylmethyl isocyanide **40a** were chosen as the model subtrates in our C–H functionalization approach. Inspired by the existing procedures, we anticipated that the combination of an iron source with an oxidant would facilitate the formation of the electrophilic iminium cation. Hence, an oxidant screening was initially carried out to evaluate the feasibility of our approach (Table 11). In this manner, the stable iron(II) acetate was initially selected as the catalyst for these first attempts.

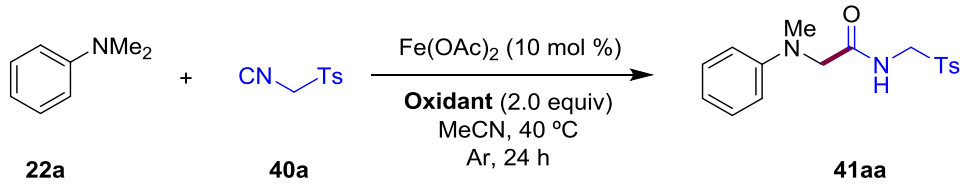

22a **40a** **41aa**

Entry	Oxidant	Yield (%)[b]
1	TBHPaq	23
2	TBPB	n.d.
3	DCP	n.d.
4	DDQ	n.d.
5	$(NH_4)_2S_2O_8$	n.d.
6	H_2O_2	23
7	O_2 (1atm)	29
8	TBHPdec	64
9	none	traces

[a] Reaction conditions: **22a** (0.5 mmol), **40a** (0.5 mmol), $Fe(OAc)_2$ (10 mol %), oxidant (2.0 equiv), MeCN (2 mL), at 40 °C, 24h. [b] Isolated yield after column chromatography. TBHPaq = *tert*-butyl hydroperoxide (70 wt. % in H_2O), TBHPdec = *tert*-butyl hydroperoxide (5.0-6.0 M in decane), DTBP = di-*tert*-butyl peroxide, DCP = dicumyl peroxide, TBPB= *tert*-butyl peroxybenzoate.

Table 11 Screening of Oxidants.[a]

In particular, organic peroxides have shown high reactivity in these types of systems based on electron transfers.[110] Similar to previous findings, *tert*-butyl hydroperoxide demonstrated the best efficiency for the coupling of **22a** and **40a** (Table 11, entry 1 and 8), whereas TBPB, DCP, DDQ or $(NH_4)_2S_2O_8$ (Table 11, entry 2-5) barely provided any product. Thus, the yield of the latter reactions was not even determined. Curiously, the use of a decane solution of TBHP resulted in a twofold increase of the yield compared to the one using an aqueous TBHP solution. Interestingly, the use of hydrogen peroxide (Table 11, entry 6) and molecular oxygen (Table 11, entry 7) led to the formation of **41aa** in low yields, providing fundamental features for a waste minimizing process. Additionally, it must be highlighted that the blank experiment evidenced the need of an oxidant to provide the cross-coupling reaction (Table 11, entry 9).

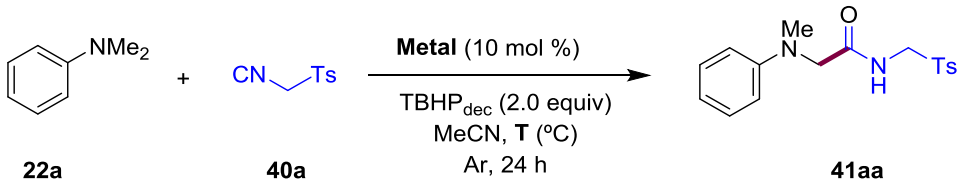

22a **40a** **41aa**

Entry	Metal	Temperature	Yield (%)[b]
1	$Fe(OAc)_2$	r.t.	44
2	$Fe(OAc)_2$	40	64
3	$FeCl_2$	r.t.	26
4	$FeBr_2$	r.t.	35
5	$FeBr_3$	r.t.	traces
6	$Fe(acac)_3$	40	46
7	CoF_3	40	34
8	CoF_2	40	30
9	$Co(acac)_2$	40	0
10	none	40	traces

[a] Reaction conditions: **22a** (0.5 mmol), **40a** (0.5 mmol), metal (10 mol %), $TBHP_{dec}$ (2.0 equiv), MeCN (2 mL), 24h.
[b] Isolated yield after column chromatography.

Table 12 Screening of Transition Metals.[a]

[110] Zhang, T.; Wu, Y.-H.; Wang, N.-X.; Xing, Y. *Synthesis* **2019**, *51*, 4531.

Once we had confirmed that iron salts were optimal for our oxidative Ugi-type reaction, the model reaction was performed with a variety of cost-efficient transition metals including both iron and cobalt salts (Table 12). Firstly, a set of iron(II)/(III) catalysts were tested at room temperature. Halogenated iron sources such as $FeCl_2$ and $FeBr_2$ provided **41aa** in 26 % and 35 % yield, respectively (Table 12, entry 3, 4), whereas the reactivity decreased with the use of $FeBr_3$ (Table 12, entry 5). The highest yield was obtained with $Fe(OAc)_2$ (Table 12, entry 1), although the result at ambient temperature shown to be comparatively lower than the one at 40 ºC (Table 12, entry 2). Next, the metal catalyst screening was repeated at 40 ºC but no significant improvement in the reaction yields was observed. This time a blank experiment was also performed in order to ensure the role of the metal (Table 12, entry 10). Interestingly, only traces of product were observed when the reaction was run in the absence of the iron catalyst. Hence, it suggested that a metal/oxidant system is necessary for the reaction to occur. Although Co-catalyzed Ugi-type oxidative processes remain unexplored, certain cobalt salts could be also employed, albeit moderate yields were obtained (Table 12, entry 7 and 8).

Concerning the reaction temperature, a slight decrease of the yield was detected when it was carried out in a more convenient room temperature (Table 13, entry 1). Then, with the purpose of raising the conversion of the starting material into the desired product, the reaction mixture was warmed up to 50 ºC and 60 ºC, which did not provide the enhancement of the α-amino amide **41aa** formation (Table 13, entry 3 and 4). Higher temperatures seemed to disfavour the cross-coupling reaction, whereas no product was observed from that temperature onwards. Thus, as shown by these initial screenings, the best result was obtained when the reaction was performed at 40 ºC (Table 12, entry 2).

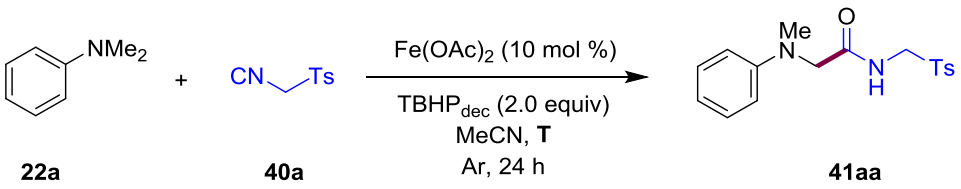

22a **40a** **41aa**

Entry	Temperature	Yield (%)[b]
1	r.t.	44
2	40	64
3	60	n.r.
4	50	41

[a] Reaction conditions: **22a** (0.5 mmol), **40a** (0.5 mmol), $Fe(OAc)_2$ (10 mol %), $TBHP_{dec}$ (2.0 equiv), MeCN (2 mL), at 40 ºC, 24h. [b] Isolated yield after column chromatography.

Table 13 Screening of Temperatures.[a]

With regard to the solvent, an extensive screening of organic solvents was carried out and the best results are collected in Table 14. Curiously, when the reagents were dissolved in chlorinated solvents, higher yields than when using non-halogenated solvents were obtained. The desired product was obtained in 63 % yield in chloroform (Table 14, entry 2) and with 60 % yield in dichloroethane (Table 14, entry 3), almost with the same effectiveness as when the reaction was performed in acetronitrile (Table 14, entry 4). We have highlighted the paramount importance of developing sustainable protocols for the assembly of α-amino amides; accordingly, acetonitrile was selected as the solvent of choice for further studies. Indeed, the area of chemical synthesis has witnessed grand innovation regarding safety issues leading to the prohibition of certain useful chemicals like dichloroethane.[111] Hence, the use of often carcinogenic halogenated solvents would be at odds with an environmentally friendly methodology and its avoidance is preferable.

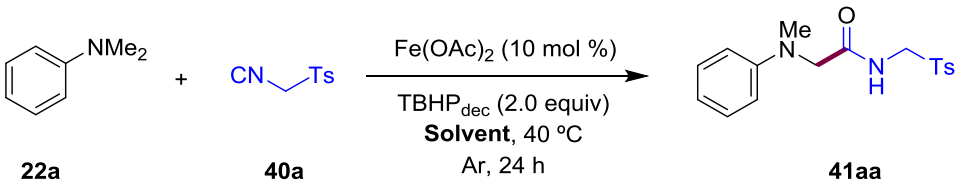

22a **40a** **41aa**

Entry	Solvent	Yield (%)[b]
1	DCM	51
2	$CHCl_3$	63
3	DCE	60
4	MeCN	64

[a] Reaction conditions: **22a** (0.5 mmol), **40a** (0.5 mmol), $Fe(OAc)_2$ (10 mol %), $TBHP_{dec}$ (2.0 equiv), solvent (2 mL), at 40 ºC, 24h. [b] Isolated yield after column chromatography.

Table 14 Screening of Solvents.[a]

Then, in order to further increase the reaction efficiency, we performed some extra experiments, and the influence of the stoichiometry on the reaction outcome was evaluated as well as some control tests were conducted (Table 15). Many times the excess of one of the coupling partners favors the reaction, thereby resulting in higher yields. This was the case when two equivalents of *N,N*-dimethylaniline **22a** were used, resulting in an excellent 81 % yield (Table 15, entry 1). As a higher amount of **22a** turned out to be significant previous changes were made in the rest of parameters. Interestingly, 5 mol % of the catalyst were also appopiate to achieve **41aa** in good yields (Table 15, entry 2), as well as the addition of just one equivalent of oxidant (Table 15, entry 5). Additionally, the reaction was not sensitive to atmospheric air and provided 75 % yield of

[111] Sherwood, J. *Angew. Chem. Int. Ed*. **2018**, *57*, 14286.

41aa (Table 15, entry 3). Although the yield was slightly lower in the latter cases (up to 75 % yield), the performance of the process with lower catalyst laoding or oxidant and under an air atmosphere ilustrates the robustness of the protocol and represents an extra bonus from a practical point of view. Moreover, we demonstrated that the scale up was possible converting 1.0 g of *p*-toluenesulfonylmethyl isocyanide **40a** into 1.54 g of α-amino amide **41aa** in an exceptional 91 % yield.

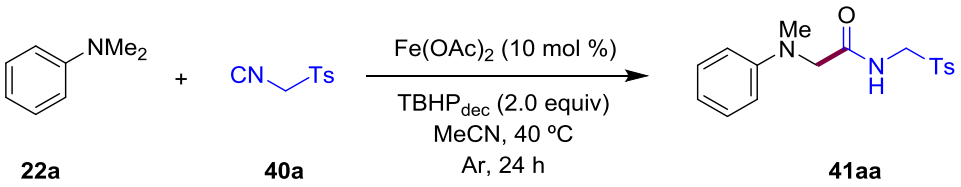

22a **40a** **41aa**

Entry	Change from standard conditions	Yield (%)[b]
1	**22a** (2.0 equiv)	81 (91)[c]
2	**22a** (2.0 equiv), $Fe(OAc)_2$ (5 mol %)	74
3	**22a** (2.0 equiv), under air	75
4	**22a** (3.0 equiv)	71
5	**22a** (2.0 equiv), TBHPdec (1.0 equiv)	74

[a] Reaction conditions: **22a** (0.5 mmol), **40a** (0.5 mmol), $Fe(OAc)_2$ (10 mol %), $TBHP_{dec}$ (2.0 equiv), MeCN (2 mL), at 40 ºC, 24h. [b] Isolated yield after column chromatography. [c] 1.0 gram-scale.

Table 15 Changes from Standard Conditions.[a]

Afterwards, the optimal reaction conditions were applied to a representative set of *N*,*N*-dimethyanilines. To our surprise, comparatively much lower yields were obtained. As an example, halogenated anilines like **22b** and **22c** resulted in 68 % and 58 % yield of their corresponding Ugi products respectively (Scheme 59). Conversely, *N*,*N*-dimethyl-*p*-anisidine afforded the target product in just 23 % yield, which could indicate that a more careful screening of the reaction conditions could be required.

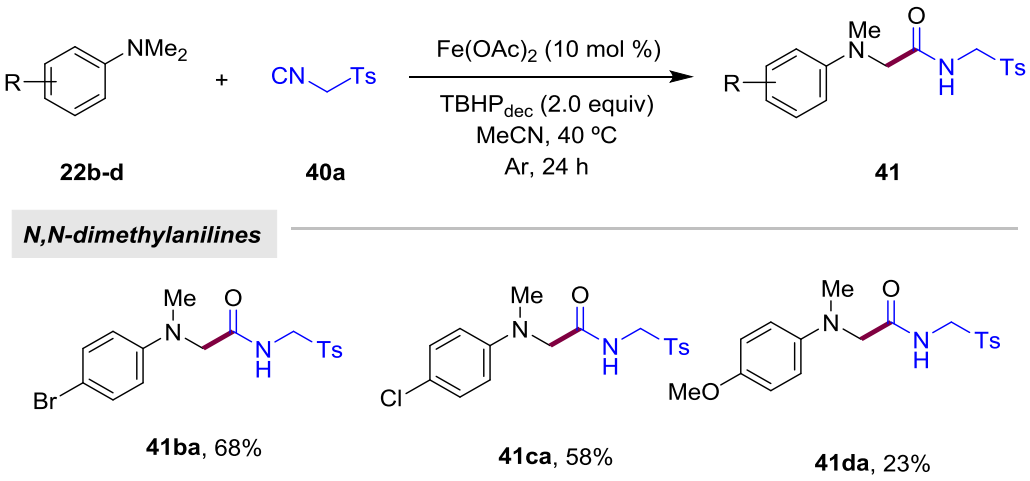

Scheme 59 First Tested N,N-Dimethylanilines.

Owing to the known ability of carboxylic acids to favor metal-catalyzed C–H functionalization reactions,[112] we next evaluated the effect of some carboxylic acids as additives in the optimal reaction conditions (Table 16). *p*-Bromo-*N*,*N*-dimethylaniline **22b** was selected as the model substrate which in the standard conditions provided a 68 % yield (Table 16, entry 1).

[112] Ackermann, L.; Vicente, R.; Althammer, A. *Org. Lett.* **2008**, *10*, 2299.

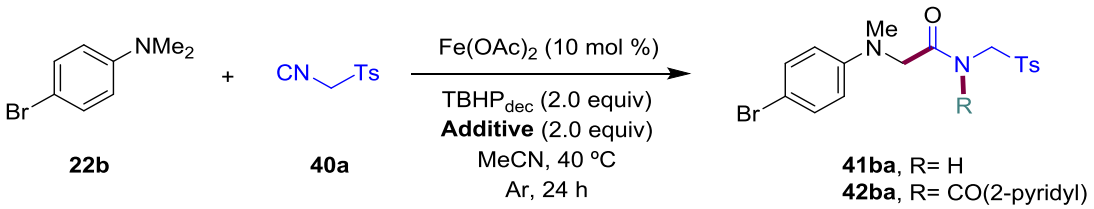

22b **40a**

41ba, R= H
42ba, R= CO(2-pyridyl)

Entry	Carboxylic acids	Yield (%)[b]
1	none	68 (**41ba**)
2	AcOH	81 (**41ba**)
3	$AdCO_2H$	81 (**41ba**)
4	PivOH	59 (**41ba**)
5	Nicotinic acid	55 (**41ba**)
6	2-Methylnicotinic acid	51 (**41ba**)
7	$MesCO_2H$	44 (**41ba**)
8	$PhCO_2H$	42 (**41ba**)[c]
9	2-Nitrobenzoic acid	n.d.
10	TFA	n.d.
11	Picolinic acid	62 (**42ba**)

[a] Reaction conditions: **22b** (1.0 mmol), **40a** (0.5 mmol), $Fe(OAc)_2$ (10 mol %), $TBHP_{dec}$ (2.0 equiv), MeCN (2 mL), at 40 ºC, 24h. [b] Isolated yield after column chromatography. [c] 21% yield of the benzoylated amide was obtained along with **41ba**. nd = not determined.

Table 16 Screening of Carboxylic acids.[a]

To our delight, the addition of either acetic acid or 1-adamantanecarboxylic acid had a positive impact raising the yield of **41ba** to an excellent 81 % (Table 16, entry 2, 3). On the other hand, some other tested carboxylic acids shown to slighly decrease the reactivity of the model reaction achieving yields between 40-60 % (Table 16, entry 4-8), while the low conversion observed with the use of trifluoroacetic acid and 2-nitrobenzoic acid was not even determined (Table 16, entry 9 and 10). At this point, it must be highlighted the exclusive formation of **41ba** in the presence of carboxylic acids instead of an expected Ugi-3CR α-amino imide **42ba**. Likewise, the selectivity of our protocol was demonstrated with the preferable formation of α-amino amide as the sole product. However**,** the addition of picolinic acid turned out to be an exception providing the unique formation of the corresponding picolinamide **42ba** in a promising 62 % yield (Table 16**,** entry 11). This case would be an alternative to the iron-catalyzed oxidative Ugi 3-CR of Batra and co-workers,[107] which was limited to primary

amines. Comparatively, our methodology could be carried out under lower temperature and the expensive TEMPO oxidant would be substituted by a more cost-efficient TBHP. Moreover, only four isocyanides were tested and no picolinamide example was observed in Batra's protocol. Therefore, the exclusive use of picolinic acid in our model reaction could lead to a novel Ugi-type 3-CR with the possibility of broadenig the existing scope**.**

3.3.2. Scope of Fe-Catalyzed C(sp^3)–H Functionalization of N,N-Dimethylanilines with Isocyanides

With the optimized conditions in hand, we next evaluated our iron-catalyzed oxidative Ugi-type reaction toward the assembly of novel α-amino amide compounds (Scheme 60). Regarding the *N,N*-dimethylanilines, some of them were commercially available, whereas others had to be synthesized. To transform the starting anilines into their corresponding *N,N*-dimethylated analogues, *method A* was applied where three equivalents of potassium carbonate and methyl iodide in acetonitrile were necessary. Alternatively, *Method B* enabled the synthesis of differently substituted *N,N*-dimethylanilines through esterification reactions.

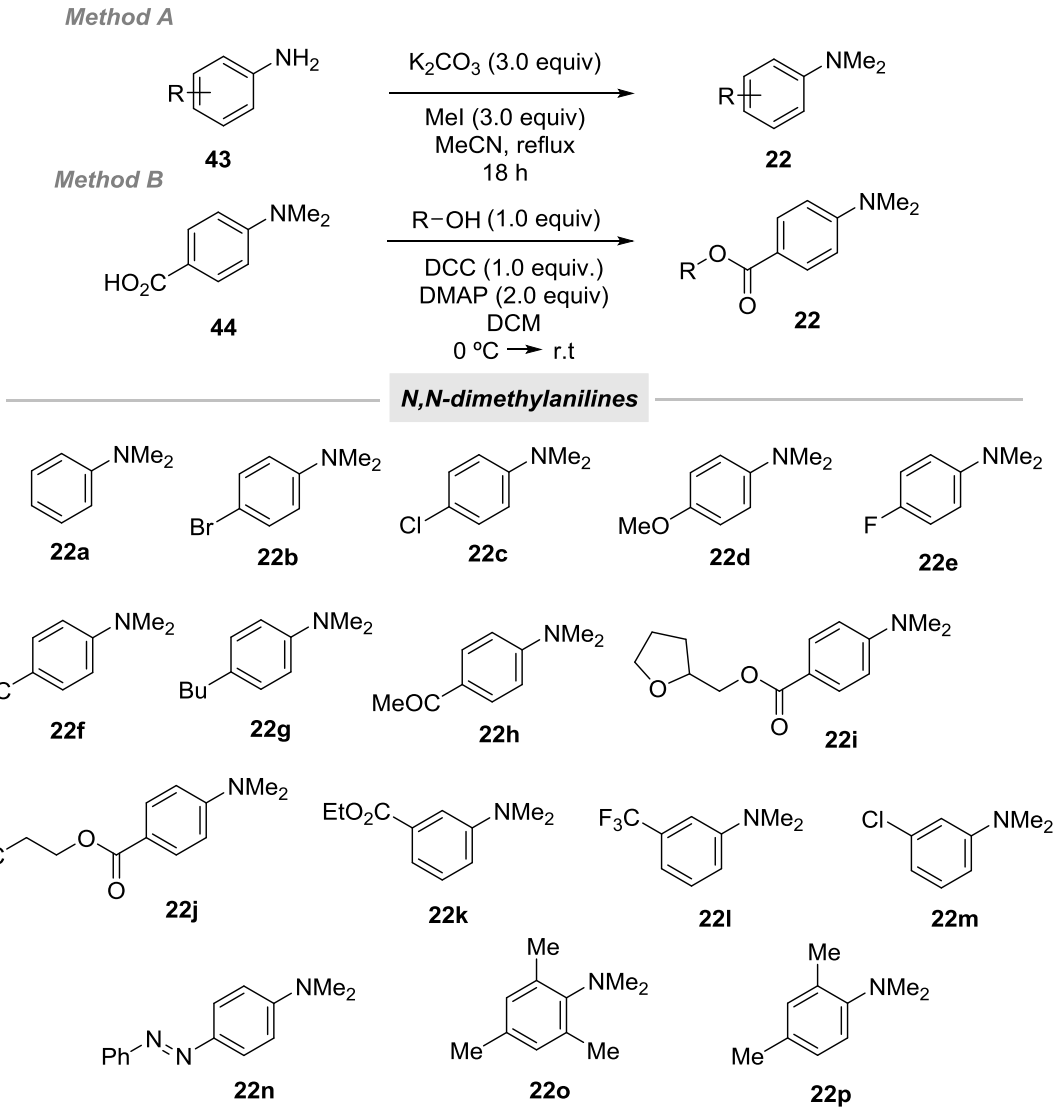

Scheme 60 Substrate Scope

Notably, the addition of AcOH enhanced considerably the yields of previously tested **22b** and **22c** anilines reaching excellent results of the corresponding products. 4-Fluoro-*N*,*N*-dimethylaniline **22e** also required the carboxylic acid additive to obtain a better conversion into **41ea**. The formation of these halogen-containing amino acid type derivatives are of great significance as they allow to take a step forward to further modifications with cross-coupling reactions. Alternative position of halogenated functional groups turned out to have no effect, and high yields like 77 % and 78% for **41ma** and **41la**, respectively, were achieved. Halogens aside, other *p*-substituted anilines exhibited high reactivity toward the assembly of α-amino amides (**41da-41ja**). One more time, the positive impact of acetic acid in previously poor-yielding compounds such as **41da** must be highlighted. The additive provided the increase in three-folds the prior yield for the coupling between 4-methoxy-*N*,*N*-dimethylaniline **22d** and **40a**. Importantly, those cases where the acid additive was required shown the formation of α-amino amide as the major product with no traces of U-3CR product.

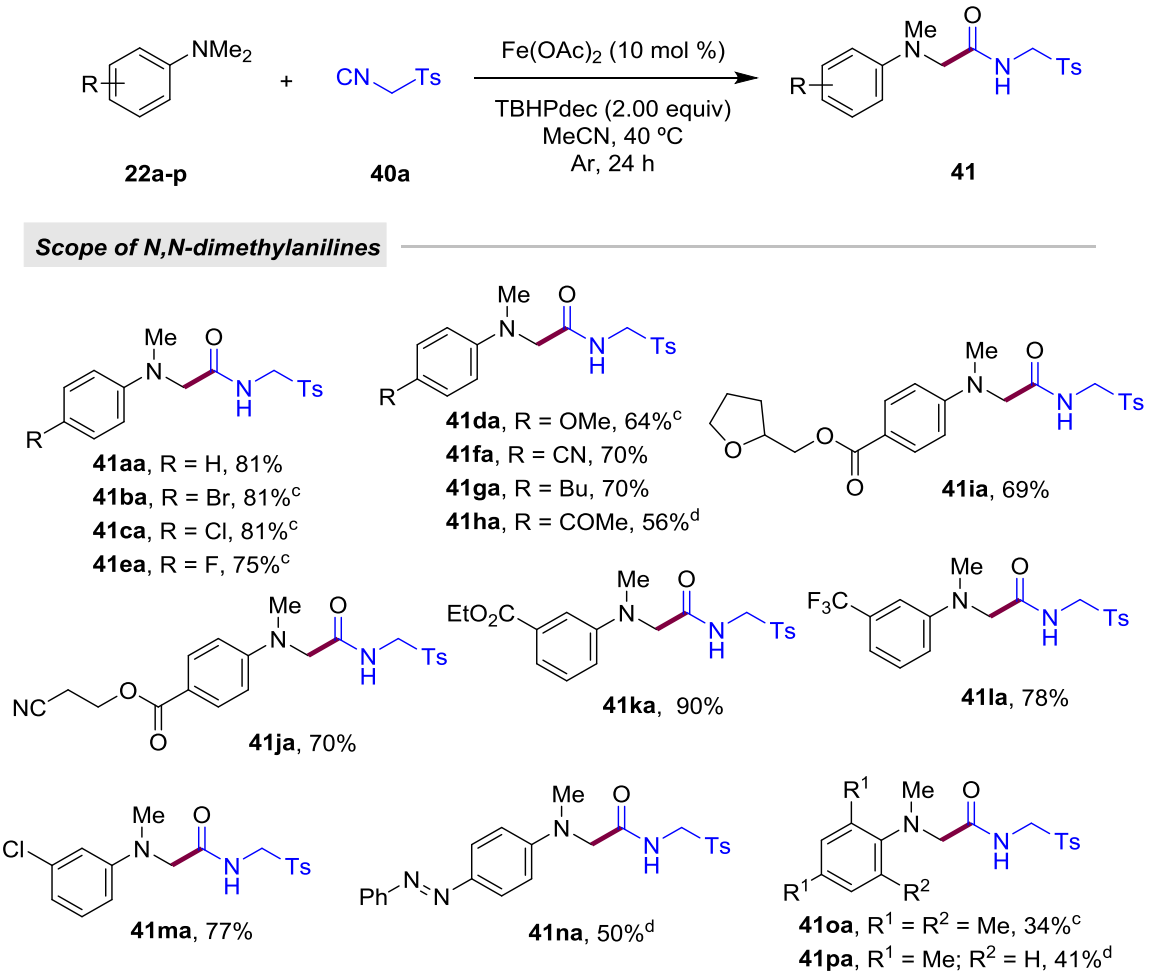

[a] Reaction conditions: **22** (1.0 mmol), **40a** (0.5 mmol), $Fe(OAc)_2$ (10 mol %), $TBHP_{dec}$ (2.0 equiv), MeCN (2 mL), at 40 ºC, 24h. [b] Isolated yield after column chromatography. [c] Addition of AcOH (2.0 equiv). [d] Reaction performed at 70 ºC.

Scheme 61 Fe-Catalyzed C(sp^3)–H Functionalization of N,N-Dimethylanilines.[a]

On the other hand, other functional groups in the aromatic ring were also found compatible with the protocol in the absence of any additive. Remarkably, *N,N*-dimethylanilines bearing nitriles (**41fa, 41ja**) and ethers (**41ia**) resulted in high yields. Taking into account that α-C(sp^3)−H bonds adjacent to either oxygen or cyano groups could be activated under oxidative reaction conditions,[113] the preferential selectivity toward the oxidation of the amines revealed the subtleties of our protocol. Furthermore, esters (**41ia, 41ja, 41ka**), ketones (**41ha**), and even azobenzenes (**41na**) provided their corresponding Ugi adducts from moderate to good yields. During the scope examination, the lack of reactivity of some substrates led us make some modifications in the reaction conditions. Thus, compounds like **41ha** and **41na** were acomplished warming up the reaction temperature to 70 ºC to ensure high yields. The latter azo-compounds, in particular, could be of paramount significance in the field of biomedicine to test their photochemical behaviour.[114] Finally, the use of *ortho* substituted anilines **22o-p** provided the target products as well, albeit in moderate yields. In any case, a vast array of dimethylanilines enable the assembly of a structurally diverse chemical library of α-amino amides evidencing the high practicality of our procedure.

We next evaluated the synthetic scope concerning the isocyanide coupling partner. Although it has been often cast doubt on their sustainability, it must be noted out that more practical and greener syntheses of isocyanides is an issue currently sought by synthetic chemists.[115] In fact, prior reported Ugi-type oxidative reactions were mainly restricted to the use of tosylmethyl isocyanide **40a**.[102] Therefore, we focused on discovering a protocol with a broader group tolerance (Scheme 62). Curiously, initial optimal reaction conditions resulted in low reactivity of certain substrates as **41bh** in 15 % yield or even in the recovering of an unreactive starting material. Consequently, previously crucial addition of acetic acid or higher reaction temperature were applied in the following attempts. In this manner, alkyl groups containing isocyanides such as pentyl, *tert*-butyl and cyclohexyl derivatives smoothly underwent the multicomponent reaction to afford the corresponding products (**41ab**, **41ac**, **41ad**). With the exception of **41ac**, all isocyanides required 70 ºC and acetic acid as additive to reach moderate to good yields.

[113] a) Zhang, S.-Y.; Zhang, F.-M.; Tu, Y.-Q. *Chem. Soc. Rev.* **2011**, *40*, 1937. b) Chu, X.-Q.; Ge, D.; Shen, Z.-L.; Loh, T.-P. *ACS Catal.* **2018**, *8*, 258.
[114] Grathwol, C. W.; Wössner, N.; Behnisch-Cornwell, S.; Schulig L.; Zhang, L.; Einsle, O.; Jung, M.; Link, A. *ChemMedChem*. **2020**, *15*, 1480.
[115] Waibel, K. A.; Nickisch, R.; Möhl, N.; Seim, R.; Meier, M. A. R. *Green Chem.* **2020**, *22*, 933.

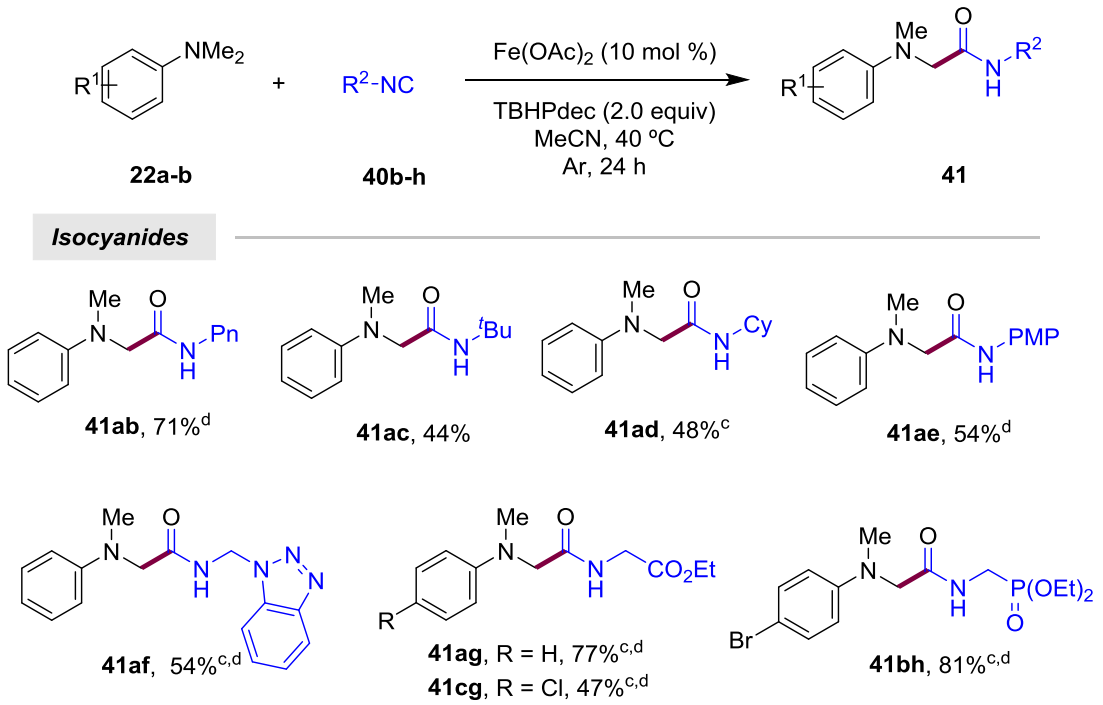

[a] Reaction conditions: **22** (1.0 mmol), **40** (0.25 mmol), $Fe(OAc)_2$ (10 mol %), TBHP(dec) (2.0 equiv), MeCN (1 mL) at 40 ºC, 24h. [b] Isolated yield after column chromatography. [c] Addition of AcOH (2.0 equiv). [d]Reaction performed at 70 ºC.

Scheme 62 Synthetic Scope of Isocyanides.[a]

Gratifyingly, not only alkyl isocyanides but also aromatic analogues, prone to undergo competitive SET events, could be part of the resulting Ugi-adduct (**41af**, **41ae**). The performance of the process at 70 ºC enabled the use of isocyanides **40c** and **40f** and the assembly of **41ac** and **41af**, respectively, in moderate yields. However, benzimidazole-containing **41af** was achieved in a poor 13 % yield. Hence, acetic acid was essential to raise the yield of this heteroaromatic scaffold. The introduction of relevant heterocycles like benzimidazoles, which are present in multiple bioactive compounds, enables the straightforward construction of peptide derivatives that would be truly significant for drug discovery. Increasing attention has been directed to biorthogonal reactions where a new covalent bond links two different molecules. For this reason, the phosphonate isonitrile stood out in this ample substrate scope due to the excellent 81 % yield and the crucial role of phosphonates in living organisms such as in the synthesis of nucleic acids and other metabolites. Likewise, the coupling of isocyanides bearing an ester in the α-position with different *N*,*N*-dimethylanilines provided α-amino acid derivatives **41ag** and **41cg**. These remarkable examples illustrate the utility of our method as a prominent methodology for peptide modification under mild and sustainable reaction conditions.

Overall, a larger extension of isocyanide substrates provided the desired Ugi analogue products in moderate to good yields and in a chemoselective manner. As previously highlighted, the pivotal addition of acetic acid and

higher temperature was found crucial for the formation of α-amino amides from the corresponding isocyanides. Nevertheless, during this process several substrates remained unreactive (Scheme 63). Concerning *N,N*-dimethylanilines, some *para*-substituted ones such as those bearing amides and allylic ester did not provide the desired products (**41qa**, **41ra**, **41sa**). *p*-Nitro-*N,N*-dimethylaniline **22t** having an excellent electron-aceptor nitro group was also summited to the oxidative Ugi reaction. Nonetheless, no product was obtained. On the other hand, 2-bromo-*N,N*-dimethylaniline **22v** furnished the corresponding product **41va** in low yield despite the addition of AcOH. Besides compound **41bh** and **41ag**, other attempts to construct biologically appealing products like phosphonate and amino acid derivatives **41hh** and **41jg** also resulted in moderate yield.

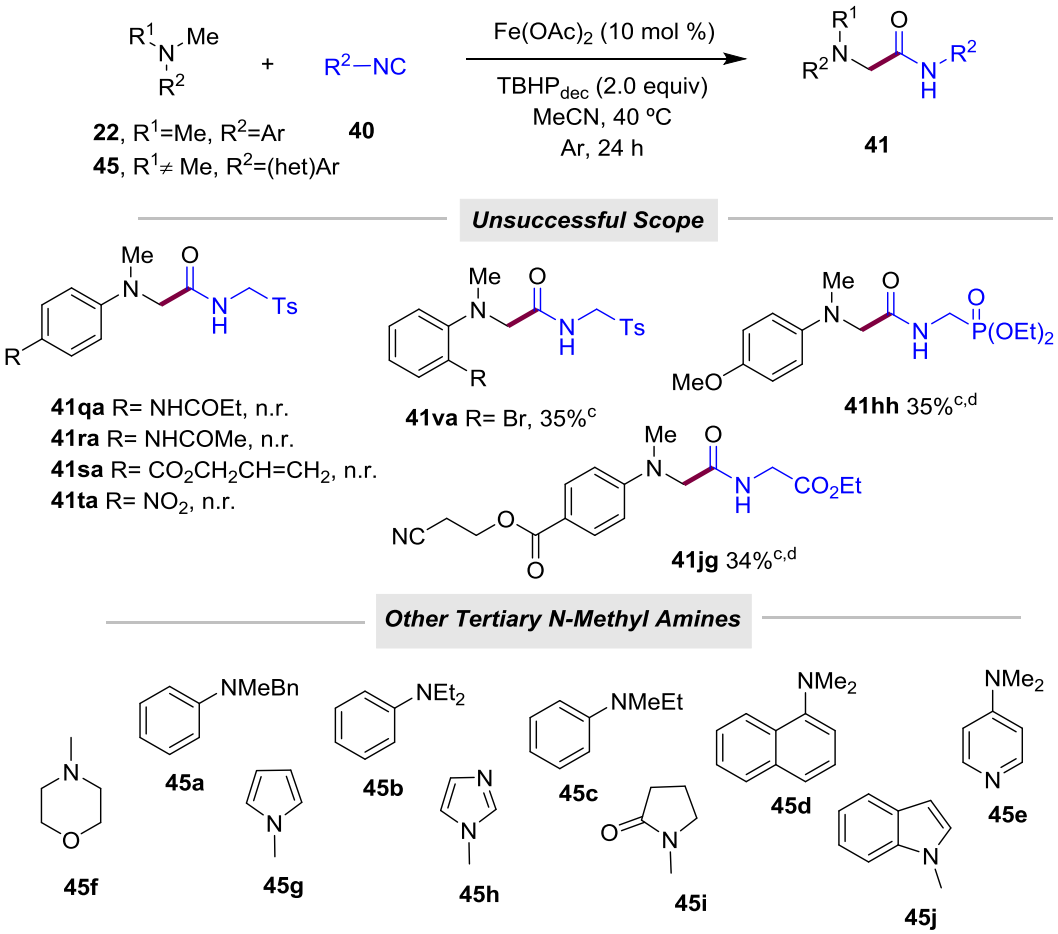

[a] Reaction conditions: **22, 45** (0.5 mmol), **40** (0.25 mmol), $Fe(OAc)_2$ (10 mol %), TBHPdec (2.0 equiv), MeCN (1 mL) at 40 ºC, 24h. [b] Isolated yield after column chromatography. [c] Addition of AcOH (2.0 equiv). [d] Reaction performed at 70 ºC.

Scheme 63 Unsuccessful Scope.

Notably, our alternative iron-catalyzed oxidative Ugi-type reaction demonstrated the selectivity toward *N,N*-dimethylanilines as the analogues ArN(Me)(Bn) (**45a**), $ArN(Et)_2$ (**45b**) and ArN(Me)(Et) (**45c**) did not react under the optimized reaction conditions. This feature was also observed in most of the previously reported

methodologies, where analogues of dialkylanilines could be rarely functionalized.[102,103a,b, 104b,c] Moreover, the electronic nature of the aromatic ring seemed to have an influence on the reactivity of the process as neither **45d** nor **45e**, bearing naphthalene and pyridine rings, respectively, provided the desired products. Additionally, when alternative heteroaromatic scaffolds like *N*-methyl-pyrrole **45g**, *N*-methyl-imidazole **45h** and *N*-methyl-indole **45j** were tested, they were incompatible with the disclosed protocol. In a final attempt, *N*-methylmorpholine **45f** and *N*-methyl-2-pyrrolidinone **45i** were submitted to our reaction conditions. Despite their similarity with isoquinoline structure,[98,104a] whose reactivity under a metal/oxidant system has been previously observed, the reaction did not occur.[116]

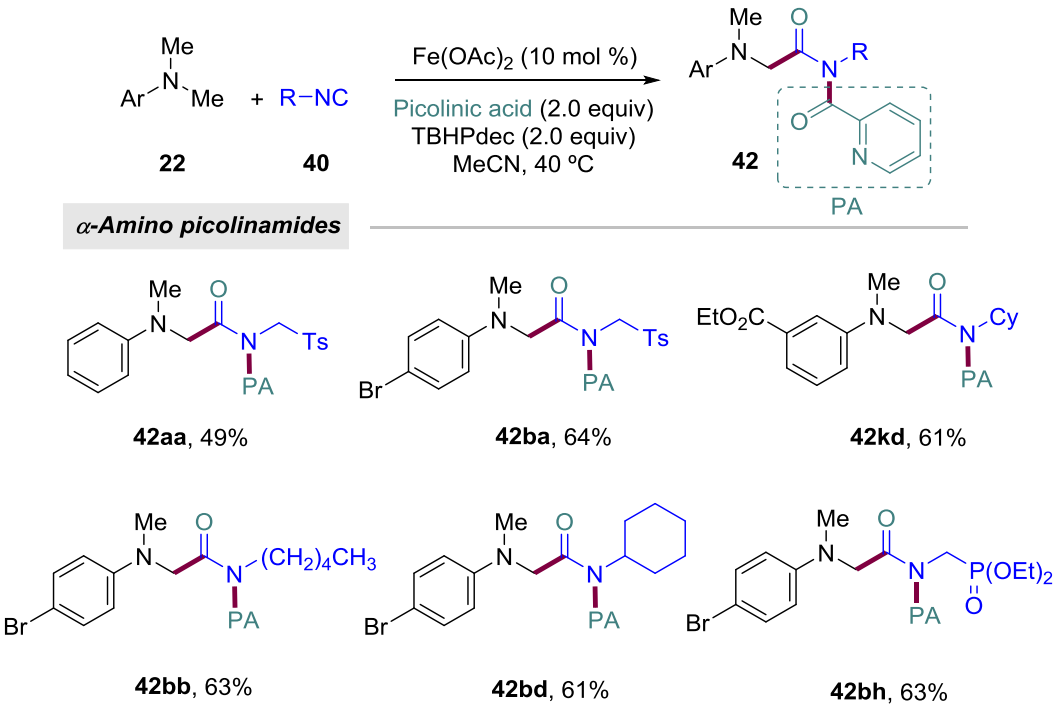

Scheme 64 Scope for Multicomponent Reaction.

To round out the reaction scope, some of the previous substrates were submitted to the iron-catalyzed 3-component Ugi type reaction in combination with picolinic acid, which led to the favorable construction of the corresponding α-amino imides (Scheme 64). In Table 16, while the use of acetic acid as an additive enhanced the yield of **41ba** to 81 %, the use of picolinic acid resulted in the exclusive formation of picolinamide **42ba** in a remarkable 64 % yield. Moreover, anilines **22a** and **22k** were also converted into their α-amino imide adducts with moderate to good yields. Then, bromo-substituted aniline **22b** was chosen as the coupling partner due to its capacity to undergo further cross-coupling transformations. In this manner, structurally complex **42bb**, **42bd** and **42bh** were synthesized with aliphatic isocyanides and biologically appealing phosponate derivative. Hence,

[116] Yuan, H.; Liu, Z.; Shen, Y.; Zhao, H.; Li, C.; Jia, X.; Li, J. *Adv. Synth. Catal.* **2019**, *361*, 2009.

the crucial addition of picolinic acid was found key for the selecive formation of picolinamides which are of widespread use in the realm of C−H activation.[117]

3.3.3. Mechanistic Proposal

To gain some insights into the mechanism, we performed some control experiments. Former disclosed oxidative Ugi-type reactions proposed the generation of the iminium ion through a SET/HAT pathway by the combination of a metal source and an oxidant, where radical species were delivered. Hence, a variety of radical scavengers were added into the reaction media together with model aniline **22a** and isocyanide **40a** with the aim of capturing some of the mentioned intermediates and verified the reaction pathway (Table 17).

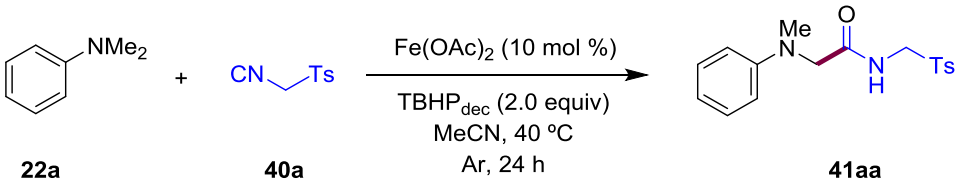

22a **40a** **41aa**

Entry	Radical trap	Yield (%)[b]
1	TEMPO	n.r.
2	1,1-diphenylethylene	n.r.
3	BHT	27

[a] Reaction conditions: **39a** (1.0 mmol), **40a** (0.5 mmol), $Fe(OAc)_2$ (10 mol %), $TBHP_{dec}$ (2.0 equiv), radical trap (1.0 equiv), MeCN (2 mL), at 40 ºC, 24h. [b] Isolated yield after column chromatography.

Table 17 Control Experiments with Radical Traps.[a]

However, while one equivalent of either TEMPO or 1,1-diphenylethylene inhibited totally the formation of **41aa**, BHT [3,5-di(*tert*-butyl)-4-hydroxytoluene] led to a detereoration of the oxidative coupling resulting in a 27 % yield. In any case, no intermediate could to be trapped and the inhibition of the reaction could suggest that radical species are likely to be involved.

On the basis of the obtained results and prior reported works,[102,103] we proposed a reaction mechanism in Scheme 66. The formation of the iminium ion is supposed to occur in the same manner as previously described within

[117] a) He, G.; Lu, G.; Guo, Z.; Liu, P.; Chen, G. *Nat. Chem.* **2016**, *8*, 1131. b) Rouquet, G.; Chatani, N. *Angew. Chem. Int. Ed.* **2013**, *52*, 11726.

chapter 2. Thus, the reaction would start with the iron(II)-assisted formation of *tert*-butoxy radical species **II**. Likewise, this species would lead to the generation of radical **III**, which undergoes a SET process resulting in the reduction of iron (III) to iron (II) regenerating the catalytic cycle and the formation of the iminium ion **IV**. Looking into literature different pathways could be envisioned for the elemental steps of the conversion of *N*,*N*-dimethylanilines into iminium ion. Although the formation of α-amino radical **II** is consistent, its further oxidation remains uncertain. In particular, Doyle and co-workers carried out a mechanistic investigation in which Fe(III) and *tert*-butyloxy radical species are known to be generated in a Fe(II)/TBHP system, but they proposed the subsequent oxidation to *tert*-butylperoxy radicals (Scheme 65). The latter is considered a thermodynamically favorable oxidant for the rate-determing step.[118]

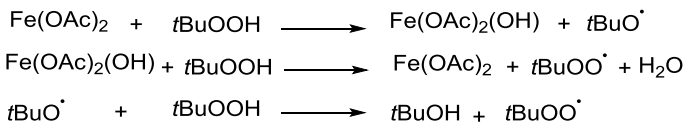

Scheme 65 Reaction of Iron (II) with TBHP.

Once the electrophilic iminium species is generated, it would be attacked by the nucleophilic isocyanide producing nitrilium ion **V**, which would be eventually trapped by water in the media and form the desired α-amino amide product. On the other hand, the phenomenon observed with the use of picolinic acid suggested that another mechanism might be operative. The preferential formation of α-amino imides indicates that the attack of the carboxylic acid may be faster that the water one into the nitrilium ion **V** to produce the cationic intermediate **VII**. Finally, the rearragenment of the latter would provide α-amino picolinamides. However, this latter favorable formation of imides over amides must be higlighted and attributed to the exclusive use of picolinic acid, as no α-amino imides was observed utilizing other carboxylic acids. Furthermore, derivatives of picolinic acid such as 2-methylnicotinic and nicotinic acids did not provide the same product either. We considered that this might be owing to not only the metal-coordination ability of the nitrogen atom in the picolinic acid but also because the position of this atom in the aromatic ring.

[118] Ratnikov, M. O.; Doyle, M. P. *J. Am. Chem. Soc.* **2013**, *135*, 1549.

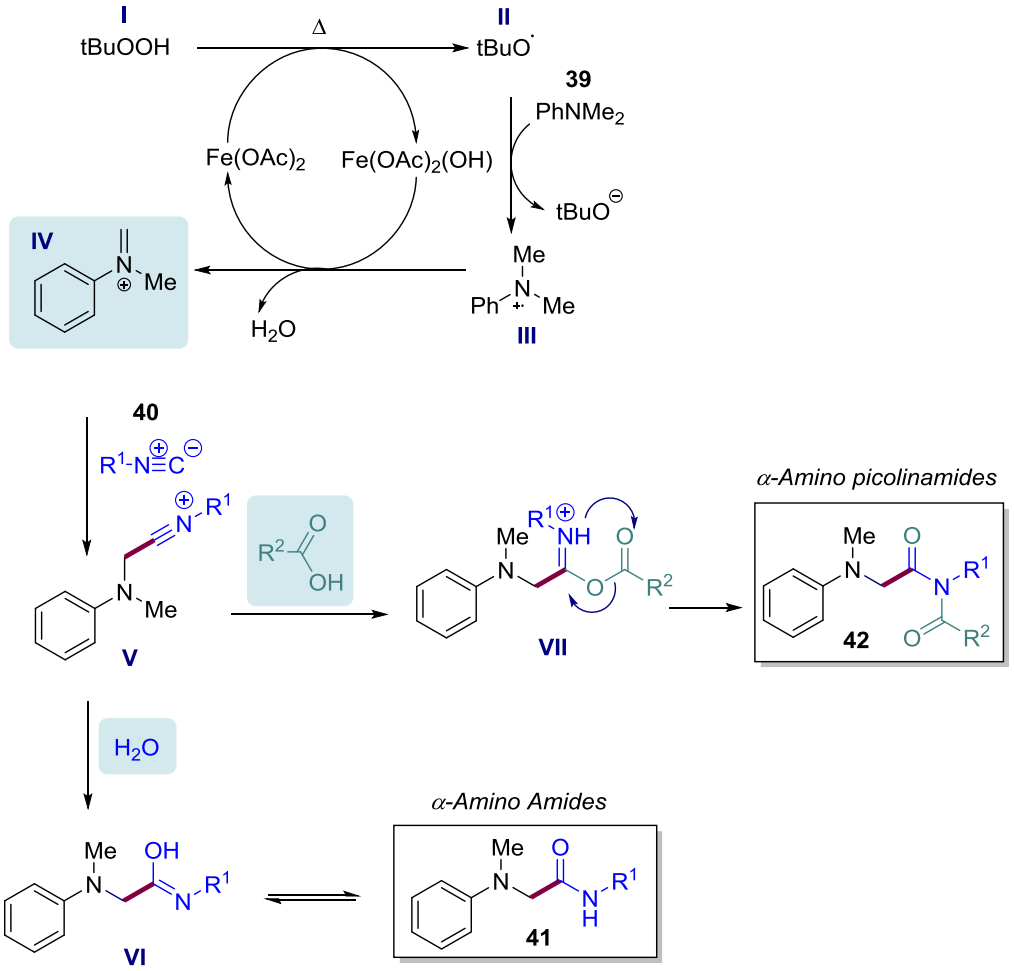

Scheme 66 Proposed Mechanism.

3.4. Conclusion

As a conclusion, an alternative oxidative Ugi-type reaction has been disclosed based on the functionalization of tertiary *N*,*N*-dimethylanilines with the low-priced iron-catalyst and *tert*-butyl hydroperoxide.[119] Not only complementary, but this operationally simple protocol provides a remarkable extention of prior synthetic scope resulting in a vast array of α-amino amides with a high functional group tolerance in good yields. Moreover, the particular addition of picolinic acid leads to the selective formation of α-amino picolinamides, whose pyridine ring constitutes a versatile moiety for medicinal chemistry. Natural products and stapled peptide synthesis are among recent applications of Ugi-3CR, where the sustainability is a major concern. Hence, due to the practicality and low-toxicity of iron salts, this method could find its application in the field of peptide chemistry.

[119] Guerrero, I.; San Segundo, M.; Correa, A. *Chem. Commun.* **2018**, *54***,** 1627.

3.5. Experimental Procedures

In this section, some representative procedures as well as the characterization of illustrative compounds are provided. For a full detailed experimental description, please see the SI of the following article.[119]

3.5.1. Fe-Catalyzed C(sp^3)–H Functionalization of N,N-Dimethylanilines with Isocyanides

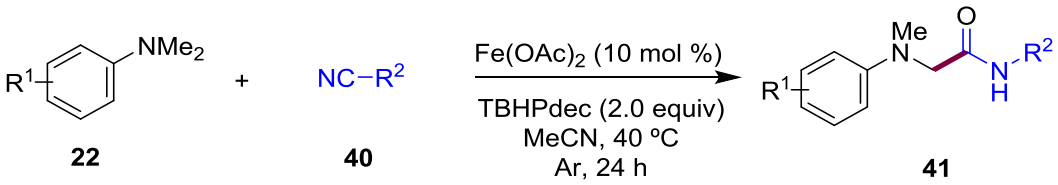

General Procedure: A reaction tube containing a stirring bar was charged with the corresponding *N*,*N*-dimethylaniline **22** (if solid) (1.0 mmol, 2.0 equiv), isocyanide **40** (if solid) (0.5 mmol, 1.0 equiv) and $Fe(OAc)_2$ (10 mol %). The reaction tube was then evacuated and back-filled with dry argon (this sequence was repeated up to three times). The corresponding *N*,*N*-dimethylaniline **22** (1.0 mmol, 2.0 equiv), and isocyanide **40** (0.5 mmol, 1.0 equiv) (if liquids), TBHP (5.0-6.0 M in decane) (2.0 equiv), and MeCN (2.0 mL) were then added under argon atmosphere. The reaction tube was next warmed up to 40 ºC and stirred for 24 hours. The mixture was then allowed to warm to room temperature, concentrated under reduced pressure and the corresponding product was purified by flash chromatography (hexanes/AcOEt 1/1), unless otherwise indicated.

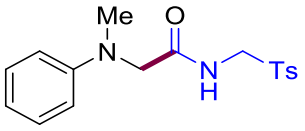

(**41aa**)

2-[Methyl(phenyl)amino]-*N*-(tosylmethyl)acetamide (41aa). Following the general procedure, using commercially available *N*,*N*-dimethylaniline (1.0 mmol, 126 µL) and *p*-toluenesulfonylmethyl isocyanide (0.5 mmol, 98 mg) provided 135 mg (81% yield) of **41aa** as a white solid. Mp 125-126 ºC (Lit.[120] 111-112 ºC). The spectroscopic data correspond to those previously reported in the literature.[121] ^{1}H NMR (400 MHz, $CDCl_3$): δ 7.82 – 7.66 (m, 2H), 7.46 (t, J = 7.0 Hz, 1H), 7.43 – 7.21 (m, 4H), 6.89 (t, J = 7.3 Hz, 1H), 6.74 – 6.61 (m, 2H), 4.68 (d, J = 6.9 Hz, 2H), 3.76 (s, 2H), 2.99 (s, 3H), 2.47 (s, 3H). ^{13}C NMR (101 MHz, $CDCl_3$): δ 170.3, 148.9, 145.4, 133.7, 129.8, 129.3, 128.7, 118.9, 113.2, 59.8, 58.3, 39.9, 21.7. *This reaction was also performed in a*

[120] Katritzky, A. R.; Mohapatra, P. P.; Singh, S.; Clemens, N.; Kirichenko, K. *J. Serb. Chem. Soc.* **2005**, *70*, 319.
[121] Yadav, A. K.; Yadav, L. D. S. *Chem. Commun.* **2016**, *52*, 10621.

*higher scale: the use of N,N-dimethylaniline (10.20 mmol, 1.29 mL) and p-toluenesulfonylmethyl isocyanide (5.12 mmol, 1.00 g) provided 1.54 g (91% yield) of **41aa** as a white solid.*

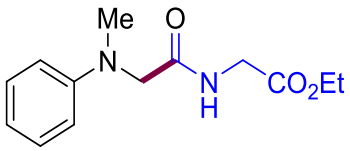

(**41ag**)

Ethyl *N*-methyl-*N*-phenylglycylglycinate (41ag). Following the general procedure adding AcOH (2.0 equiv) at 70 ºC, using *N,N*-dimethylaniline (1.0 mmol, 126 µL) and ethyl isocyanoacetate (0.5 mmol, 55 µL) provided 96 mg (77 % yield) of **41ag** as a yellow oil. ^{1}H NMR (400 MHz, $CDCl_3$) δ 7.36 – 7.26 (m, 2H), 7.08 (s, 1H), 6.87 (t, J = 7.3 Hz, NH), 6.81 (d, J = 8.0 Hz, 2H), 4.21 (q, J = 7.1 Hz, 2H), 4.08 (d, J = 5.7 Hz, 2H), 3.94 (s, 2H), 3.07 (s, 3H), 1.29 (t, J = 7.1 Hz, 3H). ^{13}C NMR (101 MHz, $CDCl_3$) δ 171.3, 169.8, 149.7, 129.7, 119.1, 113.7, 61.8, 59.1, 41.3, 40.0, 14.4. IR (neat, cm^{-1}): 3282, 2980, 1741, 1670, 1188. HRMS *calcd*. for ($C_{13}H_{18}N_2O_3$): 250.1317, *found* 250.1307.

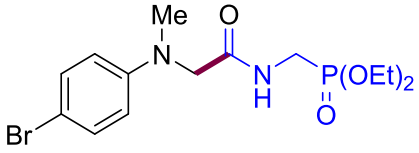

(**41bh**)

Diethyl [(2-((4-bromophenyl)(methyl)amino)acetamido)methyl]phosphonate (41bh). Following the general procedure adding AcOH (2.0 equiv) at 70 ºC, using commercially available 4-bromo-*N,N*-dimethylaniline (1.0 mmol, 200 mg) and diethyl isocyanomethylphosphonate (0.5 mmol, 80 µL) provided 158 mg (81 % yield) of **41bh** as a yellow oil. ^{1}H NMR (400 MHz, $CDCl_3$) δ 7.35 (d, J = 9.1 Hz, 2H), 6.74 (br s, 1H), 6.61 (d, J = 9.1 Hz, 2H), 4.08 (p, J = 7.2 Hz, 4H), 3.88 (s, 2H), 3.76 – 3.68 (m, 2H), 3.03 (s, 3H), 1.28 (t, J = 7.1 Hz, 6H). ^{13}C NMR (101 MHz, $CDCl_3$) δ 169.8 (d, $J_{C\text{-}P}$ = 10.1Hz), 148.0, 132.0, 114.8, 111.0, 62.5 (d, $J_{C\text{-}P}$ = 8.08 Hz), 58.5, 40.0, 35.2, 33.6, 16.3(d, $J_{C\text{-}P}$ = 10.1 Hz). IR (neat, cm^{-1}): 3268, 2980, 1751, 1495, 1208, 10020. HRMS *calcd*. for ($C_{14}H_{22}BrN_2O_4P$): 392.0501, *found* 392.0493.

3.5.2. Fe-Catalyzed Ugi-type Multicomponent Reaction with Picolinic Acid

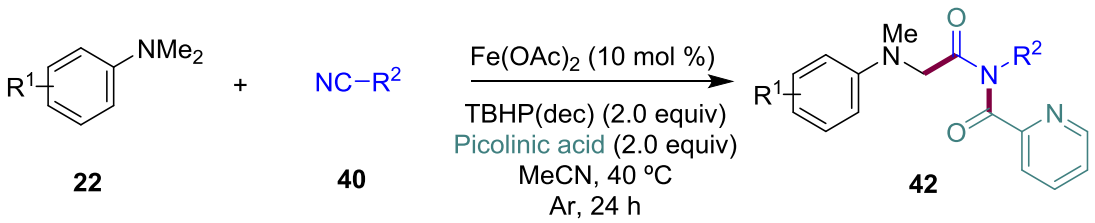

General Procedure: A reaction tube containing a stirring bar was charged with the corresponding *N*,*N*-dimethylaniline **22** (if solid) (1.0 mmol, 2.0 equiv), isocyanide **40** (if solid) (0.5 mmol, 1.0 equiv), picolinic acid (1.0 mmol, 2.0 equiv) and $Fe(OAc)_2$ (10 mol %). The reaction tube was then evacuated and back-filled with dry argon (this sequence was repeated up to three times). The corresponding *N*,*N*-dimethylaniline **22** (1.0 mmol, 2.0 equiv), and isocyanide **40** (0.5 mmol, 1.0 equiv) (if liquids), TBHP (5.0-6.0 M in decane) (2.0 equiv), and MeCN (2.0 mL) were then added under argon atmosphere. The reaction tube was next warmed up to 40 ºC and stirred for 24 hours. The mixture was then allowed to warm to room temperature, concentrated under reduced pressure and the corresponding product was purified by flash chromatography (hexanes/AcOEt 1/1), unless otherwise indicated.

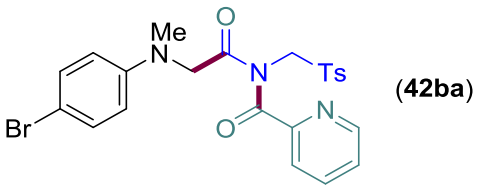

(**42ba**)

***N*-[*N*-(4-Bromophenyl)-*N*-methylglycyl]-*N*-(tosylmethyl)picolinamide (42ba).** Following the general procedure, using 4-bromo-*N*,*N*-dimethylaniline (0.5 mmol, 100 mg) and *p*-toluenesulfonylmethyl isocyanide (0.25 mmol, 49 mg) provided 82.4 mg (64% yield) of **42ba** as an orange solid. Mp 132-133 ºC. ^{1}H NMR (400 MHz, $CDCl_3$): δ 8.62 (ddd, J = 4.8, 1.6, 0.9 Hz, 1H), 8.12 – 7.84 (m, 2H), 7.71 (d, J = 8.2 Hz, 2H), 7.52 (ddd, J = 7.6, 4.8, 1.3 Hz, 1H), 7.31 (d, J = 8.0 Hz, 2H), 7.22 (d, J = 9.0 Hz, 2H), 6.37 (d, J = 8.9 Hz, 2H), 5.62 (s, 2H), 4.37 (s, 2H), 2.75 (s, 3H), 2.43 (s, 3H). ^{13}C NMR (101 MHz, $CDCl_3$): δ 172.0, 170.0, 150.4, 148.1, 147.5, 145.5, 137.7, 134.1, 131.6, 129.8, 128.9, 127.1, 126.2, 114.1, 109.7, 63.9, 57.3, 39.2 21.7. IR (neat, cm^{-1}): 1701, 1591, 1085. HRMS *calcd.* for ($C_{23}H_{22}BrN_3O_4S$): 515.0514, *found* 515.0505.

3.6.3. NMR spectra

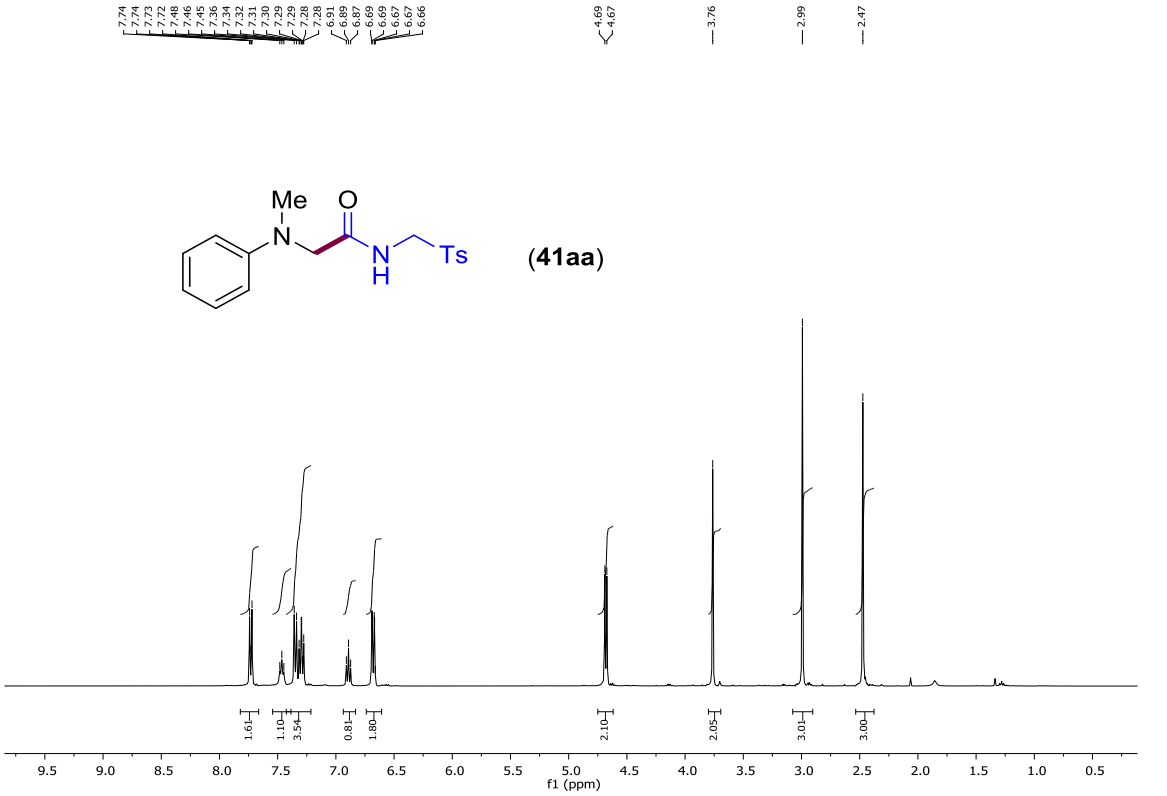

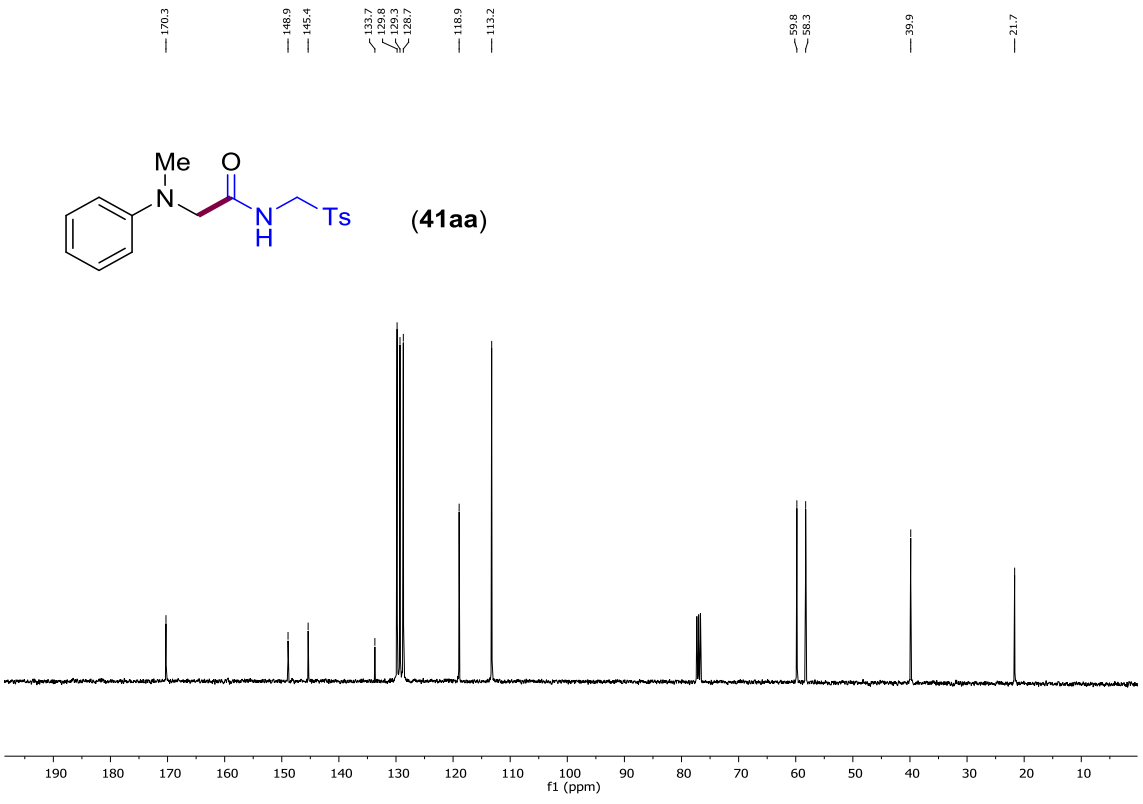

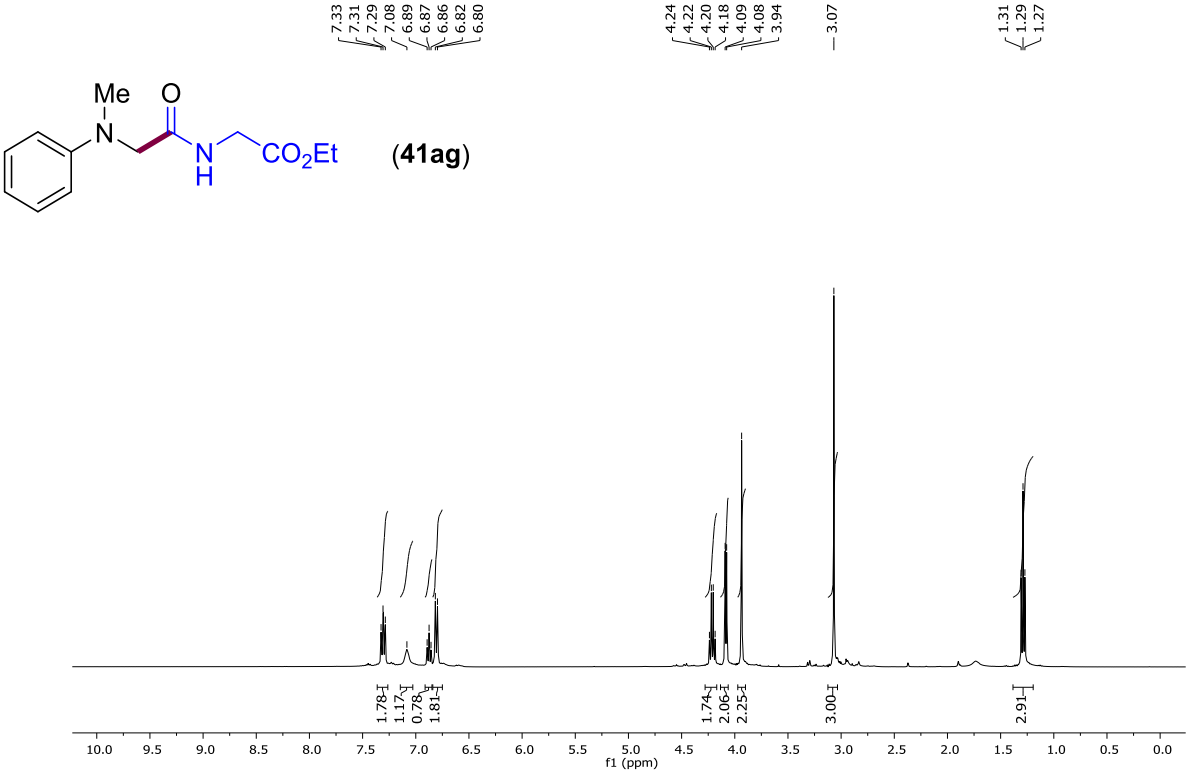
7.33
7.31
7.29
7.08
6.89
6.87
6.86
6.82
6.80
4.24
4.22
4.20
4.18
4.09
4.08
3.94
3.07
1.31
1.29
1.27
Me
O
N
N
H
CO2Et
(41ag)
1.78
1.17
0.78
1.81
1.74
2.06
2.25
3.00
2.91
f1 (ppm)

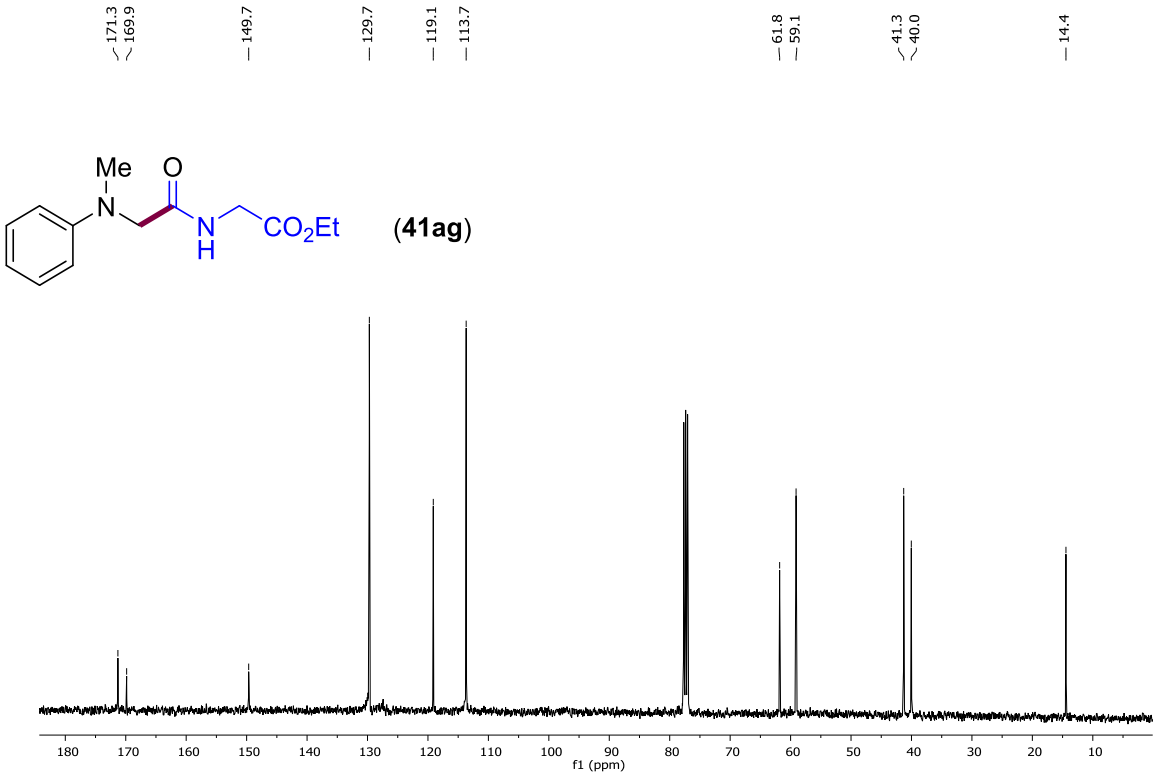
171.3
169.9
149.7
129.7
119.1
113.7
61.8
59.1
41.3
40.0
14.4
Me
O
N
N
H
CO2Et
(41ag)
f1 (ppm)

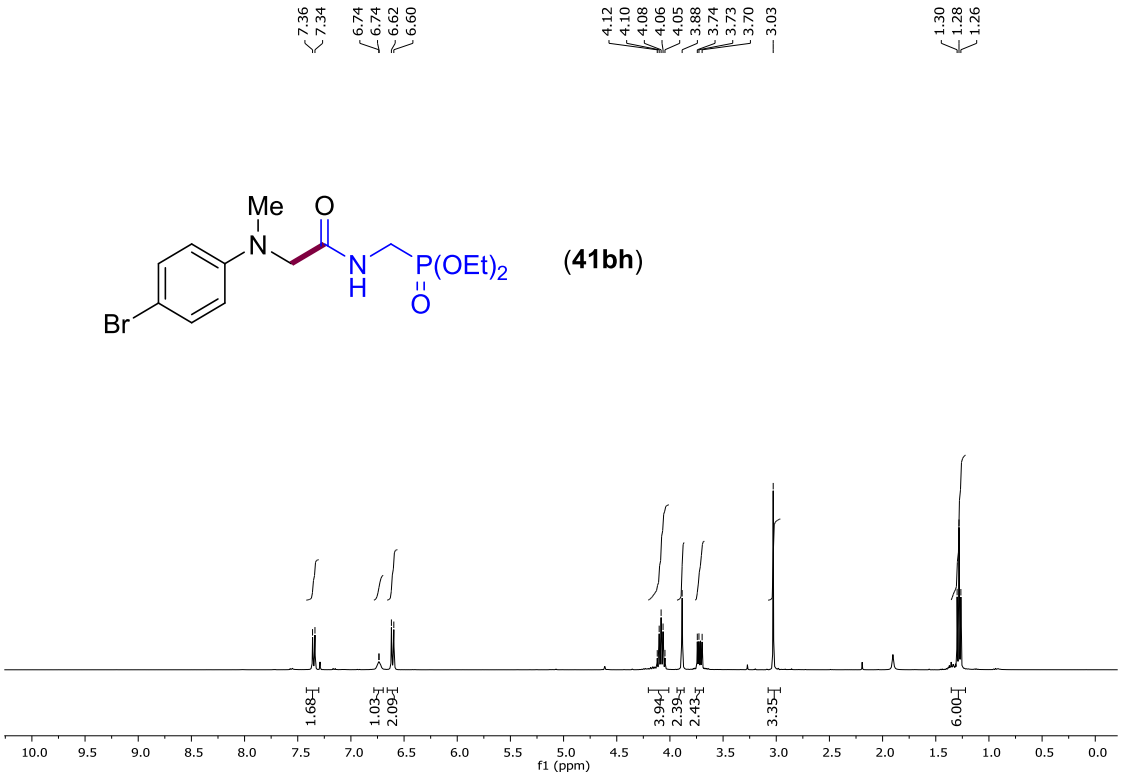
7.36
7.34
6.74
6.74
6.62
6.60
4.12
4.10
4.08
4.06
4.05
3.88
3.74
3.73
3.70
3.03
1.30
1.28
1.26
Me
O
N
N
H
P(OEt)2
O
Br
(41bh)
1.68
1.03
2.09
3.94
2.39
2.43
3.35
6.00
f1 (ppm)

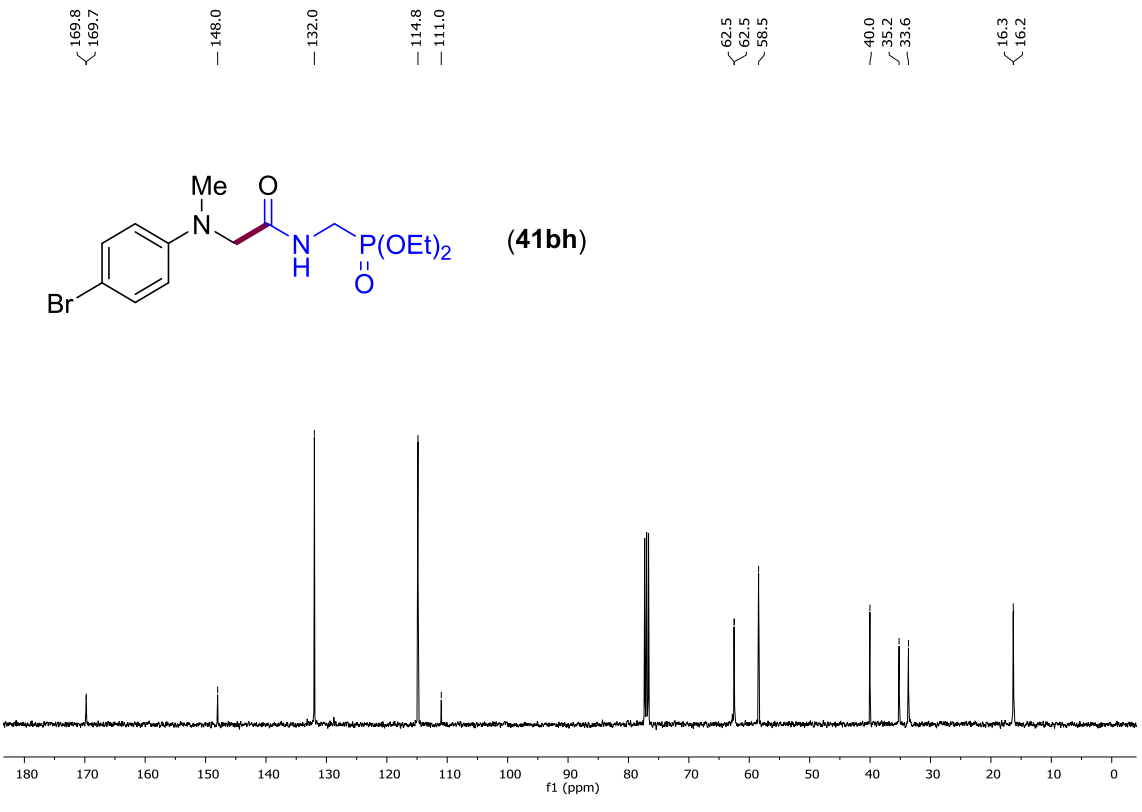
169.8
169.7
148.0
132.0
114.8
111.0
62.5
62.5
58.5
40.0
35.2
33.6
16.3
16.2
Me
O
N
N
H
P(OEt)2
O
Br
(41bh)
f1 (ppm)

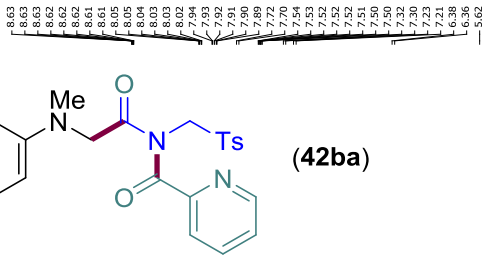

(**42ba**)

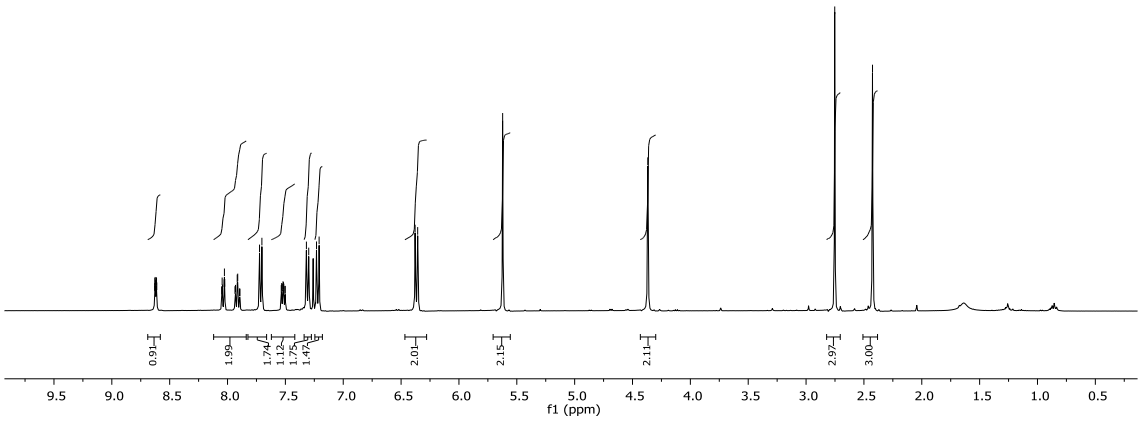

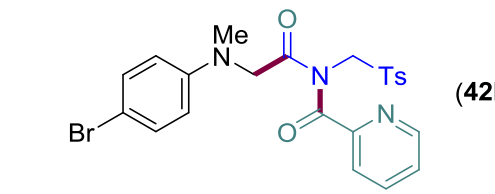

(**42ba**)

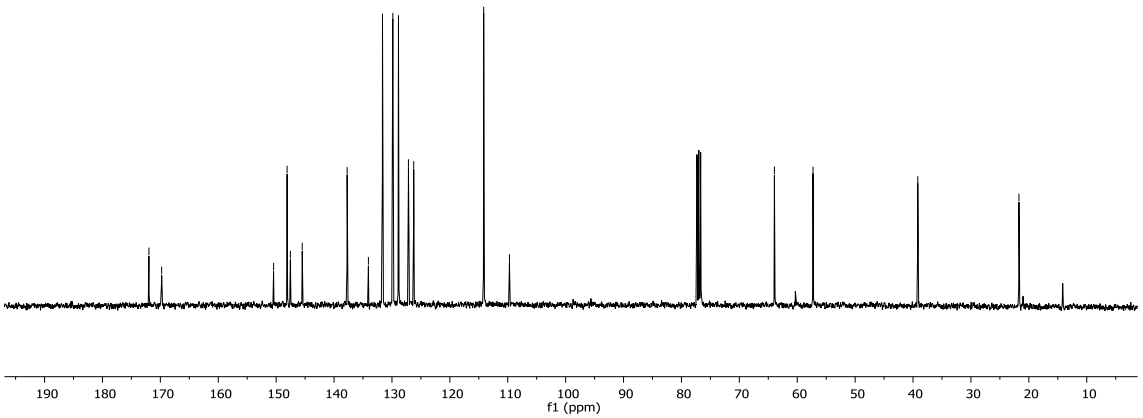

Chapter 4.

Copper-Catalyzed Site-Selective C(sp^2)–H Trifluoromethylation of Tryptophan-Containing Peptides

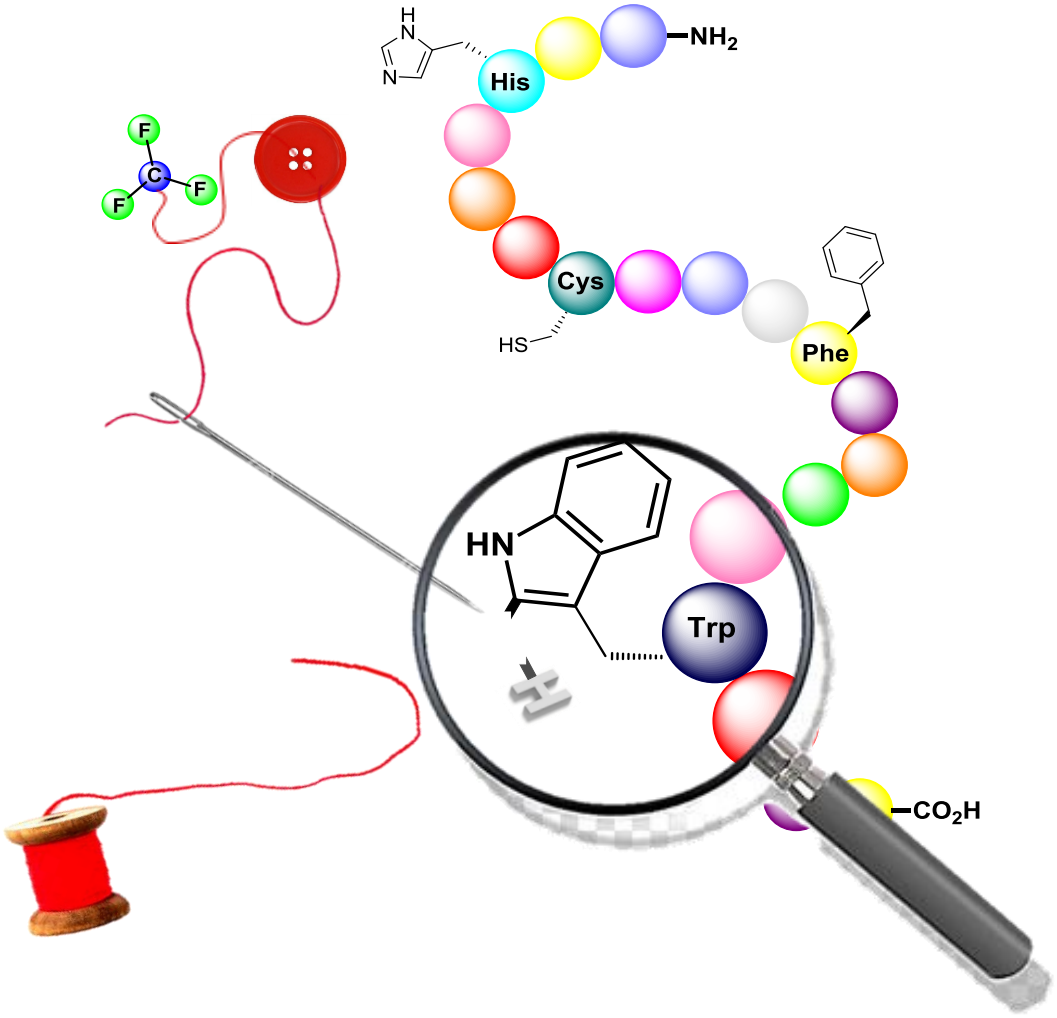

4.1. Introduction

4.1.1. Peptide Side-Chain C–H Functionalization: Tryptophan

Considering the crucial role played by peptides in living organisms,[122] the site-selective diversification of these highly ranked biomolecules has become of utmost significance. The straightforward manipulation of amino acids in peptidic scaffolds could result in the enhancement of their biological functions and pharmacokinetics, which is of great interest in proteomics.[123] Indeed, the landscape of peptide chemistry is currently experiencing an exponential growth, thereby dramatically expanding the available chemical toolbox and streamlining the rapid assembly of non-proteinogenic α-amino acids and peptides derived thereof. Despite formidable advances in the field, chemoselective functionalizaton of peptides still remains a daunting challenge. Transition-metal-catalyzed functionalization of the peptide backbone through the α-C(sp^3)–H heteroarylation of glycine derivatives has been described in Chapter 2. The methodology was based on the formation of an electrophile and its further nucleophilic attack providing a variety of modified glycine derivatives. However, the side-chain of natural amino acids can also enable the development of alternative transformations for the late-stage functionalization of complex biological structures.

A great number of selective C(sp^2)–H functionalizations are known and have been demonstrated to be feasible via transition-metal catalysis. Thus, the aromatic nature of the side-chain of phenylalanine, tyrosine, tryptophan or histidine could provide a target to modify and obtain the corresponding unnatural residues. Owing to their essential role in proteins and enzymes, their modification would be of paramount importance in medicinal chemistry. Nevertheless, the adaptation of the novel methodologies from a single amino acid unit to a more complex peptide diversification would face some previously mentioned challenges such as the presence of multiple C–H bonds, highly functionalized side-chains, multiple metal coordination sites, stereocenters that tend to racemize and the competitive chemoselectivity toward a specific aromatic moiety. A successful protocol overcoming those features would enable the late-stage functionalization of peptides in a total synthesis.

[122] a) Bucheit, J. D.; Pamulapati, L. G.; Carter, N.; K. Malloy, K.; Dixon, D. L.; Sisson, E. M. *Diabetes Technol. Ther.* **2020**, *22*, 10. b) Hedges, J. B.; Ryan, K. S. *Chem. Rev.* **2020**, *120*, 3161. c) Malonis, R. J.; Lai, J. R.; Vergnolle, O. *Chem. Rev.* **2020**, *120*, 3210. d) Blakemore, D. C.; Castro, L.; Churcher, I.; Rees, D. C.; Thomas, A. W.; Wilson, D. M.; Wood, A. *Nat. Chem.* **2018**, *10*, 383. e) Henninot, A.; Collins, J. C.; Nuss, J. M. *J. Med. Chem.* **2018**, *61*, 1382.

[123] a) Reese, H. R.; Shanahan, C. C.; Proulx, C.; Menegatti, S. *Acta Biomater.* **2020**, *102*, 35. b) Zhang, C.; Vinogradova, E. V.; Spokoyny, A. M.; Buchwald, S. L.; Pentelute, B. L. *Angew. Chem. Int. Ed.* **2019**, *58*, 4810. c) Hoyt, E. A.; Cal, P. M. S. D.; Oliveira, B. L.; Bernardes, G. J. L. *Nat. Rev. Chem.* **2019**, *3*, 147. d) Bondalapati, S.; Jbara, M.; Brik, A. *Nat. Chem.* **2016**, *8*, 407. e) Spicer, C. D.; Davis, B. G. *Nat. Commun.* **2014**, *5*, 4750.

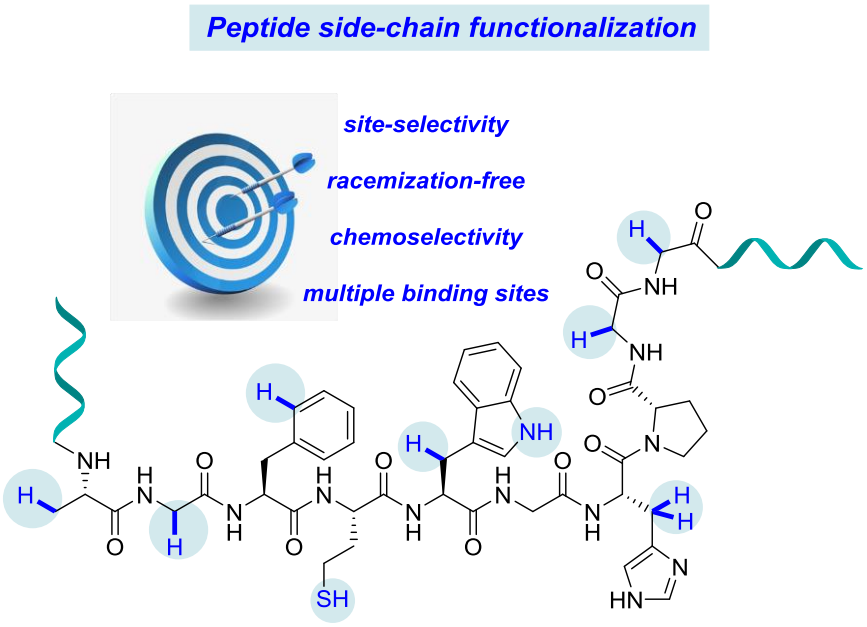

Figure 10 Challenges Observed for Peptide Side-Chain C–H Functionalization.

Among the twenty different existing natural amino acids, tryptophan is the less abundant one with a 1.4 % frequency. Nonetheless, in proteomics those complex structures that do not contain a Trp residue are unusual; it has been estimated that 90 % of proteins have at least one of this indole-based amino acid through their sequence. Furthermore, it has a significant role in protein-protein interactions.[124] Hence, targeting Trp unit would render in chemo- and site-selective bioconjugation of endogenous molecules. Currently, the development of novel synthetic pathways to assemble unnatural amino acid derivatives, including tryptophan, is a hot topic. In this way, C2-functionalization methodologies of indoles have served as a source of inspiration for targeting numerous Trp side-chain modifications.[125]

Likewise, transition-metals such as palladium and ruthenium have been exploited for several transformations in the tryptophan unit as observed in Scheme 67. On the other hand, one of the pressing goals within the field of organic synthesis is to search for alternative protocols where the sustainability is a prime issue. Hence, diversification of peptide structures through a more appealing manganese catalysis has gained a lot of attention due to its unique reactivity and environmentally friendly character. In this section, the different functionalizations carried out up to date in Trp derivatives will be disclosed.

[124] a) Bullock, B. N.; Jochim, A. L.; Arora, P. S. *J. Am. Chem. Soc.* **2011**, *133*, 14220. b) Moreira, I. S.; Fernandes, P. A.; Ramos, M. J. *Proteins Struct. Funct. Bioinf.* **2007**, *68*, 803. c) Bogan, A. A.; Thorn, K. S. *J. Mol. Biol.* **1998**, *280*, 1.
[125] a) Gruß, H.; Sewald, N. *Chem. Eur. J.* **2020**, *26*, 5328. b) Wang, W.; Lorion, M. M.; Shah, J.; Kapdi, A. R.; Ackermann, L. *Angew. Chem. Int. Ed*. **2018**, *57*, 14700. c) Brandhofer, T.; Mancheño, O. G. *Eur. J. Org. Chem.* **2018**, 6050.

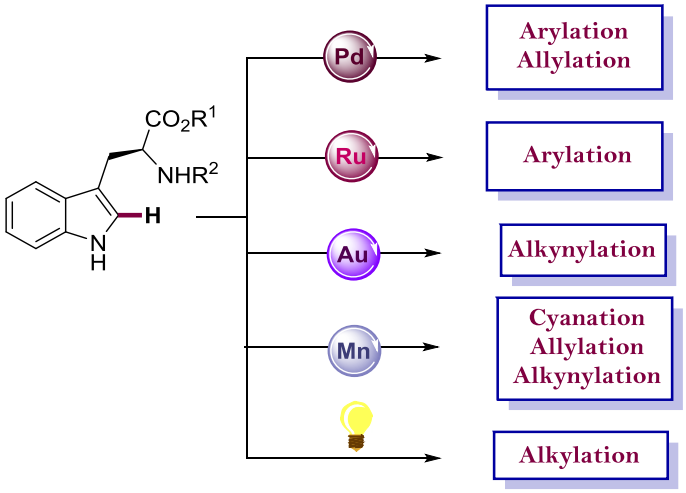

Scheme 67 Different C–H Tryptophan Functionalizations.

At the beginning of the last decade Francis and Ball described the rhodium(III)-catalyzed functionalization of tryptophan derivatives via metalocarbenoid intermediates generated by the activation of vinyl-substituted diazo compounds.[126] Despite the observed chemoselectivity toward Trp residues in proteins, the lack of regioselectivity resulted in mixtures of *N*- and C2-substituted indole products. In this manner, Linder also modified the N–H bond of the indole moiety in Trp units with dicarbonyl compounds as reversible tags.[127] Despite the significant innovation of these reports, an overall and more selective modification toward indole ring in Trp residues was still not available at that time.

4.1.1.1. Arylation

The C2-arylation of tryptophan derivatives has been the most studied reaction, where different arylating coupling partners have shown to be suitable in a variety of oxidative systems catalyzed mainly by palladium and with an isolated ruthenium example (Table 18). In 2010, Lavilla and Albericio described the C(sp^2)–H arylation of tryptophan with aryl iodides as coupling partners. The combination of $Pd(OAc)_2$ (5 mol %), $AgBF_4$ (1.0 equiv), and 2-nitrobenzoic acid (1.5 equiv) provided the C2-arylated tryptophan-containing native peptides within 5 minutes under microwave irradiation (Table 18, entry 1). Later on, this reaction was applied in an intramolecular fashion, where either Tyr- or Phe-iodinated residues were stapled with the Trp residue, obtaining cyclic peptides.[128d]

[126] a) Popp, B. V.; Ball, Z. T. *J. Am. Chem. Soc.* **2010**, *132*, 6660. b) Antos, J. M.; McFarland, J. M.; Iavarone, A. T.; Francis, M. B. *J. Am. Chem. Soc.* **2009**, *131*, 6301. c) Antos, J. M.; Francis, M. B. *J. Am. Chem. Soc.* **2004**, *126*, 10256.
[127] Foettinger, A.; Melmer, M.; Leitner, A.; Lindner, W. *Bioconjugate Chem.* **2007**, *18*, 1678.

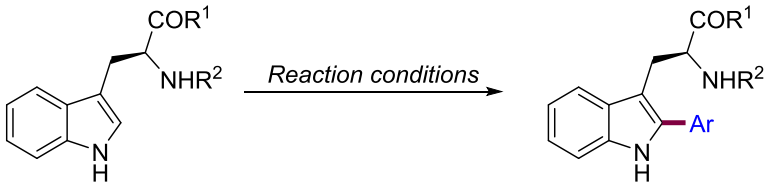

Entry	Catalyst	Oxidant	Ar source	Conditions	Yield (%)
1[128]	$Pd(OAc)_2$	$AgBF_4$	**Ar**–I	DMF, MW/2-NO_2Bz 150 °C	23–92
2[129]	$Pd(OAc)_2$	$PhI(OAc)_2$ or $Cu(OAc)_2$/air	**Ph**$B(OH)_2$	AcOH, 40 °C	8–95
3[130]	$Pd(OAc)_2$ or $Pd(OTs)_2(MeCN)_2$		**Ar**–N_2BF_4	EtOAc, r.t.	45–100
4[131]	$Pd(OAc)_2$	**Ar**$_2$IOTs		AcOH or H_2O, r.t.	41–98
5[132]		**Ar**$_2$IOTs		DMF, 100 °C	33–98
6[133]	$[RuCl_2(p\text{-cymene})]_2$		**Ar**–Br	*m*-xylene, K_3PO_4, $C_6F_5CO_2H$, 120 °C	51–97

Albericio/Lavila Fairlamb Ackermann

Table 18 C2-Arylation of Tryptophan Derivatives.

[128] a) Mendive-Tapia, L.; Preciado, S.; García, J.; Ramón, R.; Kielland, N.; Albericio, F.; Lavilla, R. *Nat. Commun.* **2015**, *6*, 7160. b) Preciado, S.; Mendive-Tapia, L.; Albericio, F.; Lavilla, R. *J. Org. Chem.* **2013**, *78*, 8129. c) Preciado, S.; Mendive-Tapia, L.; Torres-García, C.; Zamudio-Vázquez, R.; Soto-Cerrato, V.; Pérez-Tomás, R.; Albericio, F.; Nicolás, E.; Lavilla, R. *Med. Chem. Commun.* **2013**, *4*, 1171. d) Ruiz-Rodríguez, J.; Albericio, F.; Lavilla, R. *Chem. Eur. J.* **2010**, *16*, 1124.

[129] a) Reay, A. J.; Williams, T. J.; Fairlamb, I. J. S. *Org. Biomol. Chem.* **2015**, *13*, 8298. b) Williams, T. J.; Reay, A. J.; Whitwood, A. C.; Fairlamb, I. J. S. *Chem Commun.* **2014**, *50*, 3052.

[130] Reay, A. J.; Hammarback, L. A.; Bray, J. T. W.; Sheridan, T.; Turnbull, D.; Whitwood, A. C.; Fairlamb, I. J. S. *ACS Catal.* **2017**, *7*, 5174.

[131] Zhu, Y.; Bauer, M.; Ackermann, L. *Chem. Eur. J.* **2015**, *21*, 9980.

[132] Zhu, Y.; Bauer, M.; Ploog, J.; Ackermann, L. *Chem. Eur. J.* **2014**, *20*, 13099.

[133] Schischko, A.; Ren, H.; Kaplaneris, N.; Ackermann, L. *Angew. Chem. Int. Ed.* **2017**, *56*, 1576.

Next, Fairlamb and co-workers reported two similar palladium-catalyzed Suzuki-type oxidative reactions with boronic acids and Trp derivatives (Table 18, entry 2). The reactions proceeded in the presence of an oxidant like $PhI(OAc)_2$ or atmospheric air with $Cu(OAc)_2$ as co-catalyst. In general, milder reaction conditions were achieved with a significant decrease in the reaction temperature to 40 ºC. It was also Fairlamb's group, who developed another Pd-catalyzed C–H arylation of tryptophan derivatives. This time with the use of aryldiazonium salts as the coupling partner (Table 18, entry 3). Although the process took place at room temperature and gave excellent yields for C2-arylated tryptophan units, only a couple of peptide examples were submitted to the reaction conditions. Ackermann and co-workers also contributed to this field with three more arylation methods. Initially, they succeeded in a metal-free C–H modification of non-natural peptides with user-friendly diaryliodonium salts[134] as arylating partners (Table 18, entry 5). In spite of the developed arylation protocols, features such as high reaction temperatures, elevated stoichiometric amounts of reagents (2-5 equiv) or expensive and toxic silver oxidants represented significant restrictions for further late-stage peptide diversification. In this context, a milder Pd-catalyzed procedure was further described, where the modification of peptides could be performed at room temperature and with 1.5 equivalents of the arylating reagent in a more environmentally-friendly aqueous media (Table 18, entry 4). Finally, the same group developed the first site- and chemoselective cost-effective ruthenium(II)-catalyzed C(sp^2)–H arylation of Trp-containing peptides (Table 18, entry 6). All type of aryl bromide sources turned out to be compatible with the reported reaction conditions leading to the corresponding arylated Trp-containing oligopeptides with no racemization of the existing stereocenters. In stark contrast, this methodology provided an outstanding scope where α- and β-amino acids were functionalized, arylated peptides with fluorescence properties were obtained and more interestingly chemical ligation of two different peptides was achieved (Scheme 68). The selective C–H functionalization was ensured by the installation of a pyridine ring acting as the directing group.

[134] Pacheco-Benichou, A.; Besson, T.; Fruit, C. *Catalysts* **2020**, *10*, 483.

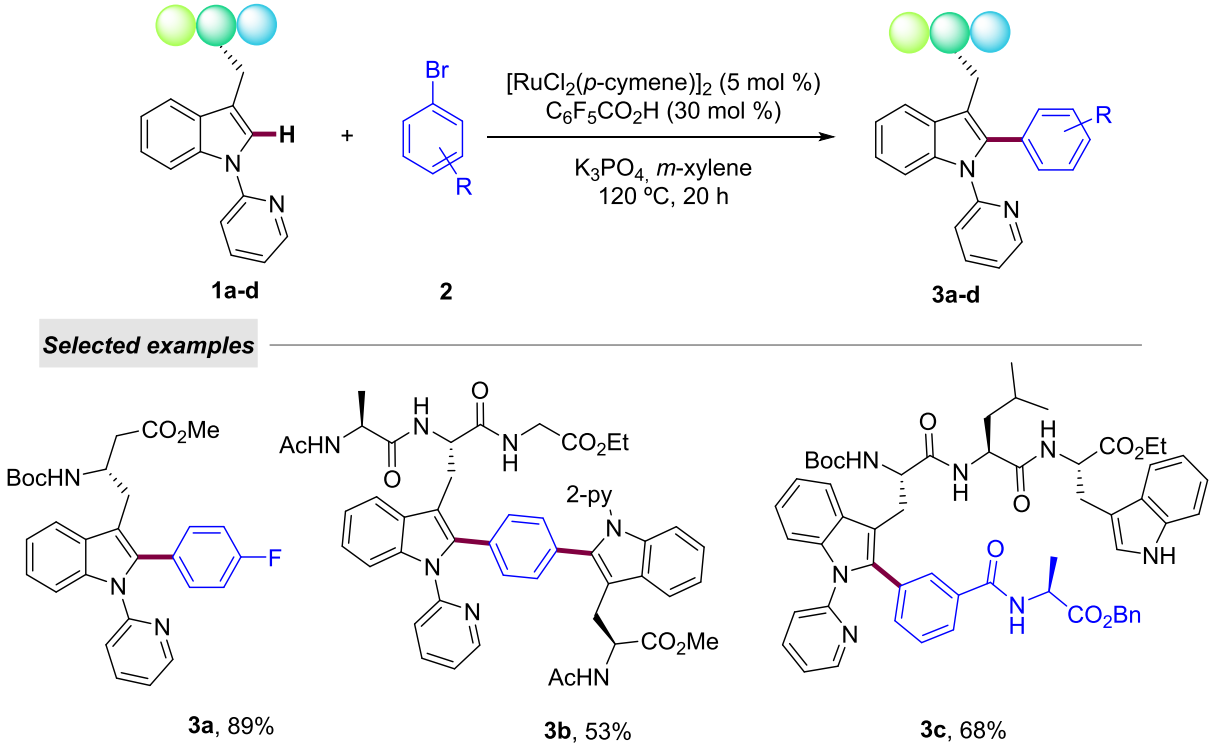

Scheme 68 Ruthenium(II)-Catalyzed C–H Arylation Enabling Chemical Ligation of Peptides.

4.1.1.2. Alkynylation

The installation of the versatile alkynyl group is of great value and enables further manipulation of any molecule such as the reaction with an azide for the formation of triazole compounds upon "click chemistry".[135] Based on a previously reported tryptophan C2-alkynylation protocol,[136] Hoeg-Jensen and co-workers developed a gold-catalyzed C(sp^2)–H alkynylation of tryptophan compounds utilizing TIPS-EBX as ethynyl donor in acetonitrile at room temperature (Scheme 69).[137] Not only peptides but also proteins like apomyoglobin and melittin were submitted to the reaction conditions and gave the corresponding adducts in good yields. However, in some cases stoichiometric amount of the gold source was necessary to obtain full conversion.

[135] Kolb, H. C.; Finn, M. G.; Sharpless, K. B. *Angew. Chem. Int. Ed.* **2001**, *40*, 2004.
[136] Tolnai, G. L.; Brand, J. P.; Waser, J. *Beilstein J. Org. Chem.* **2016**, *12*, 745.
[137] Borre Hansen, M.; Hubálek, F.; Skrydstrup, T.; Hoeg-Jensen, T. *Chem. Eur. J.* **2016**, *22*, 1572.

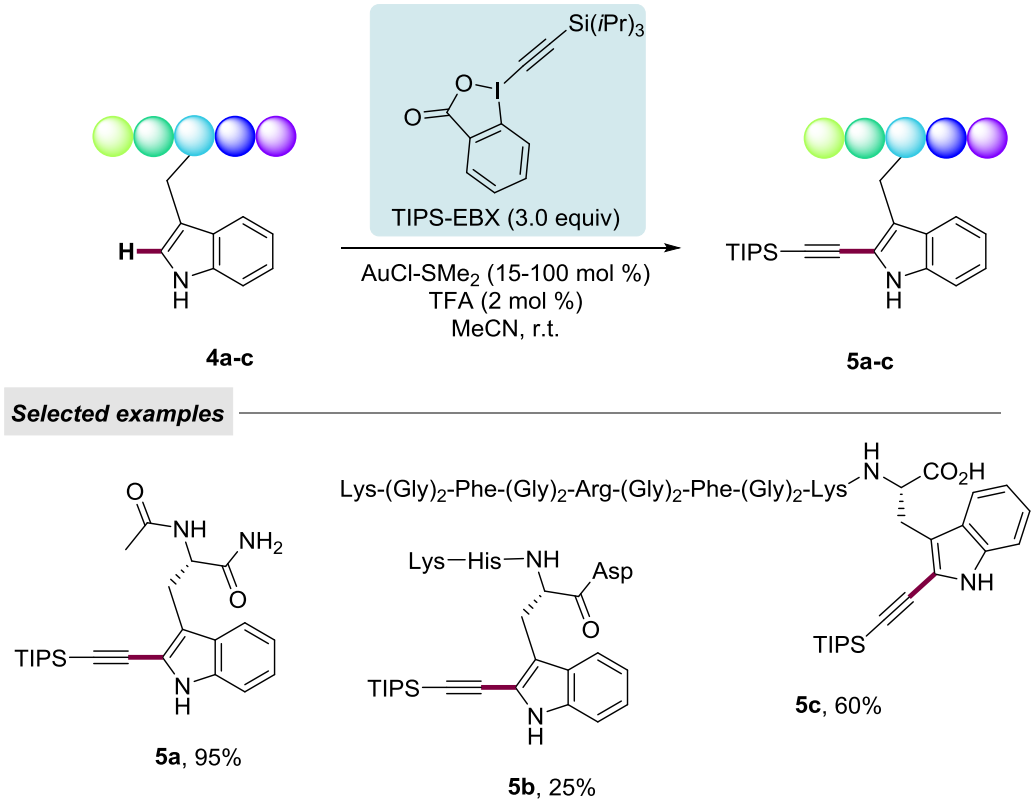

Scheme 69 Gold-Catalyzed C–H Alkynylation of Tryptophan-Containing Peptides.

As it has been justified all along this Thesis, the use of precious metals has been avoided to apply earth-abundant and less toxic base metals like manganese, whose complexes have shown to be able to mediate some C–H functionalization processes in a 'Pd-like' manner, raising hopes that this could provide a robust alternative to current methods.[138] Precisely, in 2017 Ackermann's group disclosed an alkynylation reaction of indoles with bromo alkynes catalyzed by $[MnBr(CO)_5]$.[139] The protocol led to the modification of novel peptidic structures like compound **7**, which was formed by the macrocyclization of substrate **6** (Scheme 70). The installation of the pyrimidine ring in the N–H bond of the indole was required as the directing group to enable the site-selectivity towards the C2-position. Likewise, after the C–H activation step the migratory insertion of the alkynyl bromide provided the organometallic species **III,** which rendered the desired product **VI** upon β-elimination.

[138] a) Liu, W.; Ackermann, L. *ACS Catal.* **2016**, *6*, 3743. b) Liu, W.; Groves, J. T. *Acc. Chem. Res.* **2015**, *48*, 1727.
[139] Ruan, Z.; Sauermann, N.; Manoni, E.; Ackermann, L. *Angew. Chem. Int. Ed*. **2017**, *56*, 3172.

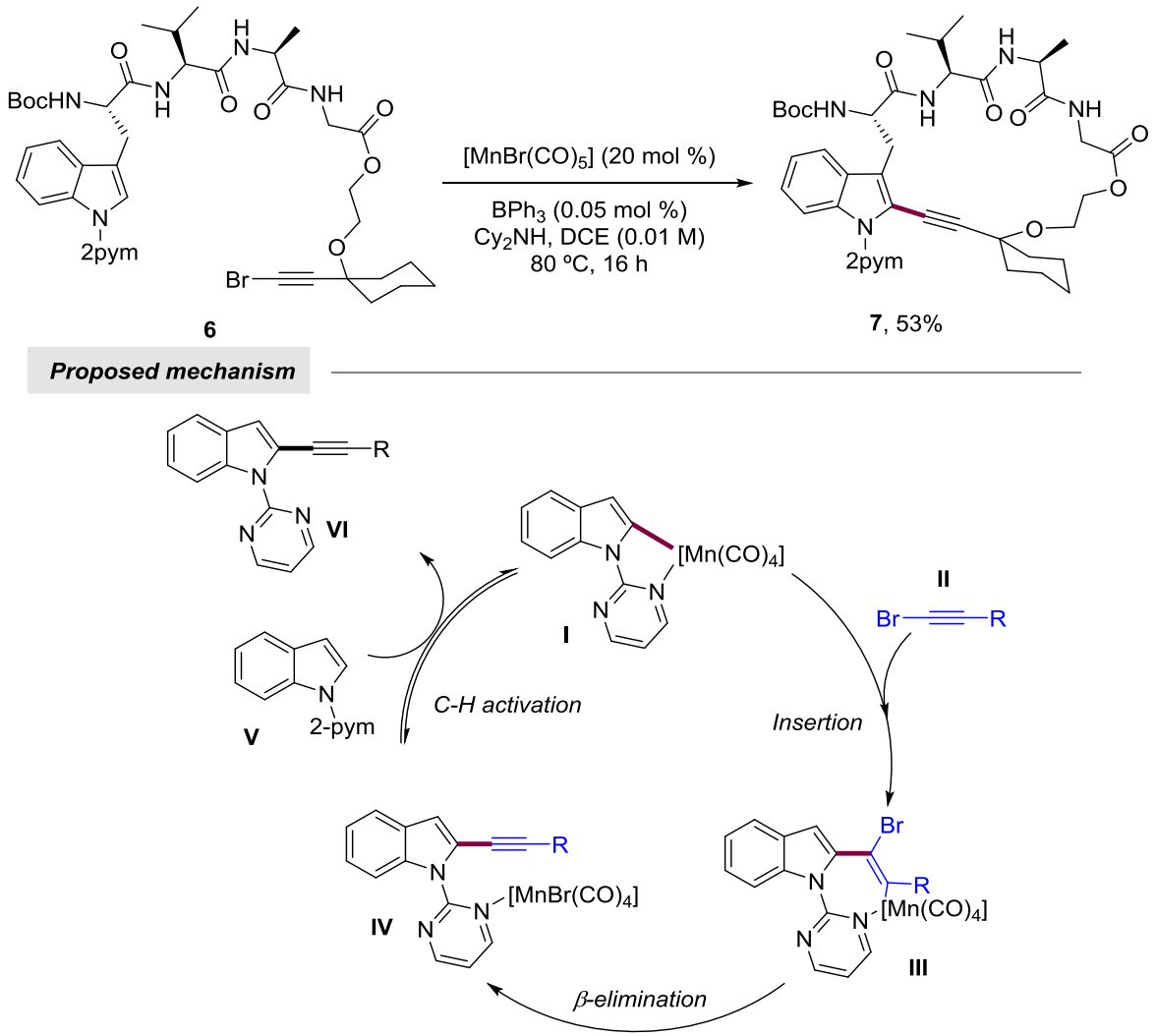

Scheme 70 Manganese-Catalyzed C–H Alkynylation.

4.1.1.3. Cyanation

As part of his interest in sustainable development, Ackermann reported a Mn-catalyzed cyanation of indole derivatives including a few Trp examples.[140]

[140] Liu, W.; Richter, S. C.; Mei, R.; Feldt, M.; Ackermann, L. *Chem. Eur. J.* **2016**, *22*, 17958.

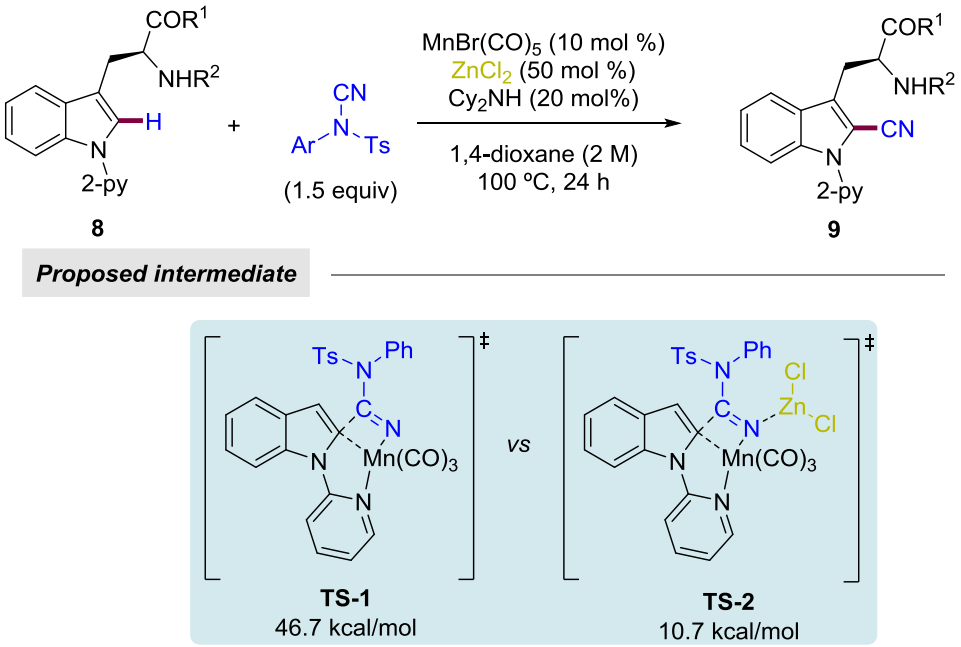

Scheme 71 Heterobimetallic Catalysis for C–H Cyanation Tryptophan Derivatives.

Catalytic amounts of $MnBr(CO)_5$, $ZnCl_2$ and Cy_2NH in ethereal solvent at 100 °C provided the coupling between *N*-pyridine tryptophan derivatives and Beller's NCTS (*N*-cyano-*N*-aryl-*p*-toluenesulfonamide)[141] in moderate yields and with no change in the existing stereocenter (Scheme 71). The crucial role of the additives must be highlighted as in their absence no reaction took place. DFT studies revealed that the coordination of the Zn(II) additive with the cyclomanganated intermediate led to a more stable transition state **TS-2** with 10.7 kcal·mol^{-1} in comparison with the **TS-1** with 46.7 kcal·mol^{-1} in its absence, which unraveled the synergistic action of a heterobimetallic catalysis regime.

4.1.1.4. Allylation

More recently, Cross and co-workers have reported the palladium-catalyzed olefination of tryptophan residues in peptides. Based on their previous phenylalanine functionalization methodology,[142] model dipeptide Ac-Gly-Trp-OMe, where the indole unit remained unprotected as the NH-free unit, was submitted to the following reaction conditions: $Pd(OAc)_2$ (10 mol %), AgOAc (2.5 equiv) and 4 equivalents of styrene at 130 °C in *t*-amyl alcohol. Unlike the Phe-analogue, the reaction with the tryptophan derivative **10a** did not proceed to produce the product **12a**. After several control experiments, they came to the conclusion that *tert*-butoxycarbonyl

[141] Anbarasan, P.; Neumann, H.; Beller, M. *Chem. Soc. Rev.* **2011**, *40*, 5049.
[142] Terrey, M. J.; Perry, C. C.; Cross, W. B. *Org. Lett.* **2019**, *21*, 104.

protecting group was essential.[143] Thus, the latter would act as a DG, whereas the amide in the amino acid residue could be the main backbone-based DG. The switch to toluene as the solvent and a decrease in the reaction temperature avoided the cleavage of the Boc group providing the formation of a family of modified peptides in 45-87 % yields.

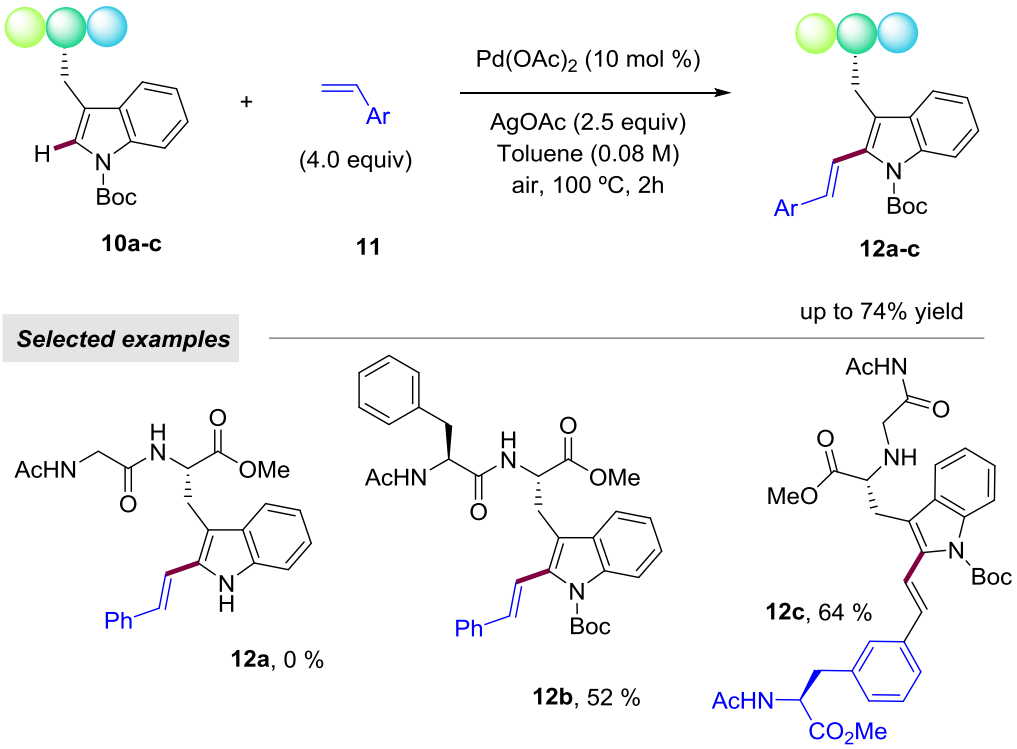

Scheme 72 Palladium-Catalyzed C2-Allylation.

Afterwards, the chemoselectivity of the reaction toward aromatic moieties was tested with both Trp and Phe containing dipeptides. Short-peptide Ac-Phe-Trp(Boc)-OMe **10b** was only modified in the Trp residue in 52% yield, whereas the absence of the Boc group resulted in the mono-olefination of the Phe residue preferentially.

[143] a) Yan, Z.-L.; Chen, W.-L.; Gao, Y.-R.; Mao, S.; Zhang, Y.-L.; Wang, Y.-Q. *Adv. Synth. Catal.* **2014**, *356*, 1085. b) Gong, B.; Shi, J.; Wang, X.; Yan, Y.; Li, Q.; Meng, Y.; Xu, H. E.; Yi, W. *Adv. Synth. Catal.* **2014**, *356*, 137. c) Lanke, V.; Prabhu, K. R. *Org. Lett.* **2013**, *15*, 2818. d) García-Rubia, A.; Urones, B.; Gómez Arrayás, R.; Carretero, J. C. *Chem. Eur. J.* **2010**, *16*, 9676.

4.1.1.5. C7-Functionalization of Tryptophan Derivatives

Site-selectivity is often an unmet challenge in the straightforward and rapid formation of engineered organic compounds. In this regard, the selective modification toward the C2-position in the indole scaffold is often achieved by the substitution of the most reactive C3-position, as it was observed previously in Trp residues. Nevertheless, the formation of two more regioisomers is possible from competitive C–H functionalization at C4- and C7-positions. Additionally, the particular introduction of functional groups into this latter side has caught great attention and several methods have been stablished for the diversification of indole moiety in alternative positions, which also included a few examples of Trp residues (Scheme 73).[144]

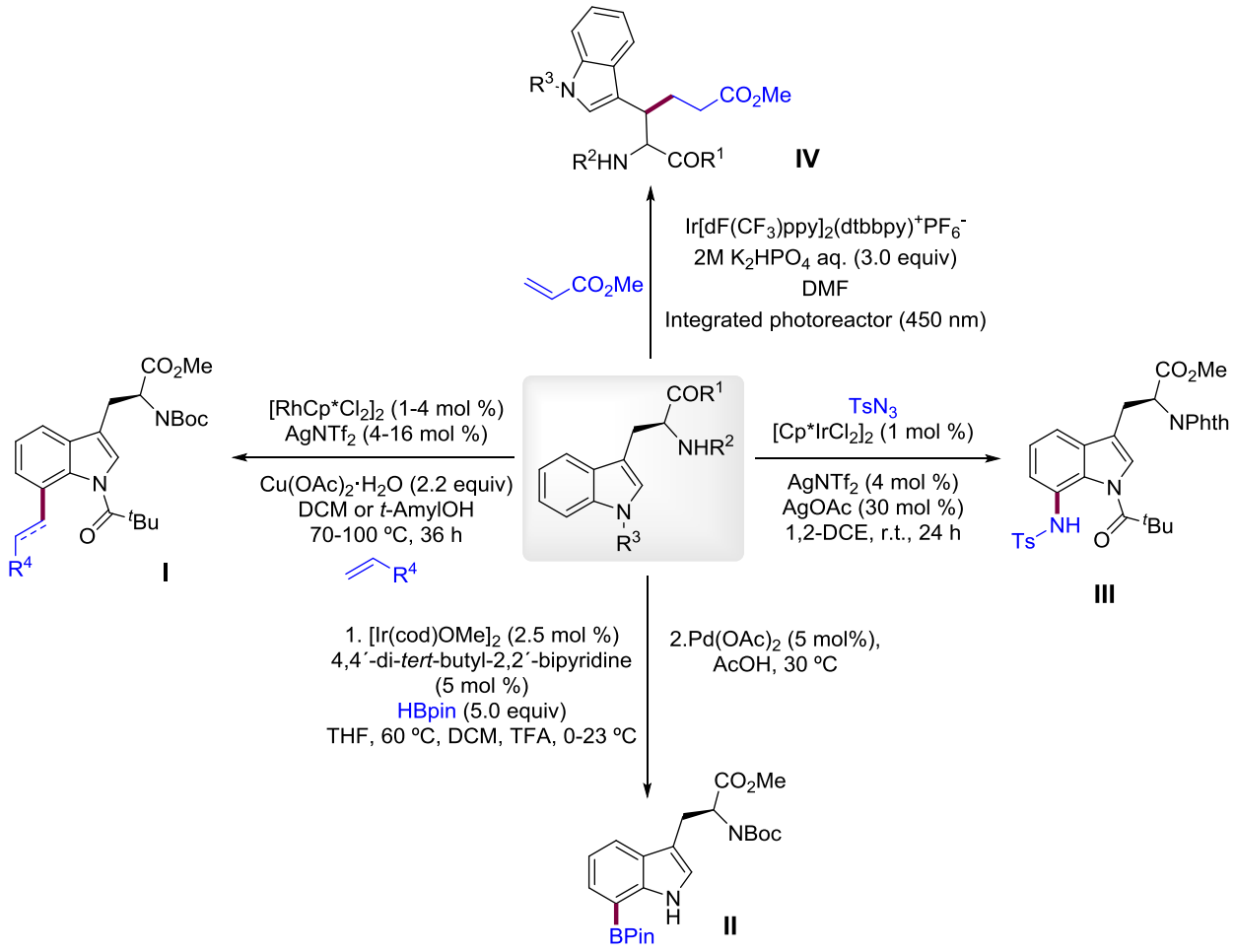

Scheme 73 C7- and β-position Functionalization of Tryptophan.

[144] Shah, T. A.; De, P. B.; Pradhan, S.; Punniyamurthy, T. *Chem. Commun.* **2019**, *55*, 572.

In 2016, Ma and co-workers disclosed the first Rh(III)-catalyzed C7-functionalization of indoles with alkenes (Scheme 73, **I**).[145] The regioselectivity of the process was attributed to the use of the bulky *N*-pivaloyl directing group, which enabled the formation of a six-membered ruthenacycle. Moreover, DFT studies determined the role of copper(II) acetate and silver additive for the formation and stabilization of the active catalytic species after the removal of the chloride anion.[146] Switching from Rh(III) to Ir(III), a similar mechanism was proposed for the formation of the active catalyst and further direct C7-amination of *N*-pivaloylindoles utilizing sulfonoazides as the nitrogen source.[147] In this occasion, the successful gram scale reaction of NPhth-Trp[C(O)^{t}Bu]-OMe was performed providing the desired product in 88% yield (Scheme 73, **III**). Iridium catalysis was also applied by Movassaghi and co-workers for the C7-borylation of C3-alkylindoles in a two-step one-pot reaction (Scheme 73, **II**).[148] The reaction consisted in the [Ir(cod)OMe]$_2$-catalyzed C2/C7-diborylation of indole derivatives, including tryptophan and tryptamine and the subsequent selective Pd-catalyzed C2-protodeboronation. Remarkably, the applicability of this valuable strategy was demonstrated when the embedded boronic acid pinacol ester motif in the C7-position of *N*-Boc-Trp-OMe could undergo further transformations in cross-coupling type reactions.

In comparison with the previous methodologies, Shi and co-workers extended the scope beyond simple amino acid units and functionalized the β-position of Trp-containing endogenous peptides via photocatalysis. Innovation aside, the described protocols required either expensive catalysts or toxic reagents, and scarcely provided peptide examples in their substrate scope. Hence, selective modification of alternative position into tryptophan residues has not reached yet its full synthetic potential and future new discoveries are expected in the challenging field of protein bioconjugation in the years to come.

4.1.2. Trifluoromethylation of Amino Acids and Peptides

The significant increase of novel methodologies for peptide modification has also led to the development of protocols that aim the installation of fluorine-containing functional groups as it can favorably tailor molecules' features. The introduction of a fluorine atom changes drastically both physical and biological properties such as solubility and lipophilicity, thereby resulting in the enhancement of metabolic stability and cellular membrane permeability.[149] The advantages presented by fluorinated compounds are reflected in areas like agrochemical and medicinal chemistry where around a 30% of the approved drugs have at least one of this halogen atom in

[145] Xu, L.; Zhang, C.; He, Y.; Tan, L.; Ma, *D. Angew. Chem. Int. Ed.* **2016**, *55*, 321.
[146] Han, L.; Ma, X.; Liu, Y.; Yu, Z.; Liu, T. *Org. Chem. Front.* **2018**, *5*, 725.
[147] a) Xu, L.; Tan, L.; Ma, D. *J. Org. Chem.* **2016**, *81*, 10476. b) Song, Z.; Antonchick, A. P. *Org. Biomol. Chem*. **2016**, *14*, 4804.
[148] Loach, R. P.; Fenton, O. S.; Amaike, K.; Siegel, S. D.; Ozkal, E.; Movassaghi, M. *J. Org. Chem.* **2014**, *79*, 11254.
[149] Szpera, R.; Moseley, D. F. J.; Smith, L. B.; Sterling, A. J.; Gouverneur, V. *Angew. Chem. Int. Ed.* **2019**, *58*, 14824.

their scaffold.[150] Furthermore, ^{18}F-labelled molecules are commonly used as radiotracers, owing to their convenient half-life ($t_{1/2}$=110 min) in Positron Emission Topography (PET) enabling the diagnosis and study of biological processes *in vivo* and the pharmaceutical effectiveness of drugs in high resolution images.[151]

Hence, despite rare examples in nature, organofluorine compounds have demonstrated to be of particular interest and due to their widespread applications in pharmaceutical chemistry, agrochemistry, biomedicine and material science, the need for effective and precise incorporation of fluorine substituents into relevant biomolecules like amino acids is in grand demand.[152] For instance, in some cases the substitution of a natural amino acid in a peptide chain for its fluorinated analogue has resulted in the improvement of protein-ligand or protein-protein interactions.[153]

Notably, the incorporation of a fluoroalkyl group into a molecule such as the privileged trifluoromethyl group is of prime interest for the formation of versatile pharmaceuticals, agrochemicals, liquid crystals, dyes, and polymers with unique properties.[154] In this regard, last decades have witnessed an intense growth in transition-metal-catalyzed trifluoromethylation reactions in a late-stage fashion. Additionally, the replacement of noble metals for first-row transition metals has contributed to the outpour of more sustainable protocols. Pioneering trifluoromethylating reagents such as the gaseous CF_3I are currently avoided by pharmaceutical industries because of practicality and safety issues. Instead, a wide range of trifluoromethylating agents with distinct electronic nature can be used in these endeavors.

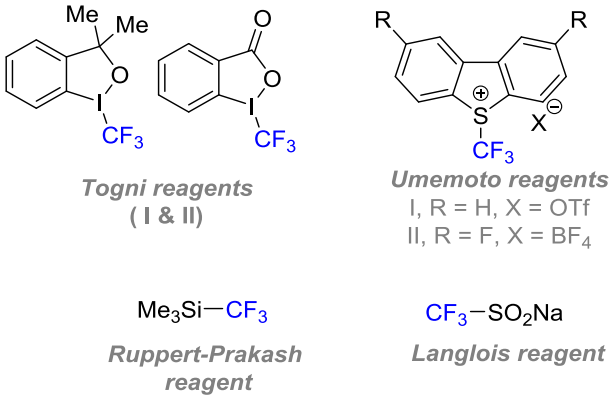

Figure 11 Common Trifluoromethylating Agents.

[150] Moschner, J.; Stulberg, V.; Fernandes, R.; Huhmann, S.; Leppkes, J.; Koksch, B. *Chem. Rev.* **2019**, *119*, 10718.
[151] a) Jacobson, O.; Kiesewetter, D. O.; Chen, X. *Bioconjugate Chem.* **2015**, *26*, 1. b) Brooks, A. F.; Topczewski, J. J.; Ichiishi, N.; Sanford, M. S.; Scott, P. J. H. *Chem. Sci*. **2014**, *5*, 4545.
[152] Molteni, M.; Pesenti, C; Sani, M.; Volonterio, A.; Zanda, M. *J. Fluorine Chem.* **2004**, *125*, 1735.
[153] Qiu, X.-L.; Qing, F.-L. *Eur. J. Org. Chem.* **2011**, *2011*, 3261.
[154] a) Furuya, T.; Kamlet, A. S.; Ritter, T. *Nature* **2011**, *473*, 470. b) Meanwell, N. A. *J. Med. Chem*. **2011**, *54*, 2529. c) Ma, J. A.; Cahard, D. *J. Fluorine Chem.* **2007**, *128*, 975.

Umemoto[155] and Togni reagents,[156] nucleophilic Ruppert-Prakash reagent[157] or Langlois reagent,[158] are some of the examples, among others (Figure 11). Whereas Langlois reagent is essentially selected to perform radical trifluoromethylation reactions, electrophilic radical trifluoromethyl species can be also generated from Umemoto and Ruppert-Prakash reagents upon reaction with an oxidant or a copper catalyst, respectively, as well as from trifluoromethylsulfonyl chloride (CF_3SO_2Cl) through photoredox catalysis.[159] Despite their common use in academic laboratories, the high price or multi-step synthesis which some of them required have limited the application of some of these CF_3 sources in industrial environments. Accordingly, the development of cost-efficient new trifluoromethyl sources represents a challenging task of capital importance to improve the performance and practicality of existing trifluoromethylation techniques in the context of downstream functionalizations of relevant biomolecules.

The incorporation of the trifluoromethyl group into amino acids within a peptide sequence results in relevant peptidomimetics with unique biomedicinal and pharmaceutical properties.[160] Driven by those outstanding applications, an upsurge of site-selective trifluoromethylations have been lately described to perform the chemoselective modification of peptides and proteins bearing cysteine (Cys), tyrosine (Tyr), histidine (His) and tryptophan (Trp) residues. In this section, some relevant protocols will be briefly commented.

For instance, the nucleophilic character of the polar thiol group in the cysteine residue has permitted the development of novel strategies in the realm of bioconjugation.[161] Encouraged by the applicability of their new electrophilic hypervalent iodine reagents,[162] Togni and Seebach groups reported a methodology capable of performing the *S*-trifluoromethylation of α- and β-Cys residues in complex peptides.[163] The combination of the Cys-containing substrates and the trifluoromethylation reagent in an aqueous solution of MeOH at cryogenic temperatures enabled the modification of peptides with up to 13 amino acid units with total selectivity toward Cys residues even in the presence of other highly reactive side-chains or unprotected terminal positions (Scheme 74).

---

[155] a) Prieto, A.; Baudoin, O.; Bouyssi, D.; Monteiro, N. *Chem. Commun.* **2016**, *52*, 869. b) Umemoto, T. *J. Fluorine Chem.* **2014**, *167*, 3. c) Umemoto, T. *Chem. Rev.* **1996**, *96*, 1757.
[156] Charpentier, J.; Früh, N.; Togni, A. *Chem. Rev.* **2015**, *115*, 650.
[157] a) Liu, X.; Xu, C.; Wang, M.; Liu, Q. *Chem. Rev.* **2015**, *115*, 683. b) Prakash, G. K. S.; Yudin, A. K. *Chem. Rev.* **1997**, *97*, 757. c) Ruppert, I.; Schlich, K.; Volbach, W. *Tetrahedron Lett.* **1984**, *25*, 2195.
[158] a) Lefebvre, Q. *Synlett* **2017**, *28*, 19. b) Zhang, C. *Adv. Synth. Catal.* **2014**, *356*, 2895. c) Langlois, B. R.; Laurent, E.; Roidot, N. *Tetrahedron Lett.* **1991**, *32*, 7525.
[159] Studer, A. *Angew. Chem. Int. Ed.* **2012**, *51*, 8950.
[160] a) Budisa, N.; Wenger, W.; Wiltschi, B. *Mol. BioSyst.* **2010**, *6*, 1630. b) Jäckel, C.; Salwiczek, M.; Koksch, B. *Angew. Chem. Int. Ed.* **2006**, *45*, 4198. c) Zanda, M. *New J. Chem.* **2004**, *28*, 1401. d) Tang, Y.; Ghirlanda, G.; Petka, W. A.; Nakajima, T.; DeGrado, W. F.; Tirrell, D. A. *Angew. Chem. Int. Ed.* **2001**, *40*, 1494.
[161] a) Gunnoo, S. B.; Madder, A. *ChemBioChem* **2016**, *17*, 529. b) Chalker, J. M.; Bernardes, G. J. L.; Lin, Y. A.; Davis, B. G. *Chem. Asian J.* **2009**, *4*, 630.
[162] Kieltsch, I.; Eisenberger, P.; Togni, A. *Angew. Chem. Int. Ed.* **2007**, *46*, 754.
[163] Capone, S.; Kieltsch, I.; Flögel, O.; Lelais, G.; Togni, A.; Seebach, D. *Helv. Chim. Acta* **2008**, *91*, 2035.

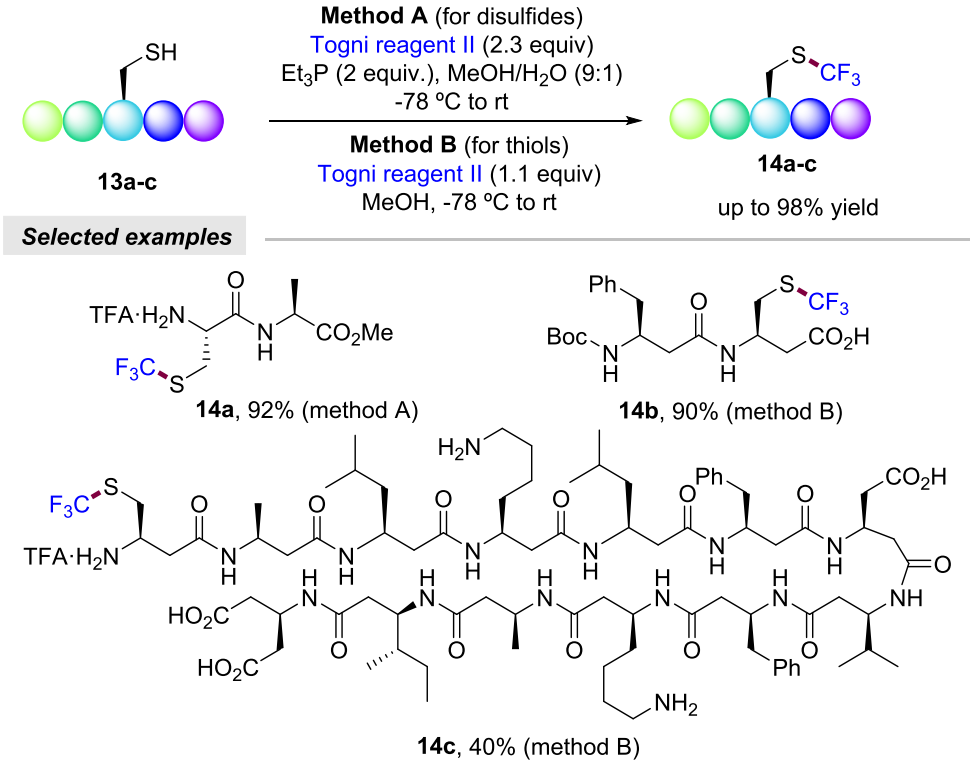

Scheme 74 S-Trifluoromethylation of Cys Derivatives with Togni reagents.

Later on, in 2016, Noël and co-workers disclosed the Ru-catalyzed *S*-trifluoromethylation and perfluoroalkylation of Cys under photoredox catalysis.[164,165] The efficiency of the process was established by the performance in continuous flow enabling the rapid (5 min in flow *vs* 2 h in batch), high yielding and scalable assembly of trifluromethylated and perfluoroalkylated simple Cys units even with the use of gaseous CF_3I.

[164] Bottecchia, C.; Wei, X.-J.; Kuijpers, K. P. L.; Hessel, V.; Noël, T. *J. Org. Chem.* **2016**, *81*, 7301.
[165] Straathof, N. J. W.; Tegelbeckers, B. J. P.; Hessel, V.; Wang, X.; Noël, T. *Chem. Sci.* **2014**, *5*, 4768.

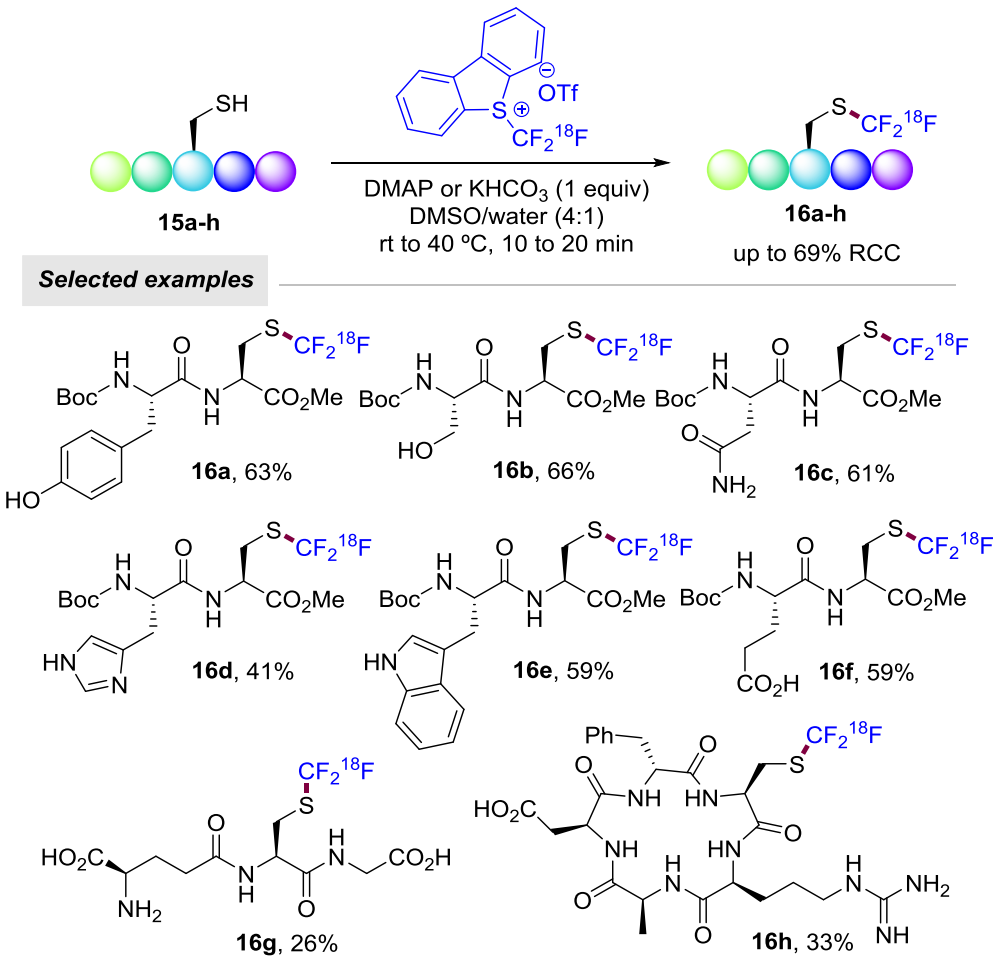

Scheme 75 ^{18}F-Trifluoromethylation of Cys-Containing unmodified Peptides (RCC=radiochemical conversion).

With reference to fluorine containing drugs' applications, in 2018 Davis and Gouverneur jointly succeeded in developing the synthesis of ^{18}F-labeled Cys residues in peptides utilizing ^{18}F-labeled Umemoto reagent and their further use as imaging biomarkers in an *in vivo* Positron Emission Tomography (PET)[166] study.[167] The radiolabeled reagent was prepared through a halogen exchange ^{18}F-fluorination with ^{18}F-fluoride followed by an oxidative cyclization with oxone and trifluoromethanesulfonic anhydride. A vast array of peptides underwent the ^{18}F-trifluoromethylation with high chemoselectivity toward Cys in the presence of 4-dimethylaminopyridine (DMAP) or $KHCO_3$ as base, within 10-20 minutes at room termperature with the extra bonus of the use of water as a co-solvent (Scheme 75). Owing to their use in PET studies, biologically relevant glutathione **16g** and Arg-Gly-Asp (RGD) sequence containing cyclopeptides **16h** were tagged.

[166] a) Deng, X.; Rong, J.; Wang, L.; Vasdev, N.; Zhang, L.; Josephson, L.; Liang, S. H. *Angew. Chem. Int. Ed.* **2018**, *58*, 2580. b) Willmann, J. K.; van Bruggen, N.; Dinkleborg, L. M.; Gambhir, S. S. *Nat. Rev. Drug Discov.* **2008**, *7*, 591.
[167] Verhoog, S.; Kee, C. W.; Wang, Y.; Khotavivattana, T.; Wilson, T. C.; Kersemans, V.; Smart, S.; Tredwell, M.; Davis, B. G.; Gouverneur, V. *J. Am. Chem. Soc.* **2018**, *140*, 1572.

It must be pointed out that the aforementioned procedures exhibited the preferential modification of S–H bond in the presence of harder nucleophiles such as the hydroxyl group in tyrosine residues, which is often tuned under basic conditions.[168] On the contrary, acidic and neutral conditions enable the *ortho*-C–H functionalization of the latter electron-rich phenol-containing amino acid. Although sparsely explored, the trifuloromethylation of Tyr unit has also gained attraction as this prevalent scaffold constitutes a key piece of multiple biocompounds like neurotransmitters and hormones.[169] In 1992, Kimoto and co-workers submitted for the very first time a Tyr derivative to a trifluoromethylation reaction upon ultraviolet irradiation with CF_3I and triethylamine in MeOH.[170]

In 2011, Baran and co-workers developed an excellent work where numerous heteroarenes underwent C(sp^2)–H trifluoromethylation in aqueous solution.[171] This time, CF_3 radical generation was possible through the oxidation of the Langlois reagent.[158d] Since then, the CF_3SO_2Na/^{t}BuOOH system has sparked a lot of interest due to the low-cost and stability of the easy-to-handle trifluoromethylation reagent.

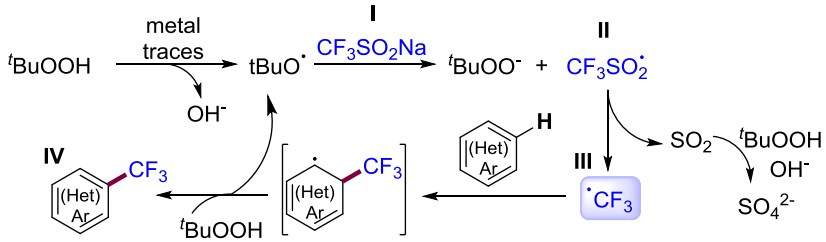

Scheme 76 Direct Radical Trifluoromethylation Mechanism with $NaSO_2CF_3$.

Baran and co-workers proposed that the reaction begins with the homolytic cleavage of *tert*-butyl hydroperoxide to form the *tert*-butoxy radical by the often remaining metal impurities observed in the commercially available Langlois reagent. The latter reacts with the Langlois reagent leading to the formation of radical **II** ($CF_3SO_2^{\bullet}$) which after releasing SO_2, generates the trifluoromethyl radical **III**. $CF_3^{\bullet}$ reacts with the corresponding (hetero)arene substrate followed by oxidation/deprotonation to obtain the desired trifluoromethylated adduct **IV**.[172]

[168] DeGruyter, J. N.; Malins, L. R.; Baran, P. S. *Biochemistry* **2017**, *56*, 3863.
[169] a) Lee, J.; Ju, M.; Cho, O. H.; Kim, Y.; Nam, K. T. *Adv. Sci.* **2019**, *6*, 1801255. b) Chávez-Béjar, M. I.; Báez-Viveros, J. L.; Martínez, A.; Bolívar, F.; Gosset, G. *Process Biochem.* **2012**, *47*, 1017.
[170] Kirk, K. L.; Nishida, M.; Fujii, S.; Kimoto, H. *J. Fluorine Chem.* **1992**, *59*, 197.
[171] Ji, Y.; Brueckl, T.; Baran. P. S. *Proc. Natl. Acad. Sci. USA* **2011**, *108*, 14411.
[172] a) Billard, T.; Roidot, N.; Langlois, B. R. *J. Org. Chem.* **1999**, *64*, 3813. b) Langlois, B. R.; Laurent, E.; Roidot, N. *Tetrahedron Lett.* **1992**, *33*, 1291.

The challenging Tyr modification remained dormant until 2018, when Merck laboratories, inspired by Baran's method comented above, performed a radical C–H trifluoromethylation with sulfonate salts under a wide variety of peptides bearing Tyr residues.[173] The combination of $Zn(SO_2CF_3)_2$ and high excess of TBHP in aqueous media led to the selective trifluoromethylation of unprotected Tyr-containing dipeptides in 35-48% yields (Scheme 77, method *A*). Nevertheless, they came across chemoselectivity issues when Trp residue was present as it reacted preferably, as well as Cys residue, which was oxidized leading to its dimer analogue. On the other hand, turning to a more convenient and milder photoredox protocol, the excess of 20 equivalents of Langlois reagent afforded trifluoromethylated unprotected polypeptides of utmost importance including cyclopeptides, deltorphin I, angiotensin I and II or β-casomorphin where the mono-substituted product was the major one (Scheme 77, method B). Regarding the spectacular scope exhibited by this labelling technique, the functionalization of the four Tyr units in the recombinant human insulin must be underlined.

[173] Ichiishi, N.; Caldwell, J. P.; Lin, M.; Zhong, W.; Zhu, X.; Streckfuss, E.; Kim, H.-Y.; Parish, C. A.; Krska, S. W. *Chem. Sci.* **2018**, *9*, 4168.

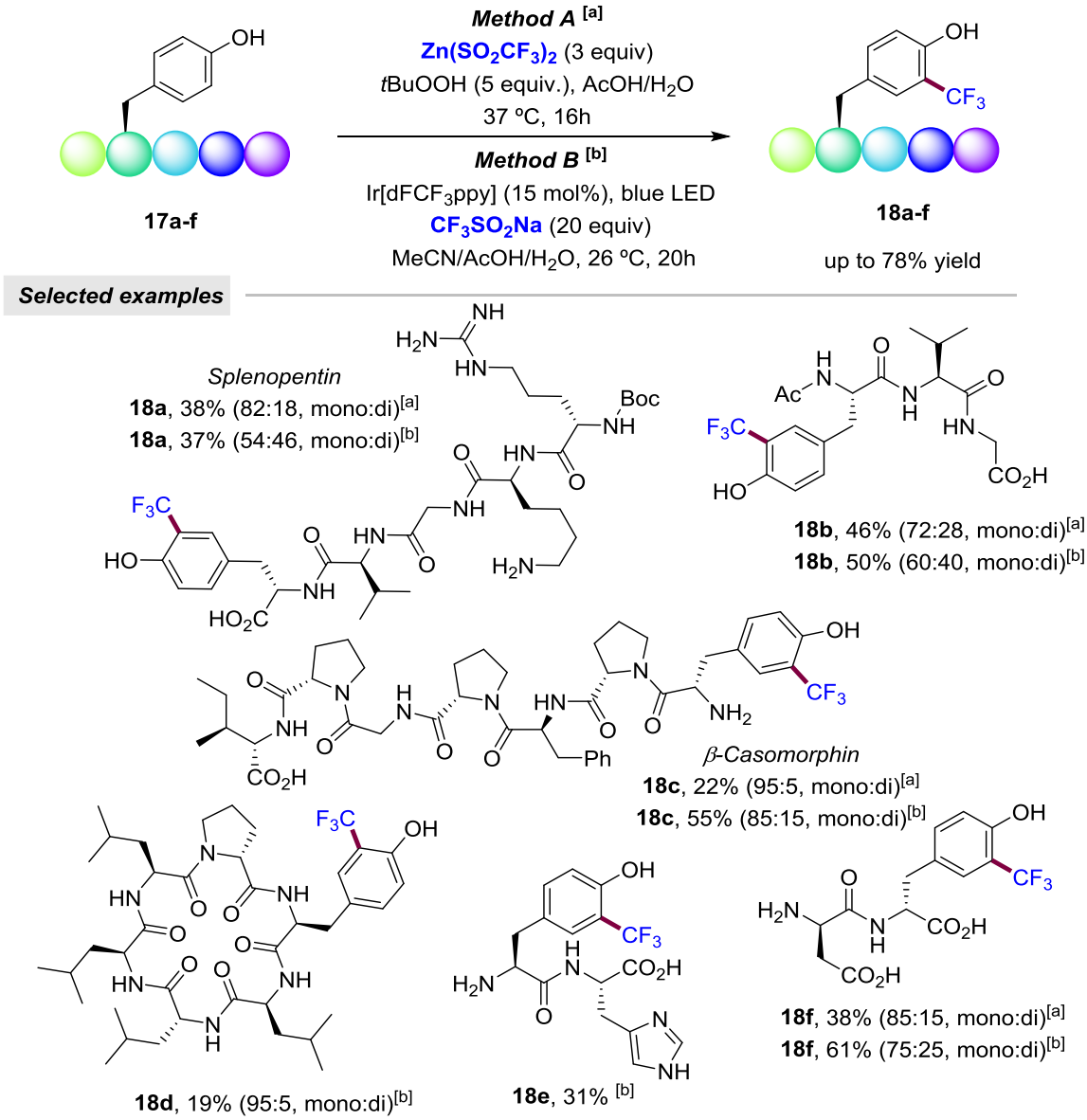

Scheme 77 ^{18}F-Trifluoromethylation of Tyr-Containing Native Peptides.

With reference to fluorine containing drugs, Gouverneur and co-workers have recently succeeded in developing an automated radiosynthesis for ^{18}F-labeled native peptides and their further use as imaging biomarkers in an *in vivo* Positron Emission Tomography (PET)[174] study.[175]

[174] a) Phelps, M. E. *Proc. Natl. Acad. Sci. USA* **2000**, *97*, 9226. b) Matthews, P. M.; Rabiner, E. A.; J. Passchier, J.; Gunn, R. N. *Br. J. Clin. Pharmacol.* **2011**, *73*, 175. c) Krishnan, H. S.; Ma, L.; Vasdev, N.; Liang, S. H. *Chem. Eur. J.* **2017**, *23*, 15553.

[175] Kee, C. W.; Tack, O.; Guibbal, F.; Wilson, T. C.; Isenegger, P. G.; Imiołek, M.; Verhoog, S.; Tilby, M.; Boscutti, G.; Ashworth, S.; Chupin, J.; Kashani, R.; Poh, A. N. J.; Sosabowski, J. K.; Macholl, S.; Plisson, C.; Cornelissen, B.; Willis, M. C.; Passchier, J.; Davis, B. G.; Gouverneur, V. *J. Am. Chem. Soc.* **2020**, *142*, 1180.

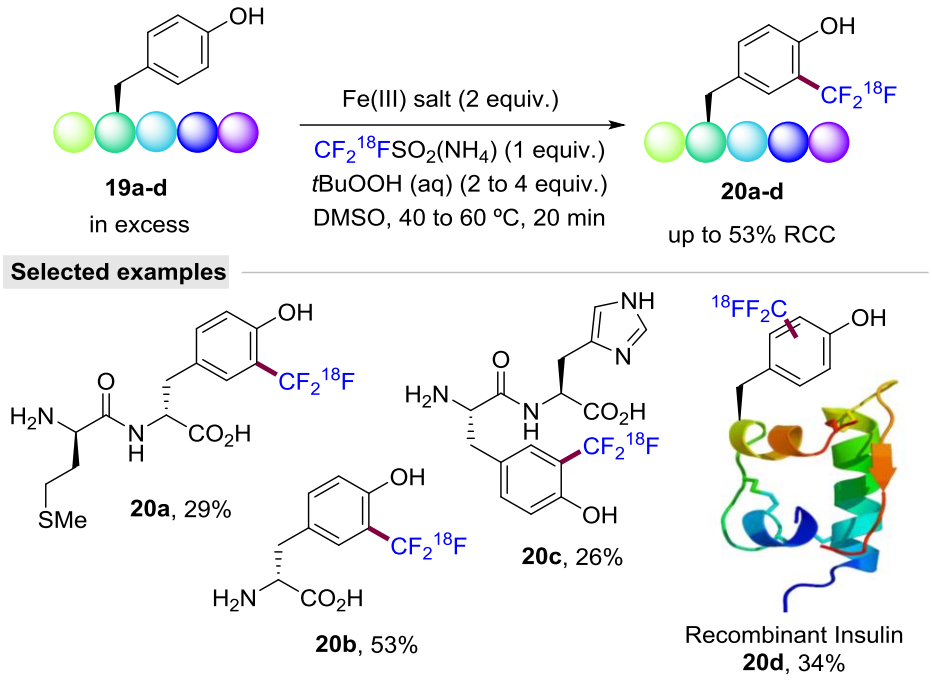

Scheme 78 ^{18}F-Trifluoromethylation of Tyr-Containing Native Peptides.

Although Langlois reagent has demonstrated excellent reactivity in a plethora of trifluoromethyaltion processes, its synthesis suffers from some drawbacks regarding sustainability and practicality issues.[176] Thus, the key reagent of this methodology consists in a one-step synthesis of a novel [^{18}F]$CF_3SO_2NH_4$, coming from PDFA, NMM·SO_2 and [^{18}F]KF/K_{222} in DMF. As a consequence of being the limiting reagent, the combination of TBHP together with double equimolar amount of an iron source in DMSO/aq. ammonium formate was necessary for the C–H ^{18}F-trifluoromethylation of Trp and Tyr containing peptides (Scheme 78). As in the method by Parish, Krska and co-workers, the Trp residue was functionalized over the Tyr one when both amino acids were present in the substrate. Remarkably, the recombinant human insulin **20d** underwent the C–H ^{18}F-trifluoromethylation at all Tyr units in 34% overall RCC.

Among the collection of natural amino acids, His is a rather versatile member that plays multiple roles in protein interactions owing to its ionizable nature at physiological conditions and its high binding ability.[177] However, the site-selective modification of such a privileged residue has been overlooked in peptide chemistry and chemoselective modification of His derivatives remains elusive.[168]

[176] a) Langlois, B. R.; Billard, T.; Mulatier, J.-C.; Yezeguelian, C. *J. Fluorine Chem.* **2007**, *128*, 851. b) Cao, H.-P.; Chen, Q.-Y. *J. Fluorine Chem.* **2007**, *128*, 1187. c) Folest, J.-C.; Nédélec, J.-Y.; Périchon, J. *Synth. Commun.* **1988**, *18*, 1491.
[177] a) Dudev, T.; Lim, C. *Chem. Rev.* **2014**, *114*, 538. b) Lu, Y.; Yeung, N.; Sieracki, N.; Marshall, N. M. *Nature* **2009**, *460*, 855.

Cohen and co-workers initiated the development of C–H trifluoromethylation of the His residue based on their previous imidazole scaffold functionalization protocol.[178] Hence, C4-trifluromethylated His derivatives together with a minor C2-modified isomer amount were achieved utilizing CF_3I in MeOH under UV light irradiation.[179]

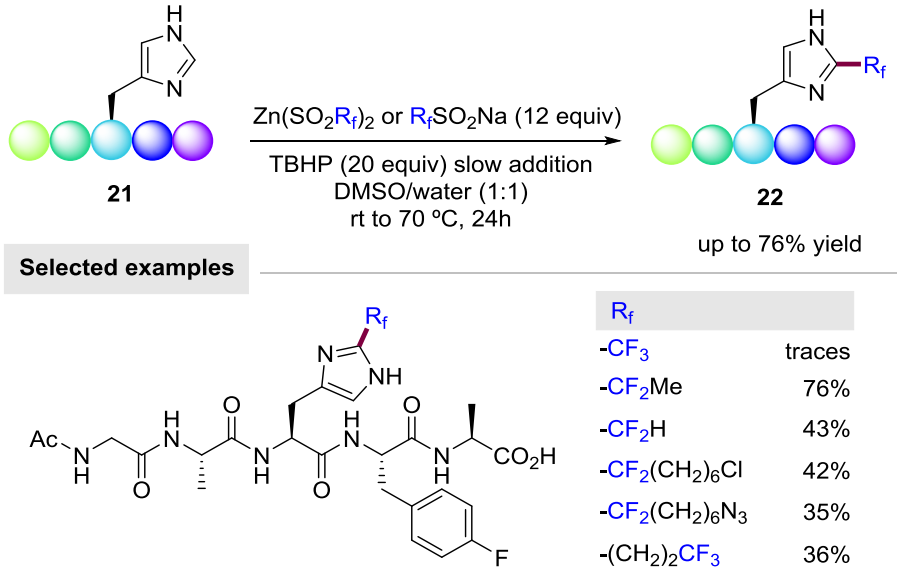

Scheme 79 Fluoroalkylation of His-Containing Unprotected Peptides.

Driven by the use of Langlois reagent for the generation of radicals under oxidative conditions,[171] Noisier, Gopalakristhnan and co-workers described the selective C2 late-stage functionalization of His-containing peptides with fluorinated moieties (Scheme 79).[180] The aqueous efficient alkylation platform was applicable to some selected AstraZeneca drugs among other relevant bioactive peptides. However, the methodology required high amounts of both fluorinated agents and TBHP to provide the modification of highly complex molecules where a great difference in reactivity could be observed. For instance, only traces of trifluoromethylated imidazole ring was obtained sometimes due to the higher reactivity toward Tyr and Trp residues present in the oligopeptide. In contrast, moieties like $–CF_2Me$, from the corresponding $MeCF_2SO_2Na$, were selectively introduced into the C2-position in a 76 % yield. [181]

[178] Kimoto, H.; Fujii, S.; Cohen, L. A. *J. Org. Chem.* **1982**, *47*, 2867.
[179] a) Labroo, V. M.; Labroo, R. B.; Cohen, L. A. *Tetrahedron Lett.* **1990**, *31*, 5705. b) Kimoto, H.; Fujii, S.; Cohen, L. A. *J. Org. Chem.* **1984**, *49*, 1060.
[180] Noisier, A. F. M.; Johansson, M. J.; Knerr, L.; Hayes, M. A.; Drury III, W. J.; Valeur, E.; Malins, L. R.; Gopalakrishnan, R. *Angew. Chem. Int. Ed.* **2019**, *58*, 19096.
[181] Chen, X.; Ye, F.; Luo, X.; Liu, X.; Zhao, J.; Wang, S.; Zhou, Q.; Chen, G.; Wang, P. *J. Am. Chem. Soc.* **2019**, *141*, 18230.

4.1.3. C(sp^2)–H Trifluoromethylation of Indole Derivatives Including Tryptophan

Several protocols have been reported for the installation of the trifluoromethyl group into (hetero)arenes and more specifically into the indole scaffold leading to versatile compounds with future applications in drug discovery.[182] The latter methodologies have been an inspiration for a facile tryptophan-containing peptides' diversification and formation of fluorinated skeletons with a great interest in pharmaceutical industry. In this section, the accomplished methodologies up to the beginning of 2020 are described, and classified according to the utilized trifluoromethylating agent.

4.1.3.1. R_f–I Reagent

In 2010, Sodeoka and co-workers developed a copper-catalyzed methodology for the C2-trifluoromethylation of indole derivatives.[183] Inspired by previous finding where the combination of a Lewis acid and hypervalent iodine reagent resulted in the latter's electrophilicity increase,[184] Togni reagent was utilized as the trifluoromethylating source together with catalytic copper(I) acetate.

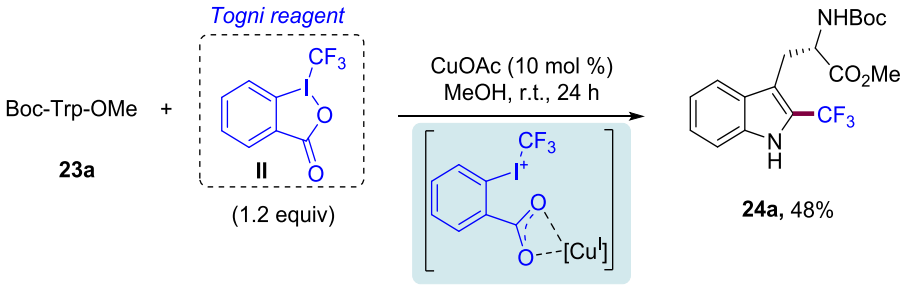

Scheme 80 Copper-Catalyzed C2-Selective Trifluoromethylation of Boc-Trp-OMe.

Among 3-substituted indoles, the single and first example of tryptophan derivative **23a** gave the corresponding product **24a** under the optimized reaction conditions in 48 % yield (Scheme 80). The commercially available Togni reagent represented an alternative of utmost importance in the field of trifluoromethylation chemistry as previous toxic and corrosive radical precursors such as CF_3I (gas), CF_3Br (gas) and CF_3SO_2Cl were avoided.[185]

---

[182] Alonso, C.; Martínez de Marigorta, E.; Rubilaes, G.; Palacios, F. *Chem. Rev.* **2015**, *115*, 1847.
[183] Shimizu, R.; Egami, H.; Nagi, T.; Chae, J.; Hamashima, Y.; Sodeoka, M. *Tetrahedron Lett.* **2010**, *51*, 5947.
[184] a) Allen, A. E.; MacMillan, D. W. C. *J. Am. Chem. Soc.* **2010**, *132*, 4986. b) Fantasia, S.; Welch, J. M.; Togni, A. *J. Org. Chem.* **2010**, *75*, 1179. c) Koller, R.; Stanek, K.; Stolz, D.; Aardoom, R.; Niedermann, K.; Togni, A. *Angew. Chem. Int. Ed.* **2009**, *48*, 4332.
[185] a) Herrmann, A. T.; Smith, L.; Zakarian, A. *J. Am. Chem. Soc.* **2012**, *134*, 6976. b) Nagib, D. A.; MacMillan, D. W. C. *Nature* **2011**, *480*, 224. c) Kino, T.; Nagase, Y.; Ohtsuka, Y.; Yamamoto, K.; Uraguchi, D.; Tokuhisa, K.; Yamakawa, T.

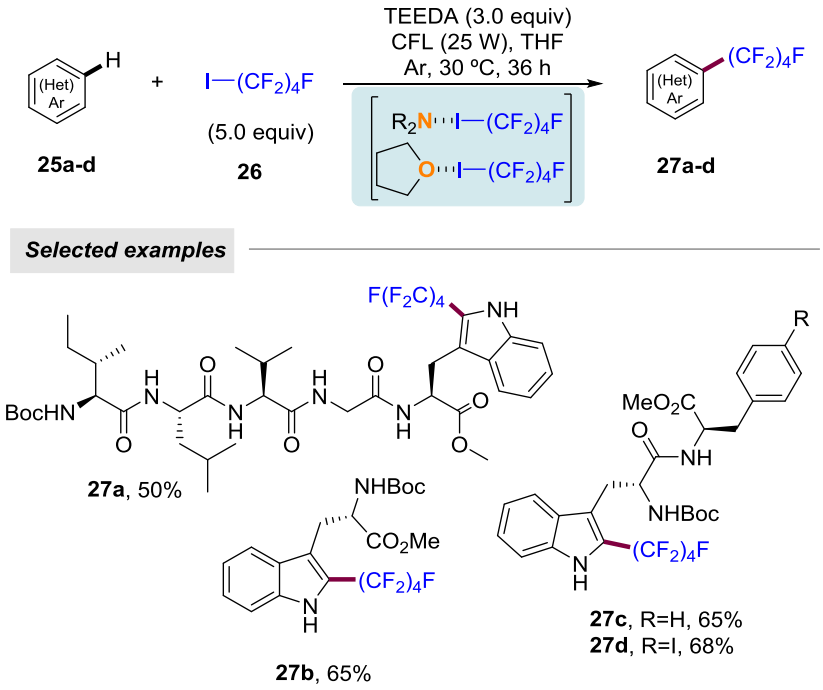

Scheme 81 C(sp^2)–H Perfluoroalkyaltion of Heteroarenes.

On the other hand, Chen's group developed a protocol for the modification of a few examples of tryptophan-containing oligopeptides in a photochemical fashion with perfluorobutyl iodide (C_4F_9–I) (Scheme 81).[186] Although trifluoromethylation reaction was not performed, the introduction of related perfluoroalkyl motifs was described. Apart from a couple of dipeptides, the more challenging selective perfluoroalkylation of Boc-Ile-Leu-Val-Gly-Trp-OMe was achieved in a 50 % yield by increasing the amount of reagents. This time together with a compact fluorescent lamp (CFL), the C2-position of the tryptophan residue was perfluoroalkylated with the aid of *N*,*N*,*N*′,*N*′-tetraethylethylenediamine (TEEDA) and THF as the solvent. Amine additives and THF were proposed to enhance the photochemical reactivity of the perfluoroalkyl iodide forming halogen bond complexes/adducts, thereby avoiding the use of a transition-metal-catalyst.

4.1.3.2. Umemoto Reagent

Umemoto reagent is together with Togni reagent, the most widely employed electrophilic agent for trifluoromethylations.[155] In 2015, Ma and You reported a metal-free C–H trifluoromethylation reaction for highly-functionalized heteroaromatic compounds, where once again a single example of a tryptophan derivative **23a** was obtained in 58 % yield (Scheme 82).[187] This efficient methodology was based on the Electron-Donor-

J. Fluorine Chem. **2010**, *131*, 98. d) Nagib, D. A.; Scott, M. E.; MacMillan, D. W. C. *J. Am. Chem. Soc.* **2009**, *131*, 10875. e) Wakselman, C.; Tordeux, M. *J. Chem. Soc. Chem. Commun.* **1987**, 1701.

[186] Wang, Y.; Wang, J.; Li, G-X.; He, G.; Chen, G. *Org. Lett.* **2017**, *19*, 1442.

[187] Cheng, Y.; Yuan, X.; Ma, J.; Yu, S. *Chem. Eur. J.* **2015**, *21*, 8355.

Acceptor (EDA) complex[188] **28** between Umemoto reagent **I** and the optimal electron-donor *N*-methylmorpholine (NMM) tertiary amine. Control experiments and theoretical calculations supported that the irreversible generation of CF_3 radical was thermodynamically favored after the reduction of the utilized trifluomethylation reagent via electron-transfer (ET) in the EDA complex **28**. Then, the addition of $^{\bullet}CF_3$ radical into **23a** led to radical **30**, which was further oxidized to cation **31,** either by NMM^+ (Path A) or Umemoto reagent **I** (Path B) and deprotonated to give the final product.

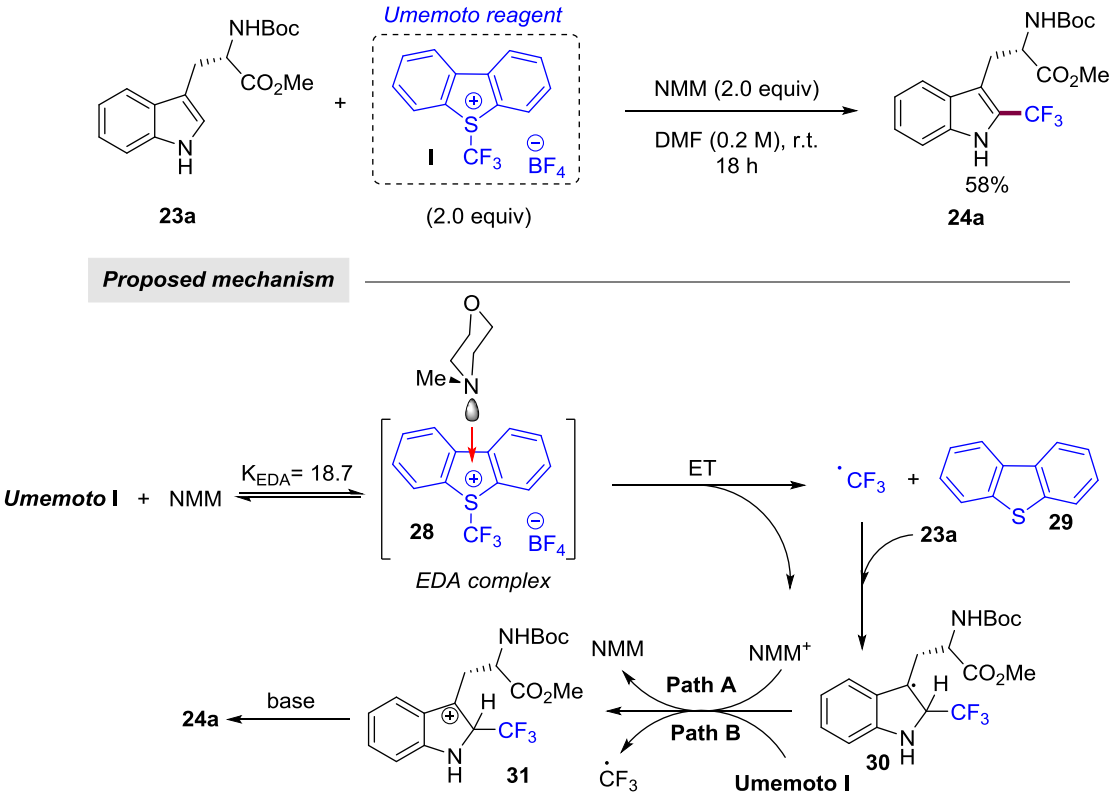

Scheme 82 C2-Selective Trifluoromethylation of Boc-Trp-OMe via an Electron-Donor—Aceptor Complex.

An EDA complex intermediate was also considered by Egami *et al.* in their photo-induced C(sp^2)–H trifluoromethylation reaction.[189] The reaction proceeded for one hour in DMSO with an excess of three equivalents of the corresponding heteroaromatic substrate with respect to Umemoto's type reagent. However, in this case when tryptophan derivative **23a** was submitted to the reaction conditions, a lower 44 % yield was observed.

[188] For selected reviews on EDA complexes, see: a) Rabie, U. M. *J. Mol. Struct*. **2013**, *1034*, 393. b) Miyasaka, H. *Acc. Chem. Res*. **2013**, *46*, 248. c) Rosokha, S. V.; Kochi, J. K. *Acc. Chem. Res.* **2008**, *41*, 641. d) Ruiz, E.; Salahub, D. R.; Vela, A. *J. Phys. Chem.* **1996**, *100*, 12265.
[189] Egami, H.; Ito, Y.; Ide, T.; Masuda, S.; Hamashima, Y. *Synthesis* **2018**, *50*, 2948.

4.1.3.3. Langlois Reagent

In 2018, Davis and co-workers, based on the plausible mechanism proposed by Baran,[171] succeeded in disclosing for the first time a selective trifluoromethylation protocol toward tryptophan residues in proteins.[190] Previous methods were usually incompatible with complex molecular structures such as proteins. Thus, it meant a major breakthrough in the field of proteomics, which seeks for operational simplicity and direct introduction of fluorine-containing functional groups into biomolecules for further medicinal applications.[191] An equimolar mixture of five native amino acid residues (Trp, Phe, Tyr, His, Cys) with CF_3SO_2Na/^{t}BuOOH was added into an aqueous media (pH=6) to study the selectivity (Scheme 83). Competition experiments revealed that the trifluoromethylation of tryptophan residue was 30 times more favorable than the rest of the amino acids that shown an insignificant yield of ~1%.

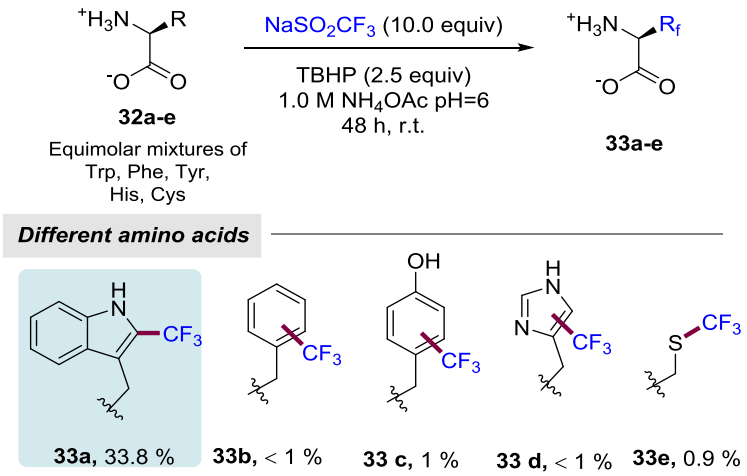

Scheme 83 Limited-Conversion Competition Trifluoromethylation Assays with Natural Amino Acids.

Interestingly, not even the nucleophilic Cys residue was functionalized. Instead, the formation of the corresponding disulfide compound was observed. This preferable selectivity was also achieved with more challenging peptides/proteins. Substrates containing one or more Trp units like Melittin (Trp19), Myoglobin (Trp7, Trp14), Panthotenate synthetase (Trp306) and enzyme lysozyme (Trp28, Trp62, Trp63, Trp108, Trp111 and Trp123) were selectively modified demonstrating no accessibility issues for buried protein sites. In these cases, the immense increase of reagents amount (200 equiv of CF_3SO_2Na and 12.5 equiv of TBHP) provided the trifluoromethylated proteins within 5 minutes.

[190] Imiołek, M.; Karunanithy, G.; Ng, W.-L.; Baldwin, A. J.; Gouverneur, V.; Davis, B. G. *J. Am. Chem. Soc*. **2018**, *140*, 1568.
[191] a) Zhou, Y.; Wang, J.; Gu, Z.; Wang, S.; Zhu, W.; Aceña, J. L.; Soloshonok, V. A.; Izawa, K.; Liu, H. *Chem. Rev*. **2016**, *116*, 422. b) Purser, S.; Moore, P. R.; Swallow, S.; Gouverneur, V. *Chem. Soc. Rev.* **2008**, *37*, 320. c) Müller, K.; Faeh, C.; Diederich, F. *Science* **2007**, *317*, 1881.

With regard to the procedures described so far, they have also demonstrated their viability for the functionalization of a limited number of simple Trp compounds. In 2017, Li and co-workers reported a redox-neutral and catalyst-free protocol to generate CF_3 radicals for the functionalization of (hetero)arenes with trifluoromethyl sulfones affording an example of Trp–CF_3 containing dipeptide.[192] Nevertheless, the aforementioned protocols resulted in limited or even none examples of peptides, except the protocol by David and Gouverneur which could be applied to a variety of complex proteins in the presence of huge excess of both oxidant and CF_3 source. Accordingly, there is still a high demand for the development of more general, yet sustainable, protocols toward the trifluoromethylation of Trp-containing oligopeptides.

[192] Liu, P.; Liu, W.; Li, C.-J. *J. Am. Chem. Soc*. **2017**, *139*, 14315.

4.2. Objective

As highlighted before, the site-selective modification of the side-chain within a peptide framework poses a challenging task of paramount synthetic relevance. Furthermore, the installation of the fluorine atom into amino acids have shown often an enhancement in their biological functions in comparison with their non-fluorinated analogues. As a result, the field of C–H trifluoromethylation of peptides has undergone a significant progress and methodologies for the functionalization of Tyr-, Cys- or His-containing residues have been developed.[193] In order to accomplish some of these protocols, the breakthroughs in the field by Baran[194] and MacMillan,[185b] among others, have inspired the use of practical trifluoromethyl sulfinate salts such as Langlois reagent for the *in situ* generation of CF_3 radicals under oxidative conditions.

Given the limitations of the existing protocols, we sought that trifluoromethylated oligopeptides could be within reach by a more practical functionalization event featuring base metal catalysis under mild reaction conditions. The main objective of this research dealt with the development a more general, modular and sustainable method for the site-selective trifluoromethylation of Trp-containing oligopeptides in a late-stage fashion. For these endeavors, we envisioned the use of cost-efficient copper catalysis, which has been comparatively unexplored within the modification of Trp-containing peptides and proteins.

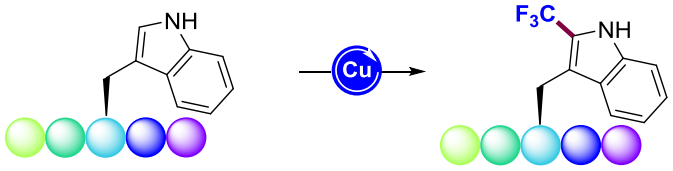

Scheme 84 Copper-Catalyzed Trifluoromethylation of Tryptophan Residue within Peptides.

[193] Guerrero, I.; Correa, A. *Asian J. Org. Chem.* **2020**, *9*, 898.
[194] a) O'Brien, A. G.; Maruyama, A.; Inokuma, Y.; Fujita, M.; Baran, P. S.; Blackmond, D. G. *Angew. Chem. Int. Ed.* **2014**, *53*, 11868. b) Fujiwara, Y.; Dixon, J. A.; O'Hara, F.; Funder, E. D.; Dixon, D. D.; Rodriguez, R. A.; Baxter, R. D.; Herlé, B.; Sach, N.; Collins, M. R.; Ishihara, I.; Baran, P. S. *Nature* **2012**, *492*, 95.

4.3. Cu-Catalyzed C(sp^2)–H Radical Trifluoromethylation of Tryptophan-Containing Peptides

4.3.1. Optimization of Reaction Conditions

To start our investigation we had a look to the trifluoromethylation reaction of heterocycles described by Baran and co-workers.[171] For the successful assembly of the trifluoromethylated compounds, 3-6 equivalents of Langlois reagent and 5-10 equivalents of *tert*-butyl hydroperoxide in a mixture of dimethyl sulfoxide and water were required (Scheme 85).

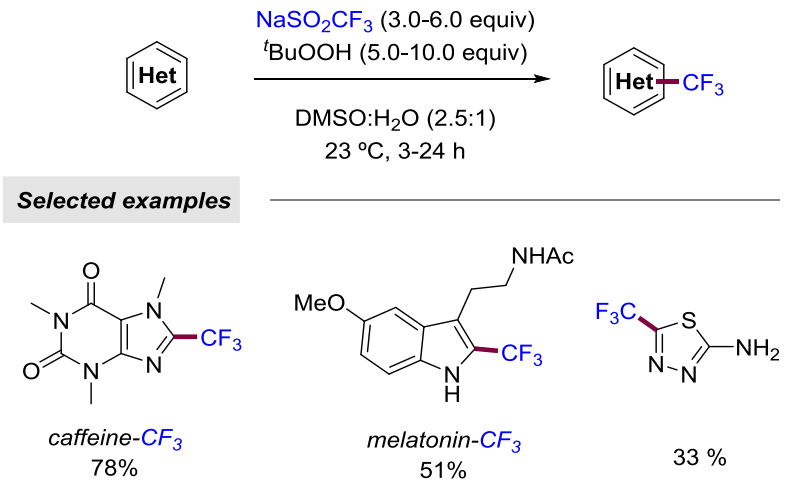

Scheme 85 Innate C–H Trifluoromethylation of Heterocycles.

The selective example of modified tryptophan metabolite melatonin drawn our attention, which was obtained in a 51 % yield. Hence, we sought that a related fluorination technique could be applied by other indole-containing substrates such as tryptophan derivatives. Accordingly, we initiated our study selecting Ac-Trp-OMe derivative as the model substrate for the optimization of the trifluoromethylation reaction conditions, which was easily synthesized in a two-step process from commercially available L-Trp-OH (Scheme 86). The first step was based on the addition of thionyl chloride to a solution of L-Trp-OH in methanol at 0 ºC. After stirring for 24 hours at room temperature, the solvent was evaporated and the resulting crude solid was washed with ether to obtain a white pure L-Trp-OMe·HCl. The latter was directly submitted to a THF solution of triethylamine at 0 ºC with the further addition of acetic anhydride. This reaction mixture led to the formation of the model substrate **35a** after two hours under reflux.

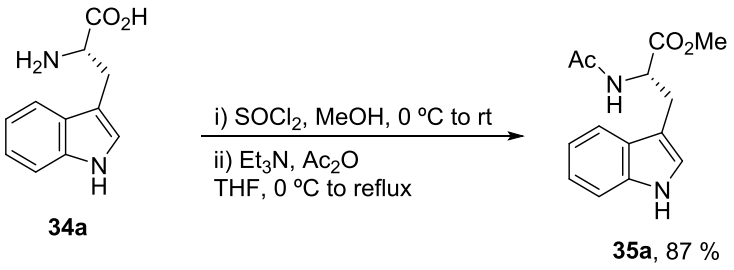

Scheme 86 Synthesis of Model Substrate Ac-Trp-OMe.

Our first attempt was carried out based on the reaction in Scheme 85, adding 3.0 equivalents of Langlois reagent in DMSO (8mL/mmol) at 80 ºC for 24 hours (Table 19). However, only two equivalents of each oxidant were added in these first attempts. Regarding the type of oxidant, both inorganic and organic ones were tested including the most convenient molecular oxygen and hydrogen peroxide, despite resulting in lack of reactivity (Table 19, entry 5 and 9). Moreover, *tert*-butyl hydroperoxide reagent is known to generate the trifluoromethyl radical and has been applied in several methodologies.[171] Thus, as expected, the aqueous solution and decane solution of TBHP provided the desired functionalized Trp derivative **36a**, while TBHP in decane gave a slightly better result of 36 % yield (Table 19, entry 1). To our delight, we observed that less hazardous $(NH_4)_2S_2O_8$[195] inorganic oxidant could also furnish the desired product with a 49 % yield (Table 19, entry 3).

[195] Mandal, S.; Bera, T.; Dubey, G.; Saha, J.; Laha, J. K. *ACS Catal.* **2018**, *8*, 5085.

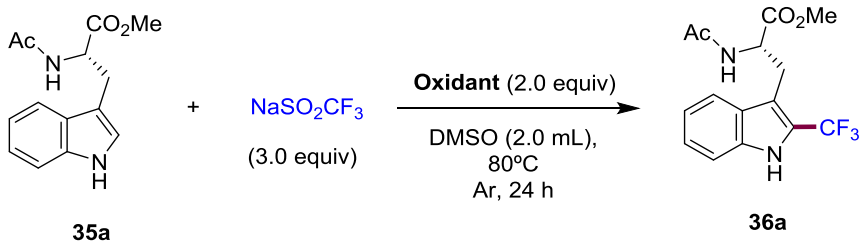

Entry	Oxidant	Yield (%)[b]
1	TBHPdec	36
2	TBHPaq	29
3	$(NH_4)_2S_2O_8$	49
4	$K_2S_2O_8$	traces
5	O_2 (1atm)	n.r.
6	DCP	0
7	DTBP	0
8	Oxone	0
9	H_2O_2	n.r.
10	PIDA	0

[a] Reaction conditions: Ac-Trp-OMe (0.25 mmol), $NaSO_2CF_3$ (0.75 mmol), DMSO (2.0 mL), 80 ºC, 24 h, under Ar. TBHPaq = *tert*-butyl hydroperoxide (70 wt. % in H_2O), TBHPdec = *tert*-butyl hydroperoxide (5.0-6.0 M in decane), DTBP = di-*tert*-butyl peroxide, DCP = dicumyl peroxide. [b] Yield of isolated product after purification by column chromatography.

Table 19 Screening of Oxidants.[a]

Next, the trifluoromethylation reaction was performed in a variety of commonly used organic solvents. However, the vast majority failed in the trifluoromethylation or provided **36a** in trace amounts, evidencing the crucial role of the solvent in the reaction outcome. In this manner, the use of DMSO provided the best result (Table 20, entry 1), probably owing to its high polarity where inorganic salts exhibit higher solubility. For the same reason, water was added as a co-solvent together with the solvents giving the best results such as acetonitrile, which provided **36a** in 30 % yield. Nonetheless, whereas aqueous media seemed to enhance the reactivity in Baran's method, in our case the addition of water resulted in lower yields of **36a** (Table 20, entry 3, 4).

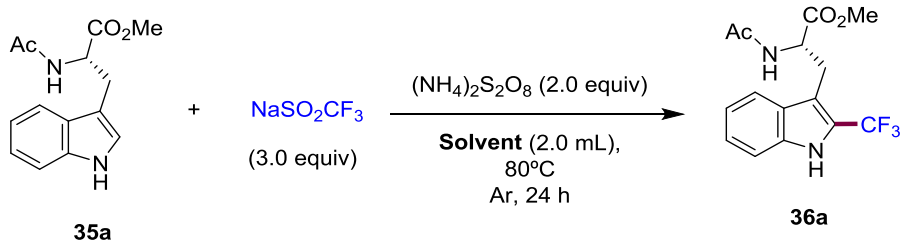

Entry	Solvent	Yield (%)[b]
1	DMSO	51
2	MeCN	30
3	MeCN/H_2O	n.r.
4	DMSO/H_2O	n.d.
5	DMF	n.d.
6	DMA	n.d.
7	NMP	n.d.

[a] Reaction conditions: Ac-Trp-OMe (0.25 mmol), $NaSO_2CF_3$ (0.75 mmol), $(NH_4)_2S_2O_8$ (2.0 equiv), Solvent (2.0 mL), 80 ºC, 24 h, under Ar. [b] Yield of isolated product after purification by column chromatography.

Table 20 Screening of Solvents.[a]

After choosing Langlois reagent and ammonium persulfate as the optimal trifluromethyl source and oxidant, respectively, **35a** was submitted to the reaction conditions at different temperatures in DMSO (Table 21). When the reaction was carried out at the most practical room temperature, almost no conversion of **35a** into **36a** could be observed (Table 21, entry 4). However, the reaction temperature could be decreased to 40 ºC becoming suitable for the formation of the trifluoromethylated product in the same yield (Table 21, entry 3). Conversely, higher temperatures (Table 21, entry1) resulted in lower yields of **36a** because other side-products were also formed under much harsh reaction conditions.

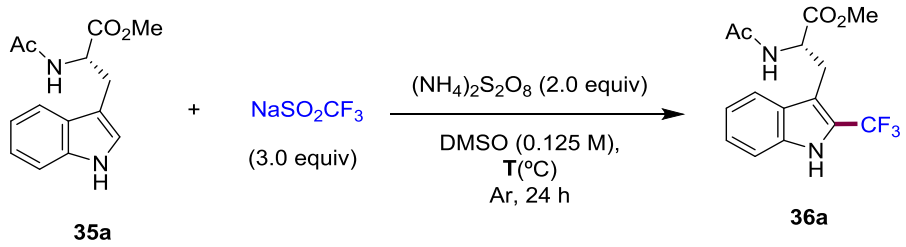

Entry	Temperature	Yield (%)[b]
1	100	24
2	80	50
3	40	52
4	r.t.	traces

[a] Reaction conditions: Ac-Trp-OMe (0.25 mmol), $NaSO_2CF_3$ (0.75 mmol), $(NH_4)_2S_2O_8$ (2.0 equiv), DMSO (2.0 mL), T, 24 h, under Ar. [b] Yield of isolated product after purification by column chromatography.

Table 21 Screening of Temperature.[a]

In order to obtain a more practical, sustainable and high-yielding procedure, we first decided to make use of first-row transition metals as catalyst instead of raising up the amount of reagents. Hence, we performed a careful screening of a vast array of cobalt, manganese, iron, silver and copper salts and the best results are collected in Table 22. Manganese catalysis has previously demonstrated its ability to perform C–H functionalization reactions in Trp residues.[139,140] Despite the fact that it would constitute a step forward from a sustainability point of view, pyridine derivatives have been often required as directing groups for the corresponding successful C2-modification processes. However, the commonly used $Mn(OAc)_2$ entirely inhibited the trifluoromethylation reaction (Table 22, entry 1). Moreover, while cobalt catalysts provided the modification of the peptide backbones in glycine derivatives (Chapter 2), low yields were achieved in our trifluoromethylation reaction (Table 22, entry 2 and 3). Indeed, they resulted in lower yields then the metal-free process (Table 22, entry 14). On the other hand, some of the tested iron and copper salts showed promising outcomes. For instance, when FeF_3 and Fe_2O_3 were added, **36a** was obtained in 65% and 72% yields, respectively. Nevertheless, we turned our attention to $Cu(OAc)_2$ and Cu(OAc) which made possible the formation of **36a** in comparatively higher yields. Furthermore, the combination of reaction conditions catalyzed by copper(I) acetate either at higher catalyst loading (Table 22, entry 13) or under air atmosphere (Table 22, entry 11) made no difference in reactivity, whereas the reaction carried out at room temperature rendered in a lower yield (Table 22, entry 12). Accordingly, in all attempts, a higher reaction concentration was applied as it was previously observed that 0.3 M provided the same result, which represents an advantage as far as minimizing waste is concerned.

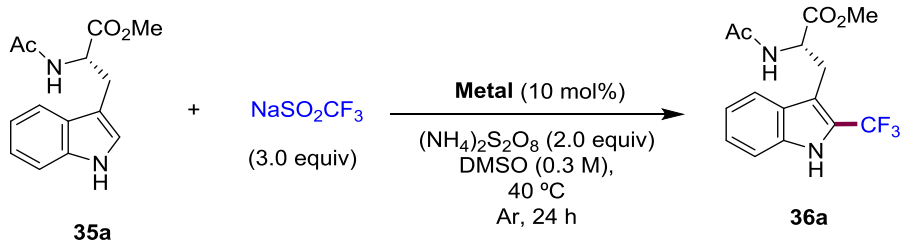

Entry	Oxidant	Yield (%)[b]
1	$Mn(OAc)_2$	0
2	$Co(acac)_2 \cdot H_2O$	27
3	$CoBr_2$	36
4	FeF_3	65
5	Fe_2O_3	72
6	CuF_2	70
7	$Cu(acac)_2$	76
8	AgOTf	30
9	$Cu(OAc)_2$	76
10	Cu(OAc)	79
11[c]	Cu(OAc)	78
12[c,d]	Cu(OAc)	61
13[c,e]	Cu(OAc)	78
14	none	52

[a] Reaction conditions: Ac-Trp-OMe (0.25 mmol), $NaSO_2CF_3$ (0.75 mmol), metal (10 mol %), $(NH_4)_2S_2O_8$ (2.0 equiv), DMSO (1 mL), 40 °C, Ar, 24h. [b] Yield of isolated product after purification by column chromatography [c] Under air. [d] at rt. [e] 50 mol % of Cu(OAc).

Table 22 Screening of Metal Catalysts.[a]

Although Cu(OAc) was selected as the optimal metal catalyst, which provided the formation of **36a** in an excellent 78% yield (Table 23, entry 1), it must be highlighted the importance of seeking for a metal-free process.[196] Thus, we accomplished last attempts to study whether we could perform the trifluoromethylation in

[196] Santoro, S.; Marrocchi, A.; Lanari, D.; Ackermann L.; Vaccaro, L. *Chem. Eur. J.* **2018**, *24*,13383.

a metal-free manner or not. The modification of **35a** was achieved in a 52% yield in the absence of a transition metal and under argon (Table 21, entry 3). However, when the last reaction was performed under air atmosphere, the reaction yield decreased to a 30 % yield (Table 23, entry 2). Next, we considered to modify the equivalents of either the Langlois reagent or oxidant in order to obtain a better conversion of the starting material into the desired product. In this manner, it was observed that the addition of lower amounts of both reagents did not enhance the previous results (Table 23, entry 3). Interestingly, the use of four equivalents of $(NH_4)_2S_2O_8$ or other persulfates such as $K_2S_2O_8$, which had provided **36a** before, resulted in a promising 42 % and a 37 % yield, respectively (Table 23, entry 4, 5). Nevertheless, exceeding the amount of oxidant to five equivalents did not favor the reaction conversion (Table 23, entry 6), probably due to the lack of solubility of the inorganic salt into the organic solvent. Consequently, we decided to dilute the reaction mixture and as a result a 50% yield of A-Trp(CF_3)-OMe was achieved in 50 % yield (Table 23, entry 7). Furthermore, the last attempt proved that submitting **35a** to a reaction mixture of Langlois reagent (3.0 equiv), $(NH_4)_2S_2O_8$ (4.0 equiv) in 2 mL of DMSO at 60 ºC under air provided **36a** in 62% yield in the absence of a transition-metal.

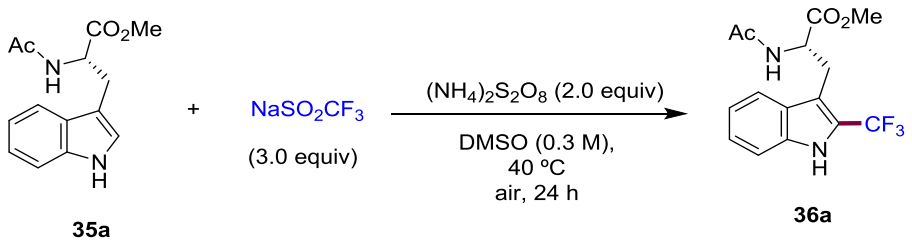

Entry	Change from standard conditions	Yield (%)[b]
1	with Cu(OAc) (10 mol%)	78
2	none	30
3	2.0 equiv of $NaSO_2CF_3$ and 1.0 equiv of $(NH_4)_2S_2O_8$	23
4	$(NH_4)_2S_2O_8$ (4.0 equiv)	42
5	$K_2S_2O_8$ (4.0 equiv)	37
6	$(NH_4)_2S_2O_8$ (5.0 equiv)	25
7	$(NH_4)_2S_2O_8$ (4.0 equiv) and DMSO (2 mL)	50
8	$(NH_4)_2S_2O_8$ (4.0 equiv), DMSO (2 mL), 60 ºC	62

[a] Reaction conditions: Ac-Trp-OMe (0.25 mmol), $NaSO_2CF_3$ (0.75 mmol), metal (10 mol %), $(NH_4)_2S_2O_8$ (2.0 equiv), DMSO (1 mL), air, 24h. [b] Yield of isolated product after purification by column chromatography.

Table 23 Metal-Free Trifluoromethylation.[a]

All these metal-free endeavors aside, the extra addition of oxidant, solvent and raising up the temperature would suppose a controversial issue as far as sustainability is concerned and the obtained yield was not as high as the one achieved with the use of Cu(I) salt to justify a metal-free process. Likewise, we considered that the copper-catalyzed trifluoromethylation of Trp derivatives would constitute a more efficient and atom-economical protocol, as the catalytic amount of benign first-row transition metal enhanced the reactivity and enabled a moderate use of reagents producing less chemical waste (Table 23, entry 1).

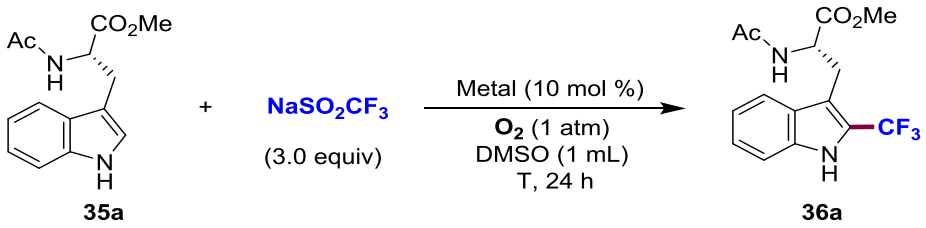

Entry	Metal	T (º C)	Yield (%)[b]
1	Cu(OAc)	40 to 80	0
2	$Cu(OAc)_2$	40	0
3	Cu(OAc)	80	traces
4	$Cu(acac)_2$	80	13

[a] Reaction conditions: Ac-Trp-OMe (0.25 mmol), $NaSO_2CF_3$ (0.75 mmol), metal (10 mol %), O_2 (1 atm), DMSO (1 mL), air, 24h. [b] Yield of isolated product after purification by column chromatography.

Table 24 Use of O_2 as the Sole Oxidant.[a]

The development of oxidative systems lead to the use of often, dangerous oxidant reagents which could be detrimental for the protocol and be discarded due to safety issues in a further industrial process. Thus, the use of molecular oxygen as the sole oxidant is a fundamental point that must be tested in this type of optimization processes.[197] Considering the best results given by Cu(OAc) and $Cu(OAc)_2$, we performed several attempts with both metal catalysts at different temperatures substituting the ammonium persulfate by O_2 (Table 24). However, when the reaction was carried out at the optimal temperature of 40 ºC no conversion of the starting material was observed (Table 24, entry 1 and 2). Warming up the reaction mixture gave same results with the last two exceptions where 80 ºC provided traces of **36a** under 1 atm of O_2 (Table 24, entry 3 and 4). Accordingly, at this stage the use of $(NH_4)_2S_2O_8$ as oxidant was found crucial for the process.

[197] Chen, B.; Wang, L.; Gao, S. *ACS Catal.* **2015**, *5*, 5851.

Once we had determined the optimal reaction conditions, we demonstrated that the process could be performed in gram-scale with a remarkable 75% yield, thus highlighting the synthetic utility and robustness of our radical functionalization method. Moreover, crystallographic analysis of **36a** confirmed that the absolute stereochemistry was identical to that of the starting Trp residue (Scheme 87).

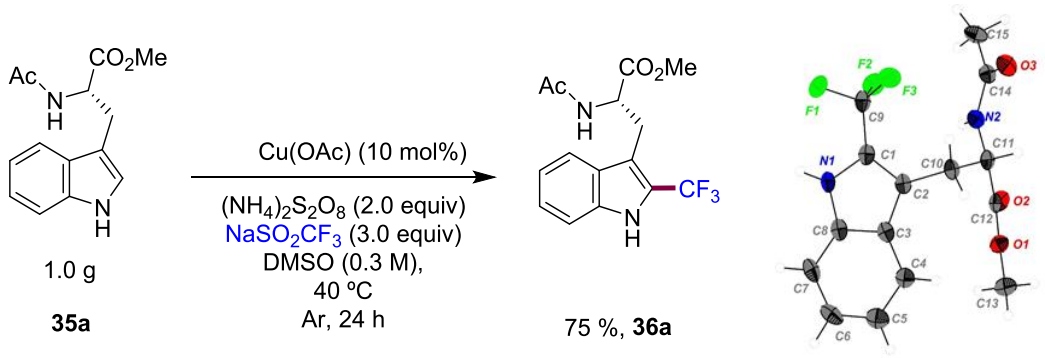

*Scheme 87 Scale Up Experiment and X-Ray Crystallography of **36a**.*

The development of novel synthetic methodologies for the modification of peptide derivatives under mild reaction conditions constitutes a prime issue as previously utilized harsh conditions exhibited disadvantages such as the racemization of existing chiral centers. Hence, in order to verify that our method provided the preservation of the α-center chirality, HPLC analysis was carried out (Figure 12). The racemic mixture of Ac-Trp-OMe was submitted to the optimal reaction conditions and product **rac-(36a)** was isolated for conducting further HPLC analysis. After a thorough search, the mixture of 95:5 Hexane:isopropanol in a Chiralpak IB type column enabled the separation of both enantiomers. Later on, when the model product **36a** was submitted to the same conditions, HPLC analysis revealed the existence of a single enantiomer, which demonstrated that our mild reaction conditions are suitable for a selective trifluoromethylation of tryptophan derivatives in a free-racemization fashion.

	Name	Retention Time (min)	Area (μV*sec)	% Area	Height (μV)
1		35.559	36062451	50.85	345106
2		40.582	34855897	49.15	292759

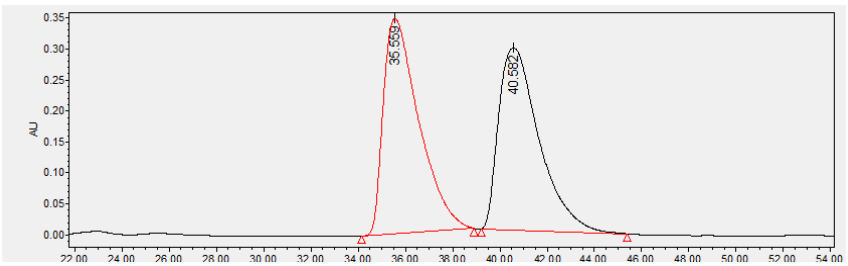

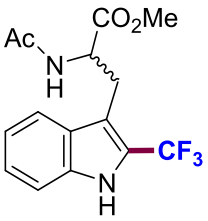

***rac*-(36a)**

Chiralpak IB; 95:5 Hexane: isopropanol; 1 mL/min, λ = 217 nm

	Name	Retention Time (min)	Area (μV*sec)	% Area	Height (μV)
1		35.607	37053237	100.00	363710

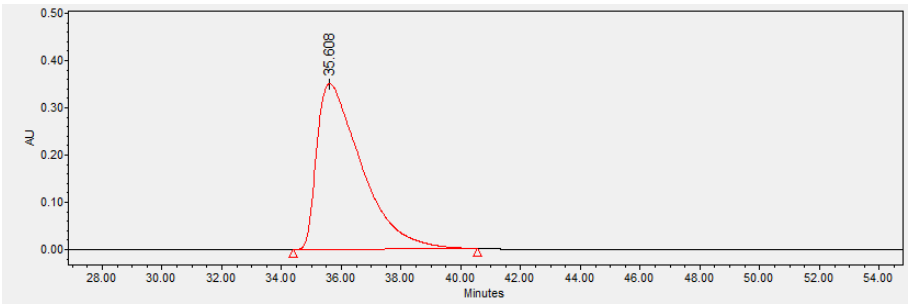

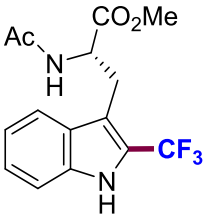

***S*-(36a)**

Figure 12 HPLC Analysis.

4.3.2. Scope of Trifluoromethylated Trp-Containing Oligopeptides

Our optimal conditions involved the use of the catalytic amounts of Cu(OAc) in combination with 2 equivalents of $(NH_4)_2S_2O_8$ and 3 equivalents of Langlois reagent in dimethylsulfoxide at 40 ºC under air, which provided the desired **36a** in 78 % yield in a practical manner. Afterwards, a wide variety of oligopeptides were synthesized (Scheme 88) and submitted to the reaction conditions to verify the efficiency of the disclosed methodology. Iniatially, a set of dipeptides were synthesized where 14 different amino acids were coupled with tryptophan. The latter could be either on the C- or N-terminal of the short-peptide. Easily prepared Boc-Trp-OH and Trp-OMe·HCl underwent further peptide couplings in the presence of standard coupling agents (EDC·HCl and HOBt) to deliver a variety of dipeptides in a simple manner (Scheme 88).[198]

[198] Montalbetti, C. A. G. N.; Falque, V. *Tetrahedron* **2005**, *61*, 10827.

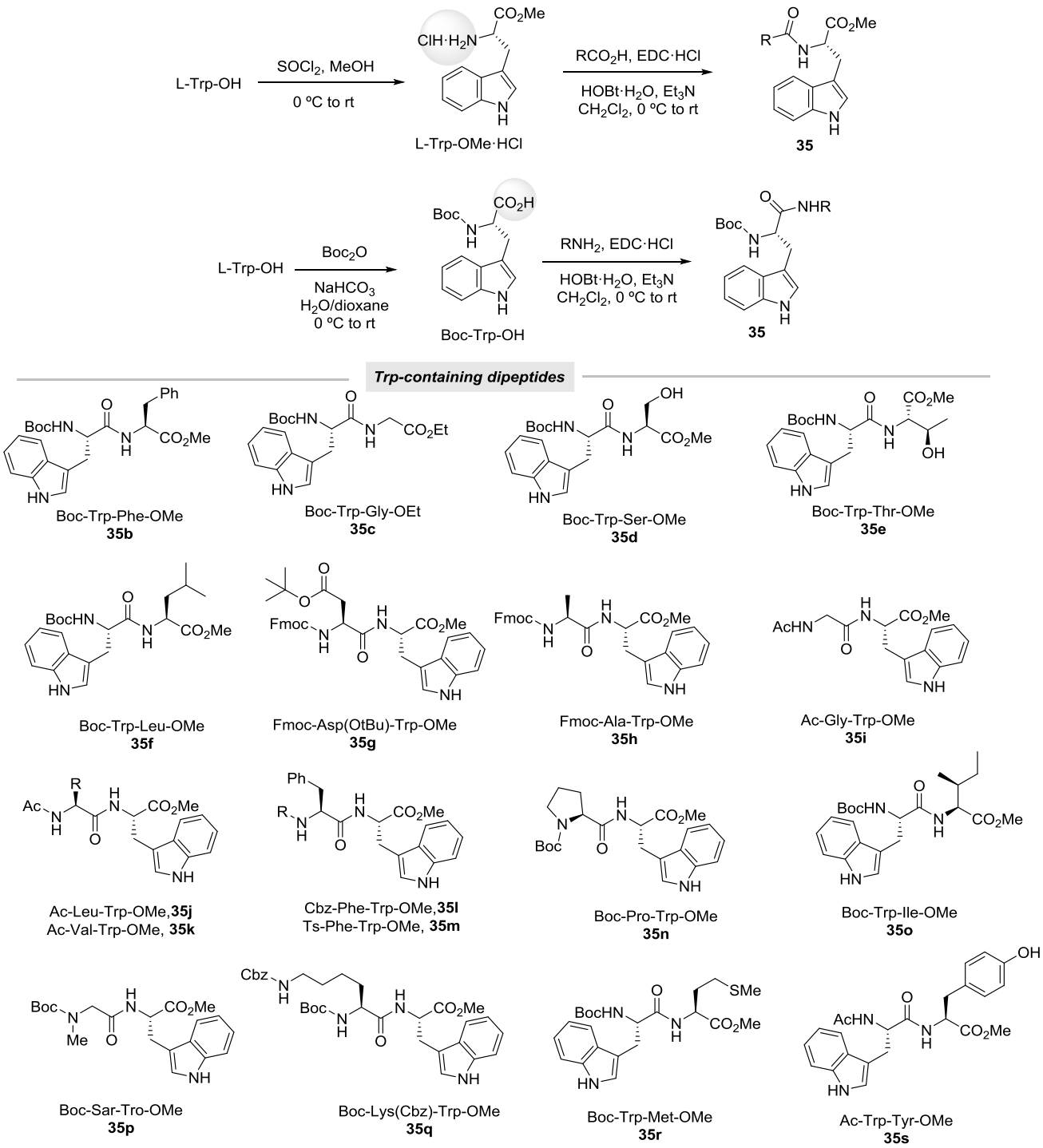

Scheme 88 Synthesis of Trp-Containing Dipeptides.

With a short-family of Trp-containing dipeptides in hand, we examined our oxidative trifluoromethylation reaction (Scheme 89). Notably, the 70% of existing natural amino acids could be tolerated and underwent the selective C2-trifluoromethylation of the Trp residue corroborating the feasibility of our protocol. As expected, amino acids bearing alkyl side-chains like Gly (**35c,i**), Leu (**35f,j**), Ala (**35h**), Val (**35k**) and Ile (**35o**) provided their fluorinated analogues with total regioselectivity and good yields. Furthermore, the presence of more than

one aromatic moiety through the peptidic structure often has diminished the efficiency of the procedure leading to product mixtures where not only the indole scaffold was functionalized.[173] In this regard, the total selectivity toward trifluoromethylated Trp unit was observed in dipeptides with phenyl rings such as Phe (**35b, 35l-m**) and Tyr (**35s**). The often obtained moderate yields were attributed to the lack of conversion of the starting materials. Precisely, the selective Trp modification of Tyr-containing dipeptide (**35s**) stood out as well as Boc-Ser-Trp(CF_3)-OMe (**36d**) and Boc-Trp(CF_3)-Thr-OMe (**36e**) which were obtained in a 45% and 46% yield, respectively, despite their oxidizable protic free-hydroxyl groups. Likewise, other functional groups such as thioether (**36r**), *N*-protected amines (**36n, p-q**) and ester (**36g**) were also suitable for this transformation. In particular, the selectivity toward indole scaffold in **36p** grabbed our attention. In the previous chapter, we have demonstrated the possibility of functionalizing the methyl group adjacent to a nitrogen atom through oxidative reaction conditions in an Ugi-type reaction. However, the developed optimal reaction conditions for our trifluoromethylation left inactive the methyl group in this case leading to the formation of a sole product. Importantly, a wide range of *N*-protecting groups boded well, and peptides protected with Boc-, Ac-, Fmoc-, Cbz- and even Ts-groups smoothly underwent the corresponding radical trifluoromethylation reaction.

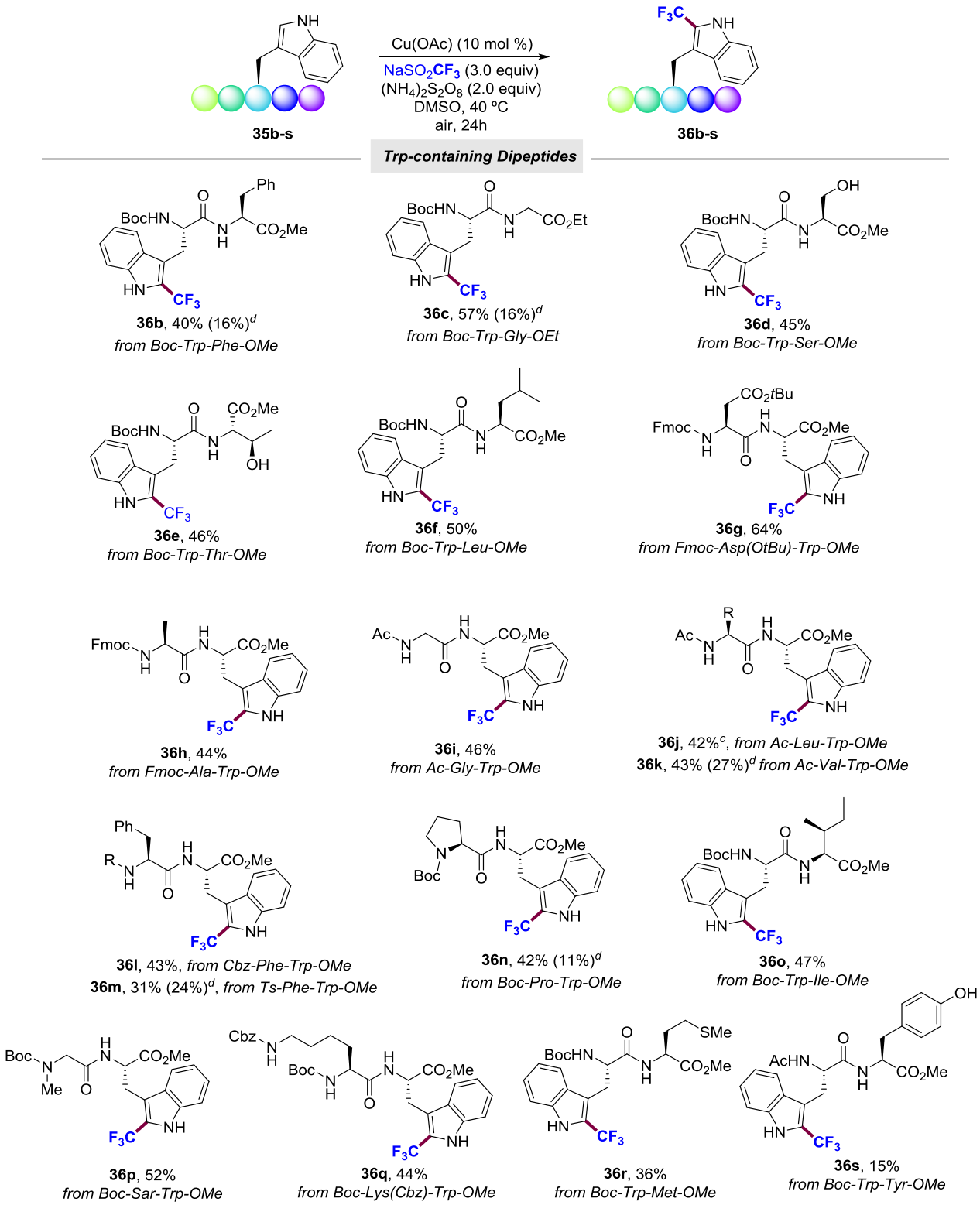

[a]As for Table 22, entry 11.[b] Yield of isolated product after column chromatography, average of at least two independent runs. [c] 48h. [d] Reaction conditions: **35** (0.25 mmol), $NaSO_2CF_3$ (0.75 mmol), $(NH_4)_2S_2O_8$ (1.0 mmol) in DMSO (0.125 M) at 60 ºC for 24 h under air.

Scheme 89 Cu-Catalyzed C(sp^2)−H Trifluoromethylation of Trp-Containing Dipeptides.[a]

A set of tri-, tetra- and pentapeptides were synthesized from the corresponding dipeptides. In this manner, either the C- or N-terminal position of the starting material had to be deprotected before the coupling with the next amino acid by the method described in Scheme 88. The peptide was treated with an excess of trifluoroacetic acid (TFA) in dichloromethane at room temperature for the deprotection of the N-terminal position, whereas basic conditions were required to obtain the terminal carboxylic acid.

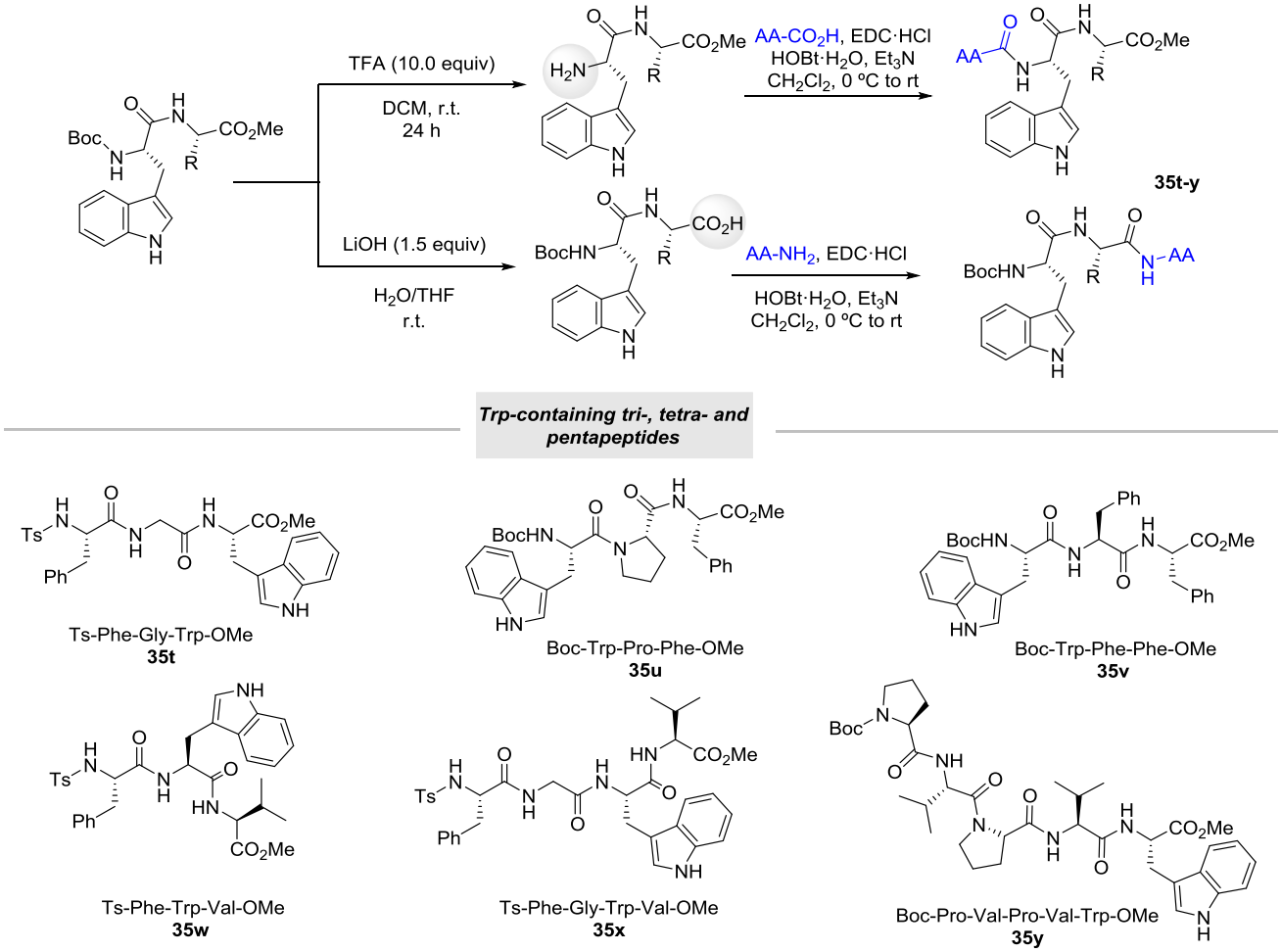

Scheme 90 Synthesis of Trp-Containing Tri-, Tetra- and Pentapeptides.

The success of the methodology did not rely on a specific position of the Trp along the peptide sequence, and was applicable to Trp residues located both at the N- and C-terminal position and in the middle of a more complex oligopeptide (Scheme 91). Tripeptide **35w** and tetrapeptide **35x** with the Trp unit in an inner position provided the corresponding adduct in moderate yields. The length of the peptidic chain was not an inconvenient to obtain good results with high selectivity (**36t-x**). Additionally, the robustness of the trifluoromethylation technique was evaluated for the diversification of a challenging pentapeptide **35y** rendering the trifluromethylated product in an excellent 52% yield. These results together with the remarkable 75% yield

achieved in gram-scale reaction for **35a** illustrate the ample opportunities of our fluorination technique in the late-stage labelling of proteins.

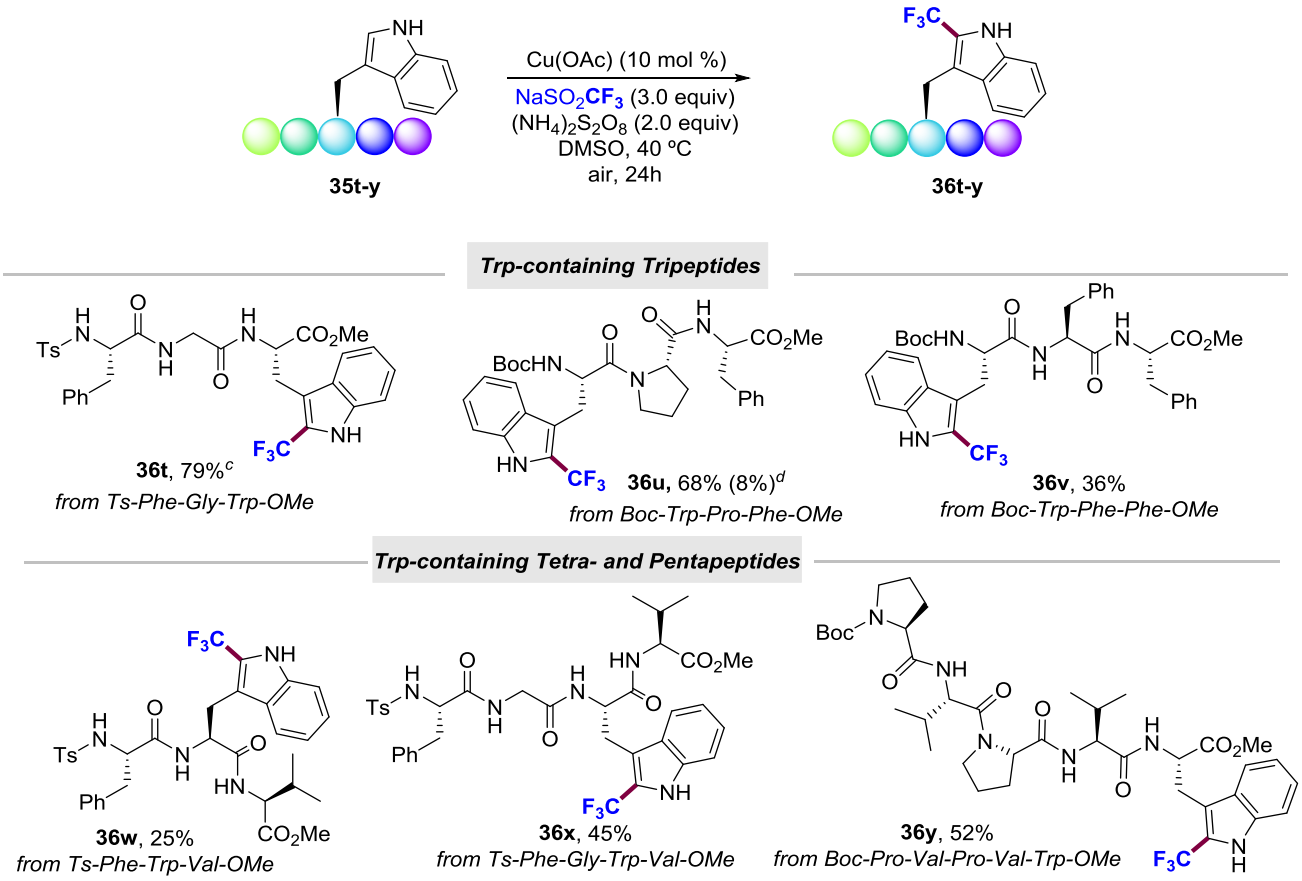

[a]As for Table 22, entry 11.[b] Yield of isolated product after column chromatography, average of at least two independent runs. [c] 48h. [d] Reaction conditions: **35** (0.25 mmol), $NaSO_2CF_3$ (0.75 mmol), $(NH_4)_2S_2O_8$ (1.0 mmol) in DMSO (0.125 M) at 60 ºC for 24 h under air.

Scheme 91 Cu-Catalyzed C(sp^2)−H Trifluoromethylation of Trp-Containing Oligopeptides.

Additionally, we decided to apply the metal-free reaction conditions disclosed in Table 23 to some of the synthesized peptides. Although the model substrate **35a** could be trifluoromethylated under metal-free conditions in a promising 65 % yield, other short-peptides displayed in Scheme 89 and 92 provided lower yields of the corresponding modified products. Trifluoromethylated tryptophan derivatives **36b**, **36c**, **36n** and **36u** were obtained in 20 % yield in the absence of the metal catalyst. Instead, the Cu-catalyzed protocol afforded comparatively higher yields in all cases, thus illustrating the clear benefits derived from the use of a Cu catalyst in this transformation. Importantly, ICP-MS analysis of some final products revealed lower amounts than 4 ppb of metal impurities, thus being insignificant levels and under the permitted range in drug discovery (Table 25).

Samples	Conc of ^{63}Cu(ppm)	RSD (%)
36b	<0.004	
36v	<0.004	
36c	<0.004	
36a	4.44	6.6

Table 25 ICP-MS Analysis.

Despite the fact that a metal-free protocol for the trifluoromethylation of tryptophan derivatives is still elusive, the results in Table 25 suggested that our methodology would provide the efficient late-stage modification of peptides under a sustainable manner and the resulting products were devoid of metal traces, which represents a prime issue in the pharmaceutical industry.

4.3.3. Scope of Trifluoromethylated Trp Derivatives

Once our methodology had demonstrated to enable the selective trifluoromethylation of a vast array of oligopeptides containing Trp residue, we decided to test the applicability of the protocol and its functional group tolerance (Scheme 92). Thus, a family of tryptophan derivatives were synthesized bearing a wide selection of functional groups such as ether (**37c**), heteroarenes (**37d-f**) or nitriles (**37h-i**). Furthermore, some known drugs and natural products were also coupled with the tryptophan unit (**37n-q**). On the other side, it must be highlighted that the diversification of natural peptides in a straightforward manner is still a challenge due to their lack of solubility in organic solvents and the high reactivity of -NH_2 and -CO_2H terminal functional groups. For that reason, native amino acids were also submitted to the optimal reaction conditions (**37a, l-m**).

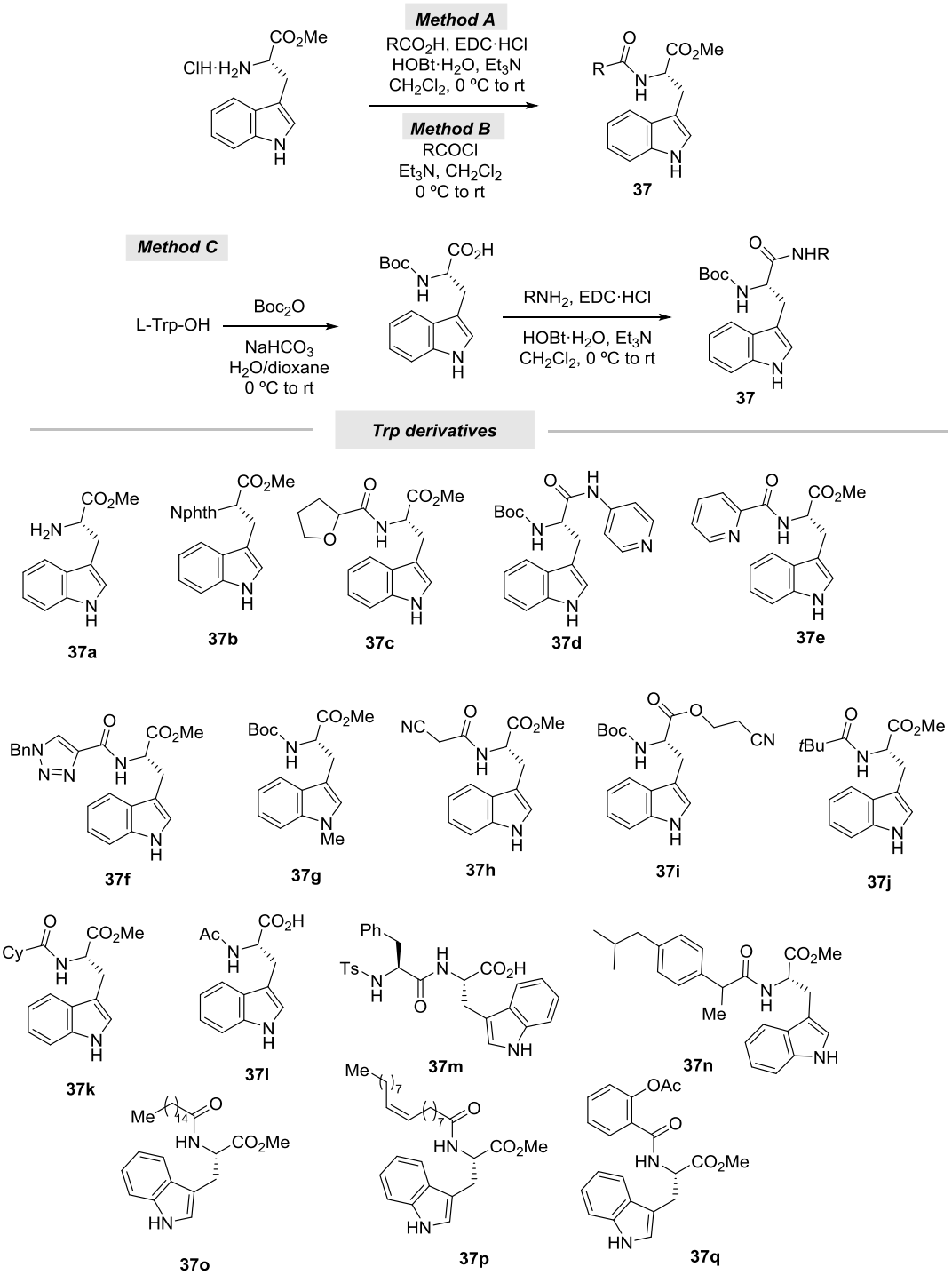

Scheme 92 Synthesis of Tryptophn Derivatives.

Hence, our trifluoromethylation manifold could occur not only with natural peptides but also with a wide variety of Trp derivatives housing functional groups (Scheme 93). According to the literature, numerous methods have been stablished for C(sp^3)–H bond oxidative functionalization of alkyl nitriles and ethers in a step-economical

fashion.[199] However, owing to the use of ammonium persulfate as a milder oxidant, tetrahydrofuryl ring (**37c**), aliphatic carboxamides (**37j,k**) or alkyl cyano groups (**37h,i**) could be accommodated among others, despite the oxidizable C(sp^3)–H adjacent bond. Another notable aspect of this protocol was the preferential trifluoromethylation of the indole ring in the presence of highly reactive heterocycles like pyridines (**37d-e**) and 1,2,3-triazoles (**37f**), which are prevalent motifs in drug discovery. Importantly, the functionalization of Trp derivatives containing bioactive drugs and natural products such as fatty acids (**37o** and **37p**), ibuprofen (**37n**) and aspirine (**37q**) were also assembled. Furthermore, the compatibility of the process in structurally more intricate contexts was demonstrated when short-peptides with either free $–NH_2$ or $–CO_2H$ functional groups gave the corresponding compounds (**37a, 37l, 37m**) in moderate yields despite their coordination ability with the metal center.

[199] a) Chu, X.-Q.; Ge, D.; Shen, Z.-L.; Loh, T.-P. *ACS Catal.* **2018**, *8*, 258. b) Batra, A.; Singh, P.; Singh, K. N. *Eur. J. Org. Chem.* **2017**, 3739. c) Guo, S.-R.; Kumar, P. S.; Yang, M. *Adv. Synth. Catal.* **2017**, *359*, 2.

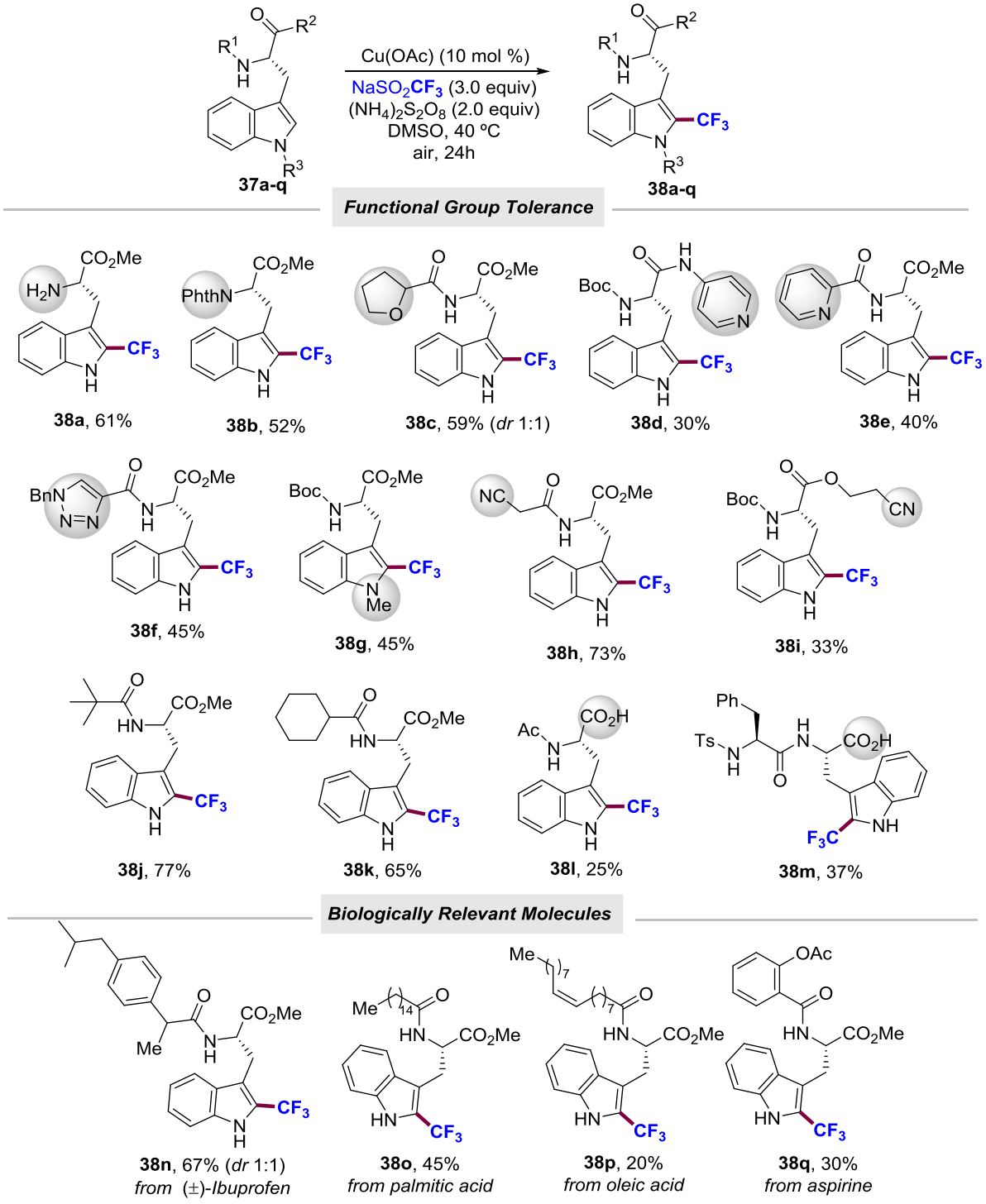

Scheme 93 Cu-Catalyzed C(sp²)−H Trifluoromethylation of Trp Derivatives.

4.3.4. *Mechanistic Proposal*

In order to gain some insights into the reaction mechanism, control experiments were performed using **35a** as the model substrate. Based on the previous literature,[200] the Cu-catalyzed trifluoromethylation of Trp-containing peptides under oxidative conditions is most likely to occur through the formation of an electrophilic trifluoromethyl radical species and further coupling upon the innate nucleophilic reactivity of the indole ring. Hence, radical traps were added into the model system to test whether the latter pathway may be operative or not (Scheme 94). Whereas the presence of TEMPO and BHT resulted in the suppresion of the transformation obtaining just traces of **36a**, when model substrate **35a** was submitted to reaction conditions with 3 equivalents of diphenylethylene no trifluoromethylated Trp derivative was detected. In contrast, compound **39**, derived from the coupling between the alkene and $^{\cdot}CF_3$, was isolated in 10 % yield. The latter suggested that radical species could be possible intermediates and accordingly the following mechanism described in Scheme 94 was proposed.

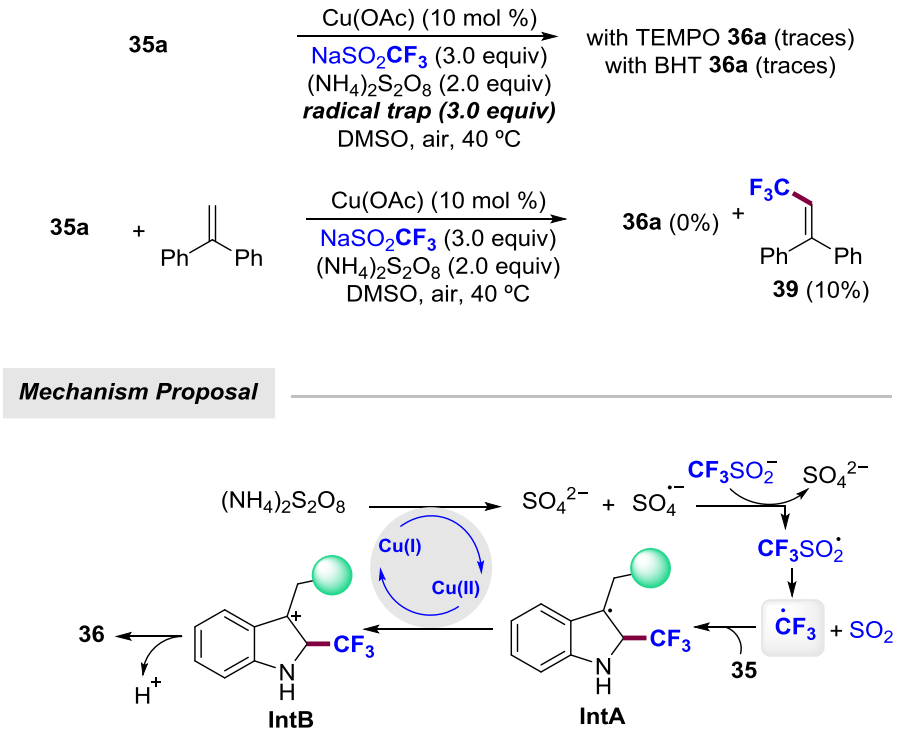

Scheme 94 Control Experiments and Mechanistic Proposal.

Firstly, copper(I) acetate would catalyzed the reduction and consequent decomposition of peroxydisulfate ion[201] into sulfate radical anion $SO_4^{\cdot -}$. The latter strong one-electron oxidant would assist a redox process where

[200] Cheng, M.; Zhang, B.; Cui, W.; Gross, M. L. *Angew. Chem. Int. Ed.* **2017**, *56*, 14007.
[201] Li, G.-b.; Zhang, C.; Song, C.; Ma, Y.-d. *Beilstein J. Org. Chem.* **2018**, *14*, 155.

$CF_3SO_2^{\cdot}$ radical would be generated, and this, in turn, would release SO_2 and $^{\cdot}CF_3$ radical species. Then, the active trifluoromethyl radical is biased by the innate reactivity of the indole ring of Trp derivative, which undergoes an electrophilic aromatic substitution at the C2-position forming the intermediate **IntA**. Following oxidation to the corresponding carbocation **IntB** would re-initiate the catalytic cycle leading to the aromatization step to afford the desired trifluoromethylated Trp derivative **36**.

At the time our research was in progress, the interest within this field has resulted in the development of other alternative trifluoromethylation protocols. Photocatalysis has evolved as a magnificent tool for C–H functionalization including fluorination reactions. The interest for late-stage modification of bioactive compounds guided Antonietti and König to develop a sustainable organic semiconductor mpg-CN photocatalyst for a variety of functionalizations of heteroarenes.[202] Different relevant molecules were submitted to the reaction conditions as well as Ac-Trp-OEt that gave a better result comparing to the 51 % yield obtained through the mpg-CN-catalyzed procedure reported four years before using CF_3SO_2Cl.[203]

However, in one of those recently published methods, Ding *et al*. disclosed an iridium-catalyzed photoredox system for the straightforward construction of trifluoromethylated peptides.[204] There, 2 mol % of photosensitizer together with blue LEDs irradiation in acetonitrile under air atmosphere provided the formation of Trp–CF_3 derivatives (Scheme 95). One more time a competition assay shown the chemo- and site-selectivity toward the Trp residue, which was reflected in short-peptides with an adjacent aromatic amino acid (Phe/Tyr) that were functionalized preferentially in the C2-position of the indole moiety (**41b**). Likewise, peptides with functional groups that could interfere within the process gave the corresponding products (**41b**, **41c**) demonstrating the efficiency of this visible-light induced protocol which occurred at room temperature and did not require any external oxidant. Furthermore, trifluoromethylated biomolecules were also obtained in a mixed-aqueous system, although in much lower yields than when using neat MeCN. Nevertheless, the expensive iridium catalyst represents a clear disadvantage and despite the functional group tolerance, the methodology exhibited limited scope with barely 12 short-peptide examples. Concerning the reaction mechanism, control experiments and electron paramagnetic resonance (EPR) studies suggested that after the photocatalyst excitation, both CF_3SO_2Na and Trp underwent individually SET steps leading to both CF_3 radical and Trp radical formation. Then, the coupling between two radicals and the following deprotonation step would render the trifluoromethylated product. However, the innate radical addition of $^{\bullet}CF_3$ to the electron rich Trp unit could not be ruled out.

[202] Ghosh, I.; Khamrai, J.; Savateev, A.; Shlapakov, N.; Antonietti, M.; König, B. *Science* **2019**, *365*, 360.
[203] Baar, M.; Blechert, S. *Chem. Eur. J.* **2015**, *21*, 526.
[204] Ding, B.; Weng, Y.; Liu, Y.; Song, C.; Yin, L.; Yuan, J.; Ren, Y.; Lei, A.; Chiang, C.-W. *Eur. J. Org. Chem.* **2019**, 7596.

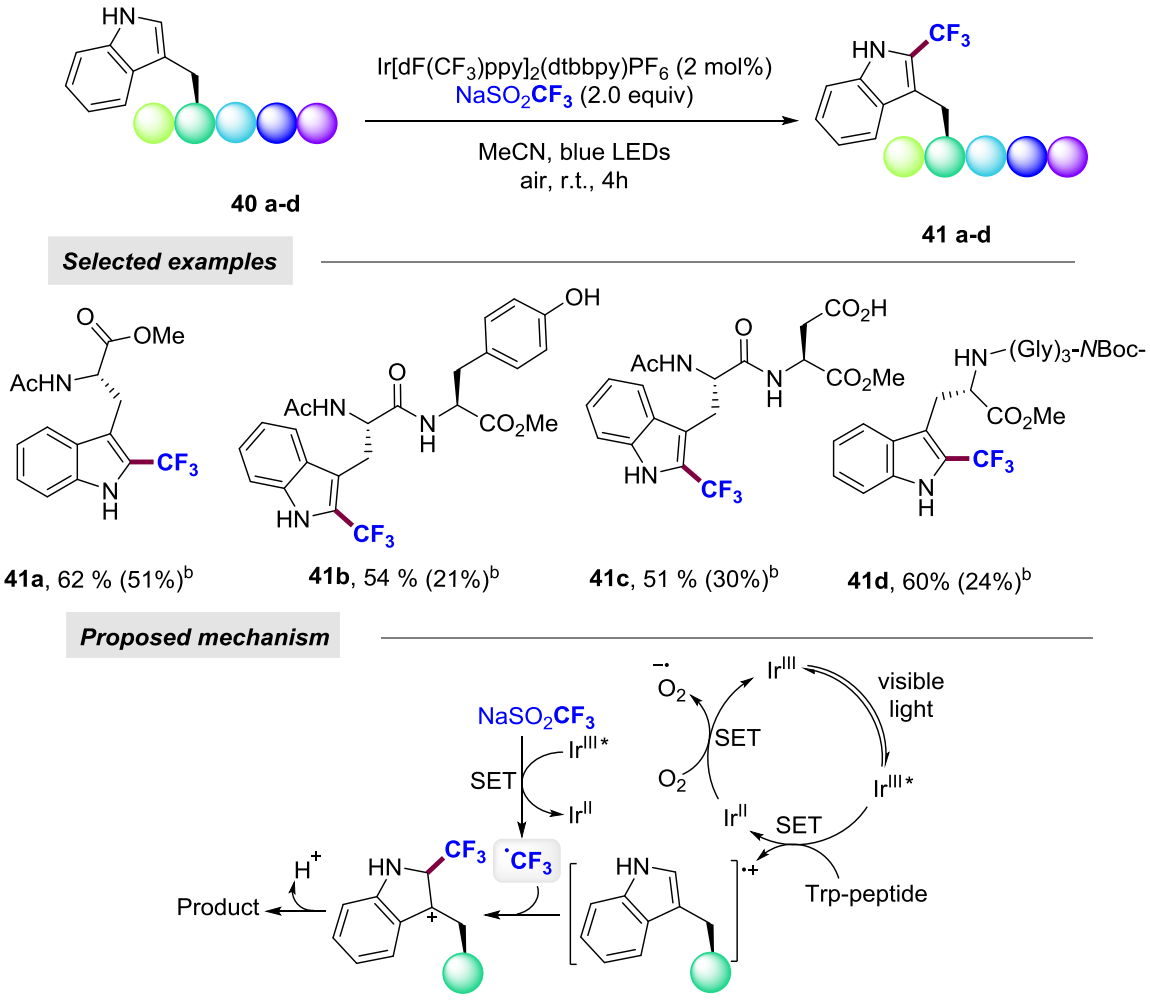

[a] Reaction conditions: **40** (0.20 mmol), CF_3SO_2Na (0.40 mmol), $Ir[dF(CF_3)ppy]_2(dtbbpy)PF_6$ (2 mol %), CH_3CN (2 mL), air, 3 W blue LEDs, room temperature, 4 h, isolated yield. $dF(CF_3)ppy$ = 2-(2,4-difluorophenyl)-5-(trifluoromethyl) pyridine; dtbbpy = 4, 4´-di-*tert*-butyl-2,2´-bipyridine.[b] CH_3CN/ H_2O (1.5 mL/1.5 mL) as solvent, 14 h, ^{19}F-NMR yield.

Scheme 95 Selective Photoredox Trifluoromethylation of Trptophan Containing Peptides.[a]

As highlighted before, Davis and Gouverneur reported the synthesis of a novel, yet efficient, radiollabeled trifluoromethylating reagent for the late-stage ^{18}F-trifluoromethylation of Tyr and Trp residues embedded into native peptides of great complexity.[175] As corroborated in previous studies, selectivity toward Trp residue instead of Tyr and other aromatic amino acids was observed where C2-modified regioisomer was the major one over the C4- and C7-analogues. Optimal reaction conditions were tested with almost twenty natural peptide structures, which resulted in their corresponding ^{18}F-radiolabeled products. Biologically versatile compounds

such as Endomorphin-1 (**43a**) (related with Alzheimer's disease)[205] or Octreotide[206] (**43b**) were selectively functionalized in their Trp units in 23% RCY (radiochemical yield) and 29% RCC (radiochemical conversion), respectively. Furthermore, the automated radiosynthesis of the latter ^{18}F-octapeptide was achieved in 133 minutes and applied in distribution and pharmacokinetic studies. Innovation aside, stoichiometric amounts of metal were required. Despite the use of the enviromentally-friendly iron source, its use as catalyst would be desirable for a more sustainable protocol.

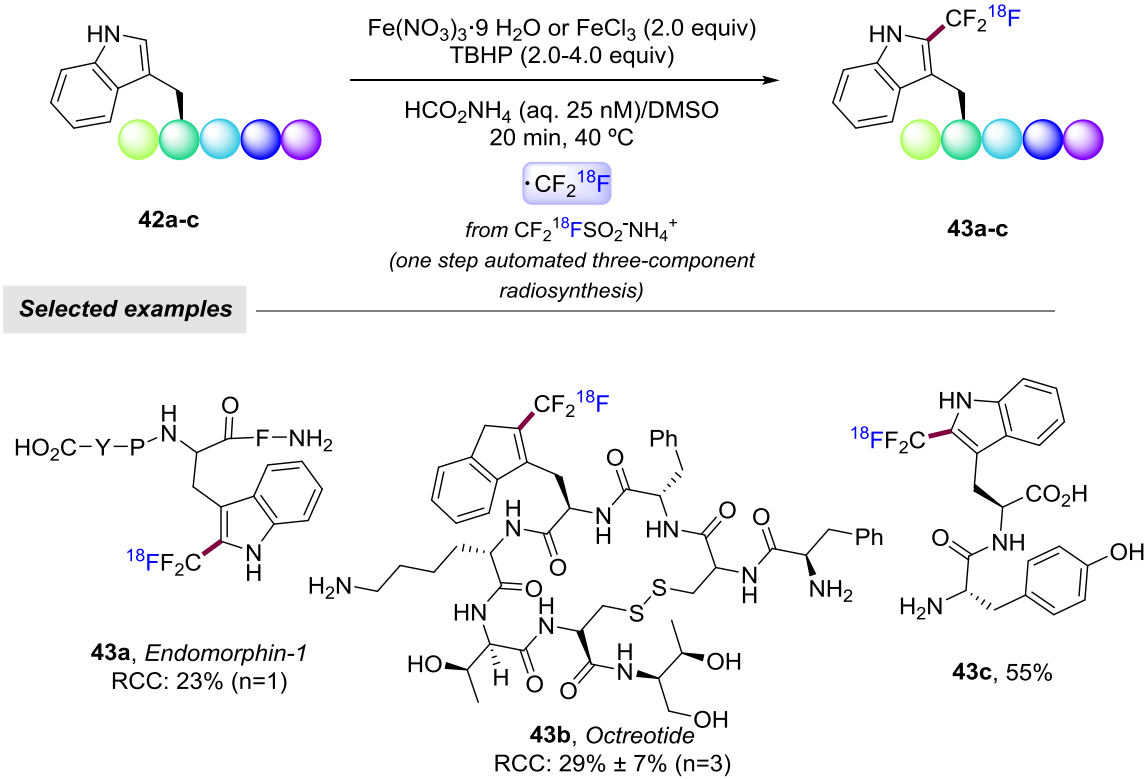

Scheme 96 Direct C–H ^{18}F-Trifluoromethylation of Native Aromatic Residues in Peptides.

[205] a) Zadina, J. E.; Hackler, L.; Ge, L. J.; Kastin, A. *Nature* **1997**, *386*, 499. b) Frydman-Marom, A.; Covertino, M.; Pellarin, R.; Lampel, A.; Shaltiel-Karyo, R.; Segal, D.; Caflish, A.; Shalev, D. E.; Gazit, E. *ACS Chem. Biol.* **2011**, *6*, 1265.
[206] Pauwels, E.; Cleeren, F.; Tshibangu, T.; Koole, M.; Serdons, K.; Dekervel, J.; Van Cutsem, E.; Verslype, C.; Van Laere, K.; Bormans, G.; Deroose, C. M. *Eur. J. Nucl. Med. Mol. Imaging* **2019**, *46*, 2398.

4.4. Conclusion

In conclusion, we have developed a radical C(sp^2)–H trifluoromethylation of Trp-containing oligopeptides assisted by copper(I) catalysis and the use of commercially available Langlois reagent.[207] In this manner, combining a non-precious first-row copper catalyst, inexpensive persulfate oxidant, avoidance of chlorinated solvents, and performance in an open-air system at relatively low temperatures resulted in excellent mild reaction conditions that enabled the assembly of enantiomerically pure modified short-to-medium-peptides with exceptional site- and chemoselectivity. Moreover, the vast array of functional groups present in the numerous substrates submitted to the process has illustrated the robustness of this C–H functionalization technique. Likewise, the recently reported trifluoromethylation of Trp residues in structurally more complex protein compounds have shown that still high levels of reagents are required for these transformations. Therefore, our Cu-catalyzed trifluoromethylation method could become an alternative for the introduction of metabolism-blocking fluoroalkyl groups in a late-stage fashion of utmost importance in the field of bioconjugation, thus providing access to new peptide entities beyond those found in native proteins.

[207] Guerrero, I.; Correa, A. *Org. Lett*. **2020**, *22*, 1754.

4.5. Experimental Procedures

In this section, some illustrative examples are included. For full details of the characterization of the products described herein, please check the SI of the already published article.[207]

4.5.1. Cu-Catalyzed C(sp^2)−H Trifluoromethylation of Trp Derivatives

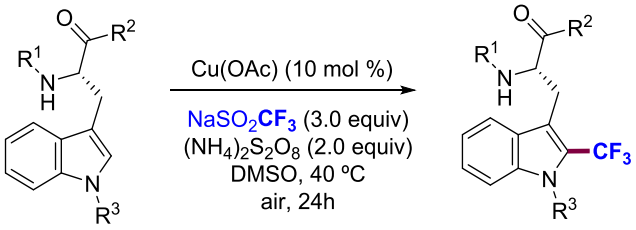

General procedure: A reaction tube containing a stirring bar was charged with the tryptophan derivative (0.25 mmol), $(NH_4)_2S_2O_8$ (0.50 mmol, 114 mg), $NaSO_2CF_3$ (0.75 mmol, 117 mg) and copper (I) acetate (10 mol %, 3.2 mg). Then, DMSO (1 mL) was added by syringe under air atmosphere. The reaction tube was next warmed up to 40 ºC in a heating block and stirred for 24 hours. The mixture was allowed to cool to room temperature, concentrated under reduced pressure and the corresponding product was purified by flash chromatography (hexanes/AcOEt).

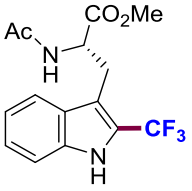

36a

Methyl (*S*)-2-acetamido-3-[2-(trifluoromethyl)-1*H*-indol-3-yl]propanoate (36a). Following the general procedure, using Ac-L-Trp-OMe (**35a**) (0.25 mmol, 65.1 mg) provided 64 mg (78 % yield) of **36a** as a white solid. Column chromatography (Hex/EtOAc 1:1). Mp 219-221 ºC. The spectroscopic data corresponded to those reported in the literature.[192] ^{1}H NMR (400 MHz, $CDCl_3$) δ 8.70 (brs, NH), 7.70 (d, *J* = 8.1 Hz, 1H), 7.38 (d, *J* = 8.2 Hz, 1H), 7.32 (t, *J* = 7.5 Hz, 1H), 7.20 (t, *J* = 7.5 Hz, 1H), 6.08 (d, *J* = 7.8 Hz, NH), 4.96 (dt, *J* = 7.9, 6.2 Hz, 1H), 3.67 (s, 3H), 3.44 (dd, *J* = 15.0, 6.6 Hz, 1H), 3.38 (dd, *J* = 14.7, 6.2 Hz, 1H), 1.94 (s, 3H). ^{13}C NMR (101 MHz, $CDCl_3$) δ 172.2, 170.0, 135.4, 127.5, 125.3, 122.7 (q, *J* = 37.4 Hz), 121.1, 121.0 (q, *J* = 269.7 Hz), 120.3, 112.3 (q, *J* = 3.0 Hz), 112.1, 52.7, 52.6, 27.2, 23.2. ^{19}F NMR (376 MHz, $CDCl_3$) δ -57.90. *This reaction was also performed in a higher scale: the use of **35a** (3.84 mmol, 1.00 g), $NaSO_2CF_3$ (1.79 g), $(NH_4)_2S_2O_8$ (1.75 g) in DMSO (15 mL) provided 1.26 g (75 % yield) of **36a** as a white solid.*

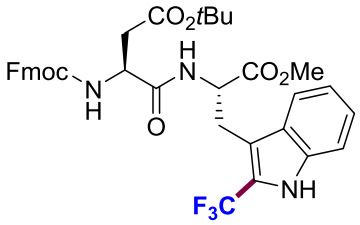

(36g)

***tert*-Butyl (*S*)-3-[(((9*H*-fluoren-9-yl)methoxy)carbonyl)amino)-4-(((*S*)-1-methoxy-1-oxo-3-(2-(trifluoromethyl)-1*H*-indol-3-yl)propan-2-yl)amino]-4-oxobutanoate (36g).** Following the general procedure, using Fmoc-Asp(O*t*Bu)-Trp-OMe (0.25 mmol, 152.9 mg) provided 108.7 mg (64 % yield) of **36g** as a white solid. Column chromatography (Hex/EtOAc 6:4). Mp 128-130 ºC. ^{1}H NMR (400 MHz, $CDCl_3$) δ 8.53 (s, NH), 7.76 (t, *J* = 7.3 Hz, 3H), 7.57 (t, *J* = 7.9 Hz, 2H), 7.41 (t, *J* = 7.3 Hz, 2H), 7.37 – 7.25 (m, 4H), 7.22 – 7.10 (m, 2H), 5.79 (d, *J* = 8.2 Hz, NH), 4.88 (dd, *J* = 16.0, 7.0 Hz, 1H), 4.57 – 4.49 (m, 1H), 4.38 (d, *J* = 7.3 Hz, 2H), 4.20 (t, *J* = 7.0 Hz, 1H), 3.62 (s, 3H), 3.38 (t, *J* = 6.9 Hz, 2H), 2.85 (dd, *J* = 17.1, 3.8 Hz, 1H), 2.56 (dd, *J* = 17.1, 6.8 Hz, 1H), 1.40 (s, 9H). ^{13}C NMR (101 MHz, $CDCl_3$) δ 171.6, 171.2, 170.4, 155.9, 143.8, 141.4, 135.4, 127.9, 127.4, 127.2, 125.3, 125.2, 122.7 (q, J_{C-F} = 34.3 Hz), 121.9 (q, J_{C-F} = 270.2 Hz), 121.2, 120.4, 120.1, 112.5, 111.9, 82.0, 67.3, 53.2, 52.5, 51.0, 47.2, 37.8, 28.1, 27.1. ^{19}F NMR (376 MHz, $CDCl_3$) δ -57.93. IR (neat, cm^{-1}): 3374, 3296, 1721, 1698, 1658, 1160, 1104, 737. HRMS (ESI) m/z: (M^+) *Calcd*. *for* ($C_{36}H_{36}F_3N_3O_7$): 679.2505, *found* 679.2510.

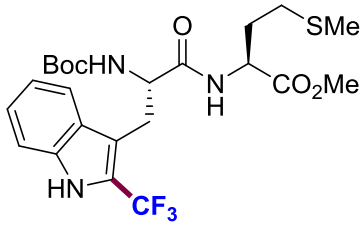

(36r)

Methyl [(*S*)-2-((*tert*-butoxycarbonyl)amino)-3-(2-(trifluoromethyl)-1*H*-indol-3-yl)propanoyl]-*L*-methioninate (36r). Following the general procedure, using Boc-Trp-Met-OMe[208] (0.25 mmol, 112 mg) for 48 h, provided 46 mg (36% yield) of **36r** as a white solid. Column chromatography (Hex/EtOAc 7:3). Mp 160-61 ºC. ^{1}H NMR (400 MHz, $CDCl_3$) δ 8.73 (brs, 1H), 7.74 (d, *J* = 8.1 Hz, 1H), 7.39 (d, *J* = 8.2 Hz, 1H), 7.30 (t, *J* = 7.6 Hz, 1H), 7.18 (t, *J* = 7.5 Hz, 1H), 6.32 (d, *J* = 7.6 Hz, 1H), 5.23 (d, *J* = 8.1 Hz, 1H), 4.53 (dd, *J* = 12.0, 6.8 Hz, 1H), 4.43 (d, *J* = 7.5 Hz, 1H), 3.62 (s, 3H), 3.47 – 3.22 (m, 2H), 2.45 – 2.28 (m, 2H), 2.02 (s, 3H), 1.97 – 1.74 (m, 2H), 1.38 (s, 9H). ^{13}C NMR (101 MHz, $CDCl_3$) δ 171.7, 171.1, 155.3, 135.5, 127.3, 125.2, 123.1, 122.9 (q, J_{C-F} = 40.4 Hz), 122.2 (q, J_{C-F} = 263.0 Hz), 120.5, 112.8, 111.9, 80.3, 55.3, 52.6, 51.6, 31.9, 29.7, 28.3, 27.5, 15.5. ^{19}F NMR (376 MHz, $CDCl_3$) δ -57.81. IR (neat, cm^{-1}): 3334, 1726, 1682, 1664, 1514, 1160, 1098. HRMS (ESI) m/z: (M^+) *Calcd*. *for* ($C_{23}H_{30}F_3N_3O_5S$): 517.1858, *found* 517.1876.

[208] Suppo, J.-S.; Subra, G.; Bergès, M.; Marcia de Figueiredo, R.; Campagne, J.-M. *Angew. Chem. Int. Ed.* **2014**, *53*, 5389.

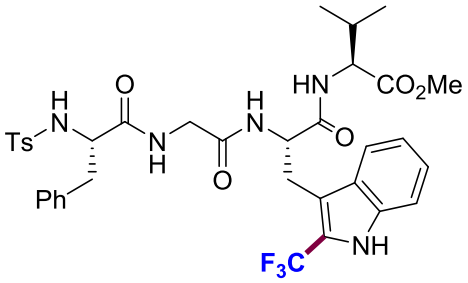

(36x)

Methyl [(*S*)-2-(2-((*S*)-2-((4-methylphenyl)sulfonamido)-3-phenylpropanamido)acetamido]-3-(2-(trifluoromethyl)-1*H*-indol-3-yl)propanoyl)-*L*-valinate (36x). Following the general procedure, using Ts-Phe-Gly-Trp-Val-OMe (0.25 mmol, 168.9 mg) provided 83 mg (45 % yield) of **36x** as a white solid. Column chromatography (Hex/EtOAc 4:6). Mp 137-140 ºC. ^{1}H NMR (400 MHz, MeOH-d_4) δ 8.30 (t, *J* = 5.6 Hz, NH), 7.83 (d, *J* = 8.7 Hz, 1H), 7.69 (d, *J* = 8.1 Hz, 1H), 7.47 (d, *J* = 8.2 Hz, 2H), 7.38 (d, *J* = 8.3 Hz, 1H), 7.24 (t, *J* = 7.6 Hz, 1H), 7.17 (d, *J* = 8.1 Hz, 2H), 7.15 – 7.08 (m, 4H), 7.01 (dd, *J* = 7.0, 2.3 Hz, 2H), 4.67 (dd, *J* = 8.3, 6.5 Hz, 1H), 4.20 (dd, *J* = 8.7, 6.2 Hz, 1H), 3.86 (dd, *J* = 9.3, 5.2 Hz, 1H), 3.74 – 3.63 (m, 2H), 3.48 (s, 3H), 3.41 (dd, *J* = 14.1, 8.6 Hz, 1H), 3.23 (dd, *J* = 14.2, 6.4 Hz, 1H), 2.98 (dd, *J* = 13.9, 5.2 Hz, 1H), 2.70 (dd, *J* = 13.9, 9.3 Hz, 1H), 2.38 (s, 3H), 1.98 (dt, *J* = 13.3, 6.6 Hz, 1H), 0.84 (dd, *J* = 6.8, 3.2 Hz, 6H). ^{13}C NMR (101 MHz, MeOH-d_4) δ 174.2, 173.0, 172.6, 170.7, 144.7, 138.0, 137.7, 137.4, 130.6, 130.2, 129.4, 128.6, 128.1, 127.7, 125.3, 123.9 (q, J_{C-F} = 37.3 Hz), 123.7 (q, J_{C-F} = 269.7 Hz), 121.2, 121.2, 113.0, 112.9, 59.8, 59.1, 55.9, 52.35, 43.5, 39.2, 32.5, 27.7, 21.5, 19.4, 18.6. ^{19}F NMR (376 MHz, $CDCl_3$) δ -57.87. IR (neat, cm^{-1}): 3293, 2963, 2927, 1730, 1638, 1157, 1119, 746, 663, 552. HRMS (ESI) m/z: (M^+) *Calcd*. *for* ($C_{36}H_{40}F_3N_5O_7S$): 743,2601, *found* 743,2575.

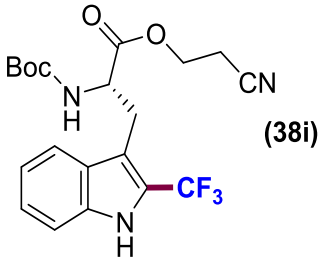

(38i)

2-Cyanoethyl (*S*)-2-[((*tert*-butoxycarbonyl)amino)-3-(2-(trifluoromethyl)-1*H*-indol-3-yl)]propanoate (38i). Following the general procedure, using **37i** (0.25 mmol, 89.3 mg) provided 35 mg (33% yield) of **38i** as a white solid. Column chromatography (Hex/EtOAc 1:1). Mp 150-152 ºC. ^{1}H NMR (400 MHz, $CDCl_3$) δ 8.53 (brs, NH), 7.67 (d, *J* = 8.0 Hz, 1H), 7.41 (d, *J* = 8.2 Hz, 1H), 7.34 (t, *J* = 7.5 Hz, 1H), 7.21 (t, *J* = 7.5 Hz, 1H), 5.10 (d, *J* = 7.9 Hz, NH), 4.64 (dd, *J* = 16.0, 7.0 Hz, 1H), 4.25 – 4.10 (m, 2H), 3.39 (d, *J* = 6.5 Hz, 2H), 2.45 (t, *J* = 6.4 Hz, 2H), 1.40 (s, 9H). ^{13}C NMR (101 MHz, $CDCl_3$) δ 171.6, 155.0, 135.4, 127.4, 125.3, 122.9 (q, J_{C-F} = 37.4 Hz), 121.9 (q, J_{C-F} =270.7 Hz), 122.3, 121.2, 120.2, 116.3, 112.3, 112.1, 80.4, 59.5, 54.2, 28.3, 27.4, 17.6.

^{19}F NMR (376 MHz, $CDCl_3$) δ -57.96. IR (neat, cm^{-1}): 3309, 2979, 2255, 1746, 1693, 1157, 1113, 737. HRMS (ESI) m/z: (M^+) *Calcd*. *for* ($C_{20}H_{22}F_3N_3O_4$): 425.1562, *found* 425.1578.

4.5.2. *NMR spectra*

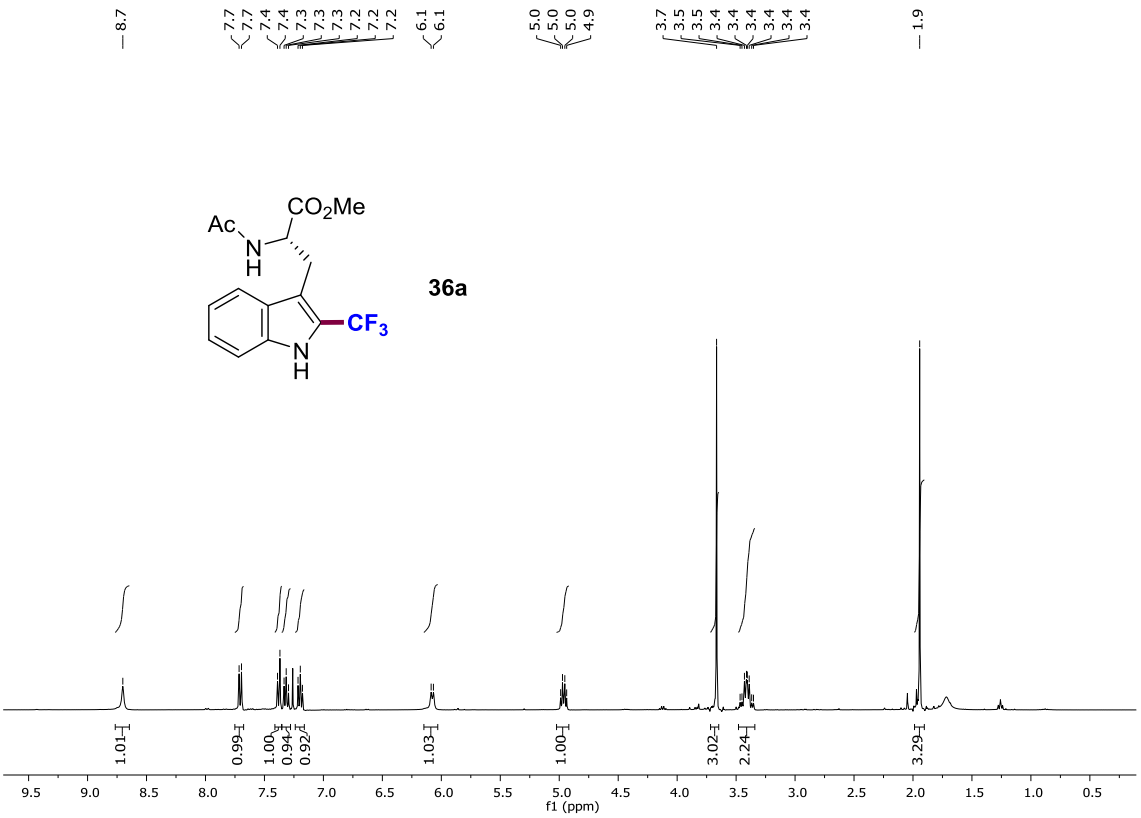

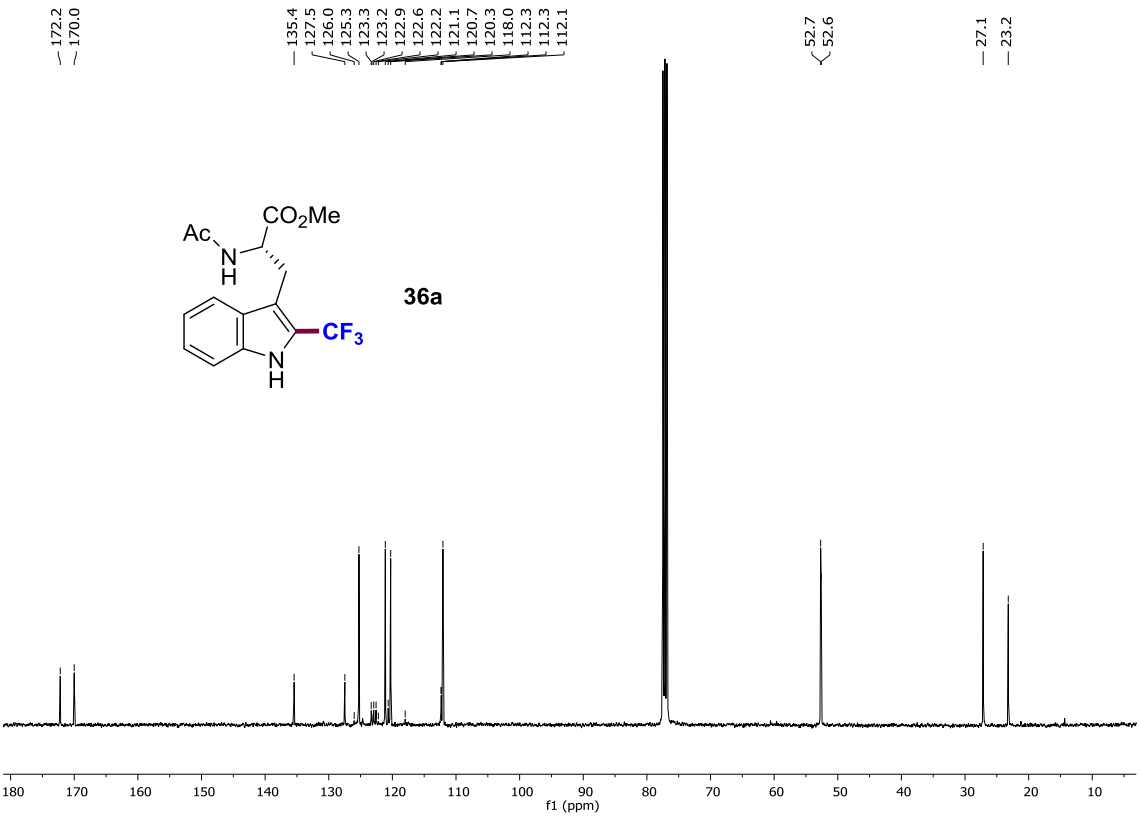

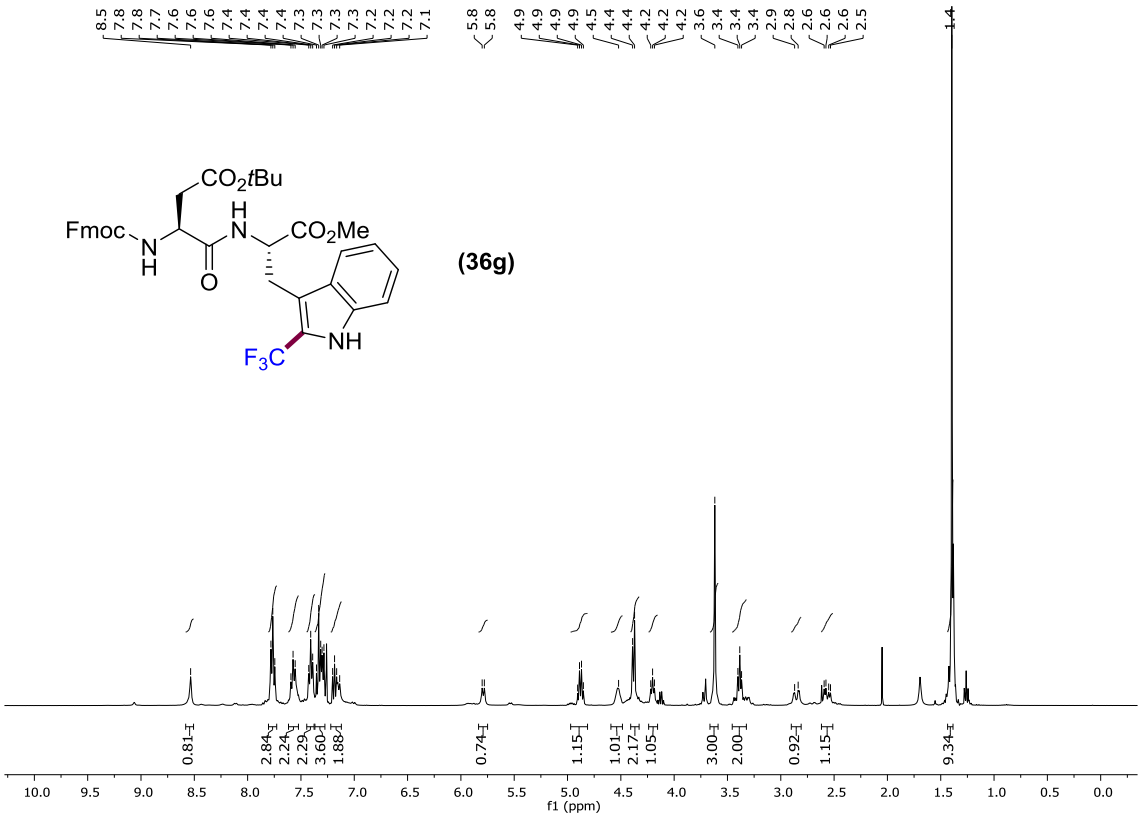
Fmoc
N
H
O
H
N
CO2tBu
CO2Me
F3C
NH
(36g)
f1 (ppm)

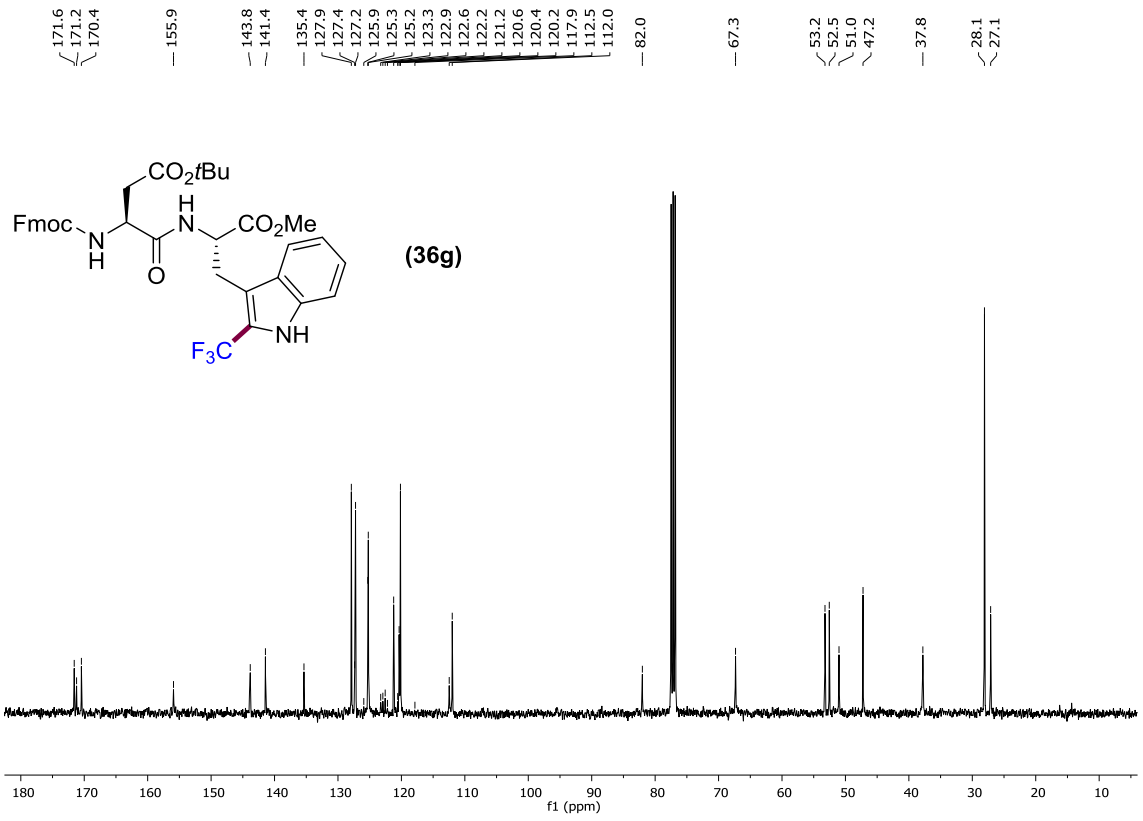
Fmoc
N
H
O
H
N
CO2tBu
CO2Me
F3C
NH
(36g)
f1 (ppm)

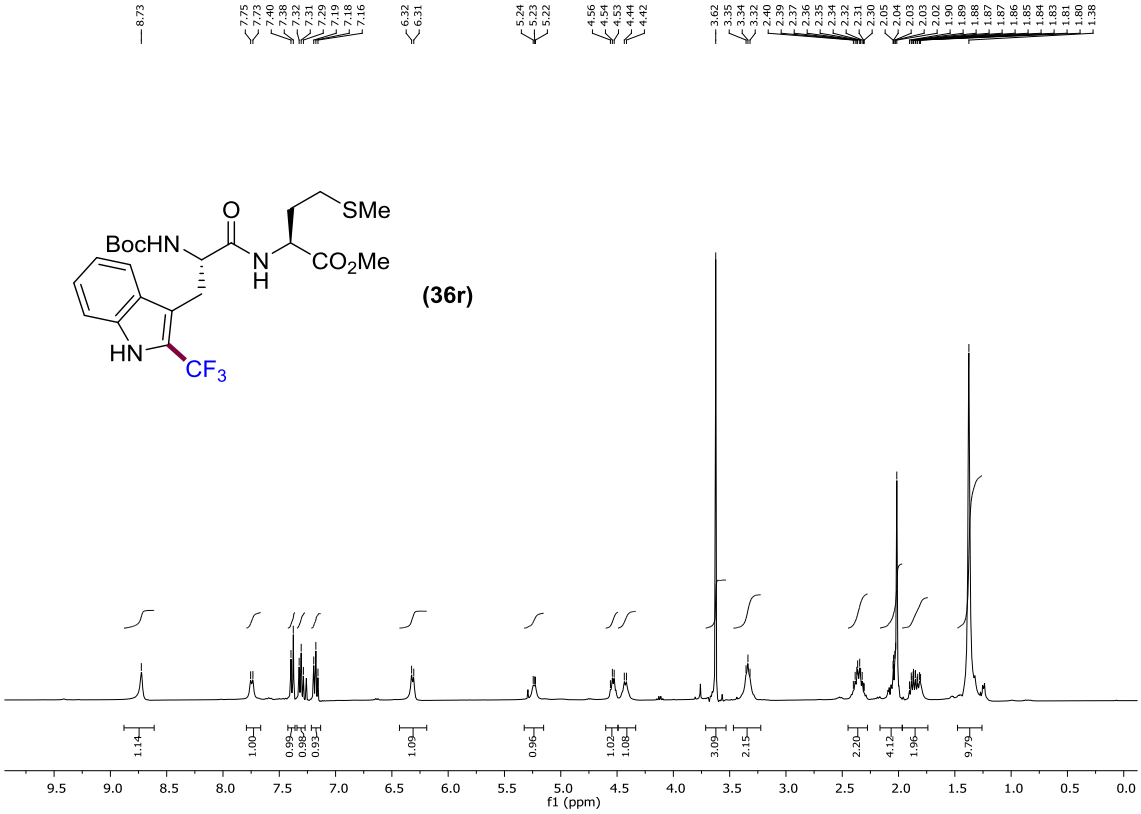
8.73
7.75
7.73
7.40
7.38
7.32
7.31
7.29
7.19
7.18
7.16
6.32
6.31
5.24
5.23
5.22
4.56
4.54
4.53
4.44
4.42
3.62
3.35
3.34
3.32
2.40
2.39
2.37
2.36
2.35
2.34
2.32
2.31
2.30
2.05
2.04
2.03
2.02
1.90
1.89
1.88
1.87
1.87
1.86
1.85
1.84
1.83
1.81
1.80
1.38
BocHN
O
N
H
SMe
CO2Me
HN
CF3
(36r)
1.14
1.00
0.99
0.98
0.93
1.09
0.96
1.02
1.08
3.09
2.15
2.20
4.12
1.96
9.79
f1 (ppm)

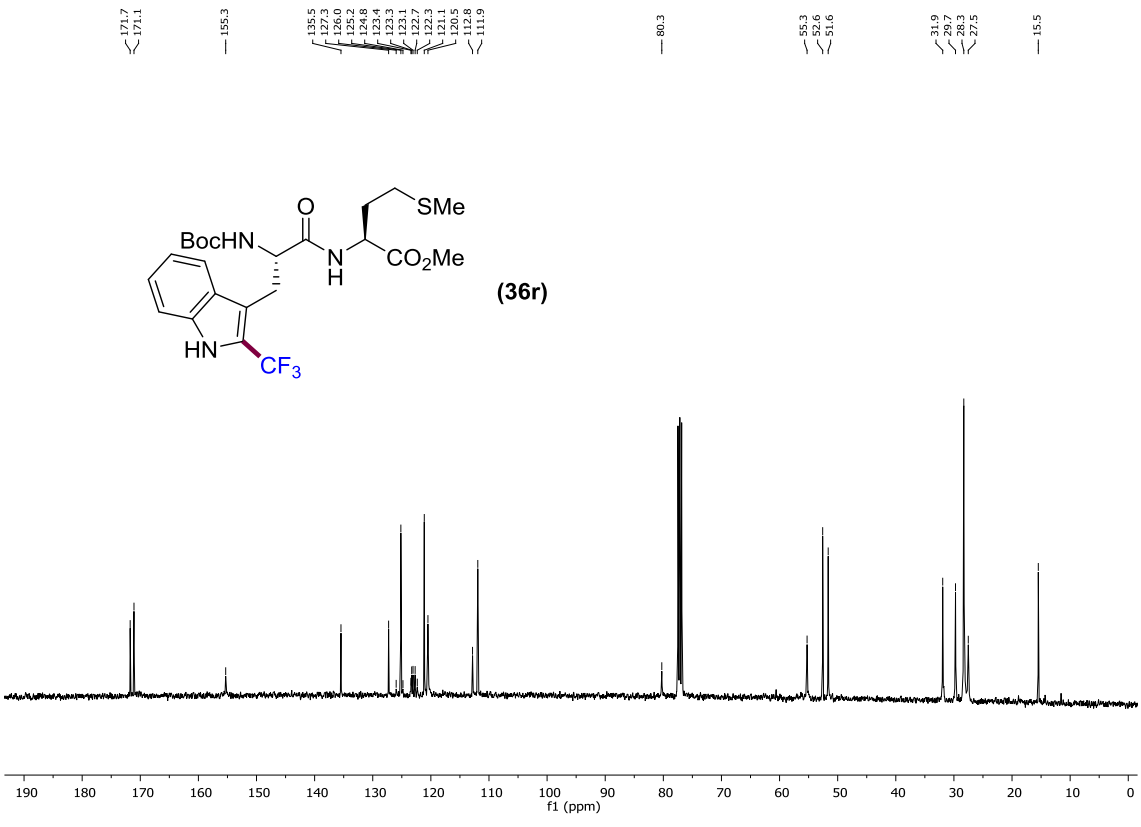
171.7
171.1
155.3
135.5
127.3
126.0
125.2
124.8
123.4
123.3
123.1
122.7
122.3
121.1
120.5
112.8
111.9
80.3
55.3
52.6
51.6
31.9
29.7
28.3
27.5
15.5
BocHN
O
N
H
SMe
CO2Me
HN
CF3
(36r)
f1 (ppm)

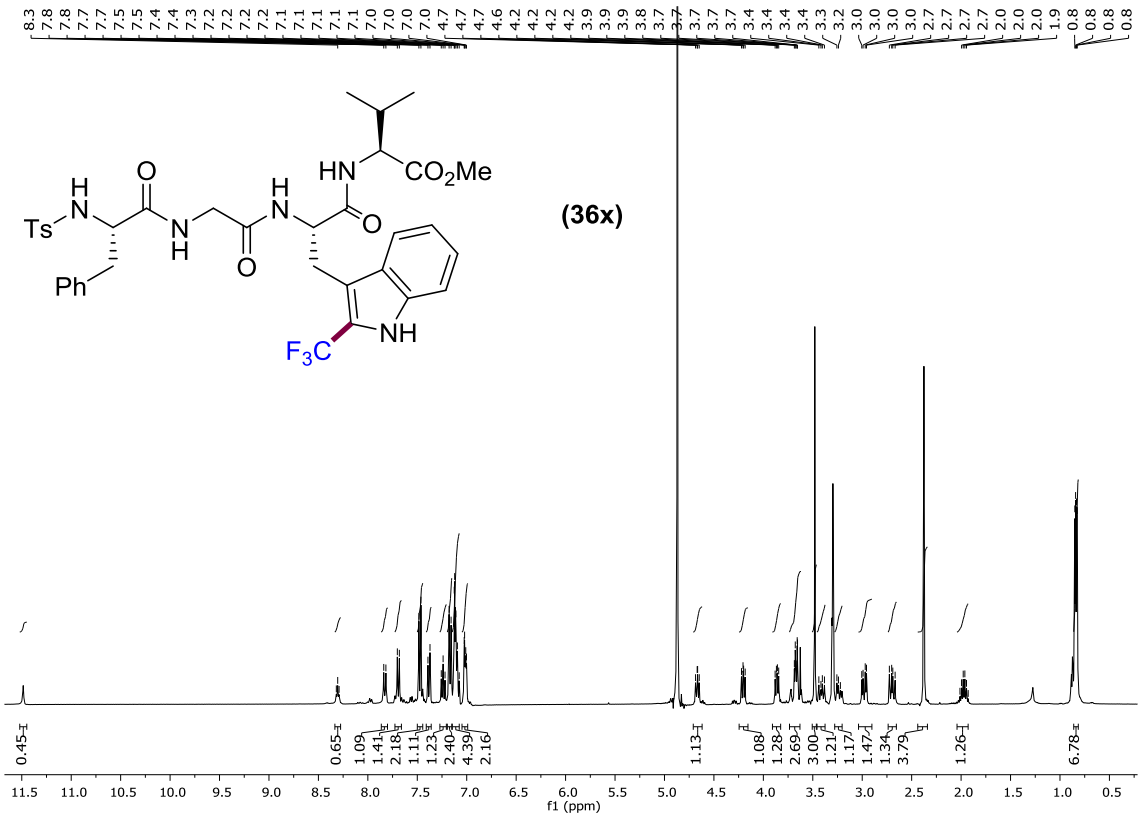
(36x)
f1 (ppm)

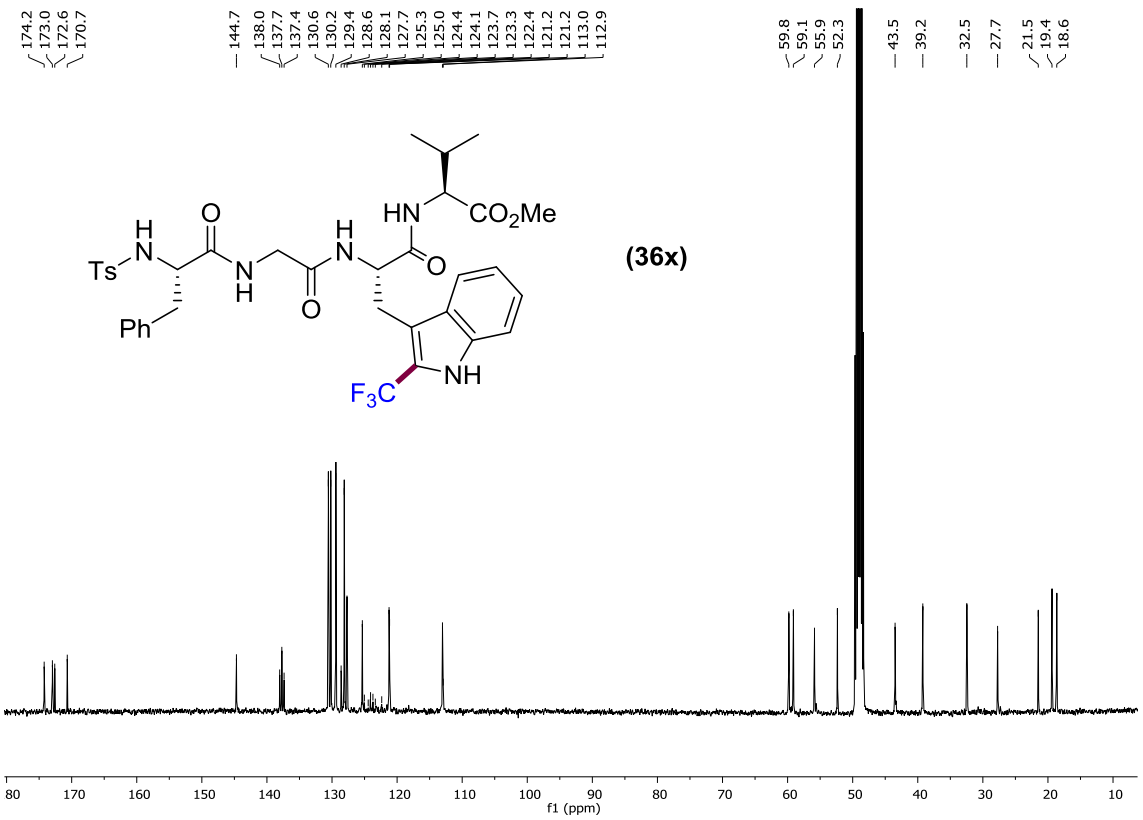
(36x)
f1 (ppm)

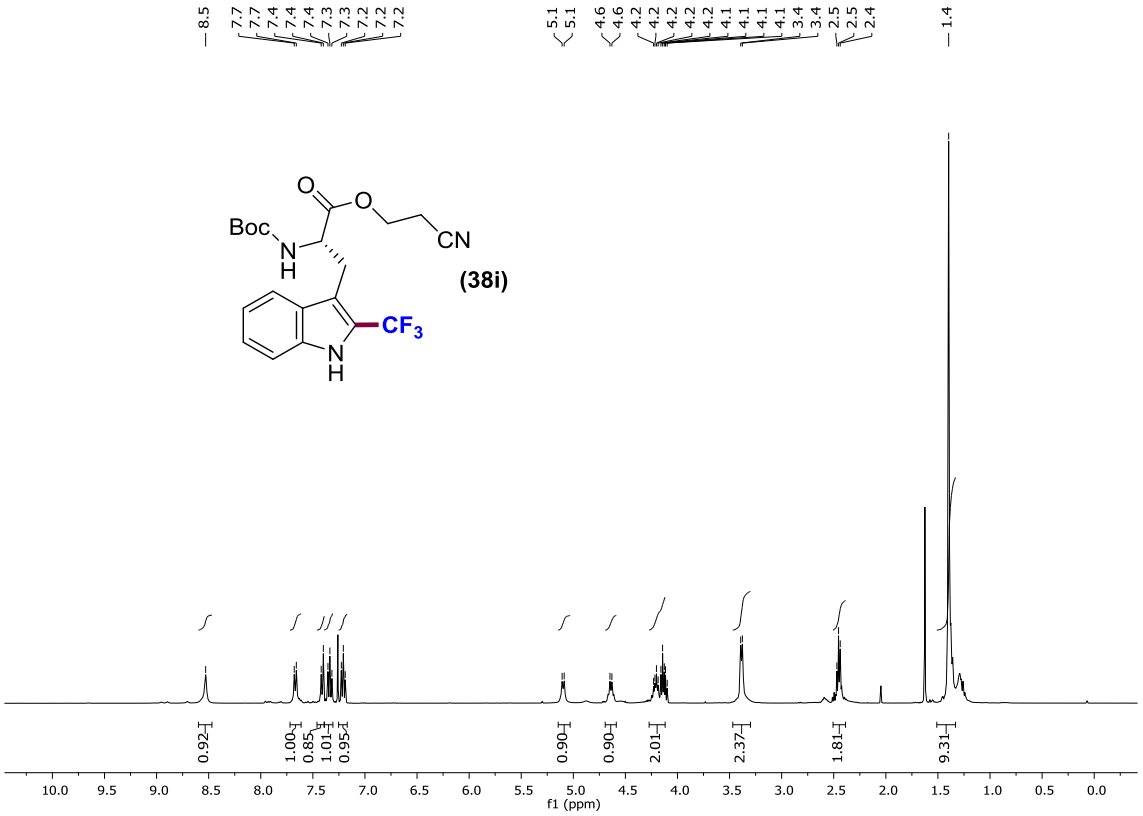
8.5
7.7
7.7
7.4
7.4
7.4
7.3
7.3
7.2
7.2
7.2
5.1
5.1
4.6
4.6
4.2
4.2
4.2
4.2
4.2
4.1
4.1
4.1
4.1
3.4
2.5
2.5
2.4
1.4
O
O
Boc
N
H
CN
(38i)
CF3
N
H
0.92
1.00
0.85
1.01
0.95
0.90
0.90
2.01
2.37
1.81
9.31
10.0
9.5
9.0
8.5
8.0
7.5
7.0
6.5
6.0
5.5
5.0
4.5
4.0
3.5
3.0
2.5
2.0
1.5
1.0
0.5
0.0
f1 (ppm)

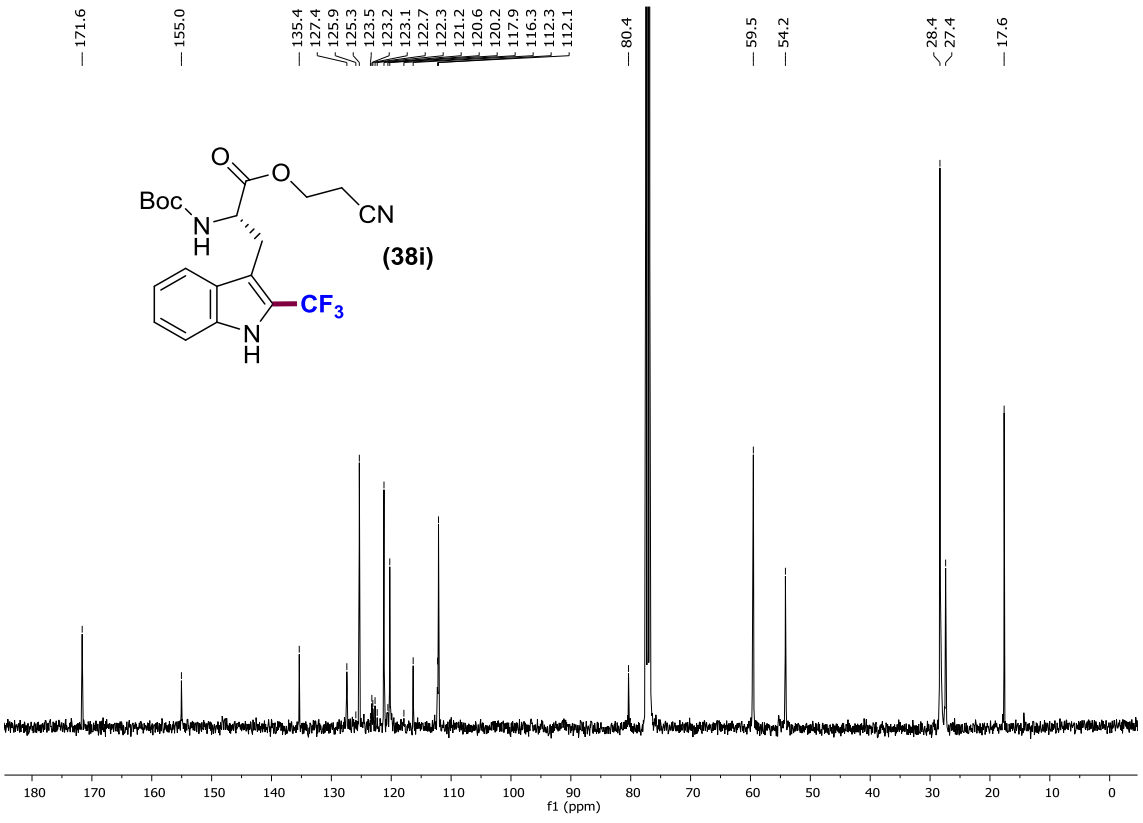
171.6
155.0
135.4
127.4
125.9
125.3
123.5
123.2
123.1
122.7
122.3
121.2
120.6
120.2
117.9
116.3
112.3
112.1
80.4
59.5
54.2
28.4
27.4
17.6
O
O
Boc
N
H
CN
(38i)
CF3
N
H
180
170
160
150
140
130
120
110
100
90
80
70
60
50
40
30
20
10
0
f1 (ppm)

Chapter 5.

Remote Ruthenium-Catalyzed C(sp^2)–H Functionalization Directed by 1,2,3-Triazoles

5.1. Introduction

5.1.1. Metal-Catalyzed C–H Functionalization Assisted by "Click" Triazoles

Thanks to their high atom-economy and sustainable character, direct C–H functionalization processes[209] have certainly changed the landscape of organic synthesis, enabling the development of unprecedented tactics through innovative bond disconnections. Because of the wide variety of C–H bonds often present in an organic molecule, a prime issue in these reactions is achieving high control over the regioselectivity. One of the most practical avenues involves the introduction of a Lewis basic functional group, commonly named a directing group (DG), which upon coordination with the metal catalyst can lower the energy barrier for the cleavage of a specific C–H bond (Scheme 97). As previously mentioned in the general introduction of this Thesis, a significant role of the DG itself in the resulting compounds is an extra bonus, which avoids additional synthetic steps for its cleavage.[210]

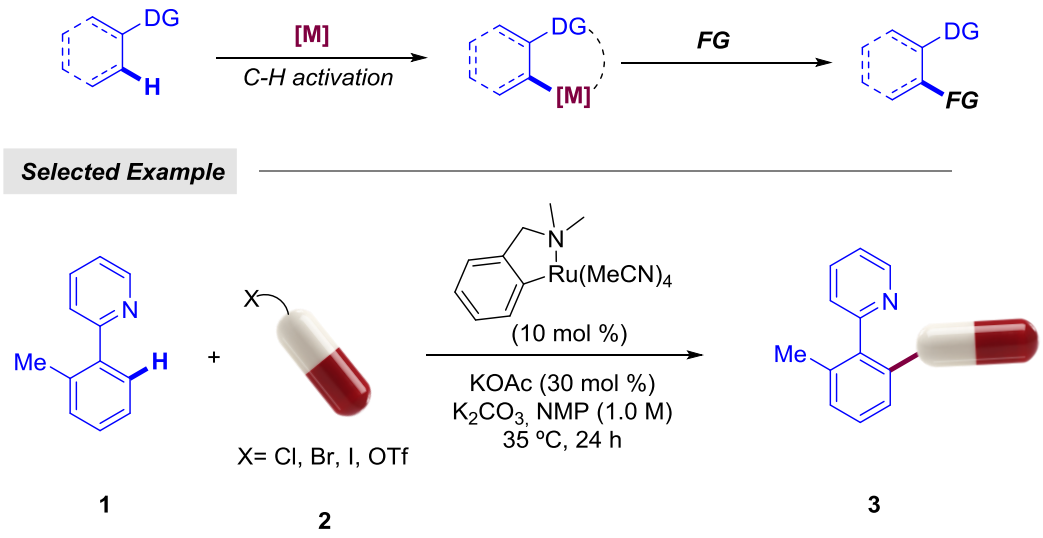

Scheme 97 Directed Metal-Catalyzed ortho-Functionalization.

In this respect, a plethora of molecules with relevant activity in medicinal chemistry or agrochemistry incorporate Lewis basic heterocycles as key frameworks[211] that exhibit inherent ability to bind with a metal catalyst. As a result, the use of *N*-containing heterocycles as efficient DGs offers new synthetic opportunities of

[209] For selected reviews, see: a) Chu, J. C. K.; Rovis, T. *Angew. Chem. Int. Ed.* **2018**, *57*, 62. b) Funes-Ardoiz, I.; Maseras, F. *ACS Catal.* **2018**, *8*, 1161. c) Yi, H.; Zhang, G.; Wang, H.; Huang, Z.; Wang, J.; Singh, A. K.; Lei, A. *Chem. Rev.* **2017**, *117*, 9016. d) He, J.; Wasa, M.; Chan, K. S. L.; Shao, Q.; Yu, J.-Q. *Chem. Rev.* **2017**, *117*, 8754. e) Hartwig, J. F.; Larsen, M. A. *ACS Cent. Sci.* **2016**, *2*, 281. f) Newhouse, T.; Baran, P. S. *Angew. Chem. Int. Ed.* **2011**, *50*, 3362.
[210] Rousseau, G.; Breit, B. *Angew. Chem. Int. Ed.* **2011**, *50*, 2450.
[211] Vitaku, E.; Smith, D. T.; Njardarson, J. T. *J. Med. Chem.* **2014**, *57*, 10257.

paramount importance such as the modification of pharmaceuticals with 2-phenyl pyridines described by Larrosa group (Scheme 97).[212]

For instance, the high hydrogen bonding capability of 1,2,3-triazoles, metabolic stability, and amide bioequivalence make it a privileged core in distinct applied areas such as crop protection, molecular biology, drug discovery, and materials sciences, despite the absence of this scaffold in nature.[213] In this regard, its unique molecular architecture is crucial in a vast array of bioactive peptidomimetics, in compounds with important biological activities, or even in powerful ligands in asymmetric catalysis. Likewise, they are highly promising moieties for supramolecular interactions (Figure 13).

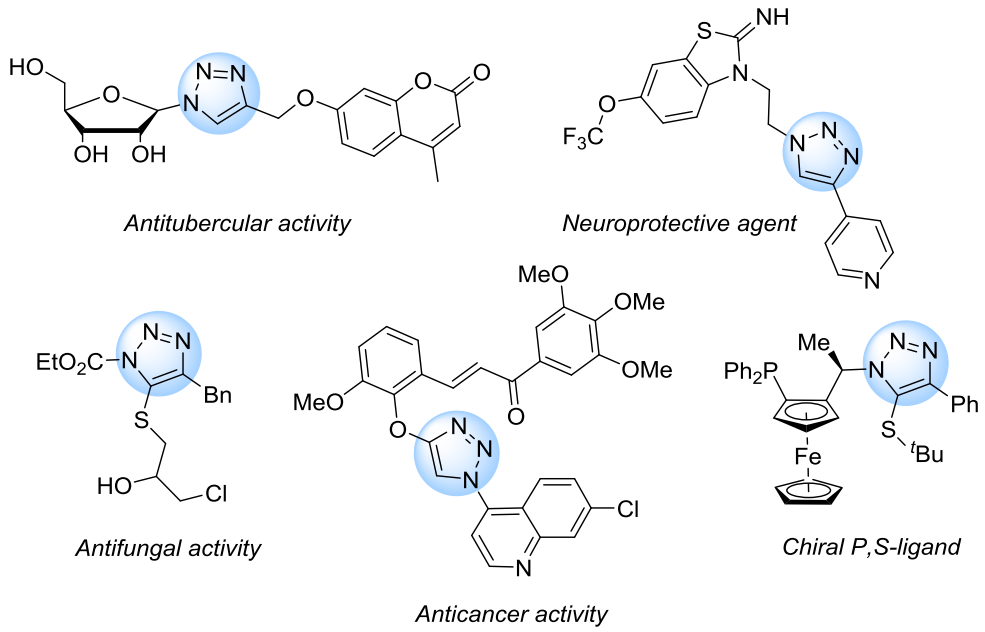

Figure 13 1,2,3-Triazole Leads in Medicinal Chemistry.

The general synthetic route for 1,2,3-triazoles is the non-catalytic Huisgen 1,3-dipolar cycloaddition, which consists in the interaction between azides and alkynes.[214] This thermal pathway leads to mixtures of 1,4- and 1,5-substituted 1,2,3-triazoles (Scheme 98). Thus, several methods have been developed to overcome the lack

[212] Simonetti, M.; Cannas, D. M.; Just-Baringo, X.; Vitorica-Yrezabal, I. J.; Larrosa, I. *Nat. Chem.* **2018**, *10*, 724.
[213] For selected reviews, see: a) Kacprzak, K.; Skiera, I.; Piasecka, M.; Paryzek, Z. *Chem. Rev.* **2016**, *116*, 5689. b) Tiwari, V. K.; Mishra, B. B.; Mishra, K. B.; Mishra, N.-I.; Singh, A. S.; Chen, X. *Chem. Rev.* **2016**, *116*, 3086. c) Thirumurugan, P.; Matosiuk, D.; Jozwiak, K. *Chem. Rev.* **2013**, *113*, 4905. d) Astruc, D.; Liang, L.; Rapakousiou, A.; Ruiz, J. *Acc. Chem. Res.* **2012**, *45*, 630.
[214] a) Breugst, M.; Reissig, H.-U. *Angew. Chem. Int. Ed.* **2020**, *59*, 12293. b) Huisgen, R.; Szeimies, G.; Mcbius, L. *Chem. Ber.* **1967**, *100*, 2494. c) Huisgen, R.; Knorr, R.; Mcbius, L.; Szeimies, G. *Chem. Ber.* **1965**, *98*, 4014.

of regioselectivity such as the use of ruthenium catalysts for the formation of the 1,5-regioisomer as the major product.[215]

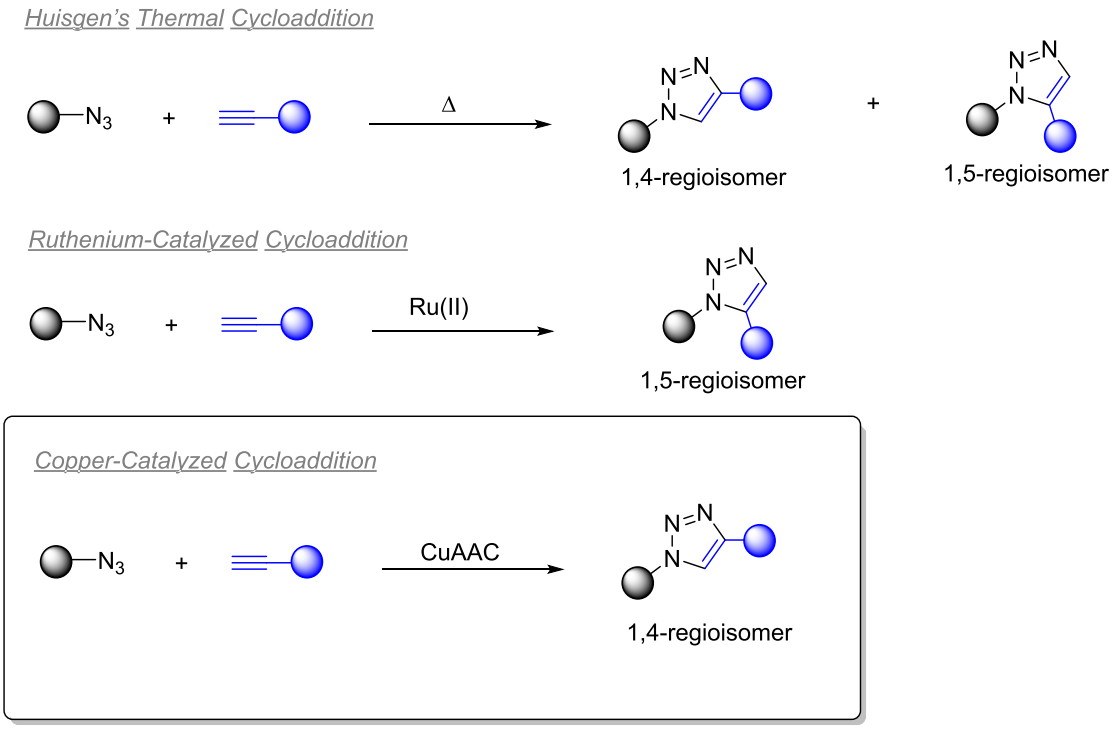

Scheme 98 Synthesis of 1,2,3-Triazoles.

On the other hand, despite the existence of different methods,[216] one of the most practical method for the assembly of 1,2,3-triazoles, often termed as "click process",[217] features a Cu-catalyzed azide–alkyne [3+2] cycloaddition (CuAAC) to deliver selectively 1,4-disubstituted triazoles.[218] Concerning the mechanism, Fokin and co-workers have lately proposed a revised reaction pathway with a dinuclear copper intermediate (**V**) based on prior literature[219] and experimental evidence (Scheme 99).[220]

[215] Johansson, J. R.; Beke-Somfai, T.; Said, S. A.; Kann, N. *Chem. Rev.* **2016**, 116, 14726.
[216] Efimov, I. V. *Chem. Heterocycl Compd.* **2019**, *55*, 28.
[217] Kolb, H. C.; Finn, M. G.; Sharpless, K. B. *Angew. Chem. Int. Ed.* **2001**, *40*, 2004.
[218] a) Tornøe, C. W.; Christensen, C.; Meldal, M. *J. Org. Chem.* **2002**, *67*, 3057. b) Rostovtsev, V. V.; Green, L. G.; Fokin, V. V.; Sharpless, K. B. *Angew. Chem. Int. Ed.* **2002**, *41*, 2596.
[219] a) Kuang, G.-C.; Guha, P. M.; Brotherton, W. S.; Simmons, J. T.; Stankee, L. A.; Nguyen, B. T.; Clark, R. J.; Zhu, L. *J. Am. Chem. Soc.* **2011**, *133*, 13984. b) Ahlquist, M.; Fokin, V. V. *Organometallics* **2007**, *26*, 4389. c) B. F. Straub, *Chem. Commun.* **2007**, 3868. d) Rodionov, V. O.; Presolski, S. I.; Díaz, D. D.; Fokin, V. V.; Finn, M. G. *J. Am. Chem. Soc.* **2007**, *129*, 12705. e) Himo, F.; Lovell, T.; Hilgraf, R.; Rostovtsev, V. V.; Noodleman, L.; Sharpless, K. B.; Fokin, V. V. *J. Am. Chem. Soc.* **2005**, *127*, 210. f) Rodionov, V. O.; Fokin, V. V.; Finn, M. G. *Angew. Chem. Int. Ed.* **2005**, *44*, 2210.
[220] Worrell, B. T.; Malik J. A.; Fokin, V. V. *Science* **2013**, *340*, 457.

The reaction begins with the coordination of the Cu(I) species to the corresponding alkyne to form intermediate **II** and lowering the energy barrier of the C–H bond of the terminal alkyne. In this way the subsequent formation of σ,π-di(copper)acetylide **III** is achieved.[221] Afterwards, the addition of the corresponding azide leads to key intermediate **V**, which undergoes reductive elimination affording **VI**. Further protonolysis delivers the desired 1,2,3-triazole compound regenerating the catalyst and closing the catalytic cycle.

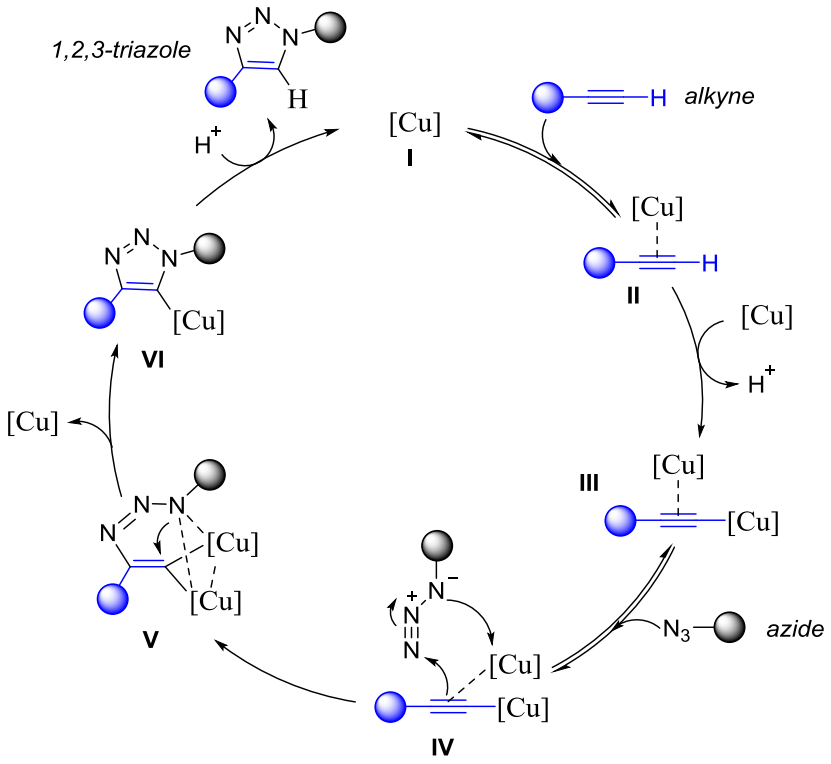

Scheme 99 Cu-catalyzed azide–alkyne [3+2] cycloaddition (CuAAC): Mechanistic Proposal.

In particular, 4-aryl 1,2,3-triazoles resulting from the atom-economical CuAAC stand out as ideal substrates for the development of new directed C–H functionalization events. These represent powerful techniques for the chemoselective late-stage derivatization of "click compounds". Our group reported a microreview that covers the literature from 2008 up to May 2018, and it highlights the latest developments in the use of both simple "click" 1,2,3-triazoles and triazole-containing amides as versatile mono- and bidentate DGs, respectively, in the field of C–H functionalization.[222] The main achievements in this area of expertise have been briefly summarized in Scheme 100 according to the nature of the bond formed in the oxidative process.

[221] Jin, L.; Tolentino, D. R.; Melaimi, M.; Bertrand, G. *Sci. Adv.* **2015**, *1*, e1500304.
[222] Guerrero, I.; Correa, A. *Eur. J. Org. Chem.* **2018**, 6034.

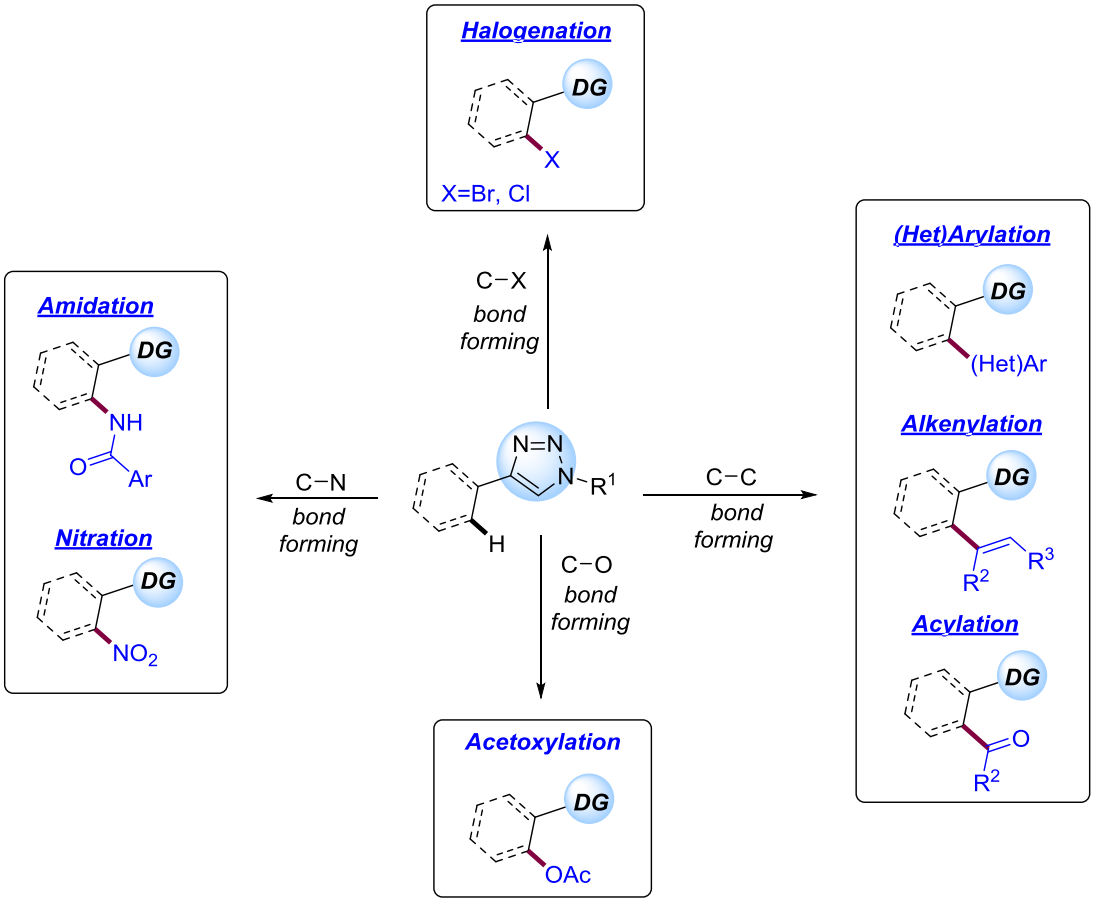

Scheme 100 "Click" & Go.

Among the C−C bond forming reactions, C−H (hetero)arylation has been the most exploited functionalization since Ackermann and co-workers observed that, unlike in previous reports, the switch of palladium or copper catalysts to ruthenium catalysis resulted in the exclusive and selective directed C−H arylation of the arene ring in 1-aryl-1,2,3-triazoles with aryl bromides (Scheme 101).[223]

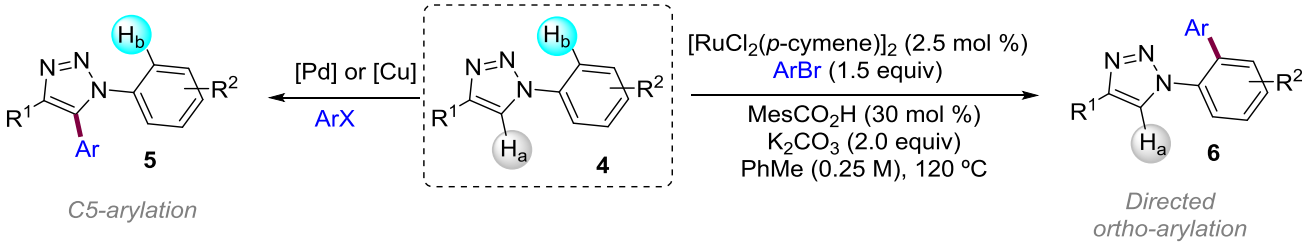

Scheme 101 Regioselectivity of Direct Arylation in 1-Aryl-1,2,3-triazoles.

[223] Ackermann, L.; Vicente, R.; Althammer, A. *Org. Lett.* **2008**, *10*, 2299.

Aryl chlorides were also found to be suitable for these types of transformations with either 1-aryl or 4-aryl-1,2,3-triazoles.[224] Moreover, the less attractive aryl iodides were utilized as aryl sources in a series of palladium-catalyzed C–H functionalization assisted by the heteroaromatic scaffold.[225] Afterwards, the interest for the use of the triazole moiety as DG enabled the introduction of different functional groups into the arene ring such as alkene and acyl groups. As an illustrative example, a Ru-catalyzed alkenylation developed by Ackermann is depicted in Scheme 102. [226] The combination of the triazole derivative and an alkene with $AgSbF_6$ and $Cu(OAc)_2 \cdot H_2O$ in toluene ensured the catalyst performance and mechanistic studies suggested a BIES as the key elemental step to provide the corresponding rutenacycle **I**. Subsequent migratory insertion with the corresponding acrylate would deliver rutenacycle **II**, which would ultimately furnish the coupling product upon β-hydride elimination. Finally, the released Ru(0) species would be then reoxidized by the copper oxidant (Scheme 102).

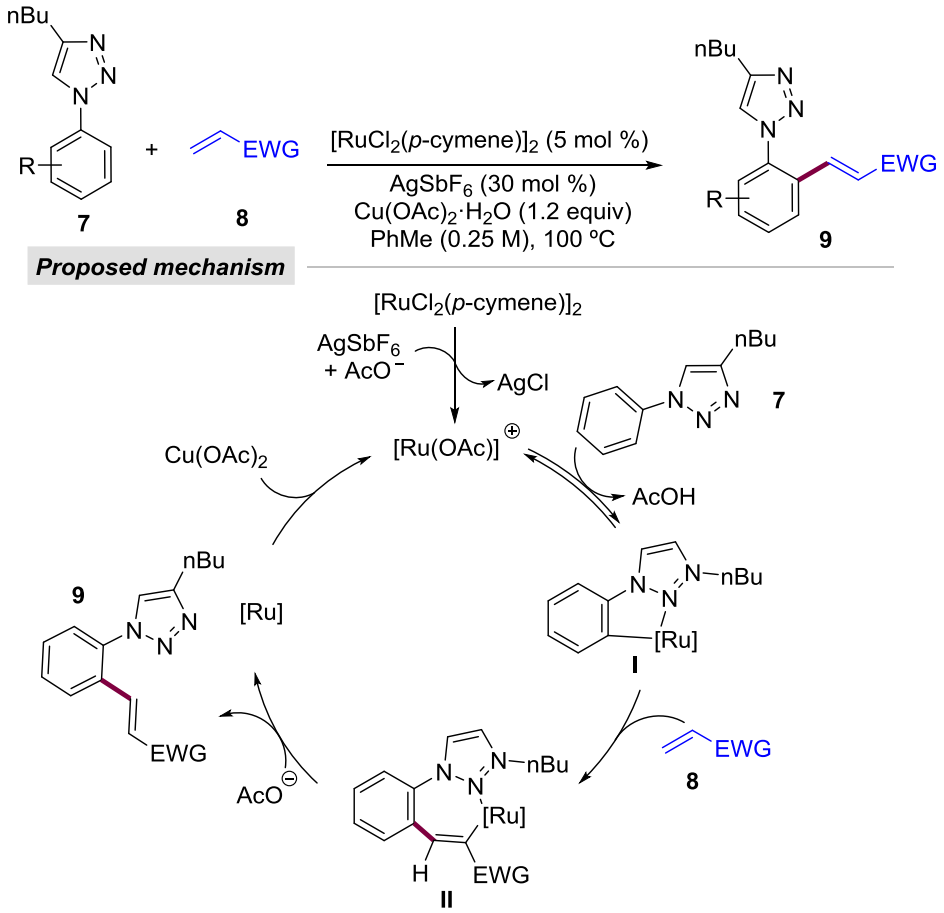

Scheme 102 Triazole-Assisted Ru-Catalyzed Alkenylation with Alkenes.

[224] a) Ackermann, L.; Novák, P.; Vicente, R.; Pirovano, V.; Potukuchi, H. K. *Synthesis* **2010**, *13*, 2245. b) Ackermann, L.; Born, R.; Vicente, R. *ChemSusChem* **2009**, *2*, 546.
[225] a) Zhao, F.; Liu, Y.; Yang, S.; Xie, K.; Jiang, Y. *Org. Chem. Front.* **2017**, *4*, 1112. b) Shi, S.; Liu, W.; He, P.; Kuang, C. *Org. Biomol. Chem.* **2014**, *12*, 3576.
[226] Tirler, C.; Ackermann, L. *Tetrahedron* **2015**, *71*, 4543.

Additionally, metal-catalyzed *ortho*-C–H functionalizations where a heteroatom-containing motif is introduced in arenes upon 1,2,3-triazole assistance have been also described. In particular, inspired by previous protocols, our group described a C(sp^2)–H oxygenation procedure featuring the use of simple "click" triazoles as monodentate DGs (Scheme 103).[227] Notably, the corresponding mono-oxygenated arenes and even alkenes were obtained with DG- and substrate-controlled selectivity. Interestingly, the particular use of 5-iodotriazoles resulted in exclusive mono-oxygenation, by a DG-controlled reaction pathway. The ample potential of the resulting 5-iodo-oxygenated compounds was illustrated by the assembly of fully decorated 1,2,3-triazoles through conventional Pd-catalyzed cross-coupling techniques. Moreover, the following year our group disclosed a Pd-catalyzed C(sp^2)–H halogenation of arenes directed by modular "click" triazoles.[228] In particular, it was found that the use of *N*-bromosuccinimide together with PivOH and $PhI(OAc)_2$ was decisive for the halogenation of "click" compounds. Control experiments and computational studies supported the intermediacy of pivaloyl hypobromite (PivOBr, formed *in situ*) as the most plausible brominating agent.

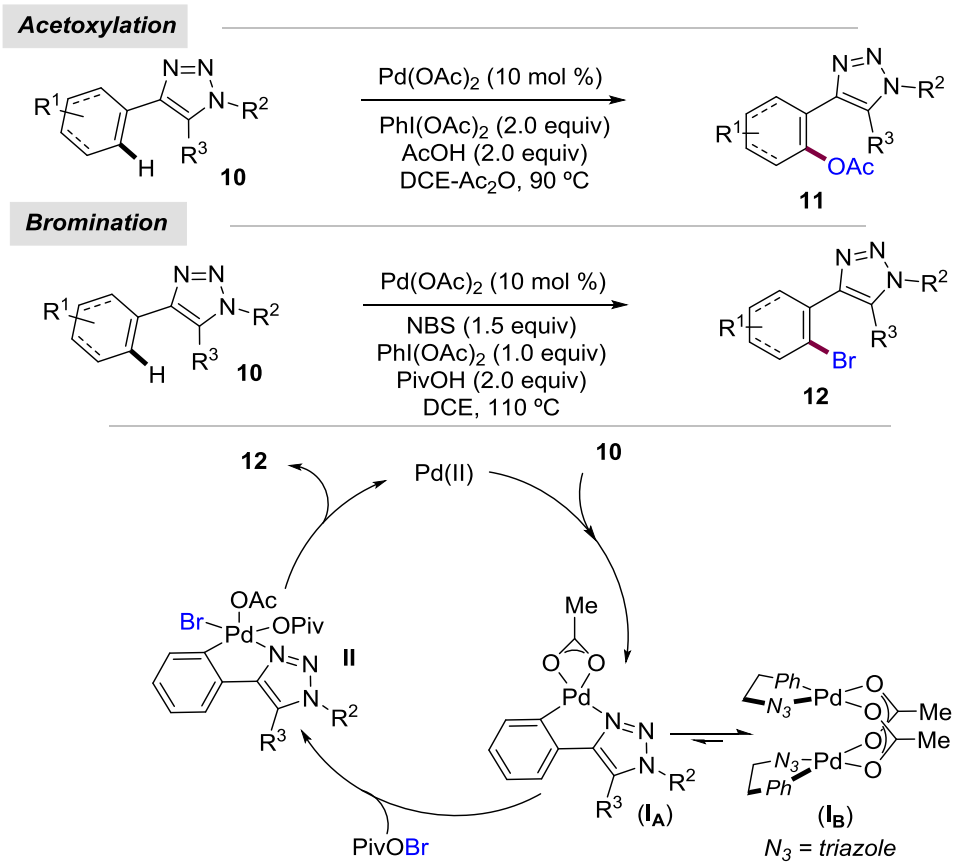

Scheme 103 4-Aryl-1,2,3-triazole C–H Acetoxylation and Bromination Reactions.

[227] Irastorza, A.; Aizpurua, J. M.; Correa, A. *Org. Lett.* **2016**, *18*, 1080.
[228] Goitia, A.; Gómez-Bengoa, E.; Correa, A. *Org. Lett.* **2017**, *19*, 962.

On the other hand, in 2016, the seminal work by Daugulis[229] and Nakamura[230] on the use of 8-aminoquinoline (AQ) motif as a powerful bidentate DG inspired Ackermann and co-workers to design a novel family of highly versatile triazole-derived amides for the efficient iron-catalyzed arylation of arenes, alkenes and even alkanes through the activation of both C(sp^3)−H and C(sp^2)−H bonds (Scheme 104).[231] Control experiments revealed the superior activity of the triazolyldimethylmethyl (TAM) group, where the acidic free NH group played a crucial role in the catalyst activation mode.

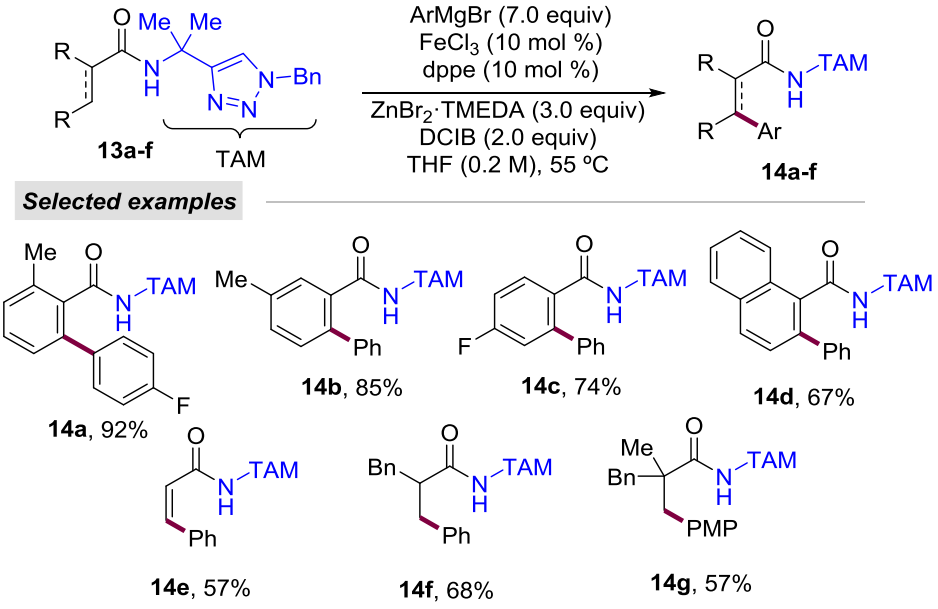

Scheme 104 Fe-Catalyzed Direct Arylation of Triazole-derived Amides.

The finding of Ackermann group set up the stage for further developments of many other methodologies featuring the employment of a bidentate "click" triazole-containing DG. Palladium and iron catalysis were mainly utilized[232] in this type of protocols based on the base-assisted cyclometallation where the nitrogen of the amide and the N1 of the triazole provided double coordination of the metal center. In this manner, functionalizations such as the installation of unsaturated moieties or simple methylation were carried out (Scheme 105). Furthermore, the robustness and versatility of the strategy was illustrated by the elegant late-stage functionalization of complex biomolecules such as peptides.[233]

[229] Tran, L. D.; Popov, I.; Daugulis, O. *J. Am. Chem. Soc.* **2012**, *134*, 18237.
[230] Shang, R.; Ilies, L.; Matsumoto, A.; Nakamura, E. *J. Am. Chem. Soc.* **2013**, *135*, 6030.
[231] Gu, Q.; Al Mamari, H. H.; Grczyk, K.; Diers, E.; Ackermann, L. *Angew. Chem. Int. Ed.* **2014**, *53*, 3868.
[232] a) Cera, G.; Haven, T.; Ackermann, L. *Chem. Eur. J.* **2017**, *23*, 3577. b) Cera, G.; Haven, T.; Ackermann, L. *Chem. Commun.* **2017**, *53*, 6460. c) Santrac, D.; Cella, S.; Wang, W.; Ackermann, L. *Eur. J. Org. Chem*. **2016**, 5429. d) Ye, X.; Xu, C.; Wotjas, L.; Akhmedov, N. G.; Chen, H.; Shi, X. *Org. Lett.* **2016**, *18*, 2970. e) Zhang, G.; Xie, X.; Zhu, J.; Li, S.; Ding, C.; Ding, P. *Org. Biomol. Chem.* **2015**, *13*, 5444. f) Ye, X.; Shi, X. *Org. Lett.* **2014**, *16*, 4448.
[233] Bauer, M.; Wang, W.; Lorion, M. M.; Dong, C.; Ackermann, L. *Angew. Chem. Int. Ed.* **2018**, *57*, 203.

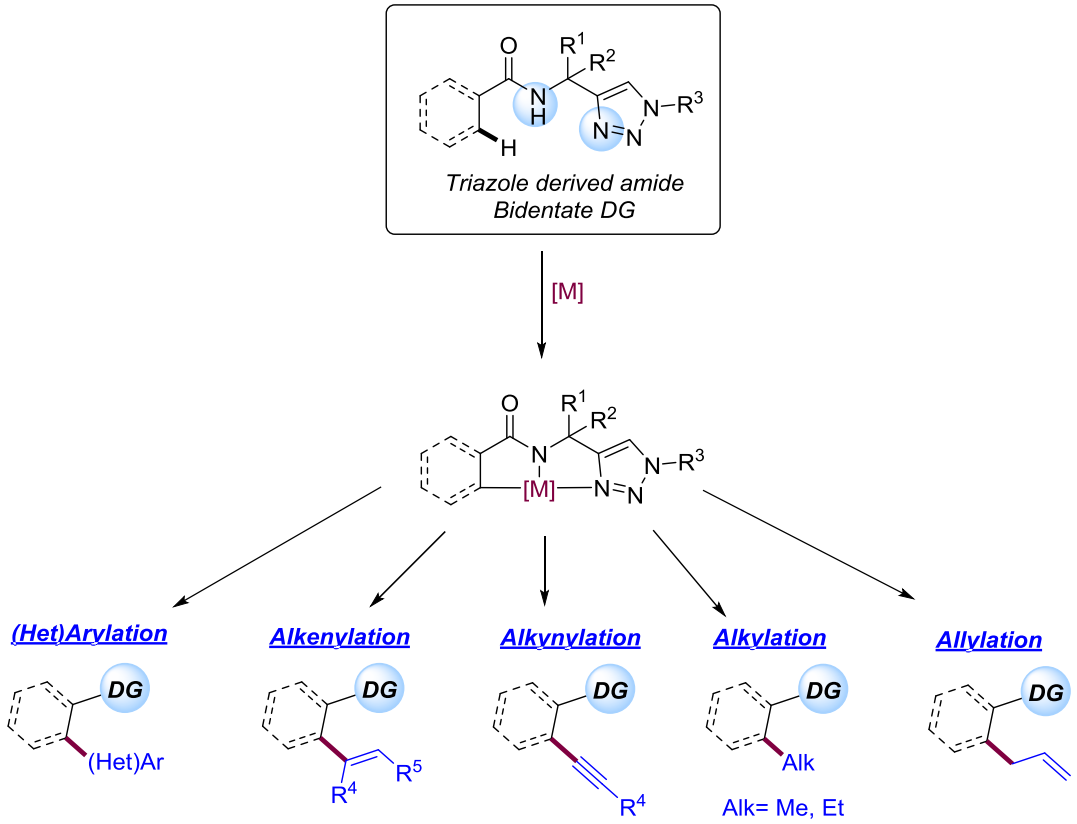

Scheme 105 Triazole Derived Amide C–H Functionalization.

Accordingly, triazole-directed C−H functionalization reactions constitute unique tools of utmost importance for the late-stage diversification of "click compounds", thus enabling the build-up of molecular diversity in a simple fashion. As described above, all the existing methodologies provide *ortho*-functionalized compounds and hence the development of more challenging *meta*- or- *para*-functionalization techniques is highly desirable and would represent an important step forward in this field of expertise.

5.1.2. Ruthenium-catalyzed σ-activation for remote meta-selective C–H functionalization

Nowadays, transition-metal-catalyzed direct C–H activation and further fuctionalization is a powerful and modern strategy, which is rarely missing in any synthesis of organic compounds. In this regard, chelation assisted *ortho*-C–H functionalization has been the most exploited one identifying a vast array of effective approaches.[234] In sharp contrast, remote *meta*- and *para*-C–H modifications still remain a challenge[235] despite the fact that site-selectivity for the assembly of fully substituted aromatic compounds is in high demand. In this context, different strategies are known to accomplish the *meta*-C–H diversification with the aid of a transition metal (Scheme 106).[236]

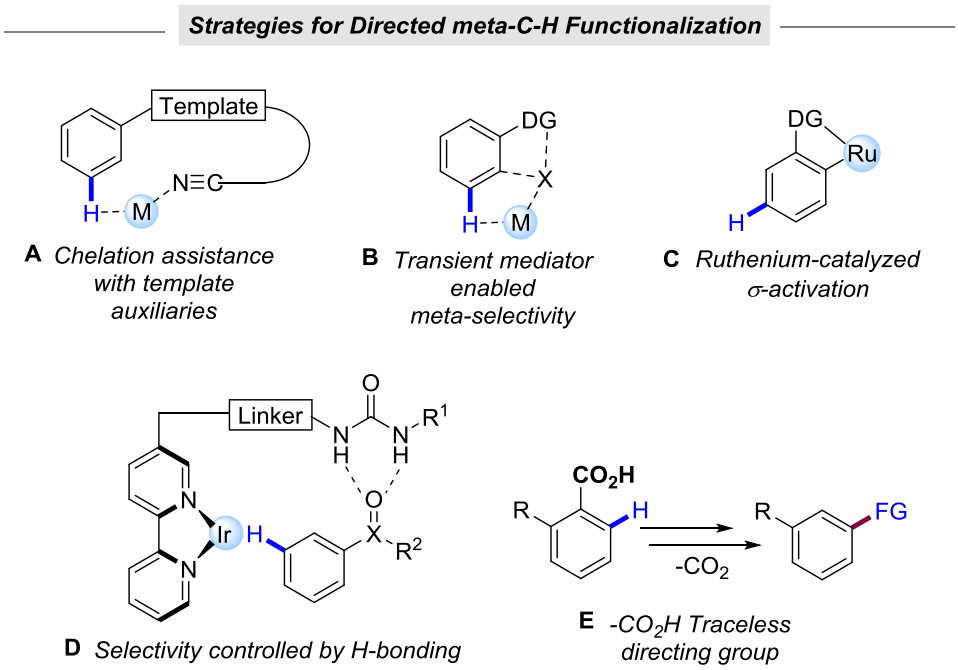

Scheme 106 Different Strategies for meta-C-H Functionalization.

Yu and co-workers were pioneers taking into account the distance and geometry to design directing templates attached to the substrate via ether for a palladium-catalyzed *meta*-alkenylation (Scheme 107).[237]

[234] Ghosh, K.; Rit, R. K.; Shankar, M.; Mukherjee, K.; Sahoo, A. K. *Chem. Rec.* **2020**, *20*, 1017.
[235] Li, J.; De Sakar, S.; Ackermann, L. *Top. Organometal. Chem.* **2016**, *55*, 217.
[236] a) Mihai, M. T.; Genov, G. R.; Phipps, R. J. *Chem. Soc. Rev.* **2018**, *47*, 149. b) Yang, J. *Org. Biomol. Chem.* **2015**, *13*, 1930.
[237] Leow, D.; Li, G.; Mei, T.-S.; Yu, J.-Q. *Nature* **2012**, *486*, 518.

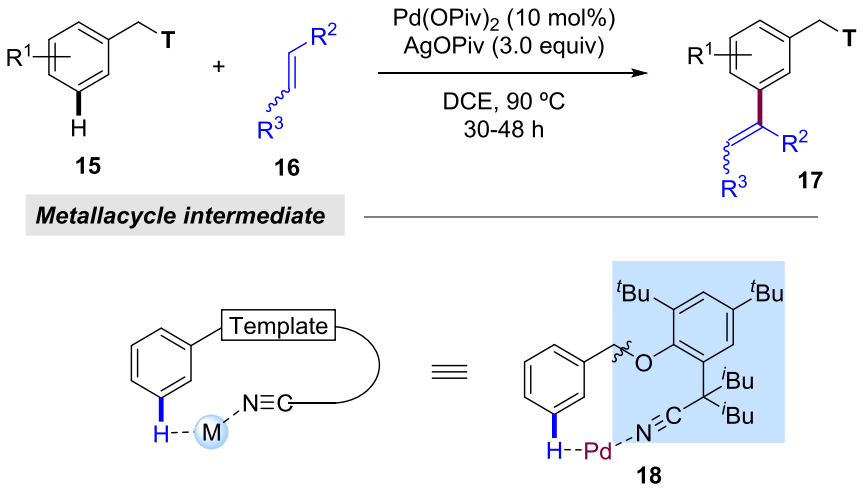

Scheme 107 Alkenylation of meta C–H Bonds Assisted by End-On Template.

This template-auxiliary approach that places the directing group proximal to the *meta*-C–H bond (Scheme 106, **A**) has given rise to the development of numerous methodologies[238] where not only ethers but also amines,[239] alcohols[240] and carboxylic acids[241] have been utilized as σ–bonding linkages.

Palladium-catalyzed DG-based reaction with transient norbornene mediator (Scheme 106, **B**),[242] also known as Catellani reaction,[243] is another recurrent strategy to decorate the *meta* position of aromatic rings.[244] The reaction pathway is depicted in Scheme 108 with the example of a *meta*-C(sp^2)–H arylation carried out by Yu's group.[245] The reaction begins with the formation of the first palladacycle **II** by the coordination of the metal catalyst with the directing group followed by the addition of norbornene transient mediator into the *ortho* position. This step relays the palladium catalyst to the closest site of the *meta* position providing palladacycle **V**. Afterwards, the oxidative addition of the aryl iodide (**VI**) and further reductive elimination results in intermediate **VII**, hence proceeding via a Pd(II)/(IV). Finally, β-carbon elimination occurs to obtain intermediate **VIII**, which undergoes a protodepalladation reaction to release the corresponding *meta*-arylated product.

[238] Dey, A.; Sinha, S. K.; Achar, T. K.; Maiti, D. *Angew. Chem. Int. Ed.* **2019**, *58*, 10820.
[239] Tang, R.-Y.; Li, G.; Yu, J.-Q. *Nature* **2014**, *507*, 215.
[240] Dai, H.; Li, G.; Zhang, X.; Stephan, A. F.; Yu, J.-Q. *J. Am. Chem. Soc.* **2013**, *135*, 7567.
[241] Deng, Y.; Yu, J.-Q. *Angew. Chem. Int. Ed.* **2015**, *54*, 888.
[242] Ye, J.; Lautens, M. *Nat. Chem.* **2015**, *7*, 863.
[243] Catellani, M.; Frignani, F.; Rangoni, A. *Angew. Chem. Int. Ed.* **1997**, *36*, 119.
[244] Yang, T.; Kong, C.; Yang, S.; Yang, Z.; Yanga, S.; Ehara, M. *Chem. Sci.* **2020**, *11*, 113.
[245] Farmer, M. E.; Wang, P.; Shi, H.; Yu, J.-Q. *ACS Catal.* **2018**, *8*, 7362.

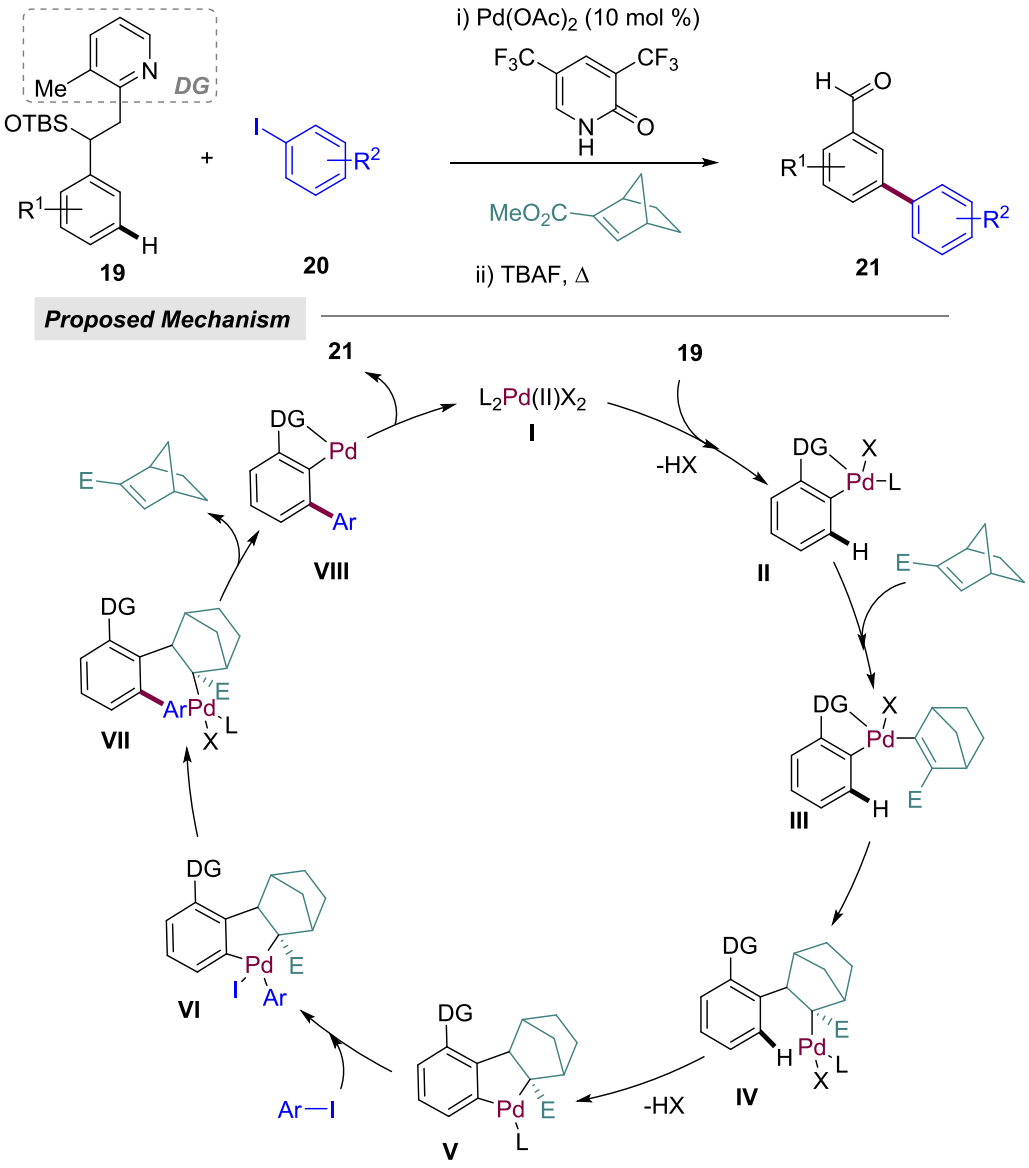

Scheme 108Palladium-Catalyzed meta-C–H Functionalization Enabled by Norbornene Transient Mediator.

Additionally, the judicious choice of hydrogen-bond-forming ligands has provided selectivity towards *meta*-C(sp^2)–H bonds (Scheme 106, **D**)[246] as well as the use of carboxylic acids as traceless directing groups (Scheme 106, **E**). The latter strategy has been well-studied by Larrosa and co-workers.[247]

[246] a) Bisht, R.; Hoque, M. E.; Chattopadhyay, B. *Angew. Chem. Int. Ed.* **2018**, *57*, 15762. b) Davis, H. J.; Phipps, R. J. *Chem. Sci.* **2017**, *8*, 864. c) Zhang, Z.; Tanaka, K.; Yu, J.-Q. *Nature* **2017**, *543*, 538. d) Hoque, M. E.; Bisht, R.; Haldar, C.; Chattopadhyay, B. *J. Am. Chem. Soc.* **2017**, *139*, 7745. e) Neel, A. J.; Hilton, M. J.; Sigman, M. S.; Toste, F. D. *Nature* **2017**, *543*, 637. f) Davis, H. J.; Genov, G. R.; Phipps, R. J. *Angew. Chem. Int. Ed.* **2017**, *56*, 13351. g) Davis, H. J.; Mihai, M. T.; Phipps, R. J. *J. Am. Chem. Soc.* **2016**, *138*, 12759. h) Kuninobu, Y.; Ida, H.; Nishi, M.; Kanai, M. *Nat. Chem.* **2015**, *7*, 712.

[247] a) Spencer, A. R. A.; Korde, R.; Font, M.; Larrosa, I. *Chem. Sci.* **2020**, *11*, 4204. b) Font, M.; Spencer, A. R. A.; Larrosa, I. *Chem. Sci.* **2018**, *9*, 7133. c) Luo, J.; Araromi, S.; Preciado, S.; Larrosa, I. *Chem. Asian J.* **2016**, *11*, 347. d) Luo, J.; Preciado, S.; Larrosa, I. *Chem. Commun.* **2015**, *51*, 3127. e) Luo, J.; Preciado, S.; Larrosa, I. *J. Am. Chem. Soc.* **2014**, *136*, 4109. f) Cornella, J.; Righi, M.; Larrosa, I. *Angew. Chem. Int. Ed.* **2011**, *50*, 9429.

Despite the widespread use of palladium catalysis for C–H bond conversions, ruthenium-catalyzed direct C–H modifications have drawn considerable attention in this field due to their remarkable behavior concerning regioselectivity, which constitutes another strategy for the *meta*- C–H functionalization through σ-activation.[248] Hence, we became interested in this type of methodologies as previous ones often exhibit shortcomings such as multistep syntheses, switch in selectivity and regioisomeric products.

In 2011, a *meta*-substituted byproduct was detected in the ruthenium-catalyzed *ortho*-C–H alkylation of ketamine derivatives reported by Ackermann and co-workers, which could be considered the first catalytic example.[249] Although the groups of Roper, Coudret and Wright had previously disclosed some *meta*-functionalization with stoichiometric ruthenium loads back in the 90's,[250] the field lay dormant until two decades later, when Frost and Ackermann reported the first catalytic reactions. The former developed a ruthenium-catalyzed *meta*-sulfonation of 2-phenylpyridine,[251] whereas the latter carried out the *meta*-alkylation with the use of secondary alkyl halides.[252] In both cases, the sole achievement of the *meta*-products were provided and they suggested that the reaction proceeded via σ-activation and S_EAr-type pathway. They proposed the depicted *ortho*-cyclometalated phenylpyridine intermediates where the crucial use of the sterically demanding 1,4,6-trimethylbenzoic acid ($MesCO_2H$) as ligand was highlighted in the alkylation reaction (Scheme 109). The regioselectivity switch toward *meta* position from palladium to ruthenium catalysis was justified with the formation of a Ru–C_{aryl} σ-bond which induces a *para*-directing effect.[250]

[248] Leitch, J. A.; Frost, C. G. *Chem. Soc. Rev.* **2017**, *46*, 7145.
[249] Ackermann, L.; Hofmann, N.; Vicente, R. *Org. Lett.* **2011**, *13*, 1875.
[250] a) Clark, G. R.; Headford, C. E. L.; Roper, W. R.; Wright, L. J.; Yap, V. P. D. *Inorg. Chim. Acta* **1994**, *220*, 261. b) Coudret, C.; Frayase, S.; Launay, J.-P. *Chem. Commun.* **199**8, 663. c) Clark, A. M.; Richard, C. E. F.; Roper, W. R.; Wright, L. J. *Organometallics* **1999**, *18*, 2813.
[251] Saidi, O.; Maragie, J.; Ledger, A. E. W.; Liu, P. M.; Mahon, M. F.; Kocick-Kohn, G.; Whitetlesey, M. K.; Frost, C. G. *J. Am. Chem. Soc.* **2011**, *133*, 19298.
[252] Hofmann, N.; Ackermann, L. *J. Am. Chem. Soc.* **2013**, *135*, 5877.

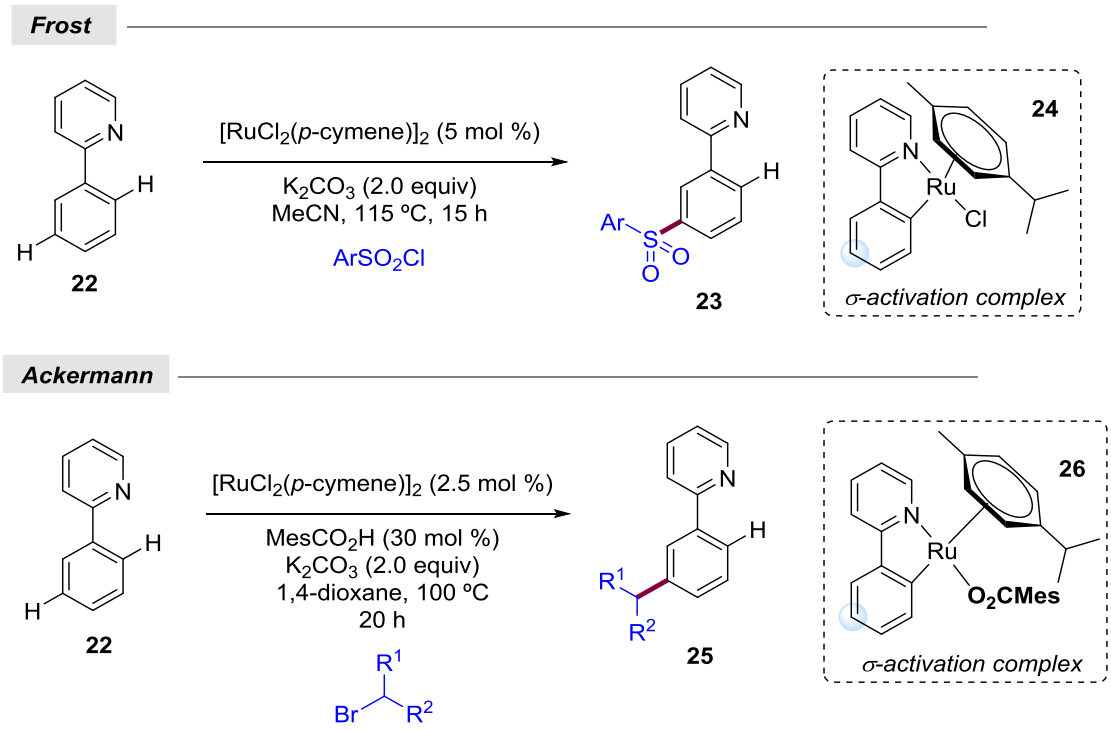

Scheme 109 First Ruthenium-Catalyzed meta-C(sp^2)–H Functionalizations.

Later in 2015, both groups simultaneously described the ruthenium-catalyzed *meta*-alkylation, this time with the use of tertiary alkyl halides.[253] Interestingly, the two new reports suggested the dual role of the metal catalyst, which enabled a radical mechanism rather than the previously proposed S_EAr. This statement was concluded by the inhibition of the reaction in the presence of radical traps and the isolation and characterization of polymeric side products carried out by Frost when tertiary α-bromo ester was used (Scheme 110). Accordingly, a distinct mechanism featuring a radical scenario was reasonably proposed. .

[253] a) Paterson, A. J.; John-Campbell, S.; Mahon, M. F.; Press N. J.; Frost, C. G. *Chem. Commun*. **2015**, *51*, 12807. b) Li, J.; Warratz, S.; Zell, D.; De Sarkar, S.; Ishikawa E. E.; Ackermann, L. *J. Am. Chem. Soc.* **2015**, *137*, 13894.

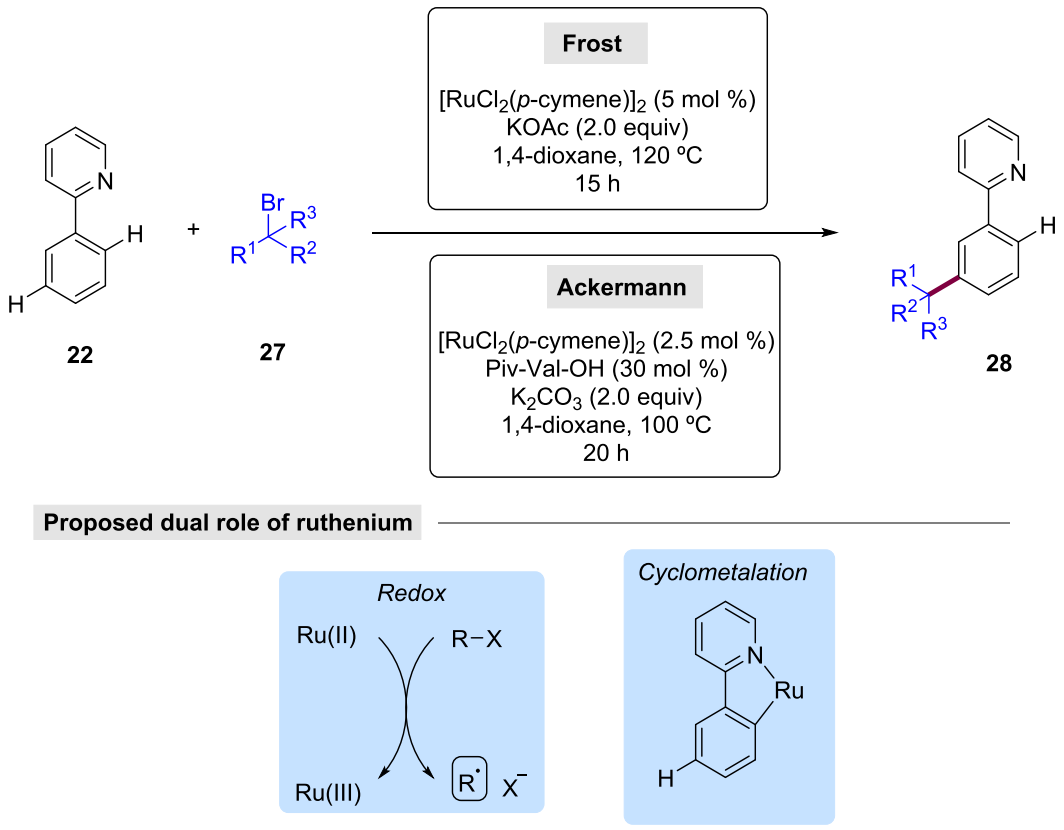

Scheme 110 Ruthenium-Catalyzed Meta-Alkylation of 2-Phenylpyridines with Tertiary Alkyl Halides.

At this point, an explanation of the mechanistic proposal could be convenient before going on with further functionalization examples based on this tactic. Owing to the lack of understanding of the achieved selectivity and deficient studies in the literature, Chen and Zhang decided to perform some DFT studies of the Ru-catalyzed *meta*-alkylation reaction with *tert*-butyl bromide to obtain more inputs about a plausible mechanism (Scheme 111).[254] Regarding regioselectivity, the alkylation step was recognized as the selectivity-determing step. Thus, the nature of the ruthenacycle **II** played a crucial role since both 2-pyridine and ruthenium atom are electron-donating and direct to *ortho*/*para* positions. It must be noted out that some groups have suggested that two C–H activations occur resulting in the formation of a bipyridyl complex, which in those cases its isolation and full characterization was achieved.[255] In this manner, DFT studies revealed that among the four possible attacks of *tert*-butyl carbonium to the different existing reaction sites (C1, C2, C3 and C4), the transition state corresponding to the attack on C3 is the most favorable one whereas C1 and C4 are the less active reaction sites due to steric repulsion. These results were verified by natural bond orbital (NBO) charge population analyses[256] and experimental evidences. Nevertheless, while secondary alkyl bromides seemed to follow the same reactivity pattern, the less bulky primary ones provided the *ortho*-substituted product corresponding to the attack in C4.

[254] Zhang, L.; Yu, L.; Zhou, J.; Chen, Y. *Eur. J. Org. Chem.* **2018**, 5268.
[255] a) Li, G.; Li, D.; Zhang, J.; Shi D.-Q.; Zhao, Y. *ACS Catal.* **2017**, *7*, 4138. b) Fan, Z.; Ni J.; Zhang, A. *J. Am. Chem. Soc.* **2016**, *138*, 8470. c) Yu, Q.; Hu, L.; Wang, Y.; Zheng, S.; Huang, J. *Angew. Chem. Int. Ed.* **2015**, *54*, 15284.
[256] Foster, J. P.; Weinhold, F. *J. Am. Chem. Soc.* **1980**, *102*, 7211.

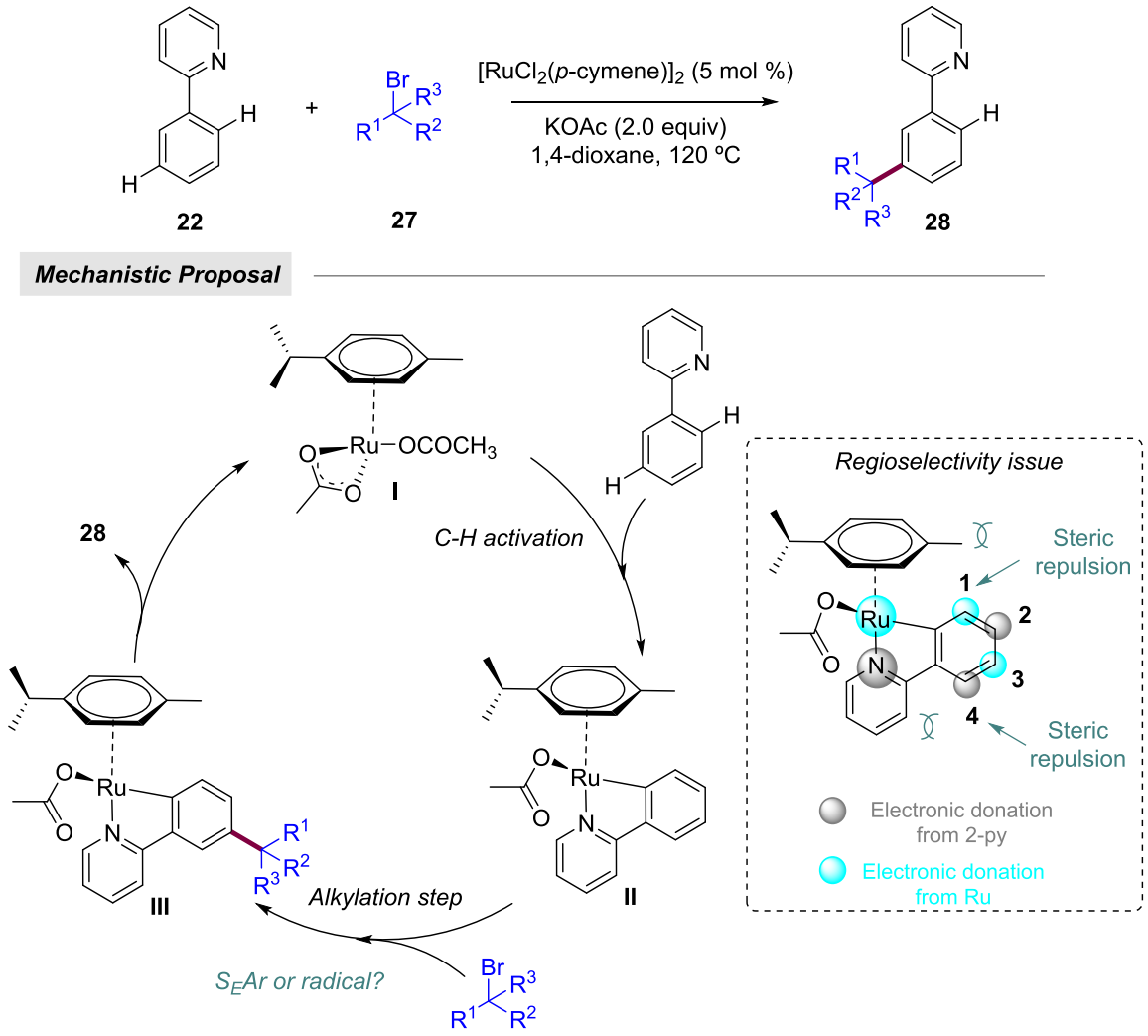

Scheme 111 Proposed Catalytic Cycle of Meta-alkylation of 2-Phenylpyridine.

Furthermore, the nature of the alkylating reagents not only could dictate the selectivity pattern but they also turned out to be decisive for the reaction mechanism. On the one hand, calculations revealed that an electrophilic aromatic substitution was more favorable to occur utilizing simple alkyl bromides. On the other hand, an alkylating reagent bearing an electron-withdrawing carbonyl group such as tertiary α-bromo ester can stabilize a radical center by conjugation but it can not do the same with a cationic center, thus favoring the radical reaction pathway, which verified the results observed by Frost.[253a] In this way, it was shown that the reactivity does not depend in a single parameter but in the reagents nature instead, and that the reaction conditions could influence and signify a change in selectivity. Likewise, 2-phenylpyridine has been a key substrate to explore deeper other

ruthenium-catalyzed *meta*-C(sp^2)–H functionalization processes such as bromination,[257a,b] nitration[257c] or sulfonylation[257d] and among the most recent advances[258] the use of photoredox stands out as a novelty in this field.[258a,b] Although pyridine is an excellent DG and its presence in a wide variety of relevant organic compounds makes it unique, its cleavage and limited scope constitute a major issue. Hence, 2-phenylpyridine directed σ-activation-based transformations brought about the expansion of this technique to other substrates bearing cleavable and versatile directing groups, which most of them have been summed up and collected in recent reviews.[236, 248]

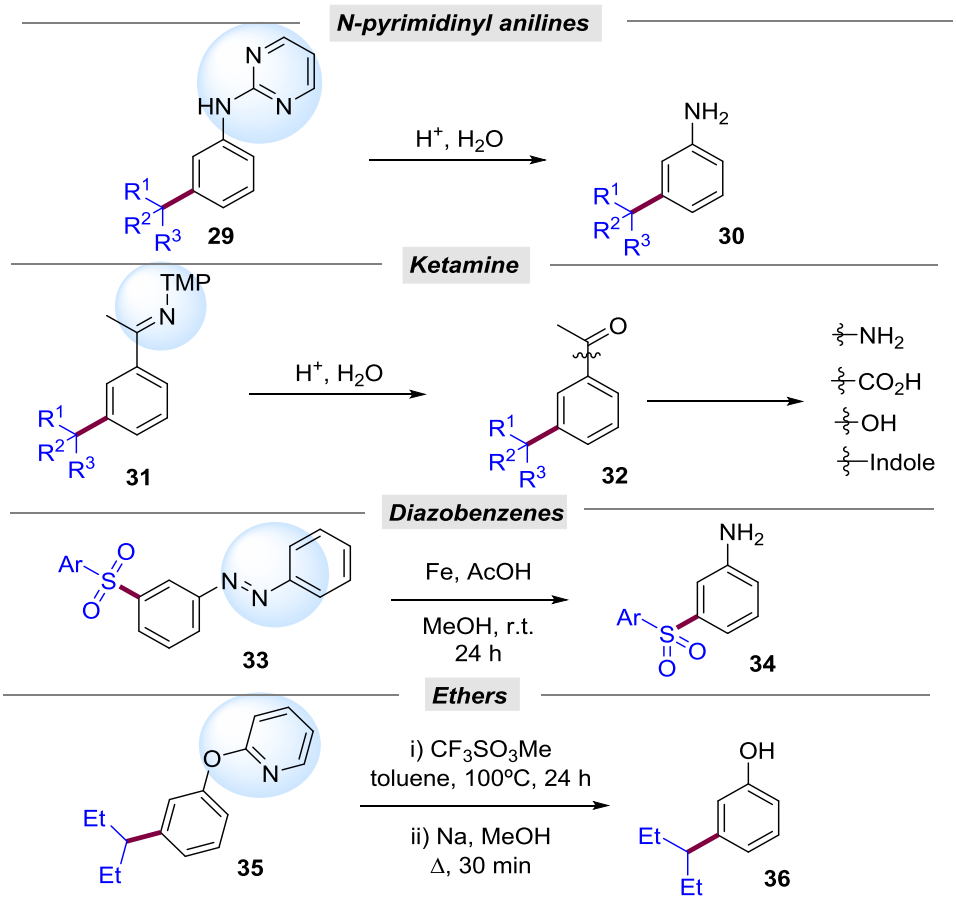

Scheme 112 Ru-Catalyzed meta-C–H Functionalization Assisted by Different Directing Groups.

For instance, some of the prior established methodologies for *meta*-functionalization reactions turned out to be suitable for substrates like *N*-pyrimidinyl anilines, ketamine, diazobenzenes or pyridyl ethers as directing

[257] a) Teskey, C. J.; Lui A. Y. W.; Greaney, M. F. *Angew. Chem. Int. Ed.* **2015**, *54*, 11677. b) Yu, Q.; Hu, L.; Wang, Y.; Zheng S.; Huang, J. *Angew. Chem. Int. Ed.* **2015**, *54*, 15284. c) Fan, Z.; Ni J.; Zhang, A. *J. Am. Chem. Soc.* **2016**, *138*, 8470. d) Marcé, P.; Paterson, A. J.; Mahon M. F.; Frost, C. G. *Catal. Sci. Technol.* **2016**, *6*, 7068.

[258] a) Gandeepan, P.; Koeller, J.; Korvorapun, K.; Mohr, J.; Ackermann, L. *Angew. Chem. Int. Ed.* **2019**, *58*, 9820. b) Sagadevan A.; Greaney, M. F. *Angew. Chem. Int. Ed.* **2019**, *58*, 9826. c) Wang, X.-G.; Li,Y.; Liu, H.-C.; Zhang, B.-S.; Gou, X.-Y.; Wang, Q.; Ma, J.-W.; Liang, Y.-M. *J. Am. Chem. Soc.* **2019**, *141*, 13914.

groups. After the transformation, the latter could be converted into the corresponding phenols or anilines demonstrating the paramount importance of the chosen DG for post-synthetic modifications (Scheme 112).

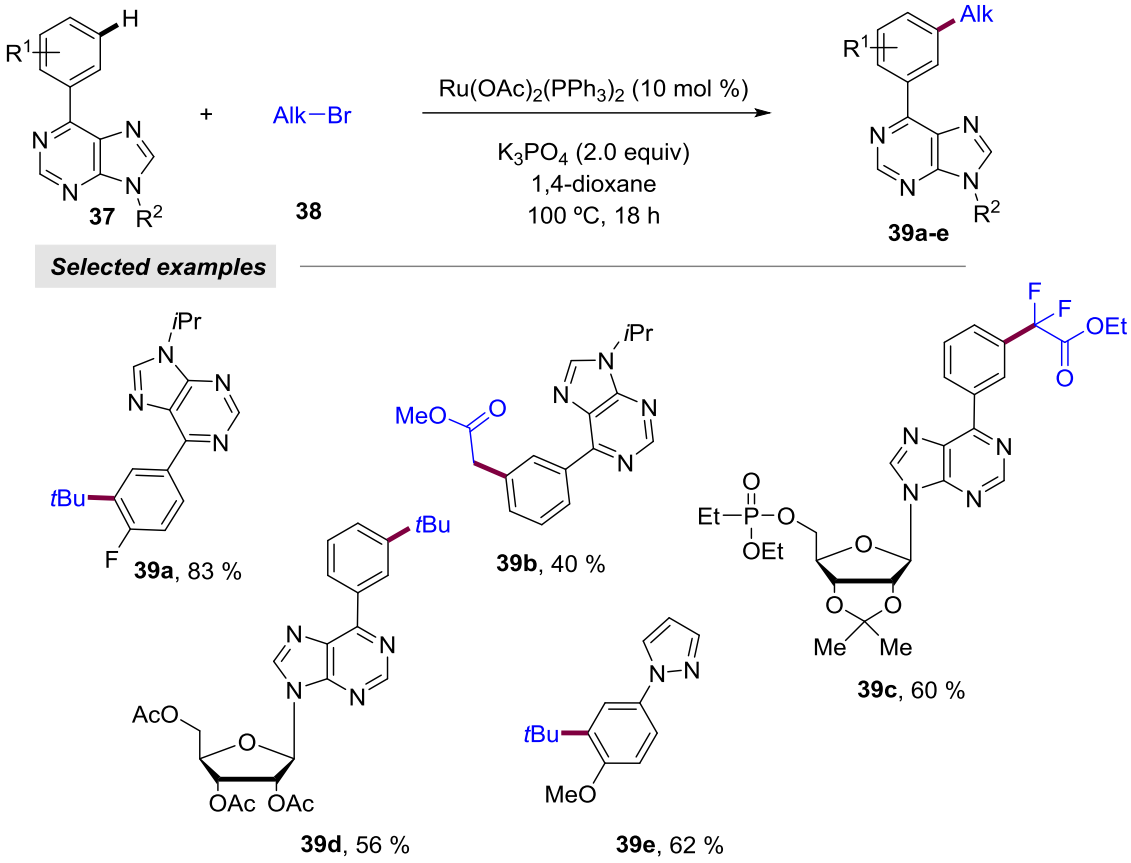

Scheme 113 Arene-Ligand-Free Ruthenium(II/III) Manifold for meta-C–H Alkylation of Purine Derivatives.

In a more recent report, Ackermann and co-workers utilized purine derivatives for a ruthenium-catalzyed *meta*-alkylation.[259] Conversely, the cleavage of the DG might not be required if its presence is pivotal for the further applications of the modified molecules as it is in this case where the purine scaffold constitutes the main part of the biologically important nucleosides. A combination of experimental evidence and DFT studies made possible the development of the first *meta*-modification with an arene-ligand-free ruthenium catalyst, where a ruthenium (II/III) manifold was suggested. The robustness of the methodology was proved by the late-stage transformation of complex nucleosides and the use of tertiary, secondary and even primary alkyl halides. Concerning the active arene-ligand-free $Ru(OAc)_2(PPh_3)_2$ catalyst, this year another mechanistic study performed by the same group[260] has revealed the crucial role of carboxylate-phosphine ligands in the stabilization of ruthenacycle complexes

[259] Fumagalli, F.; Warratz, S.; Zhang, S.-K.; Rogge, T.; Zhu, C.; Steckl, A. C.; Ackermann, L. *Chem. Eur. J.* **2018**, *24*, 3984.
[260] Korvorapun, K.; Kuniyil, R.; Ackermann, L. *ACS Catal.* **2020**, *10*, 435.

which was also observed in earlier reports.[261] Hence, the acquired knowledge and advances in this area have provided uniquely effective protocols able to perform the selective *meta*-functionalization of biorelevant compounds such as purine and urine nucleobases, lipids and amino acids and peptides.

[261] a) Ruan, Z.; Zhang, S.-K.; Zhu, C.; Ruth, P. N.; Stalke, D.; Ackermann, L. *Angew. Chem. Int. Ed.* **2017**, *56*, 2045. b) Li, G.; Li, D.; Zhang, J.; Shi, D.-Q.; Zhao, Y. *ACS Catal.* **2017**, *7*, 4138. c) Li, Z.-Y.; Li, L.; Li, Q.-L.; Jing, K.; Xu, H.; Wang, G.-W. *Chem. Eur. J.* **2017**, *23*, 3285.

5.2. Objective

"Click" triazoles have emerged as efficient directing groups owing to their practical synthesis and their ability to bind with a metal-catalyst, which offers new synthetic opportunities among C–H functionalization. Despite the advances realized, several challenges need to be addressed to render triazole-directed procedures the method of choice for the construction of those compounds in industrial environments. In this respect, while the modification of the *ortho*-C(sp^2)−H bond has been widely explored, protocols involving this *N*-containing heterocycle as DG for *meta*- functionalization remain elusive.

On the other side, ruthenium-catalyzed *meta*- C–H functionalization through σ-activation has gained a particular interest in organic synthesis. The latter represents an alternative strategy for the diversification of arene rings, avoiding tedious prefunctionalizations for the installation of templates into the substrates or the low selectivity exhibited by other tactics.

In this chapter, we will describe the preliminary results dealing with the development of a remote ruthenium-catalyzed C(sp^2)–H sulfonylation directed by 1,2,3-triazole derivatives (Scheme 114).

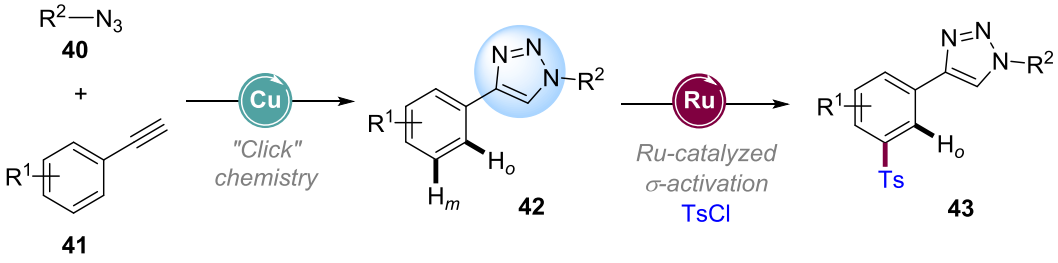

Scheme 114 Ruthenium-Catalyzed meta-C(sp^2)–H Functionalization Directed by 1,2,3-Triazole Derivatives.

5.3. Ruthenium-Catalyzed *meta*-C(sp^2)–H Tosylation Directed by 1,2,3-Triazoles

In the following section, the optimization of an unprecedented *meta*-C(sp^2)–H functionalization directed by 1,2,3-triazole is described based on a σ-activation event through ruthenium catalysis. Concerning different functionalizations, sulfonylation reaction grabbed our attention as it has been comparatively less explored. After the first catalytic *meta*-sulfonylation of 2-phenylpyridines reported by Frost and co-workers,[251] either diazobenzenes or pyridine attached to a phenol have been utilized as substrates in this remote modification strategy through ruthenium catalysis by Li and co-workers (Scheme 115).[262] Controversially, the former was suggested to proceed via S_EAr, whereas a radical pathway was proposed for the latter reaction since the use of TEMPO as a radical trap inhibited the reaction. On the other side, the synthesis of the complex-type A and its further addition into the optimal reaction conditions led to the formation of the *meta* modified product in both cases, thus it was not discarded as a possible metallacycle intermediate.

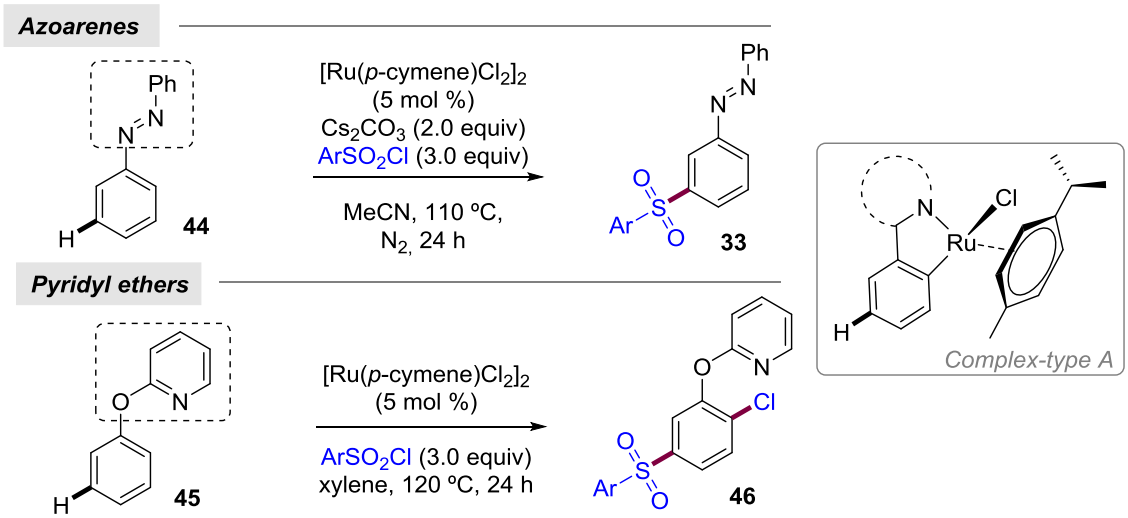

Scheme 115 Ruthenium-Catalyzed meta-Sulfonylation Directed by Azoarenes and Pyridyl Ethers.

Nevertheless, the mechanistic study of *meta*-sulfonylation of 2-phenylpyridines carried out by Frost and co-workers[257d] a year earlier enabled the isolation and characterization of rutenacycle **I** and **II** as the most probable intermediates (Scheme 116). Thus, the study revealed that *p*-cymene ligand is not essential for this reaction, which is also suggested to proceed through radical intermediates based on control experiments and previous reports.[252,253]

[262] a) Li, G.; Lv, X.; Guo, K.; Wang, Y.; Yang, S.; Yu, L.; Yu, Y.; Wang, J. *Org. Chem. Front.* **2017**, *4*, 1145. b) Li, G.; Zhu, B.; Ma, X.; Jia, C.; Lv, X.; Wang, J.; Zhao, F.; Lv, Y.; Yang, S. *Org. Lett.* **2017**, *19*, 5166.

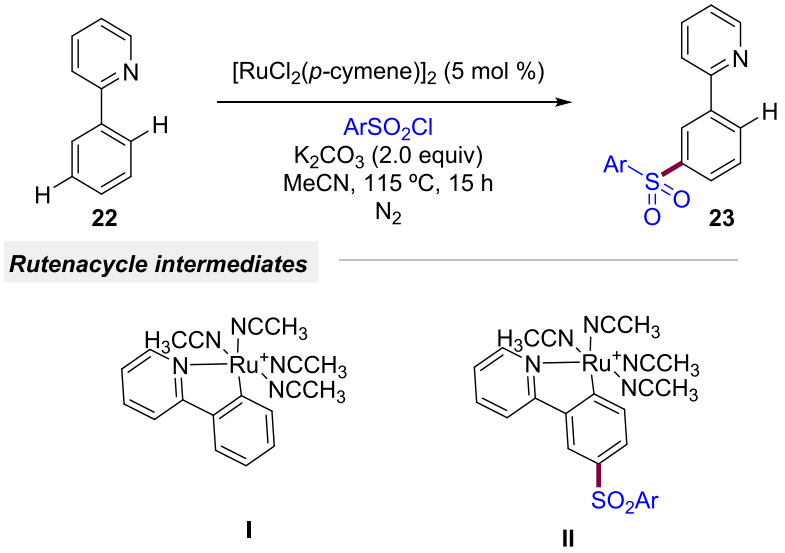

Scheme 116 Ruthenacycle Intermediates of the meta-Sulfonylation of 2-Phenylpyridines.

5.3.1. Optimization of Reaction Conditions

Accordingly, we initiated our study selecting 1-benzyl-4-phenyl-1*H*-1,2,3-triazole **42a** as the model substrate for the optimization of the *meta*-C(sp^2)–H sulfonylation reaction conditions, which was easily synthesized in a two-step process from the commercially available benzyl bromide and sodium azide. The latter reagents were mixed in a DMSO solution at room temperature to obtain the corresponding benzyl azide. This azide was later on submitted without further purification to a CuAAc "Click" reaction with phenylacetylene delivering the 1,4-substituted **42a** triazole (Scheme 117).

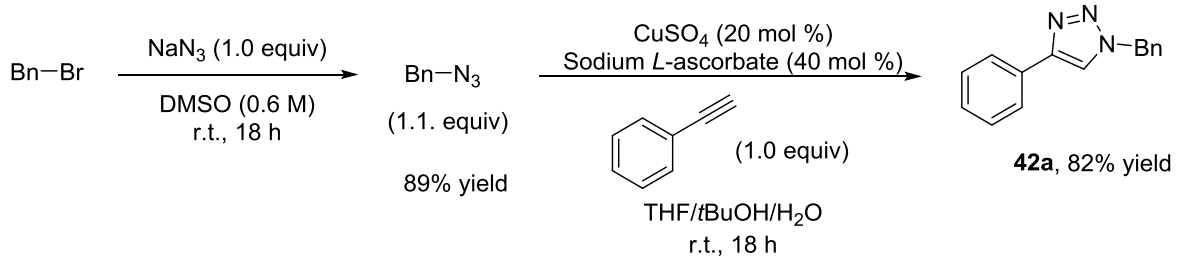

*Scheme 117 Synthesis of **42a**.*

With the model substrate in hand, a thoughtful screening process of the different reaction parameters was carried out. Nevertheless, only the most relevant results obtained so far have been commented below since the optimization of the reaction conditions is still in progress in order to reach better yields.

Owing to its widespread use in previous reports, [Ru(*p*-cymene)Cl_2]$_2$ was selected as the metal catalyst for the *meta*-C(sp^2)–H sulfonylation of **42a**. Pleasingly, the combination of *p*-toluenesulfonyl chloride, $AgSbF_6$, K_2CO_3 and Cu(OAc) in 1,4-dioxane at 130 ºC provided as a sole product **43a** in 20 % yield (Table 26, entry 1), which indicated that the 1,2,3-triazole could be used too in these remote functionalizations. Remarkably, the observed low reactivity in the absence of K_2CO_3 suggested that a base is required for the activation/deprotonation step (Table 26, entry 2). Moreover, the addition of silver(I) salts together with copper salts is known to enhance the reactivity of the ruthenium catalyst through ligand exchange.[209b] Hence, we observed that both reagents seemed to have a positive effect on the *meta*-sulfonylation reaction (Table 26, entry 3). Afterwards, a screening of copper salts revealed that the switch from Cu(OAc) to CuCl could provide a 30 % yield of the desired product (Table 26, entry 6). Besides CuCl, $CuBr_2$ and CuBr also led to the formation of **43a**, albeit in lower yields (Table 26, entry 4, 5).

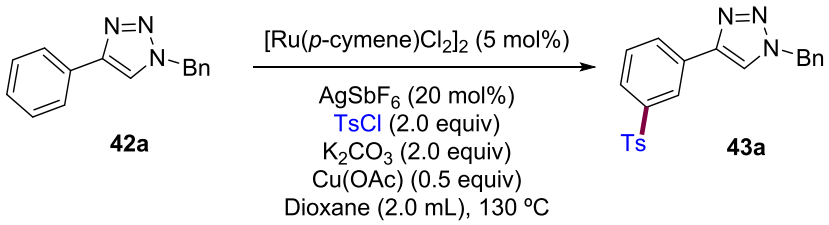

Entry	Change from standard conditions	Yield (%)[b]
1	none	20
2	No base	traces
3	No Ag(I), no Cu(I)	traces
4	$CuBr_2$ instead of Cu(OAc)	20
5	CuBr instead of Cu(OAc)	26
6	CuCl instead of Cu(OAc)	30
7	CuCl, no Ag(I)	29
8	CuCl (1.0 equiv), no Ag(I)	32

[a] Reaction conditions: **42a** (0.25 mmol), [Ru(*p*-cymene)Cl_2]$_2$ (5 mol %), TsCl (0.5 mmol), Cu(I) salt (0.5 equiv), $AgSbF_6$ (20 mol %), 1,4-dioxane (2.0 mL), Ar, 24h. [b] Isolated yield after column chromatography.

Table 26 Screening of Copper Salts.[a]

Interestingly, blank experiments shown that the addition of 50 mol % of CuCl without a silver salt was enough to obtain 30 % yield of the sulfonylated product (Table 26, entry 9). Subsequently, screening of bases, solvents and metal catalysts were carried out (Table 27). Concerning the tested inorganic bases, K_2PO_4 and K_2HPO_4 provided the best results with 25% and 27 % yields, respectively. Surprisingly, some of the commonly utilized bases and solvents by previous reports, such as cesium carbonate and toluene, exhibited low reactivity and the yields were not even determined (Table 27, entry 4, 5, 6). Additionally, and in sharp contrast to the methodology described by Frost,[257d] the use of acetronitrile as solvent did not lead to the formation of **43a** discarding in this case the previously proposed active ruthenacycle intermediates (Scheme 116). On the other hand, halogenated solvents like dichloroethane and trifluorotoluene resulted in similar yields to that obtained with dioxane (Table 27, entry 7, 9). However, the latters were avoided owing to sustainability issues.

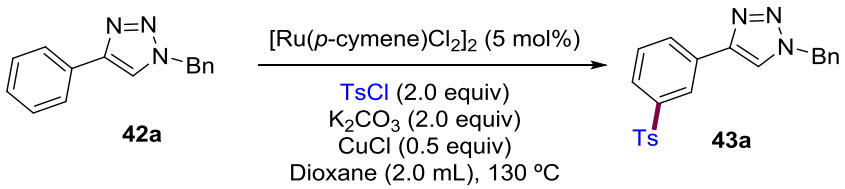

Entry	Change from standard conditions	Yield (%)[b]
1	none	30
2	K_2PO_4 as base	25
3	K_2HPO_4 as base	27
4	Cs_2CO_3 as base	n.d.
5	MeCN as solvent	n.d.
6	Toluene as solvent	n.d.
7	DCE as solvent	30
8	NMP as solvent	n.r.
9	CF_3Ph as solvent	27
10	$RuCl_2(PPh_3)_3$ as catalyst	n.d.
11	$Ru(OAc)_2(PPh_3)_2$ as catalyst	traces
12	140 ºC	29
13	Under air	traces

[a] Reaction conditions: **42a** (0.25 mmol), Ru-catalyst (5 mol %), TsCl (0.5 mmol), solvent (2.0 mL), Ar, 24h. [b] Isolated yield after column chromatography.

Table 27 Changes from the Standard Reaction Conditions.[a]

Other Ru sources showed inferior activity in the sulfonylation (Table 27, entry 10-11). Concerning to the reaction temperature, up to 100 ºC is commoly required for this type of transformations. However, when we raised the temperature to 140-150 ºC no improvement was observed in the substrate conversion (Table 27, entry 12). Furthermore, the performance of the process under inert atmosphere resulted essential for the formation of **43a** (Table 27, entry 13).

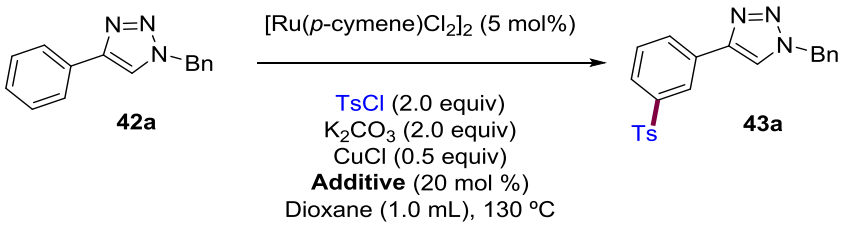

Entry	Additive	Yield (%)[b]
1	none	30
2	PPh_3	traces
3	XPhos	traces
4	^{t}BuXPhos	n.d.
5	Dppf	n.d.
6	$PCy_3 \cdot HBF_4$	n.d.
7	1,3-diisopropylimidazolium chloride	11
8	1,3-bis(2,4,6-trimethylphenyl)imidazolium chloride	31
9	Norbornene	19
10	*N*-Ac-Phe-OH	n.r.
11	*N*-Ac-Val-OH	n.d.
12	*N*-Ac-Ala-OH	n.d.
13	*N*-Ac-Gly-OH	n.d.
14	Ad-CO_2H	20
15	PivOH	n.d.
16	Picolinic acid	n.d.

[a] Reaction conditions: **42a** (0.25 mmol), [Ru(*p*-cymene)Cl_2]$_2$ (5 mol %), TsCl (0.5 mmol), CuCl (0.5 equiv), 1,4-dioxane (2.0 mL), Ar, 24h. [b] Isolated yield after column chromatography.

Table 28 Screening of Additives.[a]

At this point, we decided to investigate the influence of a vast array of commonly used additives in order to improve the formation of product **43a** (Table 28). In this manner, chelating ligands such as phosphines,

imidazolium salts and protected amino acids were added to the reaction mixture aiming to form a catalyst with higher activity. Unfortunately, only traces of the desired product were obtain with phosphines (Table 28, entry 2, 3), whereas similar or lower yields were determined with the use of carbenes (Table 28, entry 7, 8). Curiously, protected amino acids and carboxylic acid additives, which had a crucial role in prior transformations through ruthenium catalysis, resulted either in the decrease of the yield (Table 28, entry 9-13) or in the inhibition of the reaction (Table 28, entry 10).

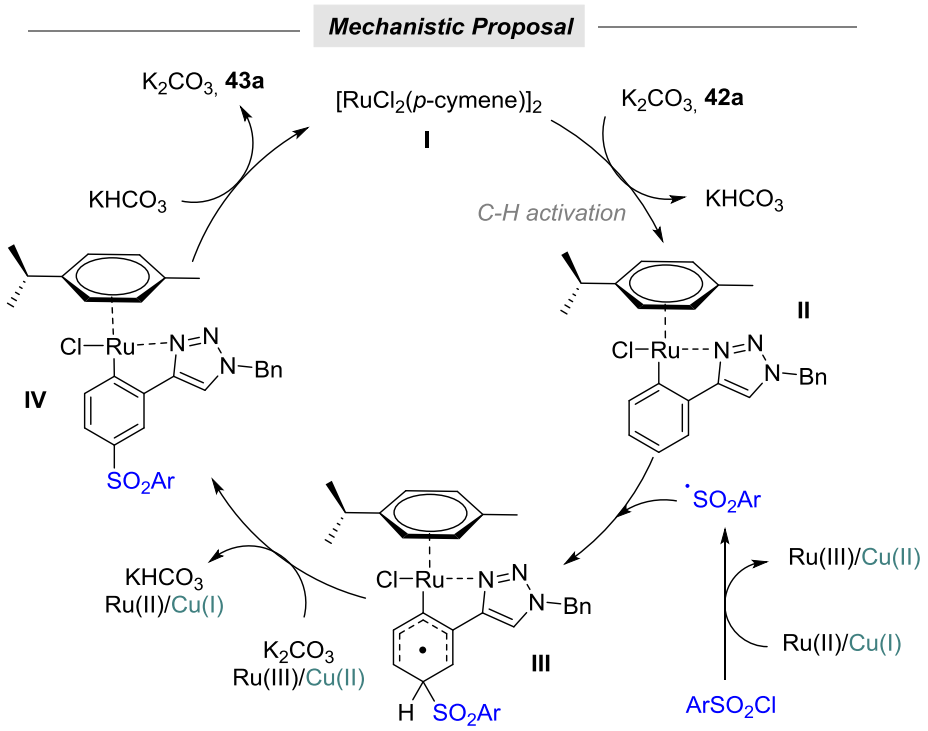

Scheme 118 Proposed Mechanism for the 1,2,3-Triazole-directed meta-Sulfonylation.

Although the reaction has not yet been optimized, on the basis of the obtained results and prior reported works,[257d] we suggested a mechanistic proposal (Scheme 118). The reaction begins with the activation of the *ortho*-C(sp^2)–H bond promoted by the Ru(II) catalyst and potassium carbonate providing the formation of ruthenacycle **II**. Then, the latter Ru-complex undergoes a radical addition of tosyl chloride at the *para* position, which is the most reactive site due to σ-activation. On the other hand, it is believed that tosyl radical can be generated by a redox process either by a Ru(II)/Ru(III) or Cu(I)/Cu(II) system. The latter would justify the better yields observed with the use of CuCl. Likewise, the same redox reaction leads to the formation of complex **IV**. Finally, the protonation/demetallation step provides the desired *meta*-modified product **43a**.

Due to the difficulties we faced in increasing reaction yields during this particular sulfonylation, we tried to expand our studies towards other ruthenium-catalyzed *meta* transformations simultaneously. In particular, the triazole assisted alkylation of *meta* position was studied with ethyl bromopropionate (Scheme 119).

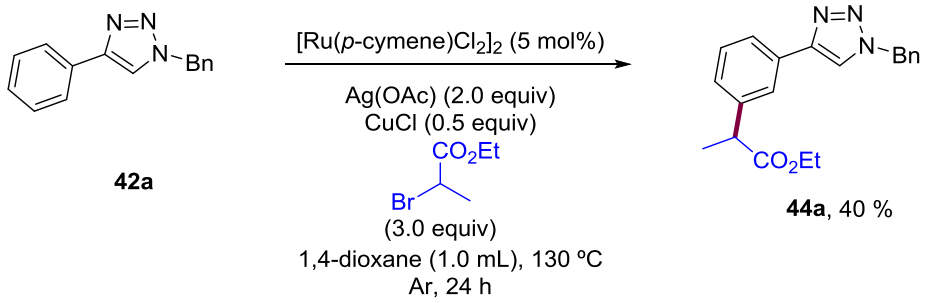

Scheme 119 Ruthenium-Catalyzed meta-alkylation Assisted by 1,2,3-Triazole.

After a screening process similar to that of *meta*-sulfonylation reaction, the coupling between triazole **42a** and ethyl bromopropionate with the use of silver acetate (2.0 equiv), copper chloride (0.5 equiv) in 1,4-dioxane at 130 ºC led to the formation of **44a** in 40 % yield.

The experiments described in this chapter supported the viability of using 1,2,3-triazoles as alternative DGs in Ru-catalyzed *meta*-functionalization processes. However, these early promising results clearly indicate that a careful screening process must be conducted to obtain the target products in synthetically useful yields and further studies are already in progress in our research group.

5.4. Conclusion

To sum up, 1,2,3-triazoles stand out not only as privileged heterocyclic scaffolds due to their ubiquity in drug discovery and their practical assembly upon “Click” chemistry, but also owing to their important role as effective DGs in *ortho* C–H functionalizations. In this light, we took a step forward and demonstrated that they could also enable the transformation of a more challenging *meta* position in an arene ring through ruthenium catalysis. In particular, triazole-directed *meta*-C(sp^2)–H sulfonylation and alkylation reactions provided promising results through the Ru-catalyzed σ-activation strategyand evidenced the feasibility of our approach.

5.5. Experimental Procedures

5.5.1. Ru-Catalyzed C(sp^2)–H Sulfonylation Directed by 1,2,3-Triazoles

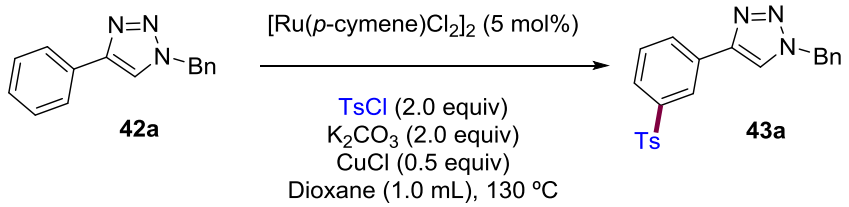

General Procedure for 43a: A reaction tube containing a stirring bar was charged with the corresponding 1-benzyl-4-phenyl-1*H*-1,2,3-triazole **42a** (0.25 mmol, 1.0 equiv), *p*-toluenesulfonyl chloride (0.5 mmol, 2.0 equiv), copper(I) chloride (0.125 mmol, 0.5 equiv), potassium carbonate (0.5 mmol, 2.0 equiv) and [Ru(*p*-cymene)Cl_2]$_2$ (5 mol %). The reaction tube was then evacuated and back-filled with dry argon (this sequence was repeated up to three times). Then, 1,4-dioxane (1.0 mL) was added and the reaction tube was next warmed up to 130 ºC and stirred for 24 hours. The mixture was then allowed to warm to room temperature, concentrated under reduced pressure and purified by flash chromatography (hexanes/AcOEt 1/1) to provide the corresponding product **43a** 30 % yield as a white solid. ^{1}H NMR (400 MHz, $CDCl_3$) δ 8.28 (s, 1H), 8.10 (d, *J* = 7.8 Hz, 1H), 7.86 (t, *J* = 7.5 Hz, 3H), 7.82 (s, 1H), 7.56 (dd, *J* = 8.1, 6.3 Hz, 3H), 7.31 (d, *J* = 8.2 Hz, 3H), 7.22 (d, *J* = 8.3 Hz, 2H), 5.56 (s, 2H), 2.41 (s, 3H). ^{13}C NMR (101 MHz, $CDCl_3$) δ 146.3, 144.2, 142.49, 138.3, 134.2, 131.9, 130.0, 129.9, 129.8, 129.2, 128.9, 128.1, 127.6, 126.8, 124.3, 120.3, 54.3, 21.5.

5.5.2. Ru-Catalyzed C(sp^2)–H Alkylation Directed by 1,2,3-Triazoles

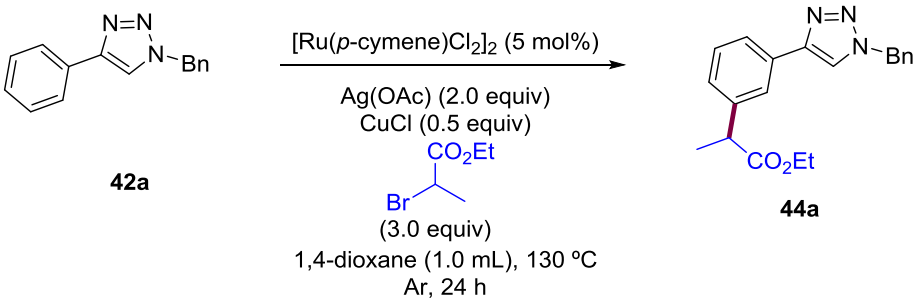

General Procedure for 44a: A reaction tube containing a stirring bar was charged with the corresponding 1-benzyl-4-phenyl-1*H*-1,2,3-triazole **42a** (0.25 mmol, 1.0 equiv), ethyl bromopropionate (0.75 mmol, 3.0 equiv), copper(I) chloride (0.125 mmol, 0.5 equiv), silver acetate (0.5 mmol, 2.0 equiv) and [Ru(*p*-cymene)Cl_2]$_2$ (5 mol

%). The reaction tube was then evacuated and back-filled with dry argon (this sequence was repeated up to three times). Then 1,4-dioxane (1.0 mL) was added and the reaction tube was next warmed up to 130 ºC and stirred for 24 hours. The mixture was then allowed to warm to room temperature, concentrated under reduced pressure and purified by flash chromatography (hexanes/AcOEt 1/1) provide the corresponding product **44a** 40% yield as a white solid. ^{1}H NMR (400 MHz, $CDCl_3$) δ 7.73 (d, *J* = 1.6 Hz, 1H), 7.72 – 7.70 (m, 0H), 7.69 – 7.68 (m, 1H), 7.41 – 7.37 (m, 2H), 7.35 (s, 0H), 7.33 (d, *J* = 6.0 Hz, 1H), 7.32 – 7.29 (m, 1H), 7.28 – 7.24 (m, 1H), 5.58 (s, 1H), 4.22 – 4.00 (m, 1H), 3.73 (q, *J* = 7.2 Hz, 1H), 1.51 (d, *J* = 7.1 Hz, 2H), 1.19 (t, *J* = 7.1 Hz, 2H). ^{13}C NMR (101 MHz, $CDCl_3$) δ 174.5, 148.2, 141.4, 134.8, 130.9, 129.3, 129.2, 128.9, 128.2, 127.4, 125.1, 124.6, 119.7, 60.9, 54.4, 45.7, 18.7, 14.2.

5.5.3. *NMR Spectra*

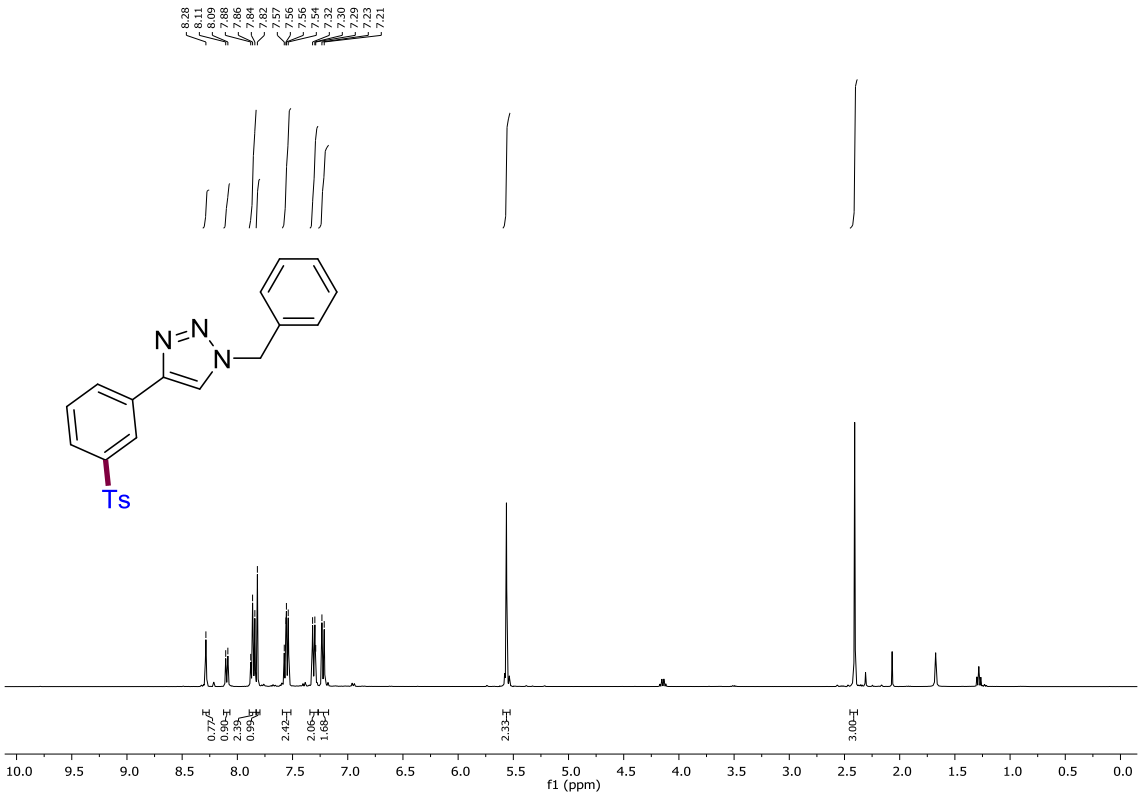

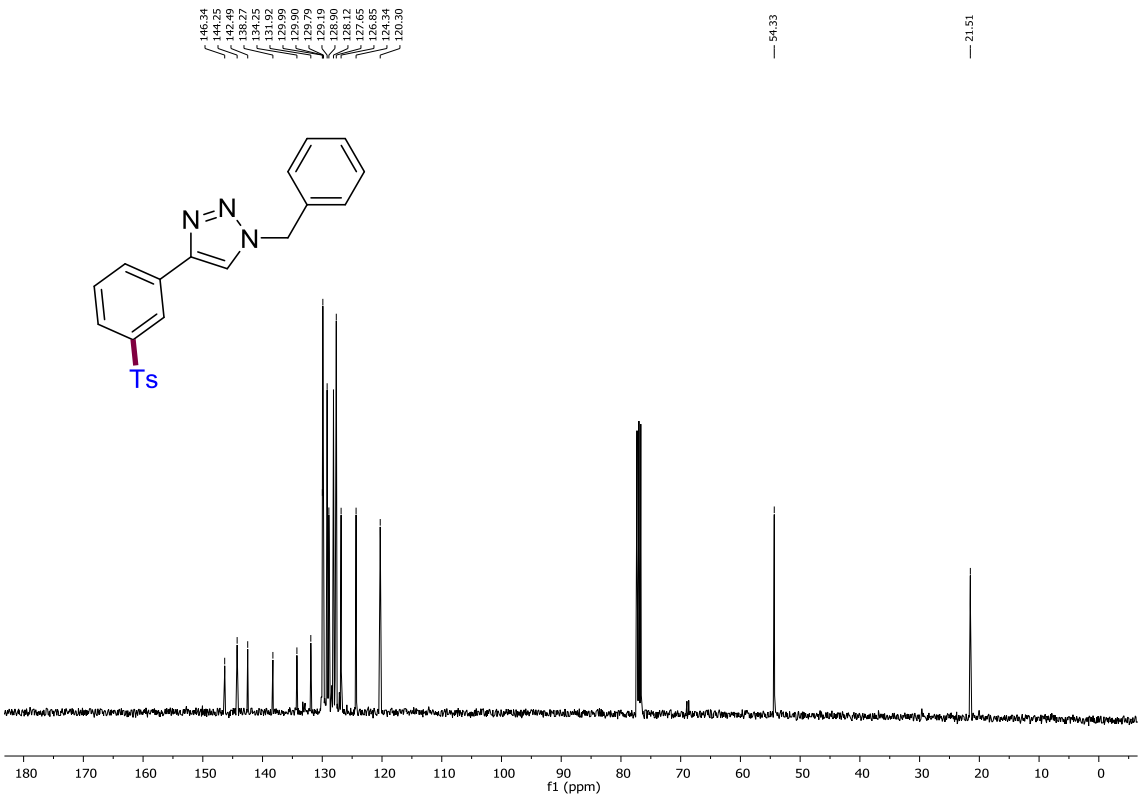

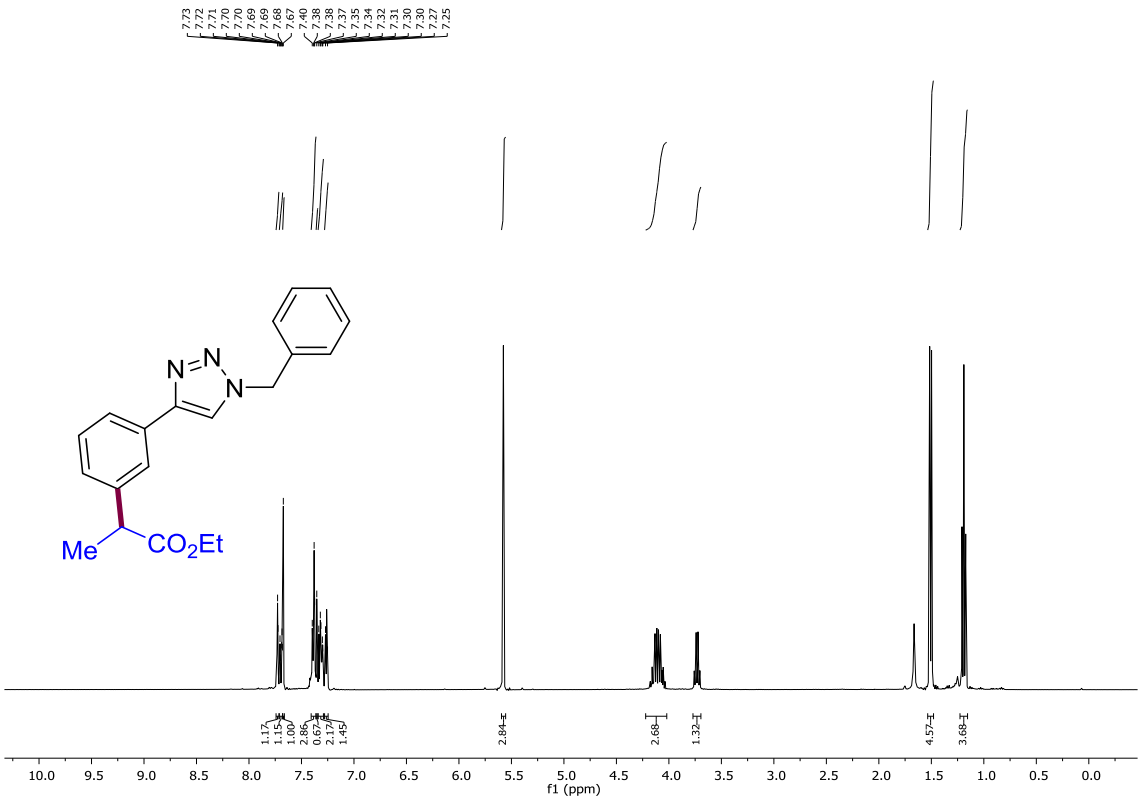
7.73
7.72
7.71
7.70
7.70
7.69
7.68
7.67
7.40
7.38
7.38
7.37
7.35
7.34
7.32
7.31
7.30
7.30
7.27
7.25
N
N
N
Me
CO2Et
1.17
1.15
1.00
2.86
0.67
2.17
1.45
2.84
2.68
1.32
4.57
3.68
10.0
9.5
9.0
8.5
8.0
7.5
7.0
6.5
6.0
5.5
5.0
4.5
4.0
3.5
3.0
2.5
2.0
1.5
1.0
0.5
0.0
f1 (ppm)

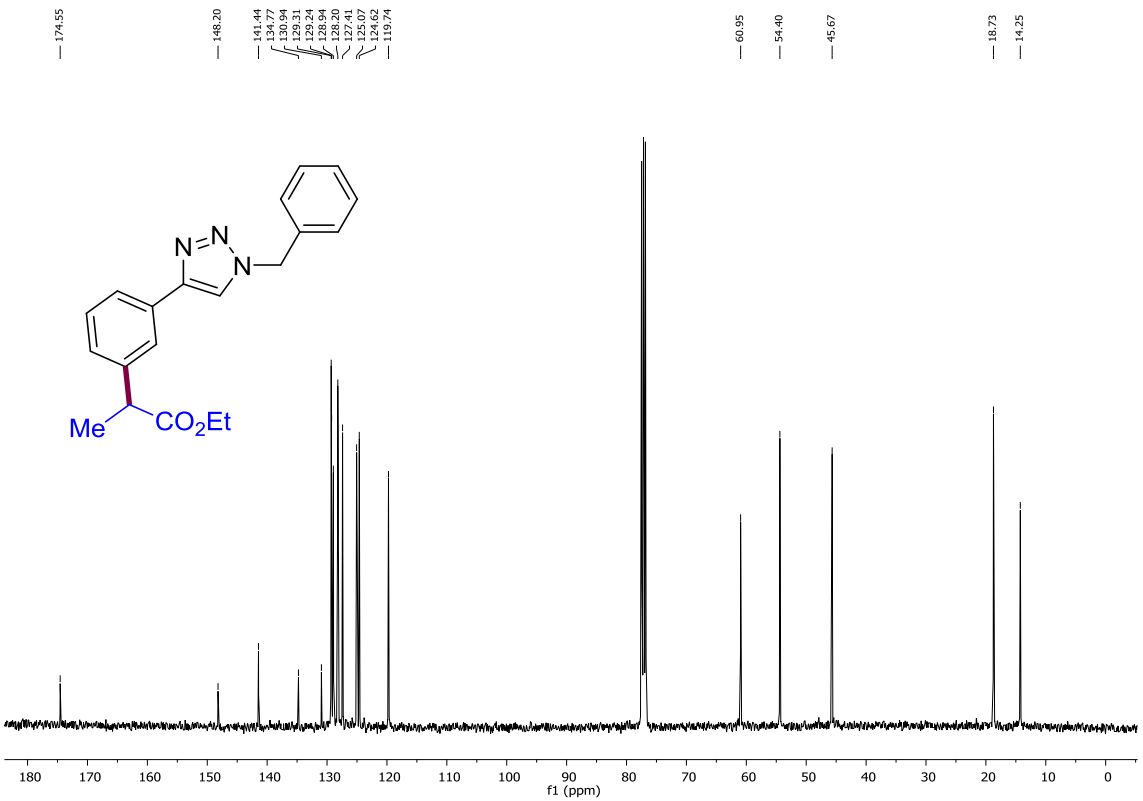
174.55
148.20
141.44
134.77
130.94
129.31
129.24
128.84
128.20
127.41
125.07
124.62
119.74
60.95
54.40
45.67
18.73
14.25
N
N
N
Me
CO2Et
180
170
160
150
140
130
120
110
100
90
80
70
60
50
40
30
20
10
0
f1 (ppm)